ABSTRACT

ROSS, KELLY ANN. Energy Flow in Multilayer Clothing Systems. (Under the direction of Trevor J. Little).

Clothing has a large part to play in the maintaining the body's heat balance especially during exercise. This research investigated how to build a layered clothing system that would optimize moisture management and performance during athletic end use. During physical activity muscles burn nutrients which releases energy in the form of heat. The human should maintain a constant core temperature of about 37 degrees Celsius, from which only a small change (+/-) ~4°C can lead to serious injury or death. There are four mechanisms that allow the body to lose heat to the environment in order to maintain its thermal balance: conduction, convection, radiation, and evaporation. This research utilizes a test method where multiple fabric layers are tested simultaneously as a person would wear multiple garment layers together. Typical existing testing procedures for the measure of heat and moisture transport in textile materials are successful in measuring one layer of fabric at a time. However, people typically wear more than one layer of clothing especially on their upper torso which could include a foundation garment such as a sports bra, undershirt or t-shirt, and an additional layer consisting of a shirt or jacket. As part of this research, a fabric testing kit was designed in order to test three different fabric layers at the same time while mounted on a human subject during exercise. This fabric testing kit measured coupled heat and moisture transfer in relation to temperature and humidity across the microclimates, the interaction between clothing to skin, and the layer to layer interactions of a clothing system.

Human subjects who participated in this research were athletic and capable of riding a stationary bicycle for an extended period of time in order to produce perspiration. Both males and females participated in this study. A total of eleven different subjects were used in this research including seven males and four females. Ten different fabrics were chosen to be evaluated by the fabric testing kit. Knowledge gained through this research can be used to design better clothing systems more suited to satisfy the needs of athletes or regular exercisers, especially those who will be perspiring for a longer time such as long distance runners and cyclists. Also, this research provides an in depth analysis of an athletes' warm up prior to training or competing, which can aid in the development of clothing systems that effectively warm muscles to a competing temperature and prevent formation of lactic acid build up before or after the competition.

Energy Flow in Multilayer Clothing Systems

by
Kelly Ann Ross

A dissertation submitted to the Graduate Faculty of
North Carolina State University
in partial fulfillment of the
requirements for the degree of
Doctor of Philosophy

Textile Technology Management

Raleigh, North Carolina

2013

APPROVED BY:

_____	_____
Trevor J. Little Committee Chair	Roger L. Barker
_____	_____
Katherine E. Carroll	Hechmi Hamouda

DEDICATION

To my mother, a wonderful woman full of strength and light. The memory of her light will always burn bright in my heart. She was an inspiration of hope and faith to all that knew her. "Do not grieve, for the joy of the LORD is your strength," Nehemiah 8:10.

BIOGRAPHY

Kelly Ann Ross was born September 1, 1979 to Steve and Ann Goforth in Shelby, North Carolina. She spent most of her youth living with her parents and two brothers, Jamie and John in Cleveland County right outside of Kings Mountain, North Carolina. She attended Bethware Elementary School and Kings Mountain Middle School before graduating from Kings Mountain High School in 1997. In May of 2005, she graduated with a Bachelor's of Science in Textile Management from North Carolina State University. In the fall of 2005, Kelly continued her education at NCSU pursuing a Master's of Science in Textiles. She was fortunate to be selected as an Institute of Textile Technology Graduate Fellow for the Class of 2007. On November 11, 2006, she married Kevin Andrew Ross, alumni and employee of North Carolina State University. Kelly graduated with a Master of Science on May 12, 2007. After graduation, Kelly began working at Glen Raven, a vertically integrated textile company located near Burlington, NC. In the fall of 2009, Kelly returned to NCSU as a graduate teaching assistant and received a Certificate of Accomplishment in Teaching in April 2011; she will graduate with her doctorate in December 2013. Her daughter Katharine Anslee Ross was born June 12, 2010. Kelly's most influential role model is her mother, a retired chemistry educator who lost her battle against cancer in April 2013.

ACKNOWLEDGMENTS

I would like to express my most sincere gratitude to my research advisor, Trevor J. Little for his advice, guidance, and support throughout my research. I would also like to thank the other members of my committee and former professors who are all special to me in their own unique ways. I am also grateful to my fellow graduate students and classmates for their encouragement and friendship. I am also grateful to my family and my church. I owe a great deal of gratitude to the NC State Cycling Club as well as the coaches and staff at Weisiger-Brown Athletics Facility. I will always appreciate their help in making this research possible.

TABLE OF CONTENTS

LIST OF TABLES

LIST OF FIGURES

CHAPTER ONE

1. Introduction

The purpose of this research was to determine how to build a multilayered clothing system that optimizes moisture management and performance during athletic end use. Clothing has a large part to play in the maintaining the body's heat balance as it modifies the heat loss from the skin surface and at the same time has the secondary effect of altering the moisture loss from the skin (Saville, 1999). When the body is in movement, active muscles require more energy and nutrients than at rest and the metabolic rate increases. When the muscles burn these nutrients, some of the energy they contain is released outside the body as external work, but the majority of it is released in the muscle as heat. The human body tries to maintain a constant core temperature of about 37 degrees Celsius, only a small change (+/-) ~4°C can lead to serious injury or death. An average adult can sustain an energy production of about 400-600 kcal/hr (jogging or bicycling) for an extended period of time. If the extra heat produced cannot escape the body, this type of activity would raise the core temperature of the body ~1.0°C every eight to ten minutes causing the effects of hyperthermia to impair body function within 25 to 30 minutes (Boron & Boulpaep, 2012).

There are only four mechanisms that allow the body to lose heat to the environment in order to maintain its thermal balance: conduction, convection, radiation, and evaporation. The research intends to characterize what properties of the fiber and/or fabric layers of a clothing system influence the heat and moisture transfer in terms of the optimizing the heat balance of the body in a variety of activity levels and environmental conditions. This

research utilizes a test method which attempts to more realistically mimic the human experience than existing testing procedures for the measure of heat and moisture transport in textile materials. This research uses a fabric test kit that can be mounted on a human subject. This fabric test kit measures both heat and moisture transfer in relation to temperature and humidity across the fabric and microclimate layers and interactions between clothing to skin and layer to layer of a clothing system.

To measure changes in the amount of heat energy and moisture flow within a fabric testing kit, the human subjects used in this study served as the heat energy and moisture source. The human subjects were recruited from active bicyclist and athletes who use the bicycle frequently in their training routines. These individuals were all athletic and capable of performing the human trial where they would be asked to ride a bicycle to produce perspiration. Both males and females participated in this study. A total of eleven different subjects were used in this research including seven males and four females. Ten different fabrics were chosen to be evaluated by the fabric testing kit. The fabric kit consisted of three layers designed to represent how a human body would dress: underwear as a base layer, t-shirt or top, and jacket as an outer shell. The choice of fabric to be used for each layer within the kit was based upon a survey of current active wear products available at several retail outlets and suitability of end use which was a consideration when building each kit. The bicycle test protocol created for this study was designed to induce perspiration from the human subjects through maintaining a specific heart rate or target range. The subjects were asked to ride the stationary bicycle: 5 minutes to warm up on bicycle during this time the subject can slowly work up to the target heart rate zone; 30 minutes at the target heart (135-

155 beats per minute), 10-15 minutes slower pace to allow the subjects heart rate to return to normal. The importance of this research is to be able to better understand how clothing systems can be designed to satisfy the needs of athletics or regular exercisers, especially those who have longer time in the competition and who will be perspiring for a longer time. Further, as athletes warm up prior to competing, the clothing system must be designed so as to warm muscles to a competing temperature and prevent formation of lactic acid build up before or after the competition.

CHAPTER TWO

2. Literature Review

Although the research is focused on heat energy and moisture movement through fabric; some initial background of comfort is required for understanding. Comfort is an essential and general need for human beings, although it is complex and difficult to define (Li, 2001). Early research on comfort in textile material focused primarily on the thermal insulation properties of fabric. Morris (1953) provides an excellent review of the pioneering research from the 1930's through to the early 1950's. The pioneer researchers found that the physiological responses of the human body could be predicted from measuring factors such as the thermal insulation and moisture permeability of the clothing, the environmental conditions, and the level of physical activity (Li, 2001). Other early researchers recognized the effect of the fabric's hand and the sensations of thermal acceptability (Bogaty, Hollies, & Harris, 1956; Hock, Sookne, & Harris, 1944; Hollies, Custer, Morin, & Howard, 1979; Facknowledged sensory factors in relation to the overall evaluation of fabric hand preference (Hoffman & Beste, 1951; Howorth & Oliver, 1958; Lundgren, 1969; Pierce, 1930). This classical research has led to the development of complex comfort theories that include physiological factors but also recognize the significance of sensory and psychological aspects of comfort. Slater (1985) defined comfort as "a pleasant state of physiological, psychological, and physical harmony between a human being and the environment." Slater defines physiological comfort as the ability to sustain life, psychological comfort as the ability to keep the mind functioning in a satisfactory state, and physical comfort as the effect

of the external environment on the body (Slater, 1985). An investigation of comfort theory provides evidence of just how difficult the term comfort is to define. The existing comfort models include differing factors related to comfort and each model illustrates a different view of the concept of comfort as it relates to human life.

2.1. Theoretical Models for Human Comfort

Researchers have developed theories and models in order to define, analyze, and understand how humans perceive comfort. To establish an understanding of comfort each of these theories and models are important. Four theories related to the clothing comfort field are presented chronologically: Fourt and Hollies' Comfort Triad (1970), Pontrelli's Comfort's Gestalt (1977), Sontag's Comfort Triad (1985-1986), and Branson's and Sweeney's Clothing Comfort Model (1991).

2.1.1. Fourt and Hollies' Comfort Triad (1970)

Fourt and Hollies (1970) created the comfort triad model which involves three elements: the wearer, the clothing and the environment where important variables and measurement methods are presented for each element of the triad. The variables used to evaluate the person included metabolism, evaporation, surface temperature, rectal temperature, tympanic membrane temperature, DuBois surface area, and heart rate. It should be noted that these are strictly physiological variables and do not include psychological, psycho-physiological, or social aspects of comfort. The clothing variables were identified as thermal insulation, resistance to evaporation or breathability, wind resistance, thickness, weight, and surface area. The environmental variables were temperature, relative humidity, air movement, and radiant heat (Fourt & Hollies, 1970).

2.1.2. Pontrelli's Comfort Gestalt (1977)

Pontrelli's Comfort Gestalt (1977) introduced a new comfort model, appropriately titled where each comfort factor is affected by or has effects on the other factors of comfort, as shown in Figure 2.1.

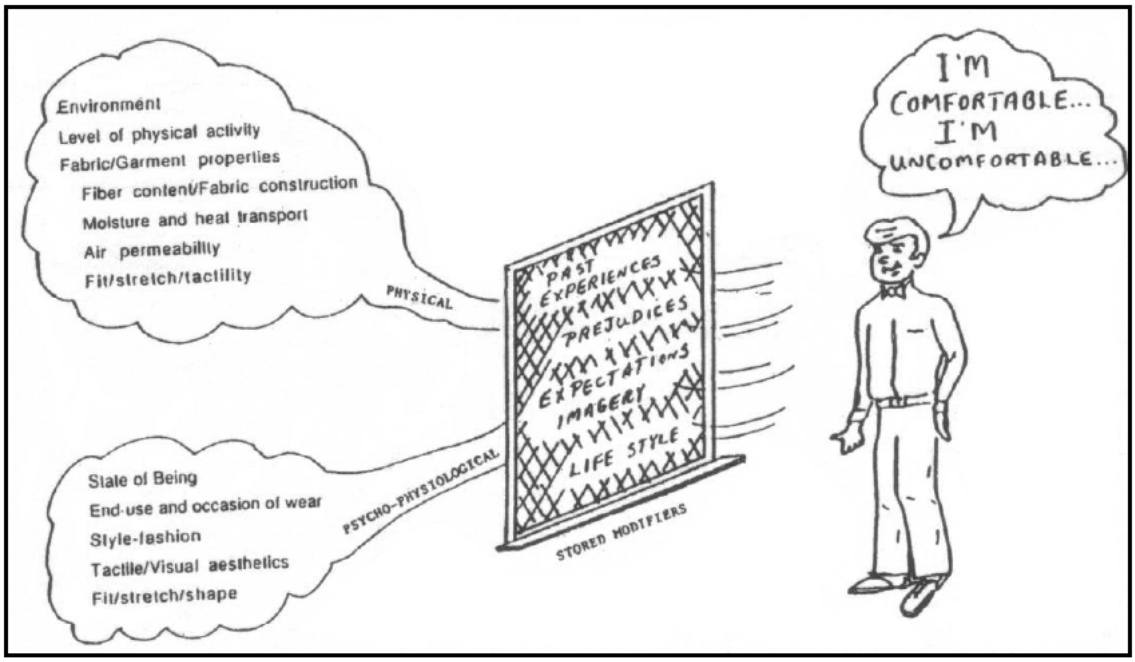

Figure 2.1: Pontrelli's Comfort Gestalt

Source: Pontrelli, G.J. (1990), "Comfort by design", *Textile Asia*, (21)1, p. 51.

This model includes physical aspects of the person, clothing, and environment from Fourt and Hollies (1970) triad model, but adds a psychophysiological aspect (Pontrelli, 1977). According to Pontrelli comfort has three main factors: Physical Variables, Psychophysiological Parameters, and Stored Modifiers. The Psychophysiological factors used by Pontrelli were state of being, end-use and occasion of wear, style-fashion, fit and

tactile aesthetics. This model also included a filter consisting of the person's "stored modifiers" which are past experiences, prejudices, expectations, imagery and life style (Pontrelli, 1977; Pontrelli, 1990). These filters affect the psychological and physical factors of the model and determine which factors will ultimately contribute the perception of comfort.

2.1.3. Sontag's Comfort Triad (1985)

Sontag (1985) further developed Fourt and Hollies' triad and Pontrelli's model as shown in Figure2.2. In this model, three concentric circles represent each of the triad dimensions, with the personal attributes as the core. The personal attributes are encircled by the clothing attributes, which are encircled by the environmental attributes. Within each circle there are variables and dimensions identified in previous models (Fourt & Hollies, 1970; Pontrelli, 1977). The interaction between the circles is shown by a double-ended arrow traveling through the three circles. Sontag's theory suggests that the attributes of the three circle's components interact with each other and filter through the person's stored modifiers to establish the perception of the garment (Sontag, 1985).

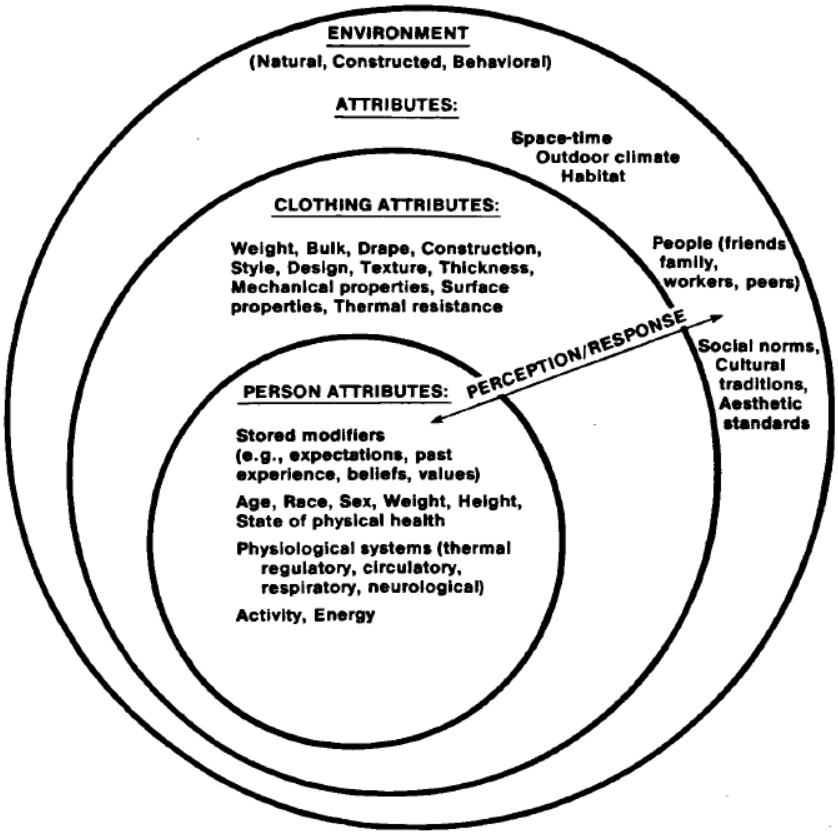

Figure 2.2: Sontag's Comfort Triad

Source: Sontag, M. S. (1985). Comfort dimensions of actual and ideal insulative clothing for older women. Clothing and Textiles Research Journal, 4(1), p. 10.

2.1.4. Branson and Sweeney's Clothing Comfort Model (1991)

The comfort model introduced by Branson and Sweeney (1991), builds upon past models as shown in Figure 2.3. This model for clothing comfort includes a triad of person, clothing, and environmental attributes but splits these attributes into two dimensions: physical and social-psychological. The model adds an additional component, the physiological/perceptual response which leads to the comfort judgment. The physiological/perceptual response includes human responses that have been generated from the interaction among the physical dimension and the social-psychological dimension. The physiological/perceptual response in

the Branson and Sweeney model represents the physical and social-psychological aspects of comfort. In this theory all the attributes and responses are reconciled through a person's individual "Filter" for determining the final perception of the garment (Branson & Sweeney, 1991).

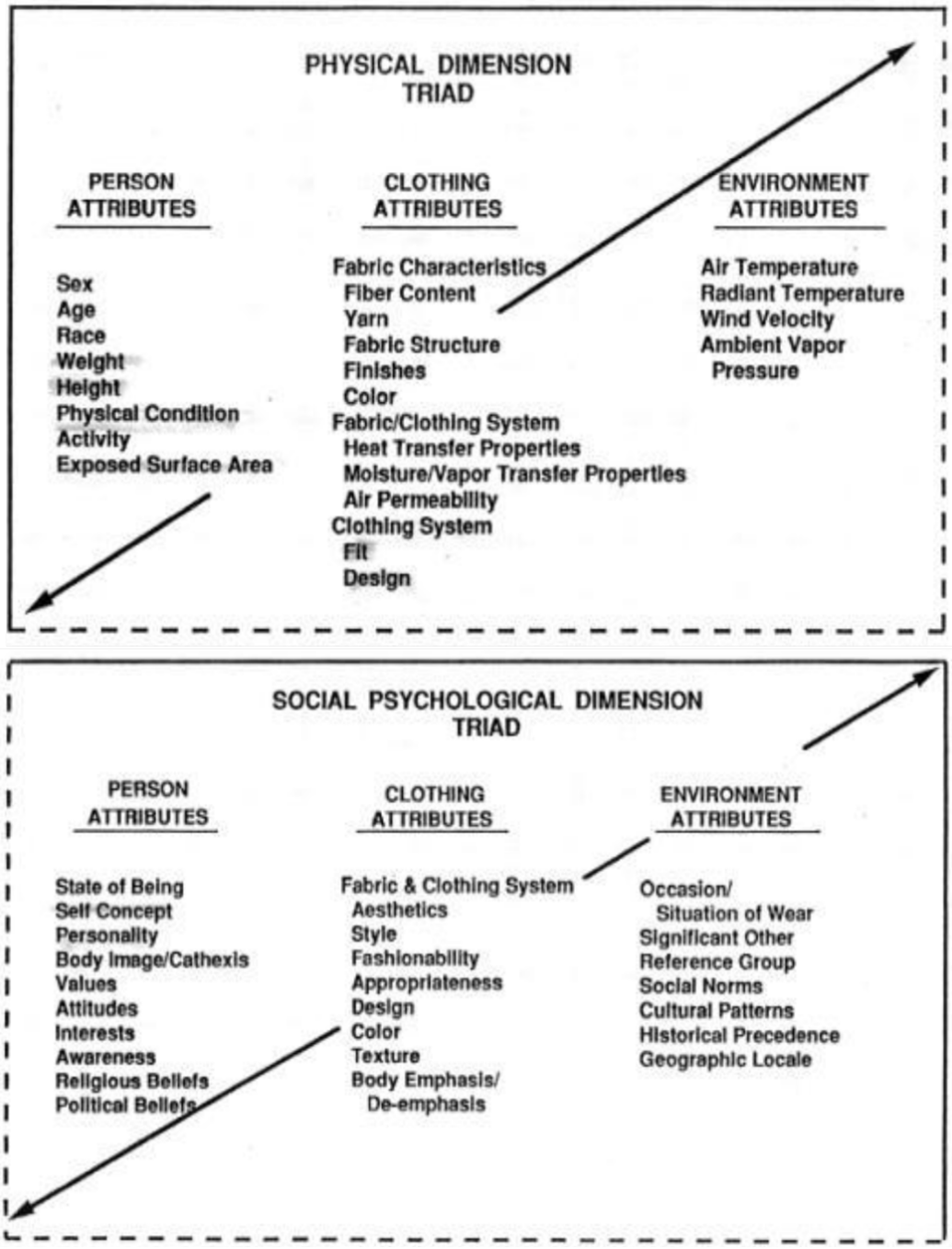

Figure 2.3: Branson and Sweeney's Clothing Comfort Model

Source: Branson, D. H. & Sweeney, M. (1991). Conceptualization and measurement of clothing comfort: Toward a metatheory. In S. B. Kaiser & M. L. Damhorst (Eds.) Critical linkages in textile and clothing subject matter: Theory, method, and practice (pp. 94-105). International Textiles and Apparel Association, Monument, CO., p. 102.

2.2. Physiological Aspect of Comfort

Each of the four comfort models introduced in Section 2.1 incorporate some aspect of the physiological state of the body. General physiological responses of the body are critical to life and can be measured such as temperature, blood pressure, heart rate, and oxygen consumption. Clothing can alter body temperature. The human body tries to maintain a constant core temperature of about 37 degrees Celsius. The body must maintain heat balance in order to function; if the body temperature rises or falls too much the event can lead to serious injury or death. Any level of physical activity above that needed to maintain body temperature will result in an excess of heat energy which must be dissipated, otherwise the body temperature will increase. According to Saville (1999) thermo-physiological comfort relates to the heat and moisture transport properties of clothing and interactions between clothing and the body's heat balance during various levels of activity. Clothing has a large part to play in the maintenance of heat balance as it modifies the heat loss from the skin surface and at the same time has the secondary effect of altering the moisture loss from the skin. The ability to manage moisture is a vital for fabrics intended to be worn during vigorous physical activity, because the human body cools itself by sweat production and evaporation during periods of high activity. If a fabric does not allow pass sufficient perspiration to pass through this leads to sweat and moisture accumulation close to the skin and discomfort. This chapter will examine different instruments to test how well fabrics shield the skin from discomfort. However, before instruments to test thermal and moisture management are discussed; the fundamental theories of heat and moisture transfer must be understood.

2.2.1. Heat Balance

Heat balance plays a very important role in maintaining a sense of comfort for the human body. Research has been conducted over the years regarding the maintenance of heat balance for a long period of time. When the body is in movement, active muscles require more energy and nutrients than at rest and the metabolic rate increases. When the muscles burn these nutrients, some of the energy they contain is released outside the body as external work, but the majority of it is released in the muscle as heat. Human body temperature is a balance between the rate of heat gain and heat loss through the management of its energy metabolism and temperature regulation (A. T. Miller, 1968). Rintamaki (2006) states that there are three key factors affecting the heat balance including: environmental thermal conditions, metabolic heat production, and thermal insulation and moisture permeability of clothing and other protective garments. Climatic parameters such as air temperature, radiant temperature, humidity, and wind speed along with personal parameters such as activity rate, clothing insulation, and sweat capacity have significant influence on the heat balance through inter-reaction among these parameters (Havenith, 2005). Body temperature changes according to the level of exertion during exercise. For body temperature to remain constant, heat losses need to balance heat production (Havenith, 1999). The body must maintain a state of heat balance with core temperature around 37°C, a rise or fall in temperature of only ± 5°C may result in injury or death (Saville, 1999).

2.2.2. Environmental Thermal Conditions

Environment influences on our sensation of thermal conditions depend on the interaction of heat, moisture, and air. The study of the interaction of these components is designated

psychrometry which is the study of water vapor in air (Franklin, Muir, & Scott, 2010). Moisture in the air does not change air temperature; instead the heat energy it holds can be released when this moisture or vapor condenses. The amount or mass of moisture in air at a specific volume and temperature is the absolute humidity or moisture content. This is measured as the humidity ratio or relative humidity of the air (Franklin, Muir, & Scott, 2010). Relative Humidity is the ratio of Vapor Pressure to the Saturated vapor Pressure. The dew point is the temperature at which atmospheric water vapor starts to condense (Franklin, Muir, & Scott, 2010). The humidity ratio (W) is used to express the mass of water vapor per unit mass of dry air in (lb_w/lb_a or kg_w/kg_a) .

$$W = \frac{M_w}{M_a} = \frac{lb_w}{lb_a} = \frac{kg_w}{kg_a}$$

According to the ASHRAE handbook, which provides the standards for design and maintenance of indoor environments, systems designed to control humidity should maintain a humidity ratio at or below 0.012, which corresponds to a water vapor pressure of 1.910 kPa (0.277 psi) at standard pressure or a dew point temperature of 16.8°C (62.2°F) (ASHRAE handbook, 2009). During exercise the body will perspire and environmental factors, such as temperature and relative humidity, affect the amount of perspiration vaporized from the skin. Outdoor environmental temperature and relative humidity varies and cannot be controlled but, clothing is worn both indoors and out of doors so, it must provide a means to manage heat and moisture for both.

2.2.3. Metabolic Rate

In human beings, the rate of internal energy production is called the metabolic rate. When food is broken down during digestion it is transformed into heat production and mechanical power in the body through oxidation (Bass & Henschel, 1956). This process can be explained by Figure 2.4.

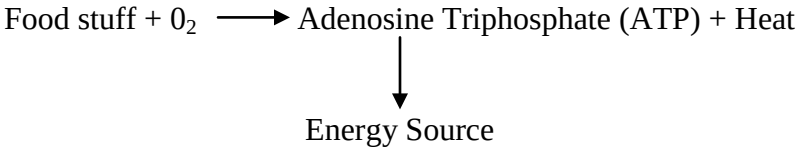

Figure 2.4: Human Body Heat and Energy Production

Different activities require different amounts of energy and the more intense the activity the more energy required. The energy required also depends on the weight of the person; a heavier person requires more energy for the same activity. The body's rate of heat production can vary from about 70 kcal/hr at rest to 600 kcal/hr while jogging (Boron & Boulpaep, 2012). Heat energy produced by human metabolic processes, can be applied into thermodynamic laws as follows:

$$\boldsymbol{H = M - W}$$

Where H is the metabolic heat production, M is the metabolic rate, and W is mechanical work (Hope, 1993; Parsons, 2002). The metabolic energy rate can be divided into heat production rate and mechanical work. The rates of *H*, *M*, and *W* can be measured by consumption of oxygen as metabolic energy consumption is directly related to oxygen consumption (Burdett & Skrinar, 1983). The unit often used for metabolic rate is "MET,"

one MET is equal to 1 kcal/kg/hour and as oxygen uptake in ml/kg/min is roughly equivalent to the energy cost of sitting or lying quietly. A MET also is defined as oxygen uptake in ml/kg/min with one MET equal to the equivalent to 3.5 ml/kg/min (Ainsworth et al., 2011). Body surface area is calculated using the formula of DuBois and DuBois:

$$BSA = (W\ 0.425\ x\ H\ 0.725)\ x\ 0.007184$$

where the weight is in kilograms and the height is in centimeters (D. DuBois & DuBois, 1916). The table below shows the metabolic heat energy produced for some common activities for a person with a BSA *1.8 m^2 (19.4 ft^2)*:

Table 2.1: Metabolic Rate for Common Activities * 1 MET = 1 kcal/kg/hr

Activity	***Met***
Lying quietly and watching television	1.0
Walking <2.0 mph, level, strolling, very slow	2.0
Walking 2.5 mph, level, firm surface	3.0
Bicycling <10 mph, leisure, to work or for pleasure	4.0
Volleyball, competitive, in gymnasium	6.0
Swimming medium speed, ~50 yards/minute, vigorous effort	8.3
Running, 10 mph (6 min/mile)	14.5

Source: Ainsworth, B. E., Haskell, W. L., Herrmann, S. D., Meckes, N., Bassett, D. R., Tudor-Locke, C., Leon, A. S. (2011). 2011 compendium of physical activities: A second update of codes and MET values. *Medicine & Science in Sports & Exercise, 43*(8), p. 1575-1581.

An average adult can sustain an energy production of about 400-600 kcal/hr (jogging or bicycling) for an extended period of time. If the extra heat produced cannot escape the body, this type of activity would raise the core temperature of the body ~1.0°C every eight to ten minutes causing the effects of hyperthermia to impair body function within 25 to 30 minutes (Boron & Boulpaep, 2012). There are only four mechanisms that allow the body to lose heat to the environment in order to maintain its thermal balance: conduction, convection, radiation, and evaporation. Figure 2.5 illustrates these four ways that heat can be transferred between the body and the environment during physical activity.

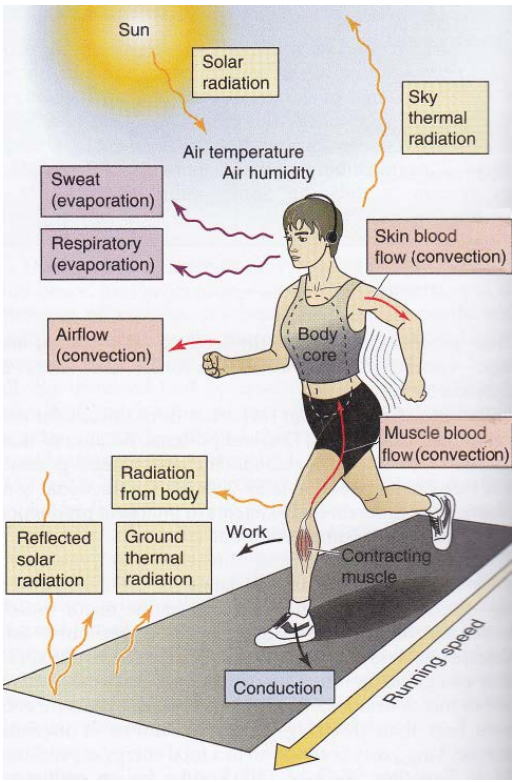

Figure 2.5: Heat balance between the body and environment during activity

Source: Boron, W. F., & Boulpaep, E. L. (2012). *Medical physiology* (2nd ed.). Philadelphia, P.A.: Saunders Elsevier.

The heat balance of the body is usually described by some variation of the following general equation:

$$M - W = q_{sk} + q_{res} + S = (C + R + E_{sk}) + (C_{res} - E_{res}) + (S_{sk} + S_{Cr})$$

where M is rate of metabolic heat production (W/m^2), W is rate of mechanical work accomplished (W/m^2), q_{sk} is total rate of heat loss from skin (W/m^2), q_{res} is total rate of heat loss through respiration (W/m^2), E_{sk} is total rate of evaporative heat loss from skin (W/m^2), C_{res} is rate of convective heat loss from respiration (W/m^2), E_{res} is rate of evaporative heat loss from respiration (W/m^2), $C + R$ is sensible heat loss from skin (W/m^2), S_{sk} is the = rate of heat storage in skin compartment (W/m^2), S_{Cr} is rate of heat storage in core compartment (W/m^2) (ASHRAE, 2009). During this process, the net heat production $(M - W)$ is transferred to the environment through the skin surface (q_{sk}) and respiratory tract (q_{res}) with any surplus or deficit stored (S) causing the body's temperature to rise or fall (ASHRAE, 2009). There are several different ways that the heat from the body can dissipate into the surrounding environment: sensible heat flow from the skin; latent heat flow from sweat evaporation and from evaporation of moisture diffused through the skin; sensible heat flow during respiration; and latent heat flow from evaporation of moisture during respiration**.** Sensible heat flow from the skin can be a multifaceted blend of conduction, convection, evaporation, and radiation for a clothed person (ASHRAE, 2009).

2.2.4. Conduction

Heat loss is accomplished by conduction through direct contact with another substance. Chandrasekaran (2009) defines heat conduction as energy flowing from a higher temperature to a lower temperature due to kinetic motion or direct impact of molecules in contact with

one another. The rate of exchange is determined by the temperature difference between the two substances and by their thermal conductivities (Saville, 1999). Heat emitted by the body can be passed onto our clothing through conduction. The amount of heat energy than can be transferred can differ according to fabric structure or fiber property (Frydrych, Dziworska, & Bilska, 2002). Therefore the thermal conductivity of different textile materials has been the subject of much interest.

2.2.5. Convection

Heat loss is accomplished by convection when heat is transferred by a moving fluid (liquid or gas). For example, cold water flowing over the body in the shower is heated by conduction as it comes in contact with the body and then carries the heat away from the body by convection. Fowler (2005) explains that convection is a gravitationally induced heat transfer. The movement of convection depends on temperature differences occurring at different levels of density and the heat energy dispersed by convection travels in the direction of the cooler high density (Fowler, 2005).

2.2.6. Radiation

Heat loss is accomplished by radiation through electromagnetic waves, defined by Guyton (2005) as "electromagnetic radiation emitted from the surface of an object due to its temperature." Radiation is usually ignored as a mechanism of losing heat because it is dependent on the temperature of an object. Radiation is more important as a means of heat gain from very hot bodies such as the sun or fire (Saville, 1999). Heat radiation and absorption by an object are both influenced by its color: black being the best as the most heat is absorbed and white being the worst as the most heat is reflected. Clothing acts to reduce

radiation loss by reducing the temperature differences between the body and the environment.

2.2.7. Evaporation

Heat loss is accomplished by evaporation when liquid is changed to water vapor. In the human body this phenomenon is called perspiration. Perspiration is the body's natural mechanism of heat regulation which allows the body to lose heat when its temperature starts to rise in order to evaporate the moisture from the skin. Evaporation requires a tremendous amount of energy, it takes 2424 J (580 calories) to evaporate one gram of water at body temperature (Saville, 1999). When water is evaporated from the skin surface the energy required is removed from the skin releasing heat and therefore cooling the skin. The evaporation of sweat is of vital importance for body temperature regulation and works to assure wellbeing in hot environments (Albert-Wallerstrom & Holmer, 1985). Other research has concluded that the latent heat of vaporization plays an important role in dispelling heat by perspiration at skin temperature (Candas, Libert, & Vogt, 1979; Givoni, 1976; Kerslake, 1972). Under normal conditions and activity levels, for example, a stroll through the inside of a shopping mall, the heat produced by the metabolism is taken up into to the atmosphere by conduction, convection and radiation and the body perspires in vapor form to maintain the body temperature. At higher activity levels and/or at higher temperatures, the production of heat increases and the heat from the skin that can be transferred to the atmosphere decreases. At this point, the sweat glands are activated to produce liquid perspiration as well (Das, Kothari, Fangueiro, & Araujo, 2007a; Das, Kothari, Fangueiro, & Araujo, 2007b). This liquid perspiration can cause discomfort as it can adversely affect the fabrics interaction with

skin. There are two forms of perspiration: insensible in which perspiration is transported as a vapor and it passes through the air gaps between yarns in a fabric, and liquid which occurs at higher sweating rates wetting the clothing in contact with the skin (Saville, 1999). The two forms of perspiration affect a fabric's ability to allow water vapor to pass through and fabric's ability to absorb or wick the sweat from the wearer's skin.

2.2.8. Thermal and Moisture Management of Clothing

A clothing system should allow the perspiration to pass through to its outside surface; otherwise it will result in discomfort. Feelings of discomfort arise from the skin being wet. If sweating occurs and the clothing moisture transfer rate is slow, the relative and absolute humidity levels between the clothing and skin increase thus suppressing the evaporation of sweat (Das, Kothari, Fangueiro, & Araujo, 2007b). Clothing vapor resistance is the standard model for calculating evaporative heat loss from the skin based on the relationship between permeability and heat resistance using the following equation:

$$R_e(m^2PaW^{-1}) = \frac{1000}{16.7F_{pcl}} = 60\left(\frac{1}{h_c} + .344I_{cl}\right)$$

where R_e is the clothing vapor resistance, F_{pcl} is the permeation efficiency factor, h_c is the convective heat transfer coeffient defined as $h_c\ (Wm^{-2}{}^{\circ}C^{-1}) = 12.1\sqrt{v_{ar}}$ and $v_{ar}(ms^{-1}) = v_a + 0.0052(M - 58)$ with v_a being air velocity(ms^{-1}), M the metabolic rate (Wm^{-2}) (Havenith, Holmer, and Parsons, 2002). Moisture accumulation in fabric degrades the thermal insulation provided by clothing systems (Sato, Nakagawa, Tokura, Zhang, & Gong, 2007). Clothing convective and radiant heat exchanges are determined by the following equation:

$$R + C = \frac{\Delta t}{I}$$

where I is thermal insulation of clothing($m^{2\circ}CW^{-1}$), Δt the temperature gradient across the clothing layer($^{\circ}C$), and R and C are the heat exchange by radiation and convection (Wm^{-2})(Havenith, Holmer, and Parsons, 2002). During normal and high activity levels and in hot and cold weather conditions, moisture transmission through clothing is important to maintain the body's heat balance.

There has been significant research leading to the development of moisture management fabrics which control of the movement of liquid sweat and moisture away from the skin to the outer surface of fabric. Traditionally, clothing made of 100% cotton absorbs perspiration well, however, cotton retains the moisture in the fabric layer next to the skin giving rise to uncomfortable feeling of wet and cold after exercise (Sarkar, Jintu , Fan, Szeto, Xiaoming & Tao, 2009). Many different techniques have been applied to the development of fabrics that have increased moisture management properties including the use of chemical and plasma treatments to alter surface energies of fabrics (Ferrero, 2003; Rodrigues, 2000).

2.3. Theoretical Background of Heat Transport

2.3.1. Thermodynamics

Thermodynamics is the study of the behavior of energy flow. The zeroth, first, second, and third law of the thermodynamics can be applied in three types of systems: isolated, closed and open system based on the method in which they interact with the exterior (Kondepudi, 2008). In the field of thermodynamics there are several established laws that explain heat and its relation to other forms of energy and work. The principle of this energy flow is

explained by the zeroth, first, second and third laws of thermodynamics. Understanding these laws is important as it relates to the heat exchanged between the human body, clothing, and the environment. The zeroth law is that "if two thermodynamic systems are each in thermal equilibrium with a third, then they are in thermal equilibrium also with each other" (Moran & Shaprio, 2008). This law is related to thermal equilibrium between systems. The first law of thermodynamics is often called the Law of Conservation of Energy. This law suggests that energy can be transferred from one system to another in many forms and cannot be created or destroyed. Energy is preserved by shifting into a variety of energy forms, for example, potential transferred into kinetic energy. The change in internal energy of the system is equal to the quantity of energy supplied to any isolated system in the form of heat (Q) minus the work done by the system (W), as shown by the following equation:

$$\Delta E = Q - W$$

The change in internal energy of the system (ΔE) consists of three factors, kinetic energy, potential energy, and internal energy and can be explained by the following equation:

$$\Delta E = \Delta KE + \Delta PE + \Delta U = Q - W$$

where ΔKE is the change in kinetic energy ($\Delta \frac{1}{2} mV^2$), ΔPE is the change in potential energy (Δmgz), ΔU is the change in internal energy of the system, m is the total mass, V is the magnitude of the velocity of the system, g is the acceleration due to gravity, z is the elevation (Moran & Shaprio, 2008). The second law states that heat energy cannot transfer from a colder to a hotter body (Kondepudi, 2008). The second law also offers a direction of the heat transfer in a system where energy transfer must have one direction and is irreversible (Logan, 1999). The third law is that as the temperature approaches absolute zero, the entropy

of a system also moves towards a minimum (Kondepudi, 2008). The third law explains that if all the thermal motion of molecules (kinetic energy) could be removed, a state called absolute zero would occur. Absolute zero is a temperature of 0 Kelvins or approximately -459.7° Fahrenheit or 273.15° Celsius.

In thermodynamics, materials or molecules can exist in four states: solid, liquid, gas, and plasma. Moran and Shapiro (2008) define the phase as the "a quantity of material that is homogeneous throughout in both physical structure and chemical composition." The material can change its state and this is called a phase change. A material normally exists in one or two phases through a process in a system. Fluid dynamics in textile materials involve two phases liquid and vapor (gas). Many researchers maintain that the phase changes in materials can be explained through molecular motion under an environmental condition. The phase change of the molecules in a system is based upon thermodynamic properties such as pressure, specific volume, and temperature (Kondepudi, 2008). This pressure (p), specific volume (v), and temperature (T) relationship is consistent with the ideal gas law ($pv = nRT$). The pressure is inversely proportional to the specific volume when temperature is constant, while temperature is directly proportional to the specific volume and pressure. If heat energy is absorbed, the molecules undergo increase in vibration which causes the bonds to be broken. The volume and intermolecular forces of the molecules are controlled by the pressure (p), specific volume (v), and temperature (T) relationship (Howell & Buckius, 1992; Stoecker & Jones, 1982).

2.3.2. The Microclimate

Albert and Palmes (1951) state that rate that the body's perspiration is vaporized is determined by environmental factors such as temperature and vapor pressure in the microclimate. In the microclimate perspiration can undergo phase changes (Albert & Palmes, 1951). As discussed in section 2.1.2,heat energy originates from metabolic activity and the body produces perspiration to help maintain heat balance. Perspiration moves from skin to the fabric through enthalpy which is a thermodynamic property used to measure the amount of heat transfer (Moran & Shaprio, 2008). Recall that the body's heat energy and perspiration are exchanged in a microclimate in four ways: evaporation, radiation, conduction, and convection. Colin & Houdas (1965) derived an equation which characterizes thermal equilibrium of the human body in terms of the first law of thermodynamics:

$$Q_E = Q_M - (Q_{CV} + Q_{CD} + Q_R)$$

where Q_E is the heat exchange by evaporation, Q_M is the metabolic production rate of heat, Q_{CV} is the heat exchange rate by convection, Q_{CD} is the heat exchange rate by conduction, and Q_R is the heat exchange by radiation (Colin & Houdas, 1965). Figure 2.6 shows the process of liquid sweat transport and phase change from liquid to vapor in the microclimate (Yi et al., 2006).

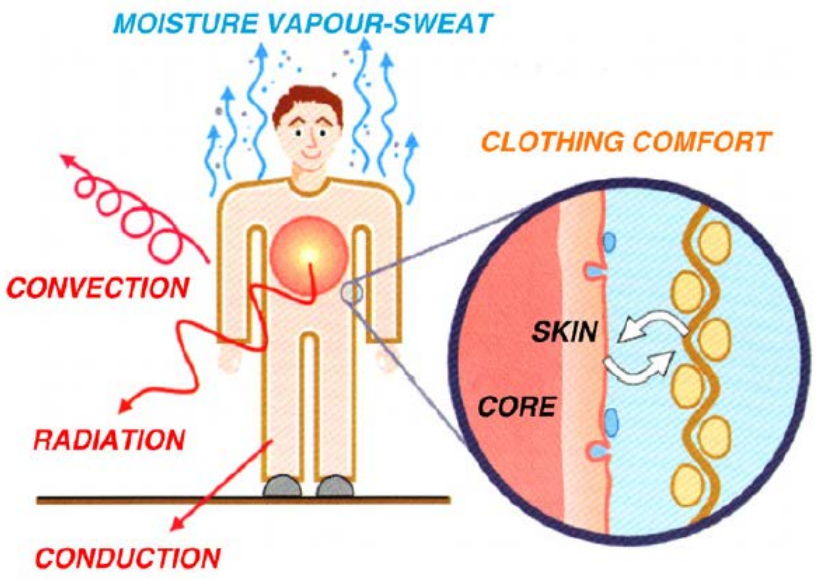

Figure 2.6: Perspiration Evaporation Movement by Heat Energy

Source: Yi, L., Aihua, M., Ruomei, W. (2006). P-smart- a virtual system for clothing thermal functional design. Computer-Aided Design, 38(7) p.728.

Liquid vapor diffusion caused by kinetic and potential energy is an important factor affecting temperature change in the microclimate (Yi et al., 2006). Theories of moisture will be discussed further in Section 2.3.

2.4. Newton's Law of Cooling

Research has been ongoing to investigate the thermal properties of the environment surrounding the human body in order to calculate the convective heat transfer coefficient. Kandjov (1999) states that the human body behaves like an open thermodynamic system that exchanges mass and energy with its surrounding environment. According to Newton's Law of Cooling, in order to calculate the amount of heat transferred during neutral convection (Q), the heat transfer coefficient (h), area (A), and a temperature difference (T_1) and (T_2) must be

known. The temperature difference is between the surface of the object and the air directly surrounding the object. Newton's Law of Cooling is shown below:

$$Q = -hA(T_1 - T_2)$$

Although, the amount of heat flow by conduction is small, it is a part of the heat energy originating from the human body.

2.5. Fourier's Law

Research has been conducted to examine thermal conductivity in textiles such as the work of Ismail (1985), Vignewaran & Chandrasekaran (2009), Wang, Kaynak, Wang, & Liu (2006), and Zhu & Li (2010). Moran and Shapiro define thermal conductivity as the "an ability of the material to conduct heat." Vignewaran and Chandrasekaran (2009) define the heat conduction as "one method of energy flow from the higher temperature to the lower temperature due to kinetic motion or direct impact of molecules." Janna (2000) explains that "the numerical value of thermal conductivity means how fast heat is conducted by the molecular effects through a material." The law of heat conduction, also known as Fourier's law, defines heat conduction as "the amount of heat flowing per unit surface area per unit time," and states that "heat current or flow is proportional to the gradient of temperature" (Moran and Shapiro, 2008). Fourier's law can be explained by the following equation:

$$Q_x = -kA\frac{dT}{dX}$$

where $Q_x$is the amount of energy transferred, A is surface certain area, dT is the temperature difference, dX is a material thickness (distance), and the proportionality constant k is a

property called the thermal conductivity, and (-) illustrates that the direction of heat flux is inversely related to temperature gradient.

After heat energy is released from the human body, heat energy will pass through the clothing worn on the body. This heat energy is transferred through the clothing fabric. The heat transfer through the fabric will vary with fabric structure and/or fiber property (Frydrych, Dziworska, and Bilska, 2002). Convection losses arise because the body loses heat to the air in contact with it. In an air temperature of 28-29℃ a person can sit comfortably without any clothing, however, if the temperature drops lower their body will begin to lose heat without the added insulation given by clothing (Saville, 1999). It important to consider fabric structure and fiber properties in order to regulate the amount of the heat energy exchanged between the human body and the environment through the fabric.

2.6. Heat Transport through Textiles

The heat flow through a fabric is due to a combination of conduction and radiation. Holcombe and Hoschke (1983) explain that heat energy is conducted by forced convection of air flow across the fabric structure, by conduction through fibers, and by radiation from the fabric. Baxter (1945) stated that the thermal conductivity of the fabric consists of two factors: "the heat transmitted through air space and the heat transmitted through a structure formed by the textile fibers." The following equation shows that thermal conductivity of fabrics k is a combination of the conductivity of the air k_A and the fiberk_F:

$$k = (1 - f)k_A + fk_F$$

where f is the fraction by volume of the fiber content of the fabric. The conductivity of air is 0.025 W/mK and fibers are 0.1 W/mK. Mao and Russell (2007) indicate that the most

important factors affecting the thermal conductivity in the fabric is the thermal conductivity of the fiber composition and the ratio of fiber to air in the fabric. Mao and Russell (2007) also describe thermal conductivity as inversely related to thermal insulation. In order to make a thermal insulated fabric; there must be balance maximizing convection and radiation effects, and minimizing conduction (Mao & Russell, 2007). According to Havenith (1999) convection is a more significant avenue for heat loss from the body than conduction when the ambient air is cooler than the skin. Radiation also plays a large role in terms of heat transfer when the surface temperature of the body is much different than the surface temperature of the objects in the environment (Havenith, 1999). Heat transfer involving clothing is typically characterized by combining conduction, convection and radiation into one term collectively known as dry heat transfer or insulation value (Holmér et al, 1999). However, a more recent study by Kyunghoon, Yangsoo, & Chongyoup (2007) found that the contributions of radiation and conduction through air are significant and account for approximately 20% each of the total heat movement.

2.6.1. Insulation

Much research has been focused on thermal insulation of clothing. The clothing property associated with insulation is effectively its resistance to dry heat transfer (R_{ct}) (Holmér et al., 1999). This value is in units of K·m²/W and includes all layers of clothing from the skin to the environment, including air layers (Holmér et al., 1999). Another unit that is used within the industry to describe a garment's insulation value is (clo) which is greatly dependent on fabric thickness and can be estimated from the relationship:

$$clo = 1.6\ X\ thickness\ in\ cm$$ (Saville, 1999).

The clo value is the equivalent to 0.155℃ m^2/W. This unit approximates the normal indoor clothing worn by sedentary workers and is the insulation required to comfortably maintain a body producing heat at 50 $Kcal/m^2/h$ at 21℃, less than 50% RH and an air flow of 10 cm/s (Saville, 1999). As mentioned, the insulation value of clothing is dependent on the whole outfit including the air gaps between the layers of clothing which can add to the total insulation value assuming the gaps do not allow for air flow within the clothing system, leading to heat loss by convection. The presence of additional air results in a higher insulation value for a multilayer garment than could be expected of a single layer garment (Havenith, 1999). Also, the fit of a garment to the body has a great influence on insulation value. Air flow has three major effects on clothing: some air clings to the body forming an insulating layer, air flow causes the fabric to compress and reduce in thickness, and air flow disturbs the air trapped within clothing by moving the fabric and penetrating through the fabric (Saville, 1999). With light air flow these effects are minor but at high air speeds they can be significant depending on the air permeability of the outer layer of the clothing.

2.6.2. Air Permeability

Air permeability is defined as the volume of air in milliliters which is passed in one second through 100s mm^2 of the fabric at a pressure difference of 10mm head of water (Saville, 1999). Air permeability is an essential characteristic of clothing fabrics. Air permeability through fabrics is a complex issue and involves a variety of factors. The air permeability is a measure how a fabric allows air to pass through and has been the subject of research for many years. Backer (1951) developed a two dimensional model to predict air permeability in fabrics. Gooijer, Warmoesjerjen, and Groot Wassink (2003a) and Rushton and Griffiths

(1971) developed three-dimensional pore models to more accurately predict the air permeability of fabrics. Other researchers have developed theoretical models to predict the air permeability and airflow resistance of single-layer woven fabrics (Gooijer et al., 2003a, 2003b; Kulichenko, 2005; Kulichenko & Van Langenhove, 1992; Rainard, 1946, 1947; Tugrul, 2006; Wang, Maze, Vahedi, & Pourdeyhimi, 2006; Xu & Wang, 2005). Research has also been conducted to predict air permeability through multiple layers of fabric such as: Clayton (1935), Elnashar (2005), Epps (1988), Havrdová (2007), Kulichenko (2005), Lord (1959), Militky and Havrdova (2001), Sundaramoorthy, Nallampalayam & Jayaraman (2011), and Xu & Wang (2005). It is thought that air permeability is related to the ability to transfer water vapor to assist in moisture management.

2.6.3. Stefan-Boltzmann Law

Guyton (2000) defines thermal radiation as "electromagnetic radiation emitted from the surface of an object due to its temperature." The Stefan-Boltzmann equation is applied to explain a radiation process for the temperature and the object's area. According to Stefan-Boltzmann law, the heat quantity depends on the fourth power of radiation temperature and heat transport is influenced by the radiation wavelength and by absorption of the material (Wilhelm, Hilmar, & Walter, 2006). The heat flow due to radiation is directed by the temperature difference between the heat emitter and the heat absorber (Saville, 1999). When the infra-red radiation enters the fabric it is either scattered or absorbed by the fibers. The fibers emit radiation which moves to the adjacent fiber and so on until it reaches the far surface of the fabric. Therefore the heat transfer from radiation between the body and the external environment depends on the absorption and emission properties of the fibers of

clothing systems (Saville, 1999). The heat flow due to radiation through a fabric can be predicted if the temperature profile is known, the following equation is used:

$$Radiative\ conductivity = \frac{8\sigma T^3 R}{f\varepsilon}$$

where σ is the Stefan-Boltzmann constant ($5.67\ X\ 10^{-8} W/m^2K^4$), ε is the thermal emissivity, R is the radius of fibers, T is the mean temperature between heat source and sink (K), f is the fractional fiber volume (Saville, 1999). The heat loss from radiation is higher at low fiber volumes (less than 5%) but is reduced by the use of fine fibers and higher fiber volumes (Farnworth, 1983; Saville, 1999). This equation is most useful at the center of a thick fabric sample but, may not be suitable to predict the conductivity due to radiation at the edges of a fabric (Saville, 1999).

2.7. Theoretical Background of Moisture Transport

The moisture transport process is attached to the heat-transfer process. Heat transfer (radiation, convection, conduction, and evaporation) through clothing responds to a human body in the microclimate. To maintain comfort, clothing systems should allow moisture in the form of sensible and insensible perspiration (Parsons, 2003) to be dispersed from the body to the environment in order to cool the body and help prevent moisture from degrading the thermal insulation of the fabric. Moisture (liquid or vapor) can be transferred through textile layers by different processes: diffusion, absorption-desorption and forced convection (Das, Kothari, Fangueiro, & Araujo, 2007b).

2.7.1. Water Vapor Diffusion

Water vapor may pass through textile layers by any of the following methods: diffusion of the water vapor through the layers; absorption, transmission and desorption of the water vapor by the fibers; adsorption and migration of the water vapor along the fiber surface; and transmission of water vapor by forced convection (Das, Kothari, Fangueiro, & Araujo, 2007b). Vapor is diffused across a fabric's surface in response to a difference in the pressure gradient. The diffusion process through a porous material is governed by Fick's law which consists of two theories:

1. The flux of a component of concentration across a membrane of unit area is proportional to the concentration differential across that plane as shown by the equation (Ostwald, 1891):

$$J = D_A \frac{\partial \emptyset}{\partial x}$$

2. The rate of change of concentration is proportional to the concentration gradient at that point in the membrane (Ostwald, 1891).

$$\frac{\partial \emptyset}{\partial x} = D_A \frac{\partial^2 \emptyset}{\partial x^2}$$

Where J is the diffusion flux in dimensions ($\frac{mol}{m^2 * s}$), D is diffusion coefficient or diffusivity in dimension ($\frac{m^2}{s}$), $\emptyset$is the concentration in dimensions ($\frac{mol}{m^3}$), x is the position, and t is the time. Essentially, the first law characterizes the diffusion change from regions of high concentration to regions of low concentration and the second law describes the rate of accumulation of concentration in the material volume (Ostwald, 1891).

Fick's law can also be represented as one equation as shown:

$$J_{Ax} = D_{AB} \frac{dC_A}{d_x}$$

where J_{Ax} in $g\ cm^{-2}\ sec^{-1}$ is the rate of moisture flux, $\frac{dC_A}{d_x}$ is the concentration gradient, and D_{AB} is the diffusion coefficient. Water vapor can diffuse through a fabric structure either by diffusion through the air spaces between the fibers and yarns or along the fiber itself (Fohr, Couton, & Treguier, 2002). When water vapor diffuses along the fiber, it travels from the inner surface of the fabric moving outward along the fibers finally reaching the outer fabric surface (Das, Kothari, Fangueiro, & Araujo, 2007b). The diffusion rate of the textile material at a specific concentration gradient depends on the porosity of the material and the water vapor diffusivity of the fiber. The diffusion coefficient of water vapor through air is 0.239 cm^2/sec and through a cotton fabric is around $10^{-7}$$cm^2$/sec (Das, Kothari, Fangueiro, & Araujo, 2007b). Moisture diffusion through the air portion of the fabric happens very rapidly, but diffusion through clothing is limited by the rate at which moisture can diffuse into and out of fibers. Diffusion through hydrophilic fibers does not obey Fick's law instead this process follows anomalous diffusion (Das, Kothari, Fangueiro, & Araujo, 2012).Water vapor diffuses through the hydrophilic fibrous system and is absorbed by the fibers causing the fibers to swell which reduces the size of the air spaces between fibers deterring the diffusion process (Pause, 1996).

Moisture diffusion through textile material can be influenced by different factors. Diffusion will decreases with an increase in fiber volume as a fraction of the material because the fraction of the material structure made up of air decreases (Das, Kothari,

Fangueiro, & Araujo, 2007b). Moisture diffusion through the fabric also decreases with an increase in fabric thickness because the porosity of the material is reduced (Li, Zhu, & Yeung, 2002). According to Wang, Wang, and Yasuda, 1991, water vapor diffusion is highly dependent on the air permeability of the fabric, permeability increases as the porosity of the fabric increases. As mentioned previously, the application of special finishes can change the surface energy of the fabric causing the material to be hydrophilic or hydrophobic, yet the finishes have virtually no effect on the diffusion process (Wang, Wang, & Yasuda, 1991). The diffusion coefficient of water vapor in air can be given as a function of temperature and pressure by the following equation:

$$D = \left[\frac{\theta}{\theta_0}\right]^2 \left[\frac{P_0}{P}\right]$$

where D is the diffusion co-efficient of water vapor in air (m^2/sec), θ is the absolute temperature (K), θ_0 is the standard temperature of 273.15 K, P is the atmospheric pressure, and P_0 is the standard pressure (Bar) (Jost, 1960). In most cases, the diffusion coefficient of fibers increases with an increase in the concentration of water in the fibers with the exception of highly hydrophobic polypropylene (Ren & Ruckman, 2003).

2.7.2. Moisture Sorption-Desorption

In the absorption-desorption process the fabric works as a moisture source to the atmosphere and helps maintain constant vapor concentration in the surrounding air (Das, Kothari, Fangueiro, & Araujo, 2007b; Wehner, Miller, & Rebenfeld, 1988). Hygroscopicity is the moisture absorption capacity of fibers where the more moisture a fiber can absorb the more hygroscopic the fiber (Hatch, 1993). A hygroscopic fabric can absorb water vapor held close

to the perspiring body and then release it in to the atmosphere (Das, Kothari, Fangueiro, & Araujo, 2007b). The amount of moisture that a fiber contains in a specific environment, temperature, and humidity is called the regain or equilibrium water content which is calculated as a percentage of dry weight.

2.7.3. Wicking and Wetting

Wicking is a term used very often to describe when a fabric takes up liquid although the driving pressure gradient is zero or negative. Wetting of textile fibers is the displacement of fiber and air (vapor) interface with fiber and liquid interface (Kissa, 1996). Wicking is described as spontaneous flow of a liquid in a porous substrate, driven by capillary forces. Wickability is the ability of a material to sustain capillary flow, while wettability describes the initial behavior of the material when brought into contact with water (Harnett & Mehta, 1984). While wetting and wicking are separate occurrences, they can be described by a single process where liquid flows in response to capillary pressure. The capillary forces that result in wicking are caused by wetting; therefore the two are coupled together (Kissa, 1996). Researchers Yoo & Barker used the Hagen-Poiseuille law to describe the effect called "demand wettability." Hagen-Poiseuille law attempts to explain laminar flow in an idealized tubular structure (S. Yoo & Barker, 2004). This law states the volumetric flow rate is proportional to the pressure drop gradient along the tube:

$$\frac{dV}{d_t} = \left(\frac{\pi R_c^4}{8\eta}\right)\frac{\Delta \mathrm{P}}{L}$$

where η is the fluid viscosity, L is the length of the tube or capillary, and ΔP is the net driving pressure. For horizontal spontaneous flow, the uptake rate is a function of the pressure

gradient ΔP and the pore size R_c (S. Yoo & Barker, 2004). Capillary pressure is the primary driving force responsible for the movement of moisture along a fabric. The magnitude of capillary pressure P_c can be expressed by the LaPlace equation:

$$P_c = \frac{2\gamma cos\theta}{R}$$

where γ is the liquid surface tension, θ is the contact angle of the liquid with the substrate, and R is the effective capillary radius. However, there exists an opposing gravity:

$$\Delta P_h = h_g \delta$$

where h is the height of elevation, δ is liquid density, and g is the accerleration due to gravity. Yoo and Barker have combined the Hagen-Poiseuille law with both the LaPlace and opposing gravity equations the result is similar to the Washburn Equation:

$$\frac{dV}{d_t} = \left(\left[\frac{2\gamma cos\theta}{R_c}\right] - h_g \delta\right)\frac{\pi R_c^4}{8\eta L}$$

The larger the pore size, the faster the rate of absorption by a fabric. A higher (cos θ) yields a better liquid uptake, and is affected by the surface tension. These two factors together are often called the 'Wettability Function" (γ cos θ) (S. Yoo & Barker, 2004).

2.7.4. Biomimicry of Moisture Management

Biomimicry or biological design is a concept that has been gaining a lot of attention related to nature's mechanisms for moisture management. The term has been defined as "a new science that studies nature's models and then imitates or takes inspiration from these designs and processes to solve human problems (Benyus, 1997)." Perhaps the most well-known application of Biomimicry in textiles is called the "lotus effect." Inspired by the extraordinary hydrophobic behavior the lotus leaf plant, researchers have made efforts to

reproduce this phenomenon through surface modification of textiles such as chemical and plasma finishes. Other research has tried to emulate the branching water transport system of plants using complex weave structures in which the yarns interchange from the bottom layer and the yarns for the top layer (Sarkar, Jintu, Szeto, & Xiaoming, 2009).

2.8. Coupled Heat and Moisture Transfer

The coupled heat and moisture transport of textile material has many implications in engineering and functional design of clothing systems. Heat transfer mechanisms in textiles include conduction by the solid material of the fibers, conduction by the air flow, radiation, and convection. On the other hand, liquid and moisture transfer mechanisms include vapor diffusion in the microclimate and moisture sorption by the fibers, evaporation, and capillary effects (Li, 2002). Extensive research on the subject of heat and moisture transfer through textile materials has been conducted such as: Gibson & Charmchi (1997), David & Nordon (1969), Henry (1939), Kondepudi (2008), Kyunghoon, Yangsoo & Chongyoup (2007), Li & Luo (1999), Li, Zhu & Luo (2001), Woodcock (1962), and Ye, Li & Sun (2010).

2.8.1. Woodcock

Woodcock (1962) describes the total heat transfer from the skin to environment through clothing with several equations and defines heat transfer from skin at any given temperature and ambient conditions. The following equation accounts for how thermal equilibrium can be maintained by an exchange between metabolic heat production and sweating:

$$H = \frac{0.309}{I}[(T_s - T_a) + i_m S(P_s - P_a)]$$

where, T_s is skin temperature; T_a is ambient temperature; I is insulation or thermal resistance of the clothing and the overlaying air layer; P_s is water vapor pressure at the skin boundary; P_a is water vapor pressure of environmental air; i_m is the permeability index, and S is the conversion factor which converts vapor pressure difference to an effective temperature difference. According to Woodcock (1962), the permeability index "supplies the missing parameter required for considering clothed man's thermal balance," the permeability index will be further discussed in section 2.10 of this paper.

2.8.2. Clausisus-Clapeyron

Kondepudi (2008) uses the Clausisus-Clapeyron Relation to explain the affect moisture vapor diffusion has on the temperature in the microclimate. Rudolf Clausius and Emlie Clapeyron define vaporization as a way of characterizing a discontinuous phase transition between two phases of matter, as shown in the equation:

$$\ln\left(\frac{P_1}{P_2}\right) = \frac{\Delta H_{vap}}{R}\left(\frac{1}{T_2} - \frac{1}{T_1}\right)$$

where T_1 and P_1 are mean temperature and vapor pressure at point 1, T_2 and P_2 are mean temperature and vapor pressure at point 2, ΔH_{vap} is the molar enthalpy of vaporization and R is the gas constant (8.314 $J\ mol^{-1}\ K^{-1}$). Clausius–Clapeyron determines the saturation vapor pressure and characterizes the transition between two phases of matter. The saturation vapor pressure is the equilibrium vapor pressure and the upper limit of the quantity of vapor that the atmosphere can hold and when this threshold is reached, no additional liquid can be evaporated (Koutsoyiannis, 2012). This equation is capable of calculating differences in enthalpy required to vaporize liquid when temperature can be predicted at a certain pressure.

2.9. Laboratory Test Methods

The testing of textile products for their ability to manage heat and moisture is very important and expensive. Heat and moisture management are properties related to the comfort associated with an actual end user experience of a garment; with that in mind humans are the ultimate test for these properties. However, it is not always feasible for a product to be tested on humans; for that reason various laboratory tests have been developed. A review of some of these tests is presented in the following sections. The table below shows a listing of the various instruments to test thermal and moisture management discussed within this paper along with the industry standard procedures for conducting these tests.

Table 2.2 Test Method and Related Industry Standard (if applicable, n/a is not applicable)

Method	**Industry Standard**
Cup Method	ASTM E 96 B Standard Test Methods for Water Vapor Transmission of Materials
Dynamic Moisture Permeation Cell	ASTM F 2298 Standard Test Methods for Water Vapor Diffusion Resistance and Air Flow Resistance of Clothing Materials Using the Dynamic Moisture Permeation Cell
Guarded Sweating Hotplate	ASTM F 1868 Standard Test Method for Thermal and Evaporative Resistance of Clothing Materials Using a Sweating Hot Plate ISO 11092 Measurement of thermal and water-vapour resistance under steady-state conditions (sweating guarded-hotplate test)
Sweating Manikin	ASTM F 2370 Standard Test Method for Measuring the Evaporative Resistance of Clothing Using a Sweating Manikin
Alambeta Instrument	n/a
Dynamic Surface Moisture Method	n/a
Human-Clothing-Environental Simulator	n/a
Moisture Management Tester	AATCC 195 Liquid Moisture Management Properties of Textile Fabrics
Wettability Test	ASTM D7334-08 Standard Practice for Surface Wettability of Coatings, Substrates and Pigments by Advancing Contact Angle Measurement
Vertical Wicking Test	AATCC 198 Horizontal Wicking of Textiles
Horizontal Wicking Test	AATCC 197 Vertical Wicking of Textiles
Gravimetric Absorbency Test System	n/a

2.9.1. Measuring Thermal Properties

Instruments that have been used to measure the thermal resistance of fabrics can be divided into two groups: steady state and transient measurement. The most common measurement is the thermal resistance in the steady state method (Bhattacharjee & Kothari, 2008). There are three types of instruments that have been most popular for measuring the thermal resistance of fabrics by the steady state method. First, the hot cylinder method which has many variations reviewed and summarized by Morris (1953). The hot semi-cylinder method was developed by Baxter and Cassie (1943) and provided a theory for measurements of thermal behavior based on Newton's law of cooling. The guarded hot plate method which is reviewed in Section 2.9.3 of this paper and the Shirley Togmeter are very similar in principle. Both devices are common steady-state methods of measurement for thermal properties. These instruments measure only the dry heat transfer of materials which is not the focus of this research.

2.9.2. Measuring Moisture Management

The ability to manage moisture is a vital for fabrics intended to be worn during vigorous physical activity, because the human body cools itself by sweat production and evaporation during periods of high activity. If a fabric does not allow pass sufficient perspiration to pass through this leads to sweat and moisture accumulation close to the skin and discomfort. This paper examines different instruments to test moisture management of fabrics including: cup method, dynamic moisture permeation cell (DMPC), gravimetric absorbency test system (GATS), dynamic surface moisture method, moisture management tester (MMT), and methods for measuring wetting and wicking.

Cup method

Introduction

The cup method is used for the measurement of water vapor permeability. This testing instrument measures the amount of moisture vapor in grams that pass through 1 m^2 of fabric in 24 hours with an air velocity of 2.8 m/s (550ft/min) applied to the fabric.

Apparatus Design

The cup method is used to measure the moisture vapor transmission rate of moisture vapor diffusion through the material in an ambient temperature between 29-30°C. This testing instrument measures the amount of moisture vapor in grams that pass through 1 m^2 of fabric in 24 hours with an air velocity of 2.8 m/s (550ft/min) applied to the fabric (Arabuli, Vlasenko, Havelka, & Kus, 2010). The fabric is sealed over the open mouth of a cup containing water and placed in the standard testing atmosphere. Each cup is filled with sufficient distilled water to give a 19mm (0.75 in) air gap between the water surface and the fabric. Self-adhesive plastic tape secures the mouth of the cup. The weight of each cup is checked within 0.1 mg as time passes (Arabuli, Vlasenko, Havelka, & Kus, 2010). According to ASTM E 96, the cup method can be carried out in two additional ways other than the method just described. The experiment is sometimes carried out with the cup inverted so that the water is in contact with the inner surface of the fabric which is used more often with hydrophilic films. The other procedure is called the desiccant method where the test cup is filled with a dry calcium chloride or a silica gel rather than water (Arabuli, Vlasenko, Havelka, & Kus, 2010). The figure below demonstrates the desiccant method (*a.*), distilled water method (*b.*), and inverted water method (*c.*).

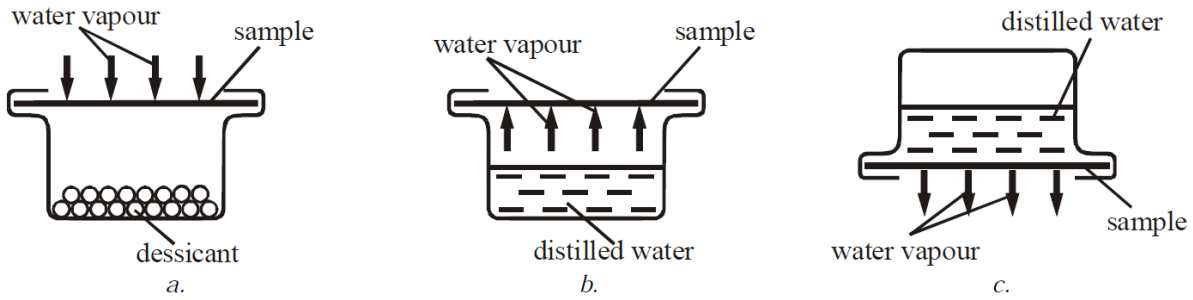

Figure 2.7 The desiccant method (a.), water method (b.), and inverted water method (c.)

Source: Arabuli, S., Vlasenko, V., Havelka, A., & Kus, Z. (2010). Analysis of modern methods for measuring vapor permeability properties of textiles. 7th International Conference - TEXSCI 2010, Liberec, Czech Republic.

Results and Analysis

Arabuli et al. (2010) conducted an analysis on the cup method and found that the water and desiccant methods measure water vapor permeability at a level for low physical activity (low sweating) adequately, but does not give the information about condensation on the fabric's surface. These methods measure the lack of vapor permeability depending on the properties of the material and also the thickness of the material (Arabuli, Vlasenko, Havelka, & Kus, 2010).

Significances of the Method

The cup method measures water vapor permeability of the sample by comparing it with a reference fabric using the following equation:

$$WVTR = \frac{G/t}{A}$$

where WVTR is the rate of water vapor transmission ($gh^{-1}m^{-2}$), G is the weight change (g), t is the time during which G occurred (h), G/t is the slope of the straight line (weight loss per unit time, (gh^{-1}), and A is the test area (m^2). Havenith (2002) discusses potential human

errors that can be made conducting the experiment, and that the test includes external environments. One must consider the amount of time it takes to perform this test and that the results of this test are recorded manually at each weighing interval. In addition, Hes and McCullough (2004) found that these testing instruments and methods require a lengthy period of time to achieve an accurate result. Perspiration emitted from the body is dynamic but this test measures moisture in a steady condition which renders the results inaccurate to measure the level of moisture management function of the fabrics (Dionne, Semeniuk, & Makris, 2003; Easter & Ankenman, 2006).

Dynamic Moisture Permeation Cell (DMPC)

Introduction

The purpose of the dynamic moisture permeation cell (DMPC) instrument is to measure the water vapor diffusion resistance and moisture vapor transmission rate. This device was devolved by Gibson et. al (1995). The test method associated with this apparatus is the ASTM F 2298, Standard Test Methods for Water Vapor Diffusion Resistance and Air Flow Resistance of Clothing Materials Using the Dynamic Moisture Permeation Cell (Huang & Qian, 2008; McCullough, Kwon, & Shim, 2003).

Apparatus Design

The DMPC device is designed so that a mixture of dry and water-saturated nitrogen can stream over the top and bottom surfaces of the test sample. The test sample is mounted between two metal plates clamped tightly by two flow cells with the inner side of the fabric facing the higher relative humidity. The nitrogen streams through the ducts of the flow cells and onto the test specimen (Gibson, Kendrick, Rivin, Charmchii, & Sicuranza, 1995; Huang

& Qian, 2008; McCullough, Kwon, & Shim, 2003). The computer system controls the flow achieving the desired relative humidity in the upper and lower streams entering the testing apparatus. The relative humidity of the nitrogen streams entering and exiting the cells is measured by sensors and the pressure gradient across the sample is also monitored. The computer calculates the water vapor diffusion resistance every minute and when the test reaches steady state conditions an average is calculated (Gibson, Kendrick, Rivin, Charmchii, & Sicuranza, 1995; Huang & Qian, 2008; McCullough, Kwon, & Shim, 2003).

Results and Analysis

McCullough, Kwon, and Shim (2003) conducted a study to measure the water vapor permeability and evaporative resistance of 26 different waterproof, windproof and breathable shell fabrics using five standard test methods including: desiccant method, inverted cup method, upright cup method, dynamic moisture permeation cell (DMPC), and the sweating hotplate test. The researchers concluded that the results from different tests were not comparable because, the magnitude water vapor permeability and evaporative resistance varied with the test method, and material (McCullough, Kwon, & Shim, 2003). Huang and Qian (2008) conducted a study to compare the testing results of the desiccant method, inverted cup method, upright cup method, dynamic moisture permeation cell (DMPC), and the sweating hotplate test with a new testing apparatus. Their analysis shows the results of the new test method being highly correlated with the other test method results with the exception of the upright cup method (distilled water method b., Figure 3.1) (Huang & Qian, 2008).

Significances of the Test

The dynamic moisture permeation cell (DMPC) instrument calculates the water vapor diffusion resistance of the test sample from the measurement of the relative humidity of the entering nitrogen flows and the exiting nitrogen flows, temperature, and gas flow rate. The following equation is used to calculate the water vapor diffusion resistance:

$$R_{dtot} = \frac{A(\Delta\phi)}{Q(\delta\phi)} = \frac{\Delta C}{\dot{m}}$$

where R_{dtot} is the total water vapor diffusion resistance (m^2), A is the area of test sample (m^2), $\Delta\phi$ is the relative humidity difference between top and bottom incoming streams, Q is the volumetric flow rate through top or bottom portion of the cell ($m^3 s^{-1}$) at the actual test temperature T , $\delta\phi$ is the relative humidity difference between incoming stream and outgoing stream in the bottom part of the test apparatus, $\dot{m}$ is the mass flux of water vapor across the specimen ($kgm^{-2}s^{-1}$), and ΔC is the log of the mean concentration difference between top and bottom nitrogen streams ($kgm^{-2}s^{-1}$) (Gibson, Kendrick, Rivin, Charmchii, & Sicuranza, 1995; Huang & Qian, 2008; McCullough, Kwon, & Shim, 2003).

Gravimetric Absorbency Test System

Introduction

The purpose of this instrument studies is to study moisture vapor transmission rate (MVT), which measures wettability of the fabric through absorbency rate, absorbency capacity, and evaporation rate (S. Yoo & Barker, 2005). This testing instrument is also able to measure the drying rate of the fabric which is correlated with the relative humidity of microclimate between the fabric and the skin (Laing, 2007). The method measures how much liquid

moisture by weight is taken away from a simulated skin surface in a given amount of time (Barker, 2002).

Apparatus Design

The (GATS) involves several devices, including capillary pressure head controller, cover with pins, frictionless bearing, and porous plate. Liquid is fed to a porous plate which has the ability to appropriately distribute it into the fabric. The cover with pins helps to distribute capillary forces generated from the pressure head controller evenly and the pins reduce the space between porous plate and fabric (Das, Kothari, Fangueiro, & Araujo, 2007b). To conduct the wettability test, the sample fabric is placed on the porous plate and the head controllers apply pressure. Figure 2.8 shows a schematic diagram of the gravimetric absorbency testing system.

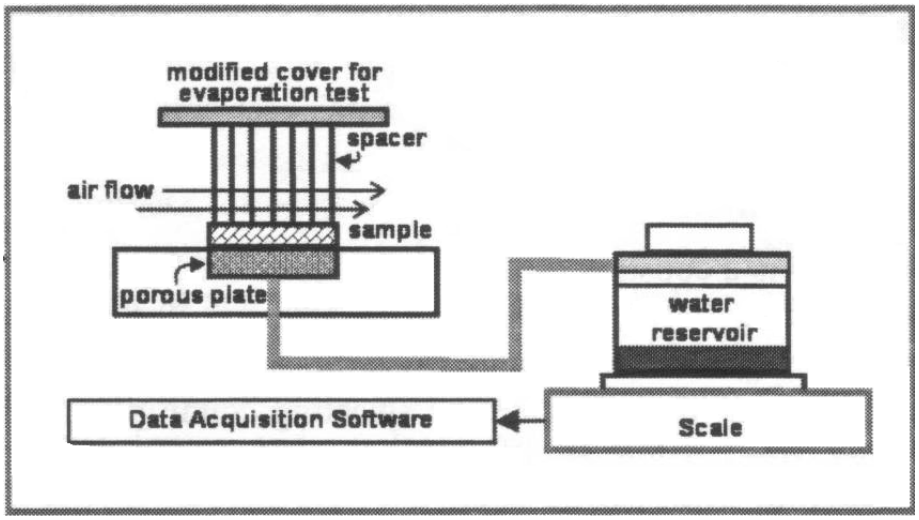

Figure 2.8: Schematic of the GATS instrument

Source: Yoo, S., & Barker, R. L. (2005). Comfort properties of heat-resistant protective workwear in varying conditions of physical activity and environment. Part I: Thermophysical and sensorial properties of fabrics. Textile Research Journal, 75, p. 523-53.

Results and Analysis

Kim et al. (2003) used this device to determine the absorption characteristics of pile and non-pile fabrics used as towels and wiping clothes from their properties of weight, density, thickness, pore size and fineness (S. H. Kim, Lee, Lim, & Jeon, 2003). A study conducted by Yoo et al (2005) used the GATS method to determine the absorption capacity, instantaneous rate of absorption, and evaporation/absorption ratio for different workwear fabrics. Liang et al. (2007) conducted experiments using GATS instrument to determine the absorptive capacity of different 100% wool knit fabrics structures shown in the table below:

Table 2.3 Fabric codes and descriptions of fabrics tested

Fabric code	Description/ structure	Fiber content 100%	Micron	Mass* (n = 5) g/m^2	Thickness (n = 5) mm	Bulk density (n = 5) g/cm^3	Yarn/stitch density[a] (n = 5) per 10 mm
KIA	Interlock	wool	18.5/19	230.88	1.15	0.201	15 × 16
KMA	Milled fleece W 405	wool	21/22	330.32	2.20	0.150	NA
KRA	Rib 3118	wool	21/22	219.28	1.12	0.196	18 × 15
KSA	Single jersey 3170	wool	21/22	356.20	1.24	0.287	9 × 12
KSC	Single jersey 3090	wool	18.5/19	150.92	0.68	0.222	20 × 19
KSD	Single jersey W3029	wool	18.5/19	197.46	0.80	0.247	15 × 16
WPA	Woven	polyamide	NA	68.41	0.14	0.488	43 × 38

[a]Wales/courses; warp/weft.
NA, not available.

Source: Laing, R. M., Niven, B. E., Barker, R. L., and Porter, J. (2007). Response of Wool Knit Apparel Fabrics to Water Vapor and Water, Textile Research Journal, 77, p. 165–171.

The GATS testing was appropriate for all the fabrics in the study except for the milled wool knit (KMA) which resisted absorption during the specified exposure time for the test. Results from the GATS test for these fabrics are shown in the table below:

Table 2.4 Results from the GATS test for the fabric codes

Test state		Fabric code KIA	KRA	KSA	KSC	KSD
Total water absorbed (g)	Mean	5.246	5.105	4.791	2.735	3.222
	s.d.	0.1207	0.0922	0.1837	0.1168	0.0582
Total water absorbed standardized for dry fabric weight (g /g)	Mean	3.600	3.617	2.160	2.850	2.506
	s.d.	0.0704	0.0453	0.0883	0.1328	0.0572
Q(Norm) standardized flow rate	Mean	1.007	1.289	2.070	0.322	0.272
	s.d.	0.0095	0.2715	0.4551	0.0165	0.0374
Evaporation (%)	Mean	16.68	17.25	17.72	26.11	22.72
	s.d.	1.0020	1.1692	3.2234	2.8302	2.8200

Source: Laing, R. M., Niven, B. E., Barker, R. L., and Porter, J. (2007). Response of Wool Knit Apparel Fabrics to Water Vapor and Water, Textile Research Journal, 77, p. 165–171.

Significances of the Method

The Gravimetric Absorbency Testing System (GATS) measures the ability of fabric to transport moisture away from the skin based on the theoretical principles of the Washburn Equation discussed in a previous section of this paper. The mechanism of this machine is to measure how much liquid moisture by weight can be taken away from a simulated skin surface in a given amount of time (Barker, 2002). This machine performs a demand wettability test, and allows fabric to simulate being on a constantly sweating skin surface, which sets it apart from other tests that determine the moisture wicking properties of a fabric when exposed to a finite and static amount of moisture. The GATS measures the fabric's ability to transport a continuously replenished moisture supply over a period of time (Barker, 2002) but, it should be noted that the milled wool fabric could not be tested.

Dynamic Surface Moisture Method

Introduction

The Dynamic Surface Moisture method was developed by Scheurell & Spivak (1985) to measure the movement of moisture through the fabric by adding cobalt chloride to the fabric before wetting and evaluating the color change that ensues with the Munsell Hue color index system. Cobaltous chloride forms hydrates with water which can take on colors ranging from blue monohydrate to pink hexahydrate (Scheurell, Spivak, & Hollies, 1985).

Apparatus Design

The testing apparatus includes a wet chamois simulating sweating skin, a hot plate representing human body temperature, and the cobalt chloride paper which indicates the moisture management of the fabric. Figure 2.9 is a schematic of the Dynamic Surface Moisture Device.

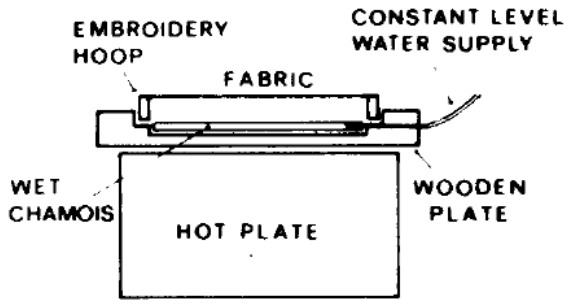

Figure 2.9: Schematic of the Dynamic Surface Moisture Device

Source: Scheurell, D.M.; Spivak, S.M. and Hollies, N.R. (1985). Dynamic Surface Wetness of Fabrics in Relation to Clothing Comfort. Textile Research Journal, (55) p. 394-399.

Results and Analysis

Cao, Wu, and Chen (2011) analyze the relationship between the dynamic surface wetness values from the Munsell Color Index and the static fabric pressure of the tight pants by creating a stepwise regression model. The research concluded that the static garment pressure of the stretch knitted pants had some relationship with dynamic surface wetness. The table below shows the Munsell values recorded from the garments tested in this study.

Table 2.7 Munsell Index of fabrics tested

Fabrics		Experimental time (min) ／Munsell color index						
		0	5	10	15	20	25	30
1.	95%C+5%S	2	2	2	2	2	2	3
2.	95%C+5%S	2	2	2	2	3	3	3
3.	95%C+5%S	2	2	2	2	2	3	3
4.	93%C+7%S	2	2	2	2	2	3	3
6.	94%C+6%S	3	5	5	5	6	6	7
7.	90%T+10%S	3	5	6	7	8	8	8
8.	88%T+12%S	3	4	5	6	6	7	7
10.	100%DTY	3	5	5	6	6	7	7
12.	95%N+5%S	2	2	2	2	2	2	2
13.	87%C+13%S	2	2	2	2	2	2	2

Source: Cao, Wu, and Chen (2011). The Stepwise Regression Model between Munsell Color Index and Clothing Pressure of Knitted Tight-Fit Sports Pants. Applied Mechanics and Materials. 58-60, p. 243-248.

Wu, Cao, and Chen (2011) conduct a study using the dynamic surface moisture method to measure dynamic permeability characteristics of 44 kinds of knitted fabrics. The researches analyze the relationships between complete label HV/C value of Munsell color space and the moisture content (Wu, Cao, & Chen, 2011). The research concludes that existing methods of testing dynamic surface moisture only include the Munsell color index evaluating dynamic

while omitting the Munsell color value and Chroma were not as comprehensive as a method considering the complete Munsell color HV/C value to establish a composite indicator of evaluation dynamic surface moisture transfer (Wu, Cao, & Chen, 2011).

Significances of the Test Method

The color of the cobaltous chloride and the fabric on which it is held is indicative of the quantity of moisture at the fabric surface at any given time. The method continuously measures the local level of moisture within the fabric while other steady state methods measure the water vapor diffusion through fabrics (Scheurell, Spivak, & Hollies, 1985).

Moisture Management Tester

Introduction

This testing instrument is developed by Hu et. al (2005) and measures liquid moisture transport ability affecting the moisture sensation of the human comfort perception. It evaluates the moisture management functionality of the fabric by comparing quantitative information of the liquid moisture transfer of a fabric in multiple directions and human subjective perceptions of moisture sensations during exercise (Hu et. al, 2005).

Apparatus Design

This testing instrument takes advantage the electric resistance of fabric. Figure 2.10 shows the portion of the MMT where a fabric sample is held flat by top and bottom copper ring sensors. Next, the perspiration solution is introduced onto the fabric by the sweat gland.

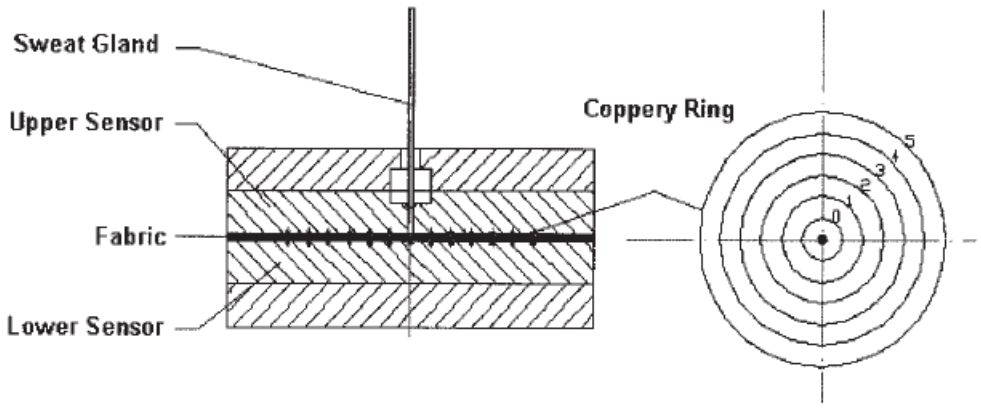

Figure 2.10: Schematic of the top and bottom copper ring sensors

Source: Hu, J., Li, Y., Yeung, K. W., Wong, A. S. W., Xu, W. (2005). Moisture Management Tester: A Method to Characterize Fabric Liquid Moisture Management Properties.

A computer program records the resistance change between each couple of neighboring copper rings individually at the top and lower sensors (Hu et. al, 2005). As a result of the experiment, the researcher is able to obtain the following parameters for both the bottom and the top side of the fabric: moisture absorption rate, spreading speed, maximum spreading radius, and one way liquid transport ability. From these parameters, researchers can infer the overall moisture management capacity ($OMMC$) using the moisture absorption rate of the bottom side (MAR), one-way liquid transport ability ($OMTC$), and moisture drying speed of the bottom side (SS) as shown in the equation below:

$$OMMC = C_1 MAR + C_2 OMTC + C_3 SS$$

where C_1, C_2, and C_3 are weighted values MAR, $OMTC$ and SS that can be determined by the experimenter according to end use of the fabric (Hu et al., 2005).

Results and Analysis

Supuren, Oglakcioglu, Ozdil and Marmarali (2011) conducted a study using the MMT device to investigate the moisture management properties of the double face knitted fabrics. The study used cotton–cotton, cotton–polypropylene, polypropylene–cotton, and polypropylene–polypropylene for face and back sides respectively. The study found that when polypropylene was used on the inside and cotton was for the outer shell fabric has better moisture management properties (Supuren, Oglakcioglu, Ozdil and Marmarali, 2011). The table below shows the overall moisture management capacity (OMMC) values of test fabrics.

Table 2.4 OMMC values of the test fabrics

	PP (inner)-PP (outer)	PP (inner), Co (outer)	Co (inner), PP (outer)	Co (inner)-Co (outer)
OMMC values	0.1111	0.5806	0.0244	0.2230
Moisture management category	Very poo r	Good	Very Poor	Poor

0–0.2: very poor, 0.2–0.4: poor, 0.4–0.6: good, 0.6–0.8: very good, >0.8: excellent.[21]
Co: cotton, PP: polypropylene.

Source: Supuren, G., Oglakcio, N., Ozdil, N., and Marmarali, A. (2011). Moisture management and thermal absorptivity properties of double-face knitted fabrics. *Textile Research Journal, 81*(13) p. 1328.

Troynikov & Wardiningsih (2011) studied the liquid moisture management properties of single jersey knitted fabrics of different wool/polyester and wool/bamboo blends of different ratios using the MMT device. The results of the study show that blending wool with polyester or wool with rayon improves moisture management properties (Troynikov & Wardiningsih, 2011).

Significances of the Method

This method is based on the principle that when moisture is introduced to a fabric it changes the contact electrical resistance and the value of the resistance changes depending on the components of the water and the water content in the fabric (Hu et al., 2005). The water content of the fabric (top and bottom) can be determined by the following equations:

$$U_t = \sum_{i=0}^{5} M_{ti} \text{ and } U_b = \sum_{i=0}^{5} M_{bi}$$

where U_t is the total water content on the fabrics top surface, U_b is the total water content on the fabric's bottom surface, and M_{ti} and M_{bi} are the water content in the area between the each couple of the copper rings at the top and bottom testing surfaces, which can be calculating by the following equation:

$$M = \frac{1}{AR_c}\frac{V_1}{V_0 - V_1}$$

where M is the moisture content which is positively and linearly related to $\frac{V_1}{V_0 - V_1}$, that is the voltage (V) principle used to measure the moisture content in the fabric, A is found from the relationship between R_f (the resistance of the fabric) and M for the individual rings, and R_c is the resistance of the resistor (Hu et. al, 2005).

Additional Methods of Measuring Moisture Management in Fabrics

Wettability Test

As stated, wicking properties are dependent upon the wettability of the fiber used to construct the fabric. A method used determine the wicking properties of fibers in a fabric is conducted by applying a water droplet to the fabric in order to measure the contact angle between a

drop of water and the plane of the fabric. ASTM D7334-08, Standard Practice for Surface Wettability of Coatings, Substrates and Pigments by Advancing Contact Angle Measurement, contains the procedural guidelines to conduct this type of test. According to ASTM D7334-08, if the contact angle is small the fabric will exhibit wicking properties but, a larger contact angle suggests the fabric will resist wicking away moisture. Figure 2.11 shows the contact angle of a water droplet test (left) with a large contact angle, and a water droplet test (right) with a smaller contact angle.

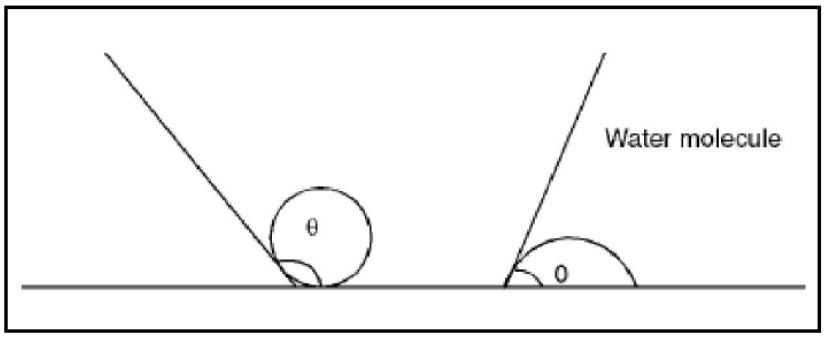

Figure 2.11: The contact angle of a water droplet test (left) with a large contact angle, and a water drop let test (right) with a smaller contact angle

Source: Ramachandran, T., & Kesavaraja, N. (2004). A study on influencing factors for wetting and wicking behaviour. Journal of the Institution of Engineers: Textile Engineering Division, 84, p. 37-41.

Vertical Wicking Test

The Vertical Wicking Test AATCC 197 is a method to measure the rate (distance per unit of time) liquid travels along and through a vertical fabric specimen by visually observation. This observation is manually timed and recorded at specified intervals. The measurement can be taking by recording the amount of time taken to reach a given distance or the

recording the distance travelled at a given time. Vertical wicking rate is calculated by dividing the wicking distance by the wicking time using the following equation:

$$W = d/t$$

where W is the wicking rate (mm/s), d is the distance (mm), and t is the wicking time (s). The Figures 2.12 and 2.13 show the specific distances (mm) marked on the sample fabric and the configuration for insertion of the test strip the opening of an Erlenmeyer flask containing liquid.

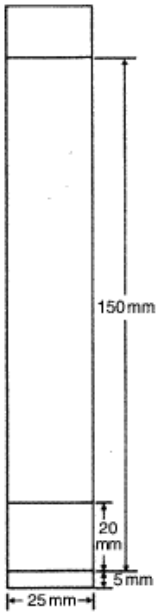

Figure 2.12: Vertical Alignment Configuration

Source: AATCC (2012). Test Method 197-2011 Vertical Wicking of Textiles, American Association of Textile Chemists and Colorists Technical Manual Research Triangle Park, N.C. p. 373-375.

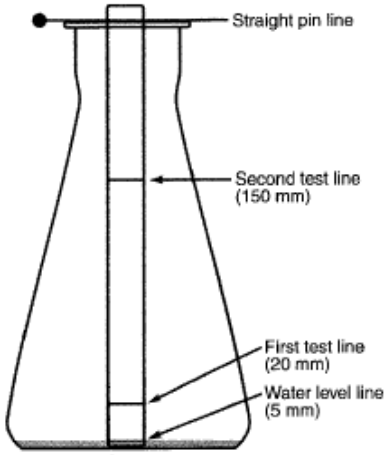

Figure 2.13: Marked Vertical Wicking Test Sample

Source: AATCC (2012). Test Method 197-2011 Vertical Wicking of Textiles, American Association of Textile Chemists and Colorists Technical Manual Research Triangle Park, N.C. p. 373-375.

Horizontal Wicking Test

The Horizontal Wicking Test AATCC 198 is a method measure the rate (area per unit time) liquid spreads over the test sample by visual observation which is manually timed and recorded a specified time intervals. The horizontal wicking rate should be calculated for five samples and then averaged. The equation for calculating the horizontal wicking rate is as follows:

$$W = \pi(1/4)(d_1)(d_2)/t$$

where W is the wicking rate ($mm2/s$), d_1 is the distance in the length direction (mm), d_2 is the distance in the width direction (mm), and t is the wicking time (s). The figure below shows the configuration where a burette distributes liquid to the sample fitted over an embroidery hoop.

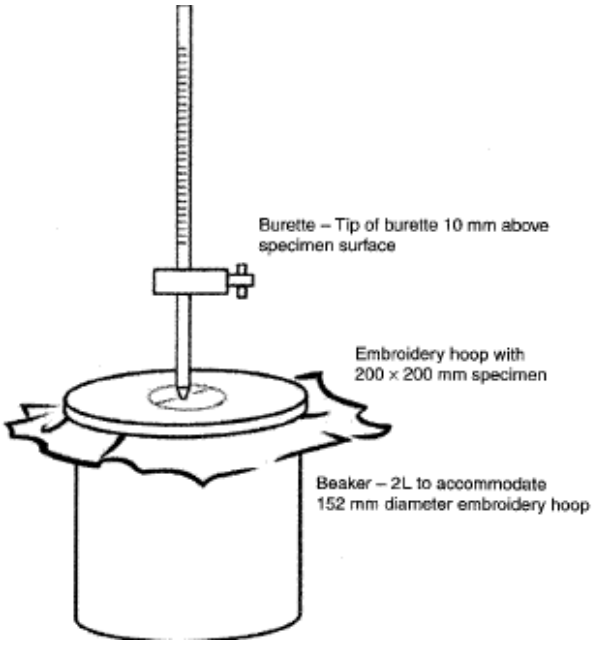

Figure 2.14: Horizontal Alignment Test Configuration

Source: AATCC (2012). Test Method 198-2011 Horizontal Wicking of Textiles, American Association of Textile Chemists and Colorists Technical Manual Research Triangle Park, N.C. p. 376-379.

2.9.3. Measuring Heat and Moisture Management Properties

It is understood that some of these tests also measure the heat resistance properties of fabrics and that thermal and evaporative resistance properties are linked together in terms of both physiological and sensational comfort. The area of moisture management to increase fabric comfort has been a subject of investigation giving rise to various recognized testing instruments and testing codes. These testing codes describe detailed testing procedures, conditions of the sample fabrics, and test instruments but also define moisture management as water vapor transmission (WVT), water vapor permeability (WVP), or water vapor resistance (Milenkovic & Skundric, 1999).

Alambeta Instrument (Permetest Model)

Introduction

Alambeta testing instrument designed by Lubos Hes, proposes to measure the water vapor permeability while improving on other testing instruments in terms of time consumption and testing costs (Hes, Bernardo, & Queirós, 1996). The determination of water vapor permeability is based on the measurement of the heat of evaporation (Hes, Bernardo, & Queirós, 1996). The Alambeta testing instrument measures water vapor permeability along with thermal resistance, and thermal conductivity with a relatively short testing time.

Apparatus Design

The Alambeta Permetest instrument has two compartments with different water vapor partial pressures separated by polymer film; the amount of liquid is measured exiting the chamber with the higher partial pressure which corresponds to saturation conditions (Hes, Bernardo, & Queirós, 1996). The figure below shows where within the instrument the heat of evaporation is measured by a direct heat flow sensor (1) in which a side of the sensor is embedded in the metal base (2), and the other side of the sensor is immersed in liquid (3) (Hes, Bernardo, & Queirós, 1996). A grid (4) supports the film which is exposed to air flow and the grid closes the measuring compartment (5). The nozzle (6) feeds the air flow to the film at a fixed humidity (Hes, Bernardo, & Queirós, 1996). Liquid is introduced into the measuring compartment onto the surface of the sensor and is kept uniform by the grid. As the liquid evaporates it diffuses through the film and to the outer layer and a temperature gradient (ΔT) develops along the sensor. The output voltage U (mV) that is proportional to the heat flux q (W/m^2) corresponds to the water vapor flow (Hes, Bernardo, & Queirós, 1996).

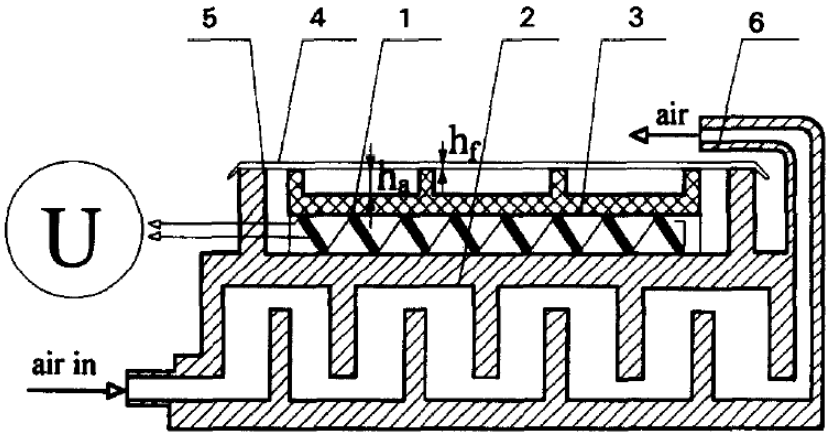

Figure 2.14 Schematic of the Alambeta Permetest instrument

Source: Hes, L., Bernardo, C. A., & Queirós, M. A. (1996). A new method for the determination of water-vapour permeability of polymer films based on the evaluation of the heat of evaporation. Polymer Testing, 15(2), p. 189-201.

Essentially, the Alambeta instrument measures the dynamic heat flow caused by the evaporation of water passing through the tested specimen, and the relative water vapor permeability is the ratio of the heat loss measured of the sample versus no sample (Tzanov, Betcheva, & Hardalov, 1999).

Results and Analysis

Tzonov et al. (1999) studied the effect of the aminofunctional silicone softeners on heat and moisture transport properties using the Alambeta instrument. Table 2.6 shows a comparison of the results for the study's untreated samples. The results show that dyed sample has higher thermal conductivity (λ) and absorptivity (b), and the amount of heat flow (q) between the instrument's measuring sensor and the sample is greater, while the thermal resistance and sample thickness are lower (Tzanov, Betcheva, & Hardalov, 1999).

Table 2.6 Comparison of untreated samples water vapor permeability

Sample	$\lambda_{(CV)} \times 10^3$ $[W/m.K]$	$b_{(CV)}$ $[W.\sqrt{s}/m^2.K]$	$r_{(CV)} \times 10^3$ $[K.m^2/W]$	$h_{(CV)}$ $[mm]$	$q_{(CV)}$ $[W/m^2]$	Water-vapour permeability (per cent)
Undyed, unthermoset	$65.1_{(1.3)}$	$333_{(2.9)}$	$6_{(1.8)}$	$0.39_{(1.9)}$	$1.49_{(2.5)}$	22.81
Dyed, thermoset	$70.4_{(1.4)}$	$400_{(3.1)}$	$5.3_{(1.5)}$	$0.37_{(1.7)}$	$1.7_{(2.4)}$	18.58

Source: Tzanov, Tzanro; Betcheva, Rossitza; Hardalov, Iva. (1999). Thermophysiological comfort of silicone softeners-treated woven textile materials. International Journal of Clothing Science and Technology, 11 (4), p. 189-197.

The study concluded that that silicone treatment to the PES blended fabrics made them better heat insulators but reduced the water-vapor permeability or breathability (Tzanov, Betcheva, & Hardalov, 1999). Gorjanc, Dimitrovski, and Bizjak (2012) conducted a study using the Permatest method along with the cup method to determine the influence on the thermal and water vapor resistance of cotton fabrics when elastane (Spandex) was added to the weft direction of the woven structure. The research concluded that cotton fabrics in twill weave structures with elastane in the weft direction have higher thermal and evaporative resistance than conventional cotton fabrics (Gorjanc, Dimitrovski, & Bizjak, 2012).

Significances of the Test Method

The Alambeta Permetest method measures the relative water vapor permeability of the textile in a steady state isothermal condition. The relative water vapor permeability (*RWVP*) the ratio (%) of heat lost when the fabric is placed on the measuring head to heat lost from the bare measuring head and is calculated by the following equation:

$$RWVP = \frac{u_s}{u_o} * 100$$

where u_s is the instrument reading without the test sample and u_o is the instrument reading of the wet measuring skin model with the test sample (Hes, 2009). This test appears to be able measure small differences in finishes as shown in the study by Tzonov et al. (1999).

Guarded Sweating Hotplate

Introduction

The sweating guarded hot plate instrument is designed to simulate heat and moisture transfer from the skin's surface through clothing material to the environment. The device measures thermal and evaporative resistance of fabrics which relate to comfort for the wearer of clothing.

Apparatus Design

Both ASTM F 1868 and ISO 11092 provide standard procedures for the assessment of heat and moisture transport through the fabrics by recording measurements of thermal and evaporative resistance. The apparatus consists of a heated test plate surrounded by a guard ring and with a bottom plate underneath. An inner heater and plate assembly is heated to 35 ºC to approximate human skin temperature (McCullough, Huang & Kim, 2004). The fabric is layered on top of the heated plate as it would be worn against the skin face cloth and the outer shell of the fabric is exposed to the outside set controlled environment of the testing apparatus. The guard ring and bottom plate are maintained at the same temperature as the test plate to ensure that no heat is lost apart from that which passes upwards through the fabric under test. The entire plate assembly is inside a test chamber that it set to keep the air at 25 ºC and 65% RH (McCullough, Huang & Kim, 2004). A fan system also located within the chamber is set to control air flow across the test sample. A computer measures the

amount of electrical power required to keep the plate at a constant temperature in steady state conditions which is proportional to heat or evaporative loss through the fabric system. The process is essentially the same for measuring evaporative as for measuring heat loss except there is liquid fed to the porous surface of the heated plate during the test for the evaporative loss test while the thermal resistance test is dry. A fluoropolymer membrane acts as a liquid barrier positioned on top of the plate to prevent water from wetting the fabric while allowing water vapor to evaporate through the fabric system (McCullough, Huang & Kim, 2004). Taking into account the thermal resistance of the particular fabric system, the new power requirement is related to the amount of water evaporating per unit time and the latent heat of vaporization (McCullough, Huang & Kim, 2004).

Results and Analysis

Prasham, Barker and Gupta (2005) used the guarded sweating hotplate along with other methods to investigate the moisture vapor transport behavior of different polyester knit fabrics. An example of the evaporative resistance (R_{et}) of a fabric tested is shown in the Table 2.7:

Table 2.7 Test Results for Round Hollow Core Polyester

Test fabrics	Evaporative thermal resistance (R_{et}), (m^2°C/watt)	Moisture vapor transmission rate (*MVTR*), g/m^2-24 hours	Microclimate drying time (T_d), minutes
Round hollow core filament	2.44	796	2.39

Prahsarn, C., Barker, R. L., & Gupta, B. S. (2005). Moisture vapor transport behavior of polyester knit fabrics. *Textile Research Journal, 75*(4), p. 346-351.

Of the fabrics tested the example shown in Table 2.7 had the highest MVTR and shared the fastest trying time with another fabric but the thermal resistance was not the lowest. The study found that moisture vapor transmission through open knit fabrics is mostly controlled by those fiber, yarn, and fabric variables that determine thickness and permeability (Prahsarn, Barker, & Gupta, 2005).

Significances of the Test Method

One theoretical basis behind this apparatus is Fick's law. The water vapor transmission rate is proportional to the vapor concentration difference. Since the sweating hot plate is a calorimetric method it can be expressed by the following equation:

$$\frac{Q}{A * T} = \frac{\Delta P}{R_{et} * \lambda}$$

where ΔP is the water vapor pressure gradient (kPa), R_{et} is the evaporative resistance ($m^2 kPa/W$), and λ the heat of vaporization of water at the plate surface temperature, J/g (Huang, 2006). There are important measures that can be calculated from data gathered by using the sweating guarded hot plate. The energy used to maintain the constant temperature of the heated plate is considered the water vapor or evaporative resistance (R_{et} [=] $kPa \cdot m^2/W$) of the fabric and can be calculated with the following equation:

$$R_{et} = \frac{A(P_s - P_a)}{H}$$

where $R_{et}$is the evaporative resistance of the specimen and surface air layer ($kPa \cdot m^2/W$), $A\ is$ the area of the test section (m^2), P_s is the water vapor pressure at the plate surface (kPa), P_a is the water vapor pressure of the air (kPa), and H is the electrical power

(W)(Huang, 2006). The thermal resistance (R_{ct}) can be calculated with the hot plate instrument using the following equation:

$$R_{ct} = \frac{A(T_s - T_a)}{H}$$

where R_{ct} is the total thermal resistance of fabrics plus the boundary air layer (m^2℃$/W$), *A is* the area of the test section (m^2), T_s is the surface temperature of the plate (℃), T_a is the temperature of the ambient air (℃), and *H* is the electrical power (W). Another valuable measure in terms of moisture management is the water vapor permeability index, i_{mt} which is the ratio of thermal (R_{ct}) and evaporative resistances (R_{et}) in accordance with equation:

$$i_{mt} = \frac{R_{ct}}{LR * R_{et}}$$

where R_{ct} is the thermal resistance LR is the Lewis relation, the ratio of mass heat transfer coefficient to convective transfer coefficient usually treated as a constant equivalent to 16.65 $^{\circ}C/kPa$ (Huang, 2006). The water vapor permeability index is dimensionless with values ranging between 0 and 1. A value of 0 implies that the material is impermeable to water vapor and a value of 1 would mean that the material is as thermally and water vapor resistant as an air layer of its same thickness (Arabuli, Vlasenko, Havelka, & Kus, 2010; Huang & Qian, 2007). Water Vapor Permeance, W_d ($g/m^2 * h - P_a$) characteristic of a textile depending on evaporative resistance and temperature in accordance with equation:

$$W_d = \frac{1}{R_{et} * \phi T_m}$$

where ϕT_m is the latent heat of vaporization of water at the temperature T_m of the heated plate (Arabuli, Vlasenko, Havelka, & Kus, 2010).

The sweating guarded hotplate can also measure to what extent a fabric can create a "buffer" for the moisture vapor or keep the skin feeling dry rather than damp or clammy. This buffering action is an important aspect of subjective sensational comfort experience of the wearer and can be measured as the Buffering Response (Bd) (S. Yoo & Barker, 2005). A higher Buffering Response indicates more moisture vapor modulating capabilities of a fabric when the body perspires. The equation for determining the Buffering Response of fabric is shown below:

$$B_{d=}(D)(S_{10} * \Delta RH_{max} * T_d)$$

where S_{10} is the rate of %RH increase in microlclimate during 10 mintutes after sweat pulse begins, ΔRH_{max} is the maximum increase in microclimate %RH during test, T_d is the time for microclimate %RH to return to steady state after test terminates, and D is the constant (1000) to give a desired range. As the equation below shows, the less the % RH increases during simulated perspiration, and the faster it returns to a normal state once simulated perspiration terminates, the higher the B_d of a fabric (S. Yoo & Barker, 2005).

Kawabata Thermo Labo

The Kawabata Thermo Labo is another device in which steady state heat and moisture transfer can be measured using a sweating hot plate featuring simulated sweating glands supplying water to the heated surface of the plate (Barker, 2002). The Thermo Labo warm/cool feeling tester became commercially available in 1984 (Kato Tech Company Ltd., 2007) and is a precursor to the guarded sweating hotplate that is still used in research today.

Sweating Manikin

Introduction

The Sweating Manikin is a measurement tool for full piece garments while taking advantage of the principles of the sweating hot plate device. The device is able to control the amount and rate of sweat supplied during long term garment testing. Garment testing allows for other parameters to be considered such as construction, fit, air layers, etc.

Apparatus Design

The water originates in a weight measured reservoir on the ceiling and then travels through the manikin's various sweat gland sites which are controlled individually. The manikin is suspended from a balance allowing the weight change on the manikin from moisture. A computer controlled system in the manikin distributes the water each of the individual sweat glands. The sweat glands are designed to continuously supply moisture to the manikin to keep its outer surface saturated throughout testing. While some manikins are supplied liquid for sweat, researchers have created a manikin can produce gaseous rather than perspiration (Fan & Chen, 2002). There are also sweating manikins that simulate walking motion in an attempt to analyze the effect of walking motion on clothing insulation and moisture vapor resistance (Fan & Qian, 2004).

Results and Analysis

Celcar, Meinander, and Geršak (2008) conducted a study to evaluate the influence of environmental and conditions on comfort using a sweating manikin dressed in ten different combinations of male business clothing systems some of which contained microencapsulated phase-change materials (PCMs). Figure 3.3 shows the evaporative heat loss, H_e (W/m^2)

results from the sweating manikin used for testing. Small differences were found between the H_e values at different ambient temperatures; the 10°C/50% RH in all combinations are only about 4.5 per cent higher than at 25°C and about 10 per cent higher than at −5°C (Celcar, Meinander, & Geršak, 2008). The evaporative heat loss H_e measurement results were shown rather than R_{et} evaporative resistance measurement; H_e is a variable needed to determine R_{et} as shown in section 2.5.4. Also, the research found only very small differences between clothing systems made of materials with PCMs and standard wool materials and wool mixtures in terms of thermal and evaporative properties tested. Also, the researchers note that they cannot confirm that these small differences exist because of the content of PCM particles (Celcar, Meinander, & Geršak, 2008).

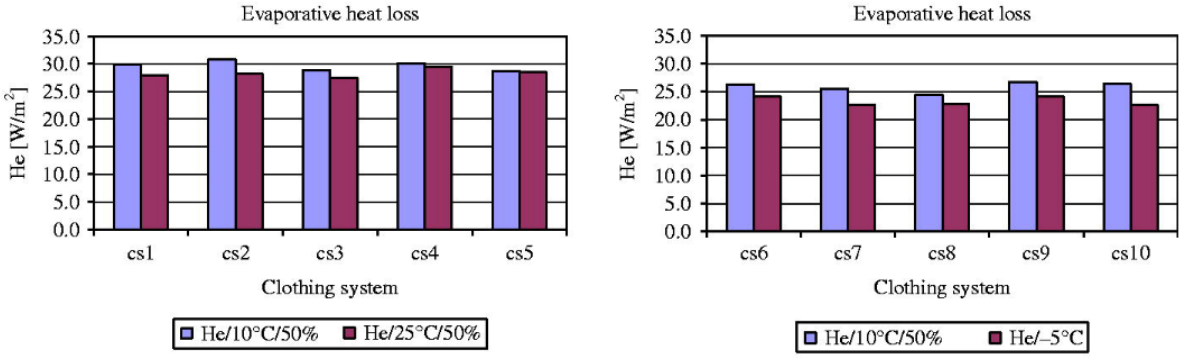

(a) 10°C/50 per cent and 25°C/50 per cent **(b)** 10°C/50 per cent and –5°C

Figure 2.15 Evaporative heat loss through clothing systems under different ambient temperatures

Source: Celcar, D., Meinander, H., & Geršak, J. (2008). Heat and moisture transmission properties of clothing systems evaluated by using a sweating thermal manikin under different environmental conditions. *International Journal of Clothing Science and Technology, 20*(4), p. 240-252.

Significances of the Test Method

As mentioned previously the sweating manikin takes the principles of the hot plate tested method. The device calculates the clothing thermal insulation and water vapor resistance rather than the fabrics. Thermal resistance is calculated from the following equation:

$$R_t = (T_s - T_a) * A/H$$

where R_t is the total thermal resistance of the clothing and surface air layer ($°C \cdot m^2/W$), A is the area of the manikin's surface (m^2), T_s is the temperature at the manikin surface ($°C$), T_a is the temperature of the air surrounding the manikin ($°C$), and H is the power required to heat manikin (W). Using the thermal resistance value the evaporative resistance can be calculated from the following equation:

$$R_{et} = \frac{[(P_s - P_a) * A]}{[H_e - (T_s - T_a) * A/R_t]}$$

where R_{et} is the evaporative resistance of the clothing and air layer ($KPa * m2/W$), P_s is the water vapor pressure at the manikin's skin (kPa), P_a is the area of the water vapor pressure in the air surrounding the clothing (kPa), A is the area of the manikin's surface that is sweating (m^2), H_e is the power required for sweating areas (W), T_s is the temperature at the manikin surface ($°C$), T_a is temperature of the air surrounding the manikin ($°C$), and R_t is the thermal resistance of the clothing ensemble and surface air layer ($°C \cdot m^2/W$).

Human-Clothing-Environment Simulator

Introduction

The human-clothing-environment simulator measures coupled heat and moisture transfer in relation to microclimate temperature and humidity changes. This device was designed to conduct testing under a various environmental temperatures.

Apparatus Design

The human-clothing-environment is a vertical-type skin model consisting of two adjacent environmental chambers, power supply with a temperature control unit, a sweating hot plate, and a data-logging system (E. Kim, Yoo, & Shim, 2006; S. H. Kim, Lee, Lim, & Jeon, 2003). Figure 2.6 illustrates the instruments components. The environmental chambers are controlled separately for cold subzero and moderate warm conditions. Test samples are placed over a copper plate attached to a panel heater which is supplied with different amounts of liquid in order to simulate various perspiration rates. Test samples can be layered in a holder designed to give appropriate air space between the layers in order to simulate clothing layers. The samples are suspended from a metal rod connecting the two environmental chambers (E. Kim, Yoo, & Shim, 2006). As Figure 2.16 shows, temperature and relative humidity sensors are located in each layer to measure the microclimate.

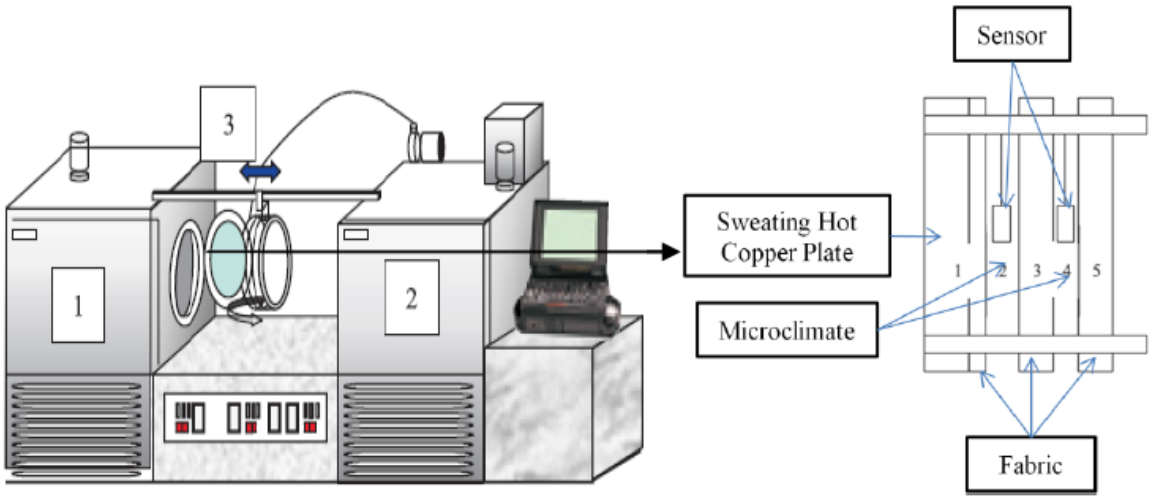

Figure 2.16 Schematic of the Human-Clothing-Environment Simulator

Source: Kim, S. H., Lee, J. H., Lim, D. Y., & Jeon, H. Y. (2003). Dependence of sorption properties of fibrous assemblies on their fabrication and material characteristics. *Textile Research Journal, 73*(5), p. 455-460.

Results and Analysis

Kim, Yoo, and Shim (2006) used the human-clothing environment simulator to evaluate the comfort performance of layered textile materials under changing environment conditions. To simulate clothing systems, layers of PET knit/fleece and PET knit/micro-porous membrane (MPM) were compared at temperatures ranging from 25 to -10°C. Their experiment found that the fleece combination had higher thermal insulation and air permeability in the cold condition compared to the MPM combination. The researchers concluded that the higher vapor pressure in the MPM combination could be attributed to condensation blocking the pores of the membrane (E. Kim, Yoo, & Shim, 2006). Yoo and Kim (2008) conducted a study using the HCE simulator to measure the effects of layer selection on heat and moisture transfer and condensation profiles for cold weather clothing ensembles. The study found

condensation mostly occurred on the outer surface of fleece fabrics and not on the inside of the waterproof breathable outer shell (S. Yoo & Kim, 2008). They concluded that the layer arrangement influenced the condensation, heat and water vapor permeability, and the distribution of condensed water on each layer of the clothing system (S. Yoo & Kim, 2008).

Significances of the Test Method

The MCE simulator device vertical skin model simulates the clothing interaction with skin in an upright fashion which is representative of how the clothes are worn on the human body. The HCE simulator uses its two environmental chambers to measure the heat and moisture transfer properties in clothing according to rapid changes in the external environment (E. Kim & Yoo, 2010).

2.10. Human Subject Testing

Humans are the ultimate test method for heat and moisture management in fabrics because they are ultimately the end users of clothing systems. Clothing when worn on the human body introduces a number of complex variables such as construction or garment design, fit on the body, physical movement as well as the individual wearer's sensory perception. Also, human testing is more expensive, complex and difficult to implement. However, there has been a lot of research into the how the body perspires and how fit and compression can help optimize athletic performance.

2.10.1. Onset of Perspiration

The body's core temperature and skin temperature are the main factors determining whether the sweat glands will produce sweat (Bligh, 1978; Houdas et al., 1978). Eccrine sweat glands are controlled by clusters of nerve cells in the hypothalamus that regulate heat-loss

and heat-gain mechanisms of the body. These nerve cells receive sensory information from skin receptors and from the circulating blood. The initial response to exercise is that the blood flow to the active muscles increases therefore increasing the transport of oxygen. As the internal temperature begins to rise, the vasodilatory response is augmented by secretion of sweat onto the skin surface for evaporative cooling to occur (Reilly & Waterhouse, 2009).

2.10.2. Predicting Perspiration Rates

Research has attempted to predict the body's perspiration rate. Macpherson's (1960) work predicted the 4 h sweat rate index (P4SR) which involves air temperature, wet-bulb temperature, air speed and a correction for the type of clothing. These factors are used for determining the maximum evaporative capacity of the environment (E_{max}) and then the P4SR is calculated taking into consideration the metabolic rate. Givoni and Berner-Nir (1967) predicted perspiration rates based on an exponential function of the ratio of evaporative cooling and the maximum evaporative capacity of the environmentE_{req}/E_{max}. Lustinec (1973) predicted sweat rates based on the linear correlation between sweat rate and $E_{req}$for low skin wettedness, but used a non-linear correlation between sweat rate, $E_{req}$and E_{max} when the skin wettedness was high. Shapiro, Pandolf, and Goldman (1982) developed the following formula:

$$\Delta m_{sw} = 18.7\ x\ E_{req} x (E_{max})^{-0.455}$$

with the limits $50 < E_{req} < 360;\ W\ x\ m^{-2}\ and\ 20 <\ E_{\ max} < 525;\ W\ x\ m^{-2}$ to predict perspiration for specific workloads, climates and clothing ensembles. According to Shapiro, Pandolf and Goldman (1982) the rate of sweat loss can be predicted (at least within +/- 20%) without the need to make physiological measurements.

2.10.3. Body Mapping of Perspiration

Evaporation is the mechanism, for heat loss during exercise. When the relative humidity is high or the skin is wet; evaporative efficiency declines significantly. When the body becomes wet with sweat the skin temperature decreases (Bullard et al., 1967; Candas et al., 1979; Kerslake,1972; McCallrey et al., 1979). The concept of skin wettedness was introduced by Gagge (1937) and is defined as the fraction of the total body area covered by sweat. Also, skin wettedness (w) is expressed as the ratio of actual evaporative heat loss to maximum possible evaporative heat loss under the same environmental conditions (Havenith et al. 2002). Skin wettedness is considered as a coefficient in a model to predict the total sweat rate (Nadel, Bullard, & Stolwijk,1971) and one of the principal indices correlated with warm discomfort (Fukazawa & Havenith, 2009). Measuring the degree of skin wettedness has been the interest of much research and a moisture detector (a hygroreceptor) for human skin has not been found (Lee, Nakao, & Tochihara, 2011). However, humans are able to recognize whether or not the skin is wet. Li (2005) points out that the perception of wetted skin could also be connected with other indirect mechanisms such as tactile and pressure sensations.

High temperature and exercise results in the greatest amount of heat loss from the body through perspiration and evaporation (Smith & Havenith, 2011). It has been established that the degree of skin wettedness influences hidromeiosis which describes the blockage of perspiration output by the wetted skin (Nadel & Stolwijk, 1973). Therefore, skin wettedness can impair the perspiration evaporative efficiency. Perspiration production in different situations forms the foundation for the body's cooling mechanism, which is

modified by aerobic fitness, acclimation state, environmental conditions, clothing, and evaporative efficiency (Candas et al. 1979; Havenith et al. 2008a; Havenith et al. 2008b; Shapiro et al. 1982). Studies have frequently found sweat rates to be greatest in the torso area particularly lumbar region of the posterior torso as well as the forehead (Cotter et al. 1995; Fogarty et al. 2007; Havenith et al. 2008a; Hertzman 1957; Kuno 1956; Machado-Moreira et al. 2008; Ogata 1935; Smith et al. 2007; Taylor et al. 2006; Weiner, 1945). Figure 2.15 shows an example of the body mapping of perspiration work of Smith and Havenith (2011), where nine athletic males were asked to exercise on a treadmill while the perspiration their bodies generated was measured. In this study, participates' perspiration was measured through the use of absorbent pads specially fitted for each participants body shape. Regional sweat rates were calculated in grams per meter square of body surface area per hour *($g/m^2/h^{-1}$)* using the weight change of each pad, the pad surface area, and the length of time the pad was kept at the skin (Smith & Havenith, 2011). The highest values of perspiration occurred in the central and lower back regions, while the lowest values were found in the hands and feet. Figure 2.16 depicts an interpretation of body perspiration mapping used by clothing designers at Addidas for optimizing athletic apparel functionality in terms of moisture and temperature management.

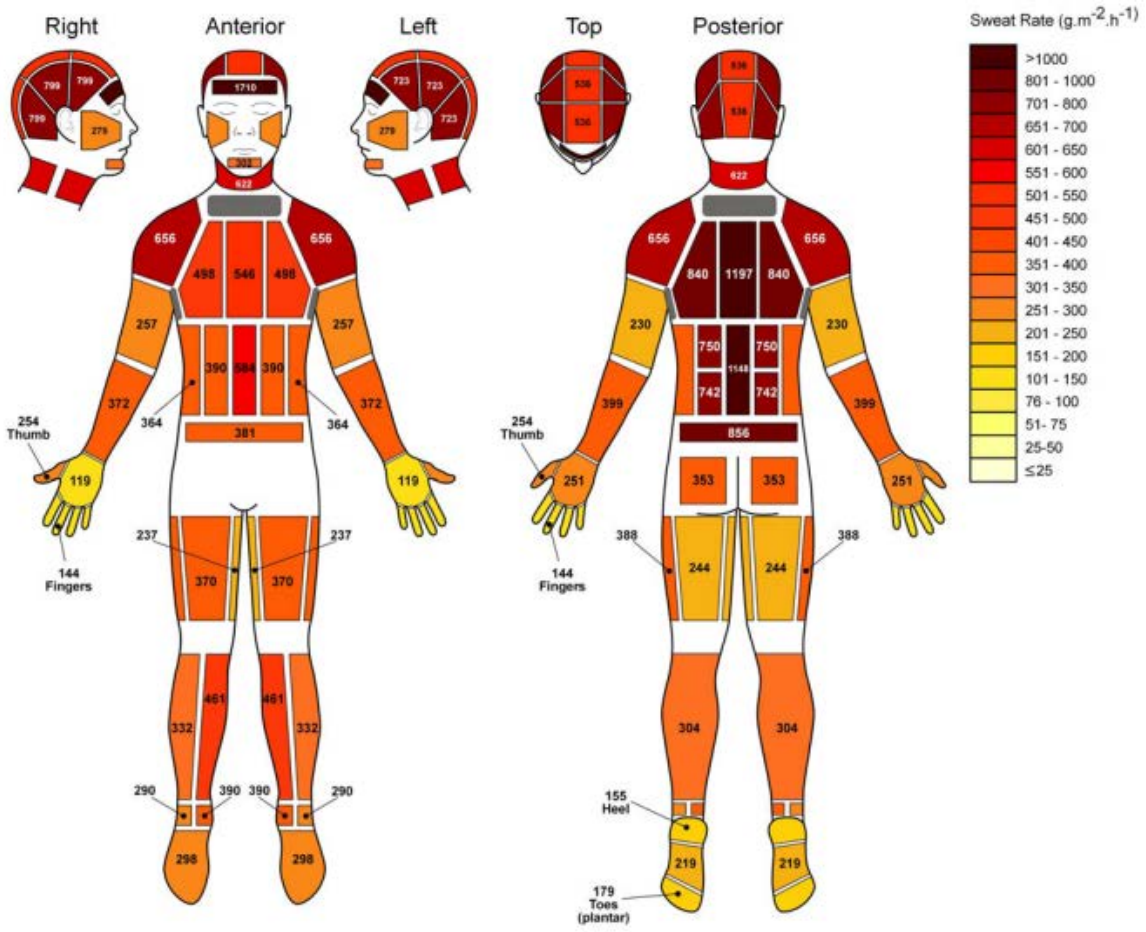

Figure 2.15: Regional Median Sweat Rates of Male Athletes at Exercise Intensity

Source: Smith, C.J. & Havenith, G. (2011). Body mapping of sweating patterns in male athletes in mild exercise-induced hyperthermia. *European Journal Applied Physiology 111*(7), p. 1397.

Figure 2.16: Temperature (left) and Perspiration (right) Guidelines for Clothing Design

Source: Smith, C.J., and Havenith, G., 2011. Sweat mapping in humans and applications for clothing design. The Fourth International Conference on Human-Environment System (ICHES 2011), Sapporo, Japan, 3-6 October, p.785.

2.10.4. Fit and Compression

Compression and form fitting garments are used widely during exercise and athletics despite little evidence or research into the benefits (MacRae, Cotter & Laing, 2011). There have been some recent studies investigating the coverage and pressure effects of compression garments (Liu, Little & Williams, 2012; MacRae, Cotter & Laing, 2011; MacRae, Laing, Niven & Cotter, 2012). Fabrics composed with Spandex material can be normally applied to sports clothes, leisure clothes, hosiery, underwear and swimwear for maintaining a stable shape of the body under changeable load (Tazelaar, 1999). The pressure caused by Spandex also reduces the microclimate between skin and fabric surface.

2.11. Fabric Developments for Moisture Management

2.11.1. Surface Energy Modification

Paraffin waxes are the easy and expensive water repellent finishes for textiles. They provide good water repellency, but limit air permeability, have poor durability, and have poor washfastness properties (Grottenmuller, 1998). Silicone finishes were most widely used in the 1970's and 80's because they can be applied in combined with other chemicals, can be applied to many textile materials, and have lower cost is compared to fluoropolymers (Holme, 2003). Since the 1980s, fluoropolymers have been widely used in the textile industry to impart water repellency as well as in applications where oil-repellent and soil-release properties can be added to fabrics. The major drawback to this method is that it is a wet process requiring high levels of thermal energy to evaporate the water and cure the fluoropolymer. In addition, fluoropolymers have recently aroused concern as to the danger they might impart to humans and the environment (U.S. Environmental Protection Agency, 2013). This concern has prompted an extensive review of existing commercial repellent finishes and renewed interest in the search for alternative chemicals and application methods for producing repellent textiles. Surface modification for water repellency and many other fabric characteristics can be achieved through plasma treatment which eliminates the need for wet processing. Plasma treatment on cotton can increase the hydrophobic properties without reducing the water vapor transmission ability of the fiber (Chinta, Landage, & Kumar, 2012); Hocker, 2002).

2.11.2. Fiber Cross-section

Special extrusion techniques can be used to create fibers with unique cross-sectional shapes which have added channels and surface area which make them more useful for wicking away moisture (Wilusz, 2012). Several bicomponent fibers are available on the athletic wear market today including Outlast, a bicomponent fiber featuring a PCM core and polyester sheath to combine heat regulation with conventional polyester fiber characteristics such as low moisture absorption (Textile World, 2011). Bicomponent fibers for moisture management are generally composed of a non-absorbent material on the inside (core) and an absorbent material on the outside (sheath). This core/sheath construction is designed to allow the absorbent material on the outside to draw the moisture away from the skin while the non-absorbent material does not allow the fabric to become saturated (Defense Update, 2007).

2.11.3. Absorption

Absorbency is also a major factor affecting moisture management. Greater absorbency increases the ability for moisture to be drawn into the fabric but, absorbent fibers may retain moisture which can lead to discomfort if the garment becomes saturated. It has been shown that fabrics which wick moisture rapidly through the fabric while absorbing little moisture help to regulate body temperature, improve muscle performance and delay exhaustion (Defense Update, 2007). Highly absorbent fibers can be paired with hydrophobic fibers in a core/sheath construction as discussed in the previous section other ways to combine these fibers is to create a multi-layer fabric or a composite spun yarn (Chen, Fan, & Sarkar, 2012; Su, Fang, Chen, & Wu, 2007).

2.11.4. Microdenier

The microfiber or microdenier moisture management mechanism is based on the theory that moisture is transported through capillary action and that the spaces between fibers effectively form tubes or capillaries that transport the liquid away from the surface. Narrower spaces between the fibers of a fabric will allow more effective moisture transport. For this reason, fabrics with many narrow capillaries are gaining popularity for moisture management end uses. Microfibers are generally used for polyester fabric which absorbs and wicks little moisture, the introduction of microfibers improve polyester's wickability allowing the fabric to dry more quickly (Sampath, Mani & Nalankilli, 2011).

2.12. Conclusion

As discussed, clothing plays an important role in the maintenance of heat balance of the body and this heat balance is essential to sustain life. Any small (+/- °5) deviation from the 37 °C core body temperature can result in injury or even death. Perspiration is the body's natural mechanism of heat regulation which allows the body to lose heat when its temperature starts to rise in order to evaporate the moisture from the skin. A clothing system should allow the perspiration to pass through to its outside surface; otherwise it will result in discomfort. In this paper various theories of thermal and moisture transport both in vapor and liquid form have been discussed including: Thermodynamic fundamentals, Newton's Law of Cooling, Fourier's Law, Stefan-Boltzmann, Fick's law, Fick's law, Hagen-Poiseuille law, and Clausius–Clapeyron relation. The literature has also advanced theories of heat balance of the body and metabolic rate. This theoretical background was established in order to more thoroughly survey different instruments to test heat and moisture management of fabrics. Of

course, humans are the ultimate test method because they are ultimately the end users of clothing systems. Clothing when worn on the human body introduces a number of complex variables such as construction or garment design, fit on the body, physical movement as well as the individual wears sensational perception. The cost and difficulty implementing human testing has driven the research towards finding an alternative method that can best represent the "real world."

The testing instruments discussed include: the cup testing method, DMPC, GATS, Alambeta (Permetest) instrument, Guarded Sweating Hotplate, Sweating Manikin, MMT, Dynamic Surface Moisture method, HCE simulator as well as methods for testing wicking and wettability. As stated, there are three key factors affecting the heat balance environmental conditions, metabolic heat production, and thermal insulation and moisture permeability of clothing and other protective garments. All of the testing instruments discussed take into account one or more of the following climatic parameters such as air temperature, radiant temperature, humidity, and wind speed. However, personal parameters such as activity rate, fitness level, and body surface area have significant influence on the heat balance of the body which would make one conclude that the metabolic heat production might be another key parameter to consider in achieving more accurate heat and moisture management measurement for clothing. These tests provide a means to compare different fabrics against one another in terms of performance but are not absolute measurements. Many of these instruments account for different thermal and moisture management measurements; the upright cup, DMPC, Permetest, and GATS measure moisture permeability while the sweating hotplate and manikin measure evaporative resistance. The

Dynamic Surface Moisture method measures the quantity of moisture, the HCE simulator measures temperature, relative humidity and vapor pressure, and MMT measures moisture absorption rate, spreading speed, maximum spreading radius, and one way liquid transport ability. Finally, the wettability test measures contact angles while the horizontal and vertical wicking tests measure liquid transport rates. Previous research and fabric testing has focused on the evaluation of single layer textile systems as far as moisture management is concerned with the exception of the Human-Clothing-Environment Stimulator (section 2.9.3.5). The proposed research sets out to characterize multi-layered textile clothing systems.

CHAPTER THREE

3. Methodology

The purpose of this research is to determine how to analyze heat and moisture transfer in a multilayered clothing system that is engineered to optimize moisture management performance during athletic end use. The research sets out to measure the moisture and heat transferred by the human body while wearing a multiple layer clothing system as the energy is transported away from the skin and out to the external environment or vice versa. The research examined energy passing through multilayer clothing system worn by human subjects through measurements taken from state of the art temperature and humidity sensors.

Major Research Hypothesis:

This research approach is based upon the theory that the properties of a clothing layer can be characterized by the changes in temperature and relative humidity flow through a fabric layer. The experiments used in this research provide detailed information regarding particular fabric types and microclimates that are ideal in order to optimize a multilayer clothing system for athletic end use. There are existing studies that support this research which illustrate a relationship between the heat energy flow and fabric. Therefore, a thorough literature review includes comfort definitions and models as well as some physiological background. The literature review defined heat and moisture (vapor and liquid) theoretical fundamentals including: thermodynamics, metabolism, evaporation, radiation, convection, and conduction. Many thermal and moisture management testing instruments are introduced within the literature review to understand the various principles involved.

3.1. Humans as Test Device

To measure changes in the amount of heat energy and moisture flow, this research utilized human subjects as the heat energy and moisture source. The literature review provided a review of the thermal and moisture management testing instruments currently used in research and industry. The trend in laboratory testing devices is to develop devices that better simulate the end use of the product. The testing devices examined usually combined one or two of the following aspects of the human experience such as: modeling skin temperature, perspiration; and the ability to test full garments, multiple layers, and changing environmental conditions. However, none of the laboratory methods reviewed simulated all of the aspects of the human clothing experience. The advantage of using human subjects as the heat and moisture source for this study is that all of the human experience factors would be combined into one test. This is especially important in understanding the warm-up and cool-down stages.

3.1. Fabric Holder

The fabric holder or kit consists of three layers and is designed to represent how a human body would actually dress. For example one might wear underwear as a base layer (Fabric Layer 1) followed by a t-shirt or top (Fabric Layer 2), and finally a jacket (Fabric Layer 3) as an outer shell; Figure 3.1 shows an internal schematic of the flexible fabric kit including approximate temperature and relative humidity sensor placement.

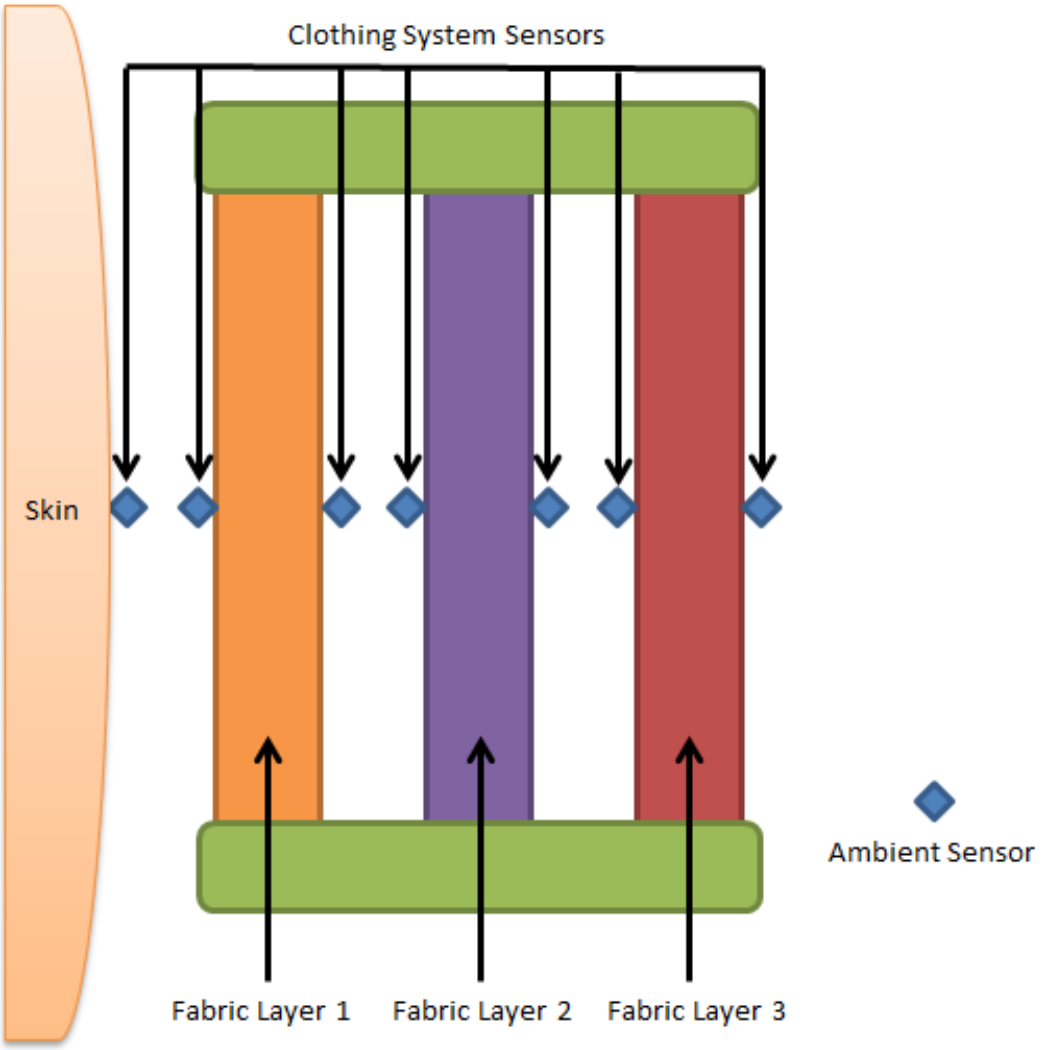

Figure 3.1: Fabric Test Kit Internal View

In order to build a fabric test kit that simulates and measure heat and moisture flow through a clothing system there were several factors to consider including issues such as size and shape of the kit, kit placement on the body, attachment of the kit to the body, and the placement of sensors within the kit.

3.1.1. Placement of Kit on the Body

The fabric kit was placed in an area of the body that maximized the perspiration passing through the fabric samples. As identified by the literature review in Chapter 2, the lumbar region of the posterior torso and the forehead area typically produce the most perspiration during exercise activity. For this study the flexible fabric kit was placed onto the lumbar region of the posterior torso or lower back rather than the forehead in order to optimize the sample size that can be tested. The flexible fabric kit was placed on the body area as shown in Figure 3.2.

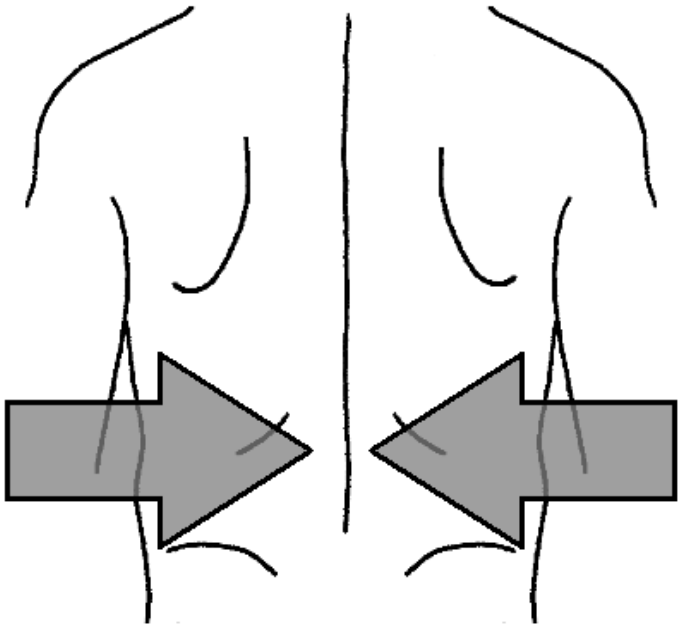

Figure 3.2: Placement of Flexible Fabric Kit on Lower Back

3.1.2. Size and Shape of the Kit

The fabric kit was designed to be mounted and fitted on the human body. The kit should be large enough in order to test a substantial fabric sample but, small enough that it will not interfere with the subject's ability to perform the trial. The various methods of measurement reviewed in Chapter 2 of this paper revealed that the fabric sample size required varied according to the instrument. However, typically the fabric sample was square. However, for this study it was found that a rectangular shape was easier to attach to the lower back. Figure 3.3 shows a schematic fabric kit.

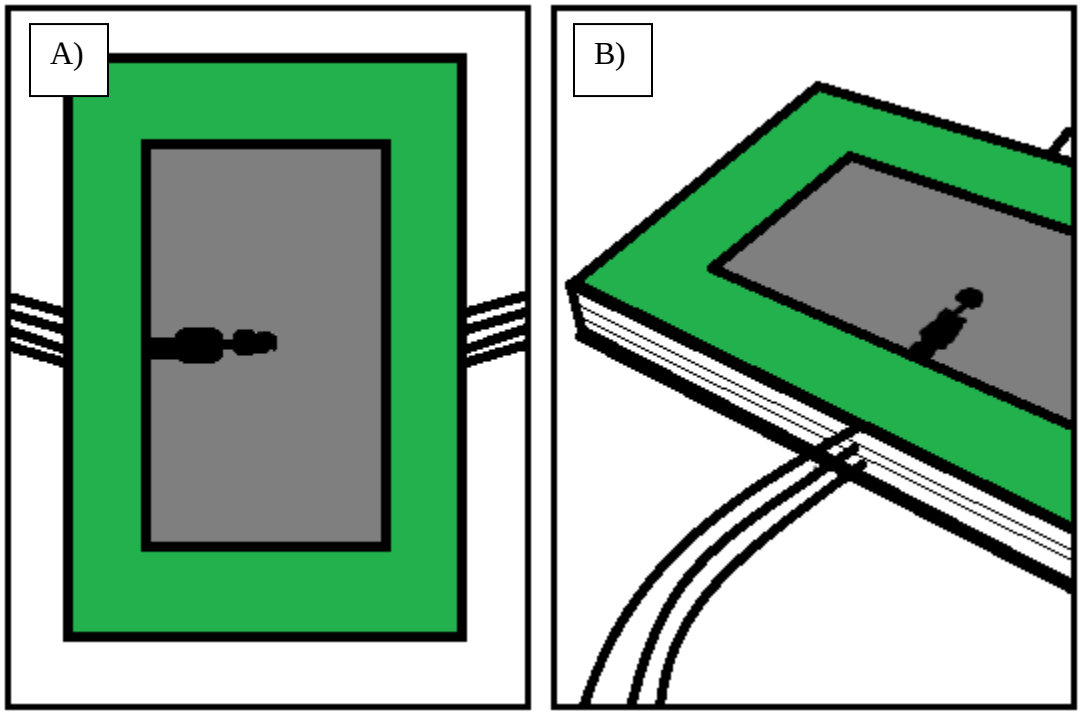

Figure 3.3: Fabric Testing Kit; A) Outside View, B) Side View

3.1.3. Attachment of the Kit to the Body

The fabric kit was made to be flexible in order to conform to the contours of the lower back comfortably and securely for the duration of the human subject testing. Medical tape was used to secure the kit on the subject's body.

3.1.4. Placement of Sensors within the Kit

The location of the two points where the heat energy flow occurs between two fabric layers was essential for the measurements taken and for the application of thermodynamic theories to the research. The microclimate distance was also important as it can alter heat energy and vapor flow. The schematic of the flexible fabric kit shown in Figure 3.1 gives an estimation of the sensor placement.

3.2. Human Trial Protocol

Human trials were used in this research which measured temperature and humidity across the fabric layers and the microclimates. Human subjects were recruited from several groups of bicycle enthusiasts. These enthusiasts ride leisurely and competitively in teams and were very familiar with riding a bicycle for an extended period of time of thirty minutes or more. Athletes who incorporate the stationery bicycle into their training routines were also recruited.

3.2.1. Stationary Bicycle Test

The Life Fitness 97C Lifecycle Upright Bike in the Weisiger-Brown Athletics Building at NC State University was utilized in this study. Both the YMCA and the American Heart Association cite advantages of using a stationary bicycle over a treadmill in terms of the ease of measuring exercise heart rate, blood pressure, and oxygen intake (Carter

et al, 2012; American Heart Association, 2012). Also, while using a stationary bicycle, the upper body movement is minimal. This is ideal for this study because the fabric test kit was attached to the lower back and this lowered the chance of the fabric kit apparatus interfering with the bicycle test protocol.

3.2.2. Bicycle Protocol

The Life Fitness 97C Lifecycle Upright Bike has 25 programmable resistance settings that progressively increase the amount of resistance applied against pedaling. For this study, it was suggested to the subjects that they use level 6 for the warm up but, many of the subjects changed the machine to settings for the remainder of the trial in order to keep their heart beat in the required range. The 97C Lifecycle manual suggests maintaining a specific heart rate while exercising as the optimal way to monitor the intensity of a workout. The subjects rode the stationary bicycle for 30 minutes vigorously in order to induce sweating using the following protocol:

1) 5 minutes to warm up on bicycle during this time the subject can slowly work up to the target heart rate zone;
2) 30 minutes at target heart (135-155 beats per minute);
3) 10-15 minutes at slower pace to allow for cool down.

As stated, the flexible fabric kit including (SHT-71) sensors was attached to each subject's lower back and measured temperature and relative humidity changes across each layer. See Appendix 1 for a copy of the IRB agreement. Figure 3.4 shows the testing set up including the stationary bicycle, testing kit, and computer system for recording data.

Figure 3.4: Stationary Bicycle Fabric Testing Kit Set-up

3.3. Materials

The fabric kit consisted of three layers designed to represent how a human body would dress: underwear as a base layer (Fabric Layer 1), t-shirt or top (Fabric Layer 2), and jacket (Fabric Layer 3) as an outer shell. The choice of fabric to be used for each layer within the flexible fabric kit was based upon a survey of current active wear products available at several retail outlets. Material composition of products offered by active wear companies such as Nike, Adidas, Under Armor, Reebok, Russell, Champion, and Hanes were documented as a guide to material selection for the experimental trials. The fabric choices for each of the three clothing layers were selected, totaling ten different fabrics to be tested. Table 3.1 describes the ten fabric choices which were used for a specified layer. However, many of the fabrics

were suitable for use in more than one layer and are charted accordingly. Before conducting human trials with the flexible fabric kits, fabric properties such as thickness were measured siroFAST instrument to allow for statistical analysis of the relationship between energy flow and fabric structure.

Table 3.1: Fabric Layers with Fabric Choices

Fabric Description	***Undergarment***	***T-Shirt or Top***	***Outer Shell***
A- 100% PET thermal-lined double jersey	✓	✓	✓
B- 100% PET French terry knit			✓
C- 100% PET Bonded three layer fleece			✓
D- 100% Recycled PET ultra-lightweight plain weave			✓
E- 100% mercerized cotton poplin	✓	✓	✓
F- 100% Mesh Fleece knit			✓
G- 86% PET, 14% Elastane single jersey knit	✓	✓	✓
H- 100% PET double knit	✓	✓	✓
I- 100% PET Mesh knit	✓	✓	✓
K- 95% Cotton, 5 % Elastane single jersey knit	✓	✓	✓

✓ indicates suitable end use

3.4. Data Collection

The data was generated by sensors (SHT-71) and data loggers (EK-H4). Within the fabric kit there was a total of eight sensors; seven sensors measuring the clothing systems microclimates including skin to clothing layer and layer to layer, and one ambient

environment sensor. Each of these sensors measured temperature and relative humidity and were pre-calibrated by the manufacturer stating typical accuracy to +/- 0.04 ˚C for temperature and +/- 3.0% for relative humidity (Sensor Performance Datasheet Appendix B). SHT-71 is produced by SENSIRION Ag the features of these sensors are shown in Table 3.2. Figure 3.5 shows its actual model and schematic diagram which are provided by SENSIRION Ag SHT-71 is a small of temperature and relative humidity sensor, it is capable of accurately measuring temperature and relative humidity in real-time simultaneously. The SHT-71 is connected with a specific cable which is specifically provided by SENSIRION Ag which is also connected to a data logger, evaluation kit (EK-H4). This data logger displays measured numerical information regarding temperature and relative humidity which are recorded by SHT-71. In this research, two data loggers were connected to eight SHT-71 sensors. During the human subject trials, temperature and relative humidity measurements are continuously stored by EK-H4 Read-Out Software Installation on a computer. This display shows real time temperature, relative humidity, and dew point data in the form of graphs of temperature and relative humidity. Figure 3.6 depicts the data logger (EK-H4) connected with sensors and EK-H4 Read-Out Software Installation software. Figure 3.7 shows a schematic diagram of connection among sensor (SHT-71), USB cable, data logger (EK-H4), and computer output graphs of relative humidity and temperature which can be exported to spreadsheet software such as Microsoft Excel which was used for this research.

Table 3.2: Features of SHT-71 Sensor by SENSIRiON Ag

Energy consumption	80uW (at 12bit, 3V, 1measurement/s)
Relative humidity operation range	0-100% RH
Temperature operation range	-40 to +125˚C
Relative humidity response time	8 seconds
Output	Digital

Source: SHT71 - Digital Humidity Sensor (RH&T). SENSIRiON Ag Retrieved on 7/15/2013 from: http://www.sensirion.com/en/products/humidity-temperature/humidity-sensor-sht71/

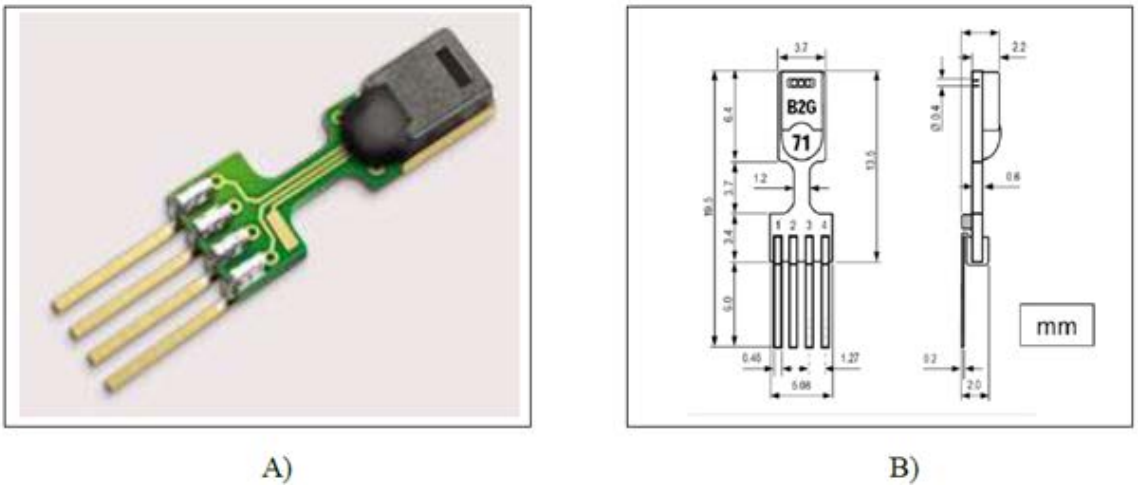

Figure 3.5: A) Actual model, B) Schematic diagram of SHT-71

Source: SHT71 - Digital Humidity Sensor (RH&T). SENSIRiON Ag Retrieved on 7/15/2013 from: http://www.sensirion.com/en/products/humidity-temperature/humidity-sensor-sht71/

Figure 3.6: A) Actual data logger (EK-H4) connected with sensors, B) EK-H4 Read-Out Software Installation

Source: SHT71 - Digital Humidity Sensor (RH&T). SENSIRON Co. Retrieved on 7/15/2013 from: http://www.sensirion.com/en/products/humidity-temperature/evaluation-kits/evaluation-kit-ek-h4/

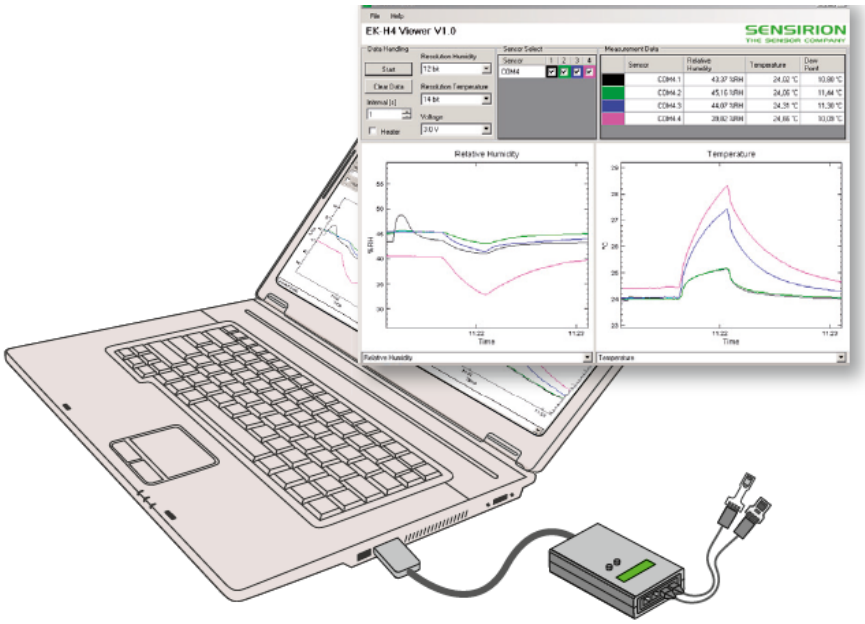

Figure 3.7: Schematic diagram of sensor (SHT-71), USB cable, data logger (EK-H4), and computer

Source: SHT71 - Digital Humidity Sensor (RH&T). SENSIRiON Ag Retrieved on 7/15/2013 from: http://www.sensirion.com/fileadmin/user_upload/customers/sensirion/Partnersaccess/Documents/Humidity/Sensirion_Humidity_EKH4_Quick_Start_Guide_Print_11.pdf

3.5. Theoretical Models

Several existing theories provided a framework to explain the heat energy flow from skin to the external environment. Heat energy flow can be described by the first and second laws of thermodynamics. The following theories were used to characterize energy flow: Clausius-Clapeyron Relation, Newton's Law of Cooling, Fourier's law, and Stefan-Boltzmann relationship. The theoretical background for this research was provided in the Literature Review (Chapter 2). The Clausius-Clapeyron Relation is central to this research as it describes both phase change and movement of water vapor. This theory explains the change in enthalpy governing the kinetic and potential energy of perspiration. Each of the theories listed require temperature differences which were measured in the both the microclimate and the across each fabric of the three layered clothing system.

3.6. Analysis of Data

Temperature and Relative humidity was measured for each clothing system through the different fabric layers. This data was used to calculate heat conductivity through microclimates and fabrics. Enthalpy was be calculated using Clausius-Clapeyron and was be related to the fabric structure and composition. This analysis shows how the energy flow is affected by different clothing systems for an athlete during a typical exercise routine which includes warm-up and cool down.

CHAPTER FOUR

4. Results, Analysis, and Findings

This Chapter discusses the results and analysis obtained using human subjects and a range of fabrics that may be found in athletic and activewear garments. First, the fabrics were measured using the SiroFAST system to obtain thickness, bending, and tensile properties. While physical properties of all the fabrics were measured using the SiroFAST system other thermal properties such as material emissivity, and material thermal conductivity were obtained from references. Physical testing results for fabric surface thickness obtained by the SiroFAST measurement system for each of the fabrics used in this research are shown in Table 4.1. Surface thickness is the difference between the fabric thickness measured at loads of $2gf/cm^2$ and 100 gf/cm^2. The human subject trial results regarding temperature and relative humidity as measured by the eight sensors revealed some very interesting patterns regarding the onset of perspiration.

Table 4.1: Fabric Thickness Measured by SiroFAST

Fabric	*Description*	*Thickness (mm)*
A	100% PET thermal-lined double jersey	0.269
B	100% PET French terry knit	0.305
C	100% PET Bonded three layer fleece	Too thick for FAST
D	100% Recycled PET ultra-lightweight plain weave	0.021
E	100% mercerized cotton poplin	0.156
F	100% Mesh Fleece knit	1.321
G	86% PET, 14% Elastane single jersey knit	0.131
H	100% PET double knit	0.124
I	100% PET Mesh knit	0.144
K	95% Cotton, 5 % Elastane single jersey knit	0.364

4.1. Fabric Testing Kit: Human Subjects as Energy Source

The fabric testing kits used for each of the human subject trials in this study was constructed of foam sheets with known thickness. The foam sheets were chosen because they were flexible, easily cut, and gave the fabric testing kit the ability to flex somewhat to the shape of the human subject. The foam sheets served as the structure to house the three fabric layers and the sensors which measured the temperature and relative humidity within the kit. Two types of foam sheets were used: 2 mm adhesive backed sheet and 6 mm non-adhesive sheet. A total of two 2 mm sheets and three 6 mm sheets were used for each kit. The 2 mm sheets were used on the outside of the kit while the three 6 mm sheets served held the sensors in

place with drilled in channels as shown in the image of a completed kit shown in Figure 4.1. To ensure that each foam sheet was cut with precision a digital pattern was created and cut using a Lectra Vector cutting system as shown in Figure 4.2. Each of the foam sheets were cut to 6" x 8 1/8" rectangles with 3 ½" x 5 ¾" internal cutouts which exposed a total area of 20.125 in^2 of the fabric samples within the kit. This kit size was chosen as it represented the maximum comfortable size of kit that could be attached to the lower back of the human subject.

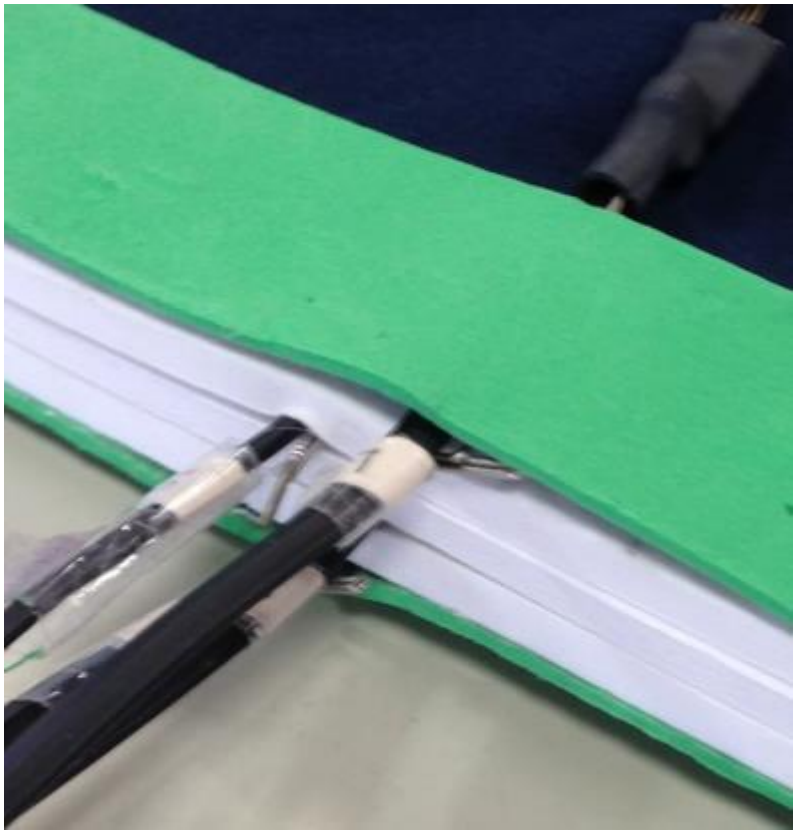

Figure 4.1: Sensor placement between foam sheets

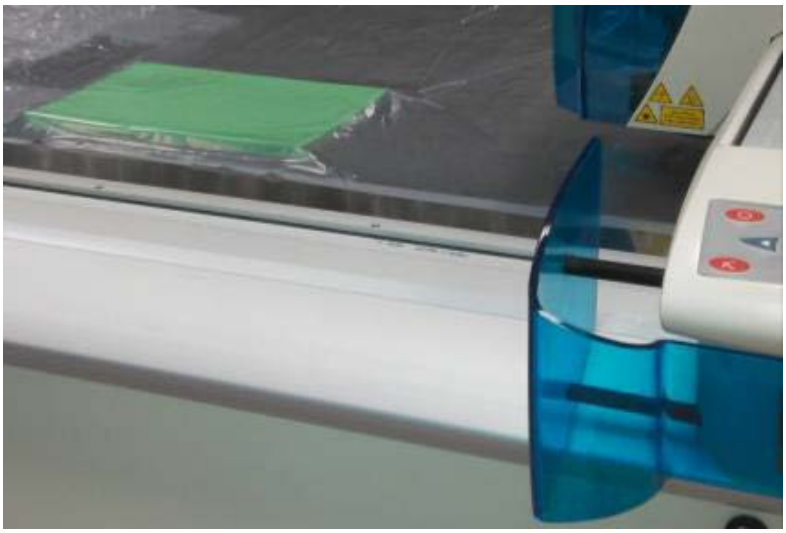

Figure 4.2: Precision cutting foam sheets

When constructing a kit, the first layer was the 2 mm adhesive foam followed by a 6 mm foam sheet with the first sensor sandwiched in between. Next, the second sensor was placed into the inside of the first 6 mm foam sheet and the first fabric then attached face up and secured with double sided tape. The third sensor was then placed on the outside or face side of the first fabric. The sensors on both sided of the fabric were stabilized with pins as shown in Figure 4.2. This was done to prevent the sensor from moving around within the kit. To further stabilize the sensors within the kit, the sensors were hand stitched/tied to attach them to the fabric. This process was repeated for the second and third fabrics. Figure 4.3 shows a kit under construction and Figure 4.4 shows a completed fabric testing kit. The first and second sensors were protected with a silicone coating to prevent sensor malfunction due to saturation/electrical shorting during the human subject trials. A new kit was built for each human subject trial using new materials.

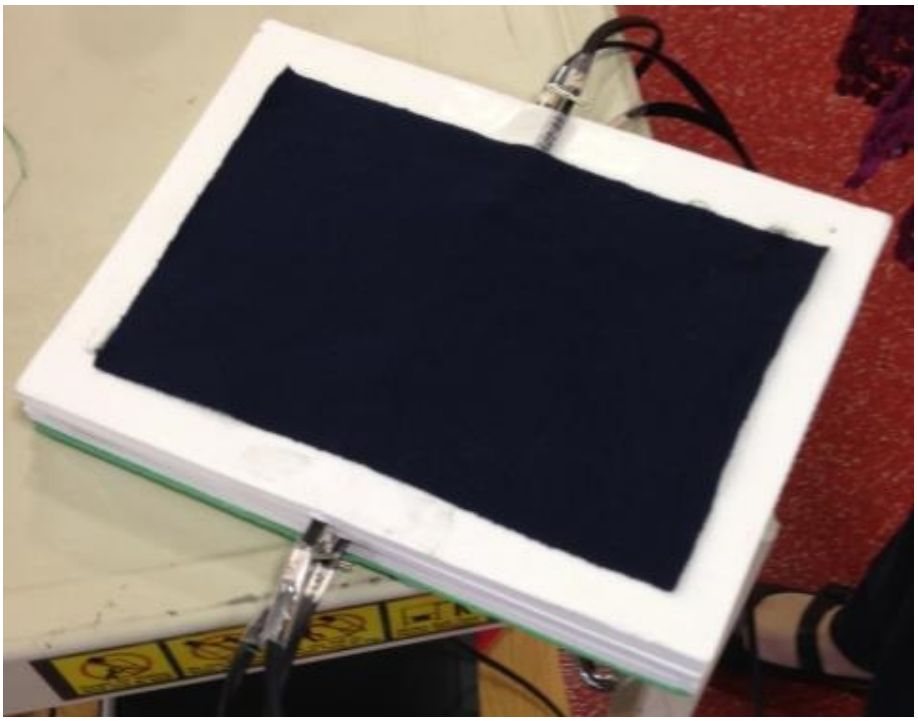

Figure 4.3: Fabric testing kit under construction

Figure 4.4: Complete fabric testing kit

4.1.1. Human Subject Profiles

Human subjects were recruited from active bicyclist and athletes who use the bicycle frequently in their training routines. All of the human subjects were accustomed to riding a bicycle for an extended period of time. These individuals were all athletic and capable of performing the human trial where they would be asked to ride a bicycle to produce perspiration. Both males and females participated in this study. A total of eleven different subjects were used in this research including seven males and four females. The height range for the males was 5 feet 8 inches to 6 feet 3 inches and for females 5 feet 5 inches to 5 feet 8 inches. The weight range for males was between 155 and 235 pounds. For females the

weight range was between 130 and 137 pounds. Figure 4.7 shows the height and weight of each of the eleven human subjects. As shown, one of the male subjects was significantly heavy than the rest while the females were very similar in terms of height and weight.

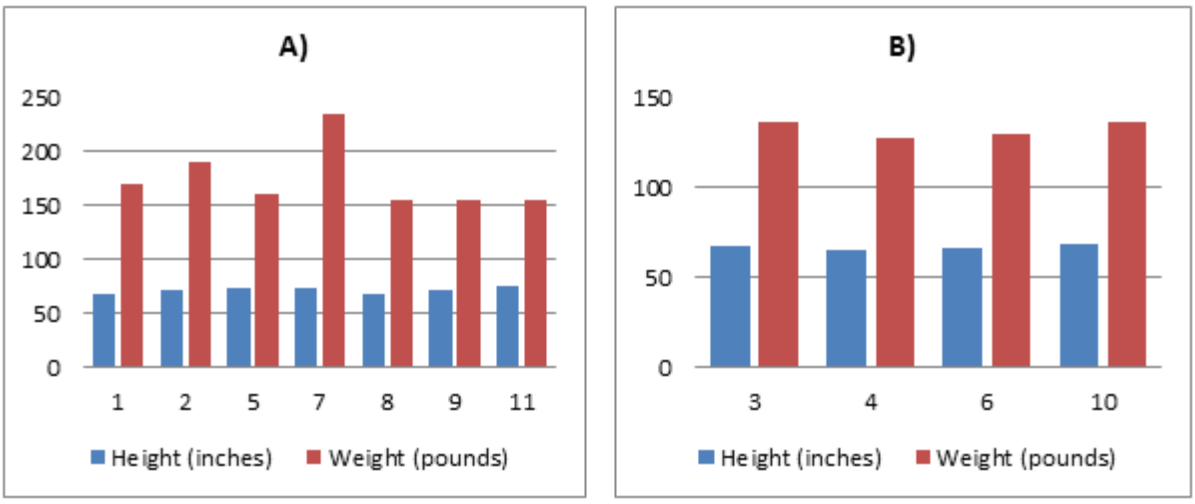

Figure 4.5: Human subject number by weight and height: A) Males, B) Females

4.1.2. Human Subject Trial Protocol

This protocol was approved by the Institutional Review Board – Human Subjects and was adhered to for every human subject and for every trial. When the human subject arrived at the athletic facility and are ready to perform the trial, they were asked questions from the survey created for this research (see Appendix). Afterwards, they were asked to make themselves comfortable sitting on the bicycle and make any seat height adjustments needed in preparation to the trial. Once the subject was situated on the stationary bicycle, several devices for monitoring the subject's vital signs were attached to their body including: heart rate, blood pressure, and blood oxygen monitors. Figure 4.6 shows the blood pressure cuff,

blood oxygen finger clip, and the display monitor for the vital signs. Once the vital sign monitoring was set-up on the subject and an initial reading had been established and recorded the fabric testing kit was be attached to the subject using approved medical adhesive tape. The sensors begin recording at the time right before the kit is attached to the subject's body in order to capture the initial response of the sensors as both the temperature and relative humidity changes immediately as it is placed near the skin even before the subject begins pedaling on the stationery bicycle. After the fabric testing kit was attached to the human subject's body as shown in Figure 4.7, the subject began pedaling at a slow pace to warm up on the bicycle.

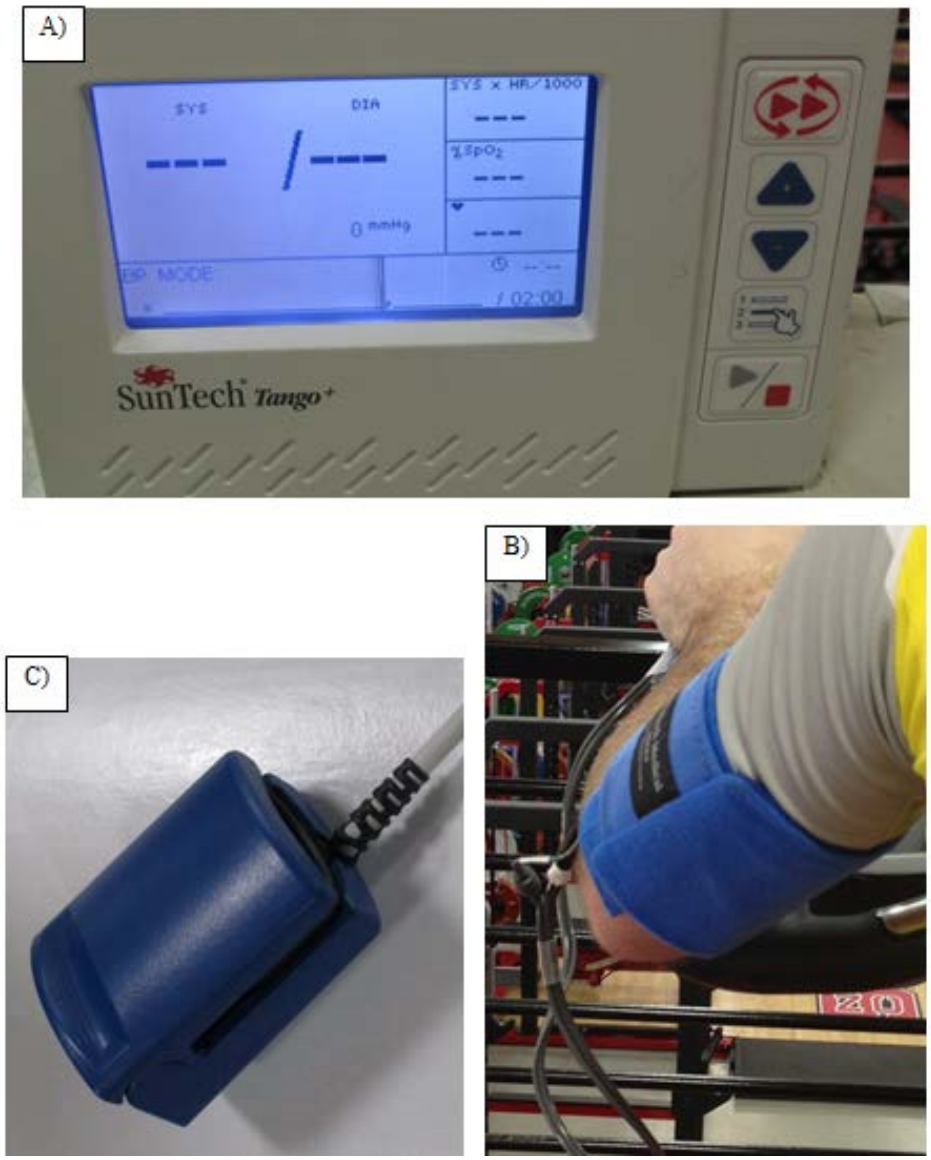

Figure 4.6: Vital Sign Monitoring: A) Display, B) Blood Oxygen Level and C) Blood Pressure Cuff

The subjects rode the stationary bicycle pedaling at a standard resistance level of 6 for five minutes and they were then asked to speed up. At this point, the subject could adjust the resistance setting in order to pedal at a rate that would keep their heart rate at the target of 135-155 beats per minute.

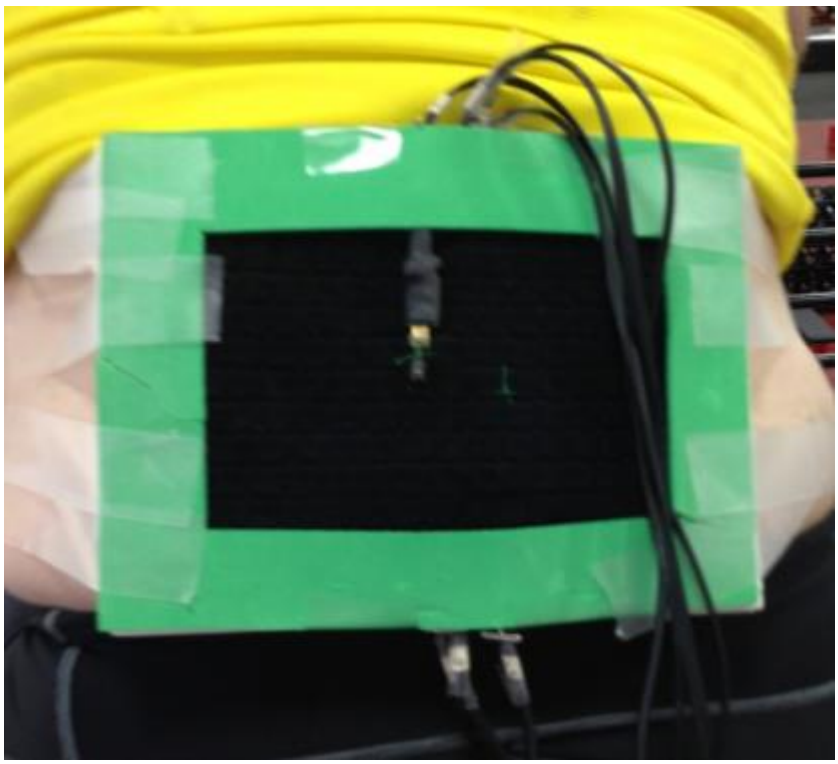

Figure 4.7: Fabric testing kit attached to subject's back

The subjects pedaled at that rate for an additional 30 minutes and then were asked to pedal slowly until their vital signs returned to the levels they had been before the trial commenced. During the trial, blood pressure, heart rate, and blood oxygen level were taken every 2 minutes and recorded. This monitoring data is not included in the dissertation as its purpose was to monitor the welfare of the human subject and not for heat and moisture transfer analysis.

Finding 1 of 17: Each trial was successful in inducing perspiration in the human subject early in the trial protocol and this particular bicycle routine in research measuring temperature and relative humidity changes during exercise. Figure 4.8 shows an image of a fabric testing kit after a trial where the fabric had become saturated and is noticeable wet.

Figure 4.8: Fabric testing kit after use showing wet area

4.1.3. Standard Kits

Initially, standard fabric kits consisting of three layers of the same fabric were used during the first series of experiments. Six out of the ten fabrics used in this study were chosen to construct the standard fabric kits. These particular fabrics were chosen because of their suitability to be used as any layer of clothing. Some fabrics were excluded because they were only suitable for outerwear garments and were either too heavy or dense to be used as a base or middle layer; these fabrics are identified in Table 3.1 of the previous chapter. Figure 4.2 shows each of the fabric testing kits and the fabric each layer consisted of as well as the

human subject number used for the particular kit. Figure 4.9 shows the temperature measurements gathered from these six human trials as recorded by an average of the first two sensors closet to the human subject's skin and before the first fabric layer of the kit. Although human subjects vary, Figure 4.9 shows that the temperature measurement profiles for each of the six standard kits were similar especially during the first twenty minutes of the trial. When initially placed on the body the sensors closet to the body all had an initial reading of around 23˚C +/- 1. There are some variations based on the time in which the sensors began recording and the time to attach the fabric testing kit to the subject's lower back. It can be assumed that the initial stable measurement is that time when the sensors were set to record but, the kit had not yet been attached to the back as both actions could not be done simultaneously. Temperatures all increased rapidly as the kit is attached to the body and heated by the skin temperature with all six of the increasing 8 to 10˚C with in the first ten minutes of the trial. All six of the kits reach their peak temperature and begin to level out about twenty minutes into the trial.

Finding 2 of 17: Throughout the first thirty minutes of the trial, the temperature measurements within the microclimate closest to the skin and before the first layer of the fabric testing kit did not vary more than 2 ˚C for the standard kits shown in Figure 4.9. While performing the bicycle protocol the human subject's body temperature will heat up and stabilize at a measurement around 33˚C +/- 2.

Table 4.2: Fabric Testing Kits

Kit Number	***Subject Number***	***Layer 1***	***Layer 2***	***Layer 3***
Kit 1	6	Fabric A	Fabric A	Fabric A
Kit 2	2	Fabric H	Fabric H	Fabric H
Kit 3	5	Fabric K	Fabric K	Fabric K
Kit 4	4	Fabric G	Fabric G	Fabric G
Kit 5	3	Fabric E	Fabric E	Fabric E
Kit 6	2	Fabric I	Fabric I	Fabric I
Kit 7	1	Fabric K	Fabric A	Fabric C
Kit 8	7	Fabric A	Fabric H	Fabric B
Kit 9	1	Fabric A	Fabric K	Fabric F
Kit 10	8	Fabric H	Fabric G	Fabric F
Kit 11	1	Fabric A	Fabric G	Fabric K
Kit 12	1	Fabric E	Fabric K	Fabric I
Kit 13	9	Fabric I	Fabric G	Fabric F
Kit 14	10	Fabric I	Fabric K	Fabric G
Kit 15	6	Fabric H	Fabric I	Fabric K
Kit 16	5	Fabric K	Fabric E	Fabric D
Kit 17	4	Fabric H	Fabric G	Fabric D
Kit 18	11	Fabric A	Fabric H	Fabric E
Kit 19	3	Fabric K	Fabric A	Fabric H

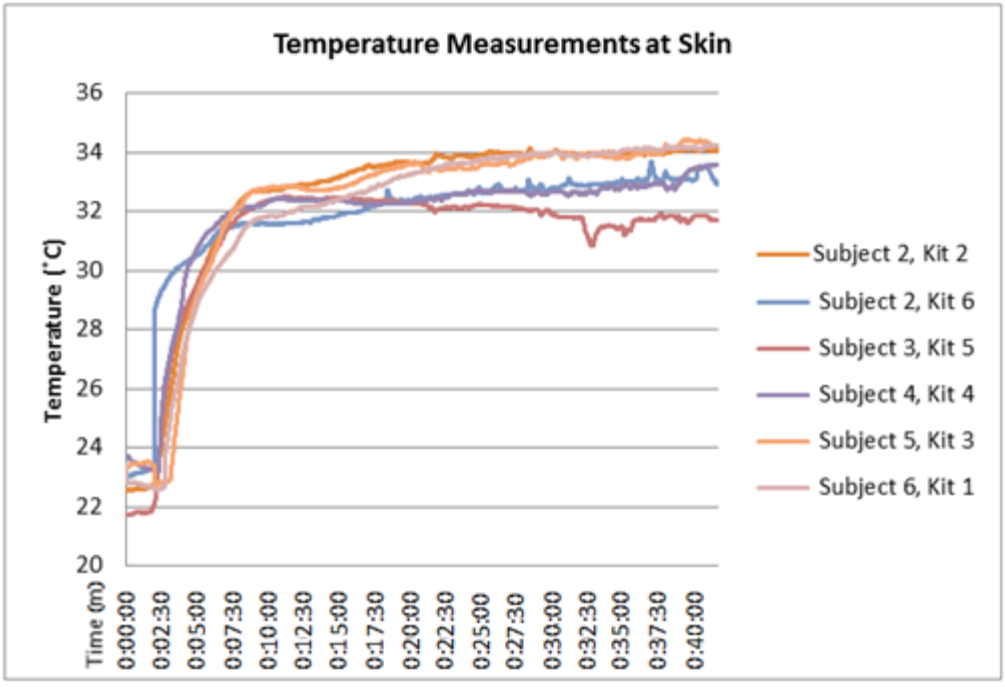

Figure 4.9: Temperature Measurement at Skin for Standard Kits

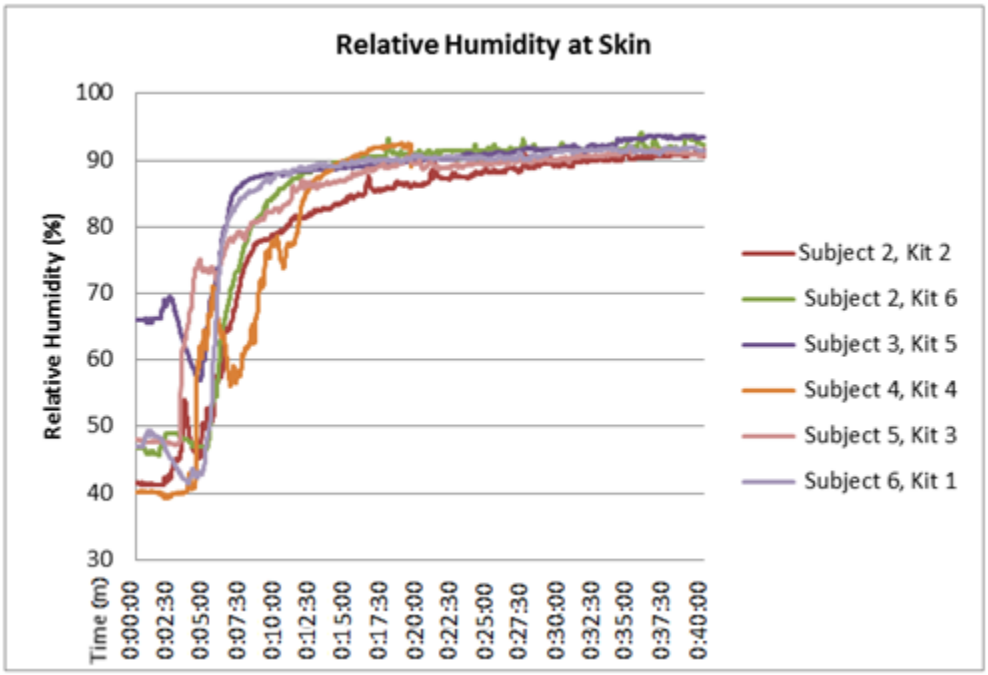

Figure 4.10: Relative Humidity Measurement at Skin for Standard Kits

The relative humidity measurement shows more variation from kit to kit. One very obvious reason this variation is that the study was conducted on site at an athletic training facility rather than a controlled laboratory environment. Initially, the range of relative humidity percentages are greater with the majority falling between 40 and 50 % RH and one kit (Kit 5) reading an initial 66 % RH. However, the relative humidity of Kit 5 quickly declined starting around the three minute mark of the trial. This decline spans approximately one minute and forty-four seconds where the humidity drops ten percent. At that point, the humidity begins to rise following a similar pattern as the other five standard fabric kits.

Finding 3 of 17: The standard kits' relative humidity relative humidity measurements were affected by the moisture released by the skin the kit is attached to the body with the majority increasing between 40-50% with in the first ten minutes of the trial. All six of the kits reach their peak relative humidity and begin to reach equilibrium (level out) at about 90% RH about twenty minutes into the trial. While performing the bicycle protocol the relative humidity in the microclimate next to the skin will reach upwards of 90% during the course of the human subject trial. A major reason for the variation in relative humidity from kit to kit could be attributed to the source of moisture in this study which was different human beings. It must be noted that human beings are very variable source for energy production especially in terms of their metabolic rate which is determined by many complex factors including but not limited to diet, physical fitness, hormone levels, mental state, etc. (all not measured in this study). A different human subject was used in each of the standard kit trials with the exception of Kit 2 and 6 in which the same human subject participated in both of these trials. The results of this initial analysis show that both relative humidity and temperature profiles

for each of the standard kits follow very similar and distinct patterns even when consisting different fabrics and using different human subjects. These initial results support this studies use of the human subject as an energy source for measuring fabric's ability to allow energy flow in the form of heat and humidity. Each test was successful in inducing a perspiration response from the human subject.

4.1.4. Human Subject Variation

Several of the human subjects participated in multiple trials; one male in four trials, three of the female and two male participates in two different fabric testing trials while the rest of the subjects participated in one trial each for a total of 17 trials each using different fabric combinations for the construction of the fabric testing kit. Figure 4.11 and 4.12 show how temperature can vary even if using the same human subject but, more importantly these figures include six instances where the fabric testing kit was attached to the body before the sensors began recording. Therefore, these kits do not include the complete warm up curve scenario where the temperature measurements show immediate response to the human subject's body. These kits have been analyzed in a different way from those kits which were set to record just prior to attaching to the human subject, i.e. time zero was defined by the event of attaching the kit. However, these trials are still valuable for all other analysis. Kit 8, 9, and 18 were started before the kit was attached to the body and are included in Figure 4.13. Figures 4.13 and 4.14 further support the evidence from the standard fabric kit analysis shown in Figure 4.9 and 4.10.

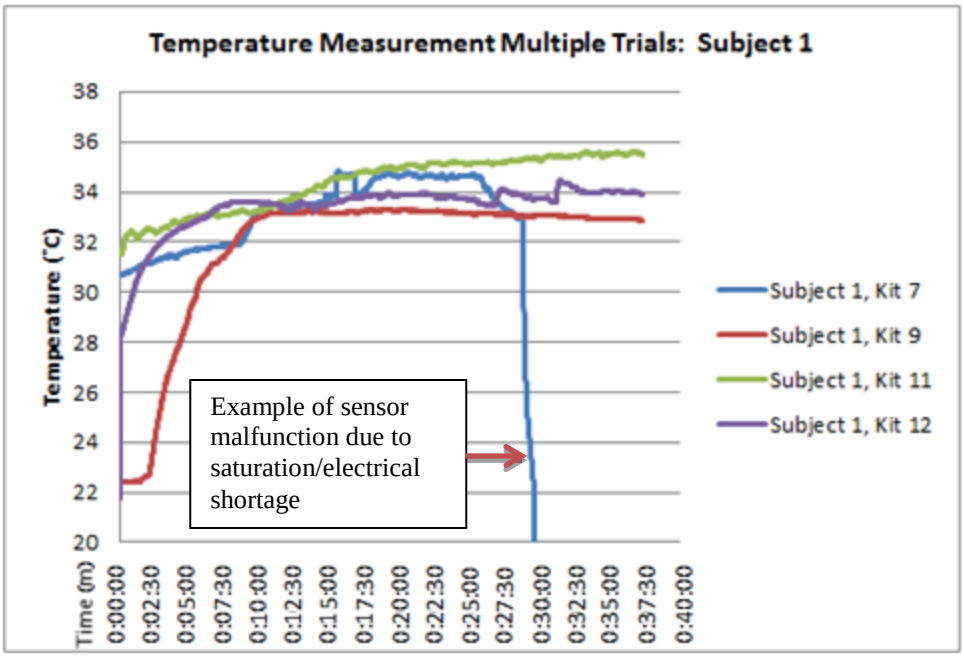

Figure 4.11: Temperature Measurement at Skin Multiple Trials with Same Subject

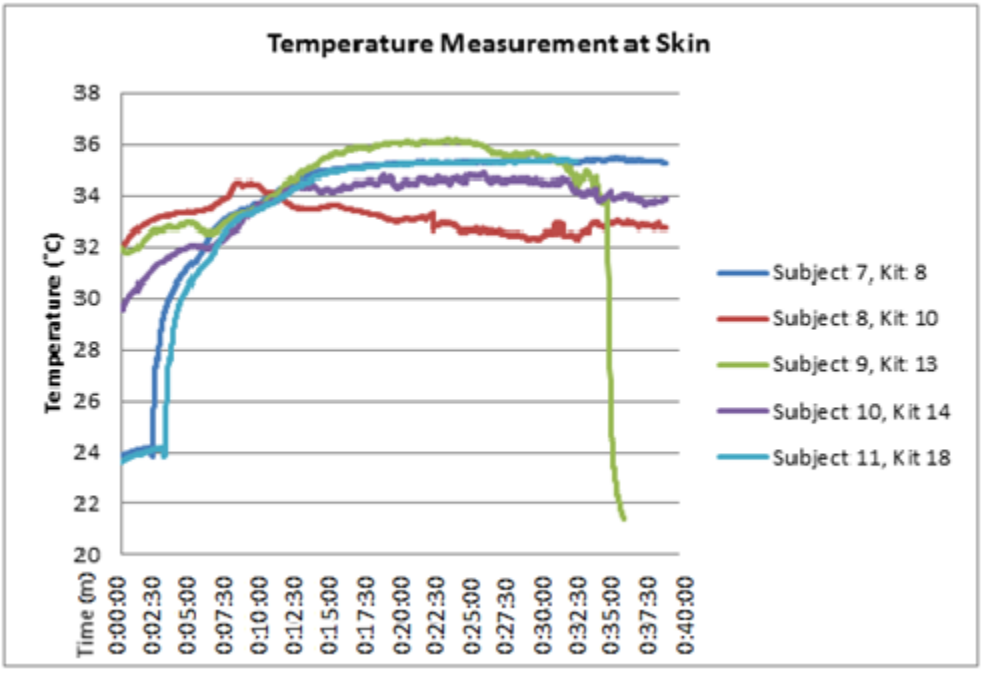

Figure 4.12: Temperature Measurement at Skin Multiple Trials with Different Subjects

Finding 4 of 17: Some very definite patterns emerge from Figure 4.13 and 4.14 which apply all the human subject trials: an immediate spike in temperature followed by humidity as the kit is attached to human subject, a period of rapid gain for the first 2-4 minutes afterward, a slower climb to steady for the next 10-12 minutes, and a continuation of this temperature and humidity from the 16 minute mark until the end of the trial. There are some fluctuations during this period but, all these instances correspond with recorded kit slippages (when medical tape became saturated kit would slip slightly on the subject's body requiring new tape and adjustment).

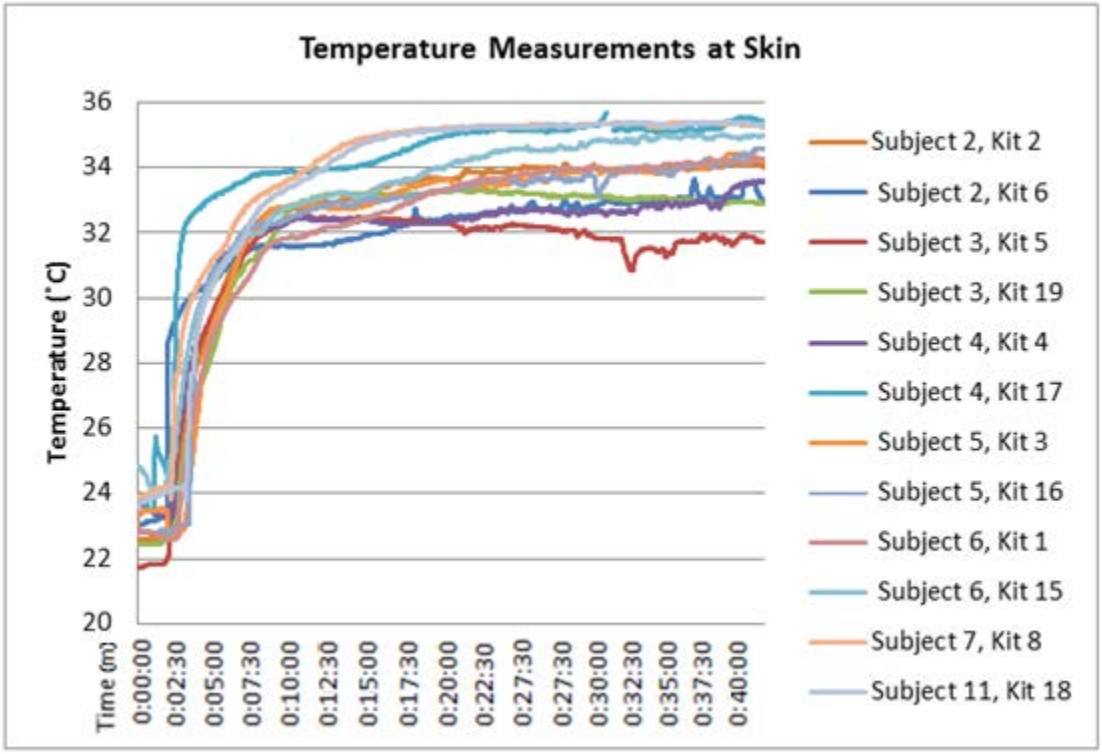

Figure 4.13: Temperature Measurement at Skin of Kits with Attachment Recorded

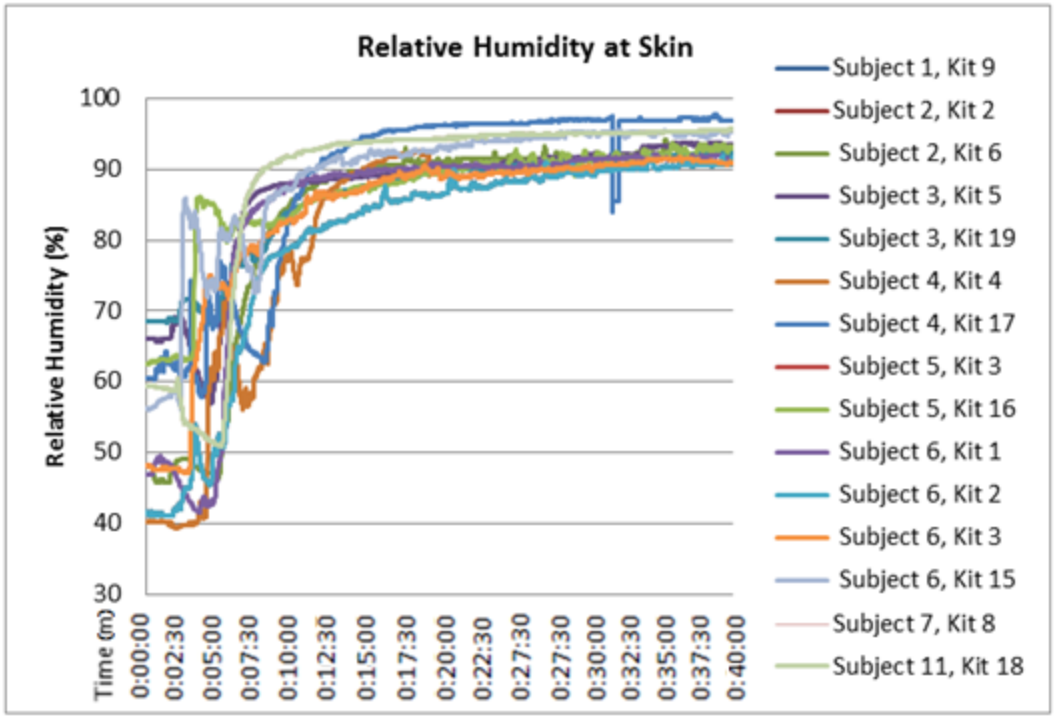

Figure 4.14: Relative Humidity % at Skin of Kits with Attachment Recorded

4.2. Onset of Perspiration

In order to analyze the vapor pressure movement within this standard fabric kit, the temperature and relative humidity was measured throughout the duration of the human subject trial. As shown in Figures 4.15 and 4.16 each of the eight sensors were able to measure temperature and relative humidity throughout the duration of the trial. This fabric testing kit (Kit 1 in Figures 4.15 and 4.16) consisted of Fabric A, H, and E. As shown, the temperatures and relative humidity measurements display distinct differences in at sensors on either side of a fabric layer. When the fabric testing kit is attached to the body there is an immediate change in temperature for the sensors closet to the skin. Initially, the relative humidity drops as the kit is attached to the skin as a response to the rise in temperature.

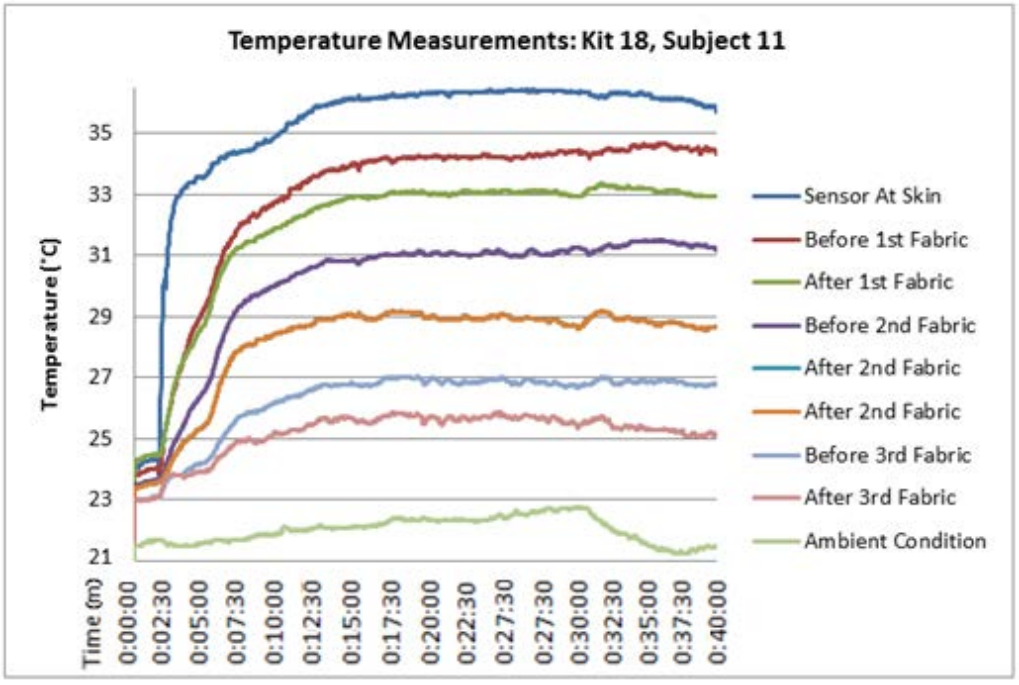

Figure 4.15: Temperature Measurement during fabric testing Kit 18, Subject 11 Human Subject Trial

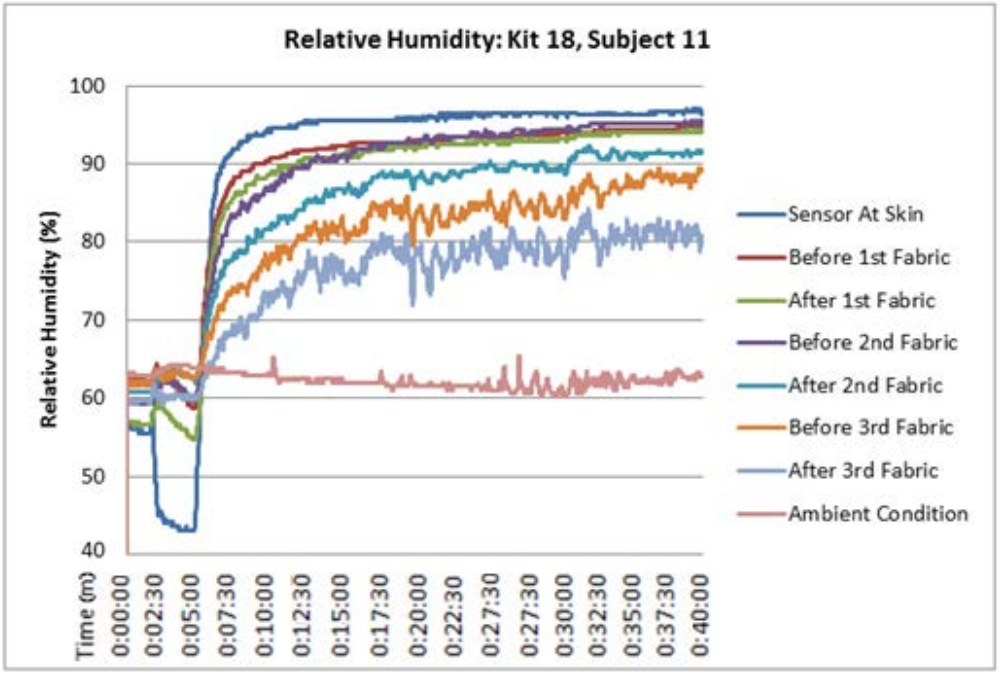

Figure 4.16: Relative Humidity Measurement during fabric testing Kit 1 Human Subject Trial

From these temperature measurements, energy flow using established thermodynamic equations which require a temperature gradient ($T_1 - T_2$) can be calculated. This analysis will be discussed later in the chapter.

Finding 5 of 17: graphing the measurements over time reveals that the eight sensors are capable of measuring differences in both temperature and relative humidity within the kit.

Finding 6 of 17: The trial temperature and relative measurements can be divided into distinct zones for analysis as shown in Figure 4.17. The first zone is the warm up zone when the kit is first placed on the body and the sensors begin responding to the body's temperature. This zone covers the first two to four minutes of the trial. The second zone, graphically shown as a slope, is the diffusion of moisture and heat taking place within the kit and this zone extends approximately eight to twelve minutes after the first zone. The third and final zone is marked by stability in the measurements and a relatively straight line on the graph which usually occurred for the last twenty minutes or more of the trial. Figure 4.17 shows the three zones graphically both for the temperature and the relative humidity. This scenario held true for all thirteen of the fabric testing kits in which measurements were began before kit was placed on the subject's body. From these results an analysis of the onset of perspiration during exercise can be conducted.

Finding 7 of 17: it was observed that, regardless of the subject or the fabric testing kit used, the onset of perspiration was sudden, graphically shown by the distinct slope caused by the rapid rate in which humidity increased inside the fabric testing kit worn by the individuals participating in this trial. As shown in Zone 2 of Figure 4.14, which started around the five minutes into the trial.

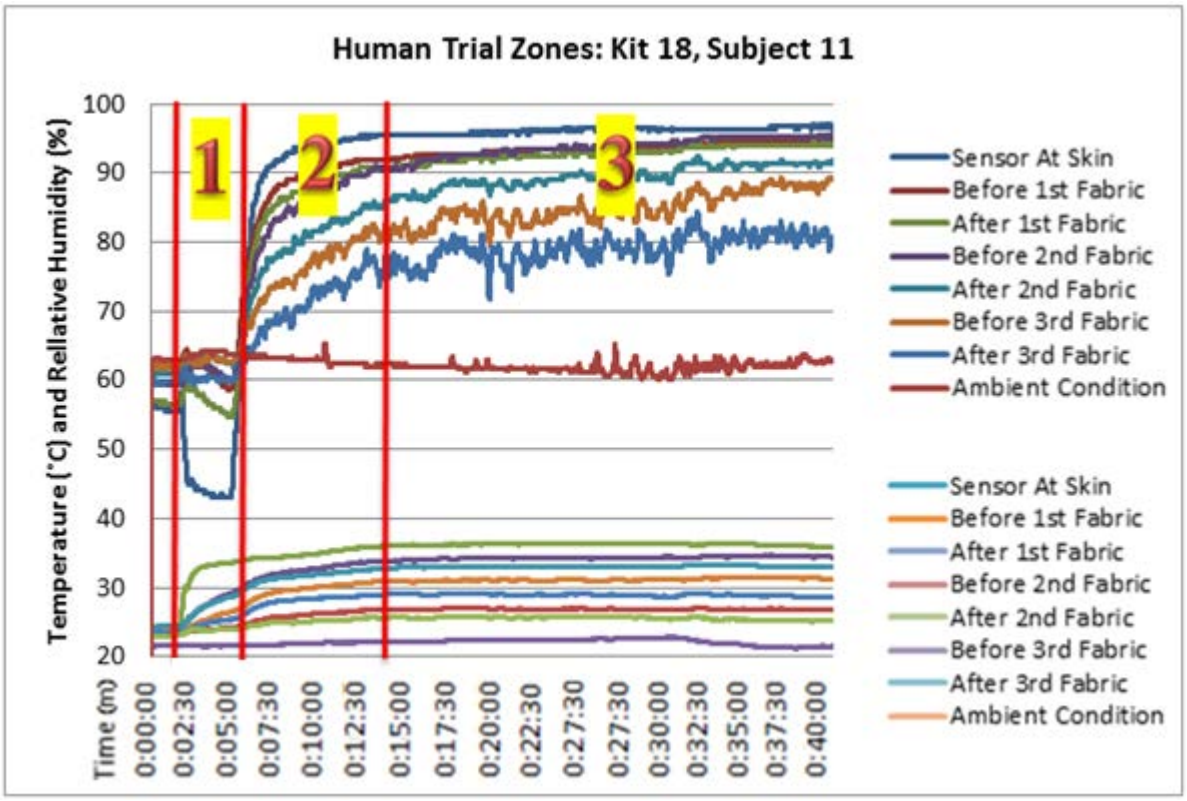

Figure 4.17: Temperature and Relative Humidity Divided into Zones

4.2.1. Vapor Pressure

Water vapor transport plays a significant role in determining the thermal comfort of a fabric since it represents the ability to transfer perspiration from the body. Perspiration leaves skin through pores, as the perspiration comes in contact with air it evaporates, turning from liquid to vapor. The movement of vapor is extremely important for moisture management fabrics (Lee & Obendorf, 2012; Mukhopadhyay & Midha, 2008). The water vapor resistance is determined by the ratio of vapor pressure gradient to heat flow, which is a parameter used by the sweating guarded hot plate instrument in terms of the measurement of the heat of evaporation (Huang, 2006; Huang, Zhanga & Qian, 2013). For our data analysis, vapor

pressure can be defined as either actual or saturated. The amount of water vapor in saturated air is dependent on the temperature of the mixture. At higher temperatures the capacity to hold water vapor is greater (Melesse & Abtew, 2013). Anderson (1936) confirmed that relative humidity percentage was not a measure of dryness but of the vapor pressure deficit, the difference between saturation vapor pressure and actual vapor pressure ($e_s - e_a$). Actual vapor pressure (e_a) is dependent on air temperature and humidity. Actual vapor pressure is computed from saturation vapor pressure (e_s) and relative humidity (Melesse & Abtew, 2013). Saturation vapor pressure can be calculated as follows:

$$e_s = 6.11x10^{(\frac{7.5\ X\ T}{237.7+T})}$$

where e_s is saturation vapor pressure in hectorPascals (hPa) and T (°C) is measured in degrees Celsius (Brice & Hall, 2009). Thus, actual vapor pressure can then be calculated for a give relative humidity as follows:

$$e_a = e_s(1 - \frac{RH}{100}).$$

The actual vapor pressure can also be derived from the dew point temperature (T_d) as follows:

$$e_a = 6.11x10^{(\frac{7.5\ X\ T_d}{237.7+T_d})}.$$

Actual vapor pressure is a measurement of the amount of water vapor in a volume of air; it increases as the amount of water vapor increases.

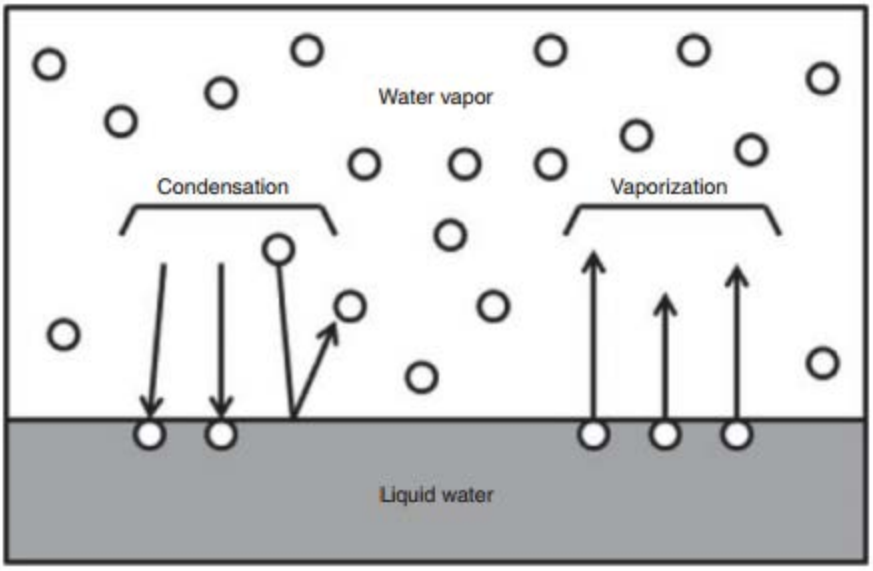

Figure 4.18: Evaporation and Condensation

Source: Shuttleworth, W.J. (2012). Water Vapor in the Atmosphere. In W. Shuttleworth (Eds.), Terrestrial Hydrometeorology. John Wiley & Sons, Ltd: West Sussex., p. 18.

When actual vapor pressure reaches saturated vapor pressure then evaporation is equal to condensation resulting in liquid water (Shuttleworth, 2012). Figure 4.18 depicts the vaporization and capture components of the evaporation process. To show how vapor pressure was analyzed for each of the human trials an example of a standard kit, Kit 1 consisting of three layers of 100% polyester thermal-lined double knit jersey fabric is used. Figure 4.19 shows the saturated vapor pressure as calculated from the temperature measurements at each of the eight sensors in this trial. Figure 4.20 shows the actual vapor pressure as calculated from the saturated vapor pressure and relative humidity measurements.

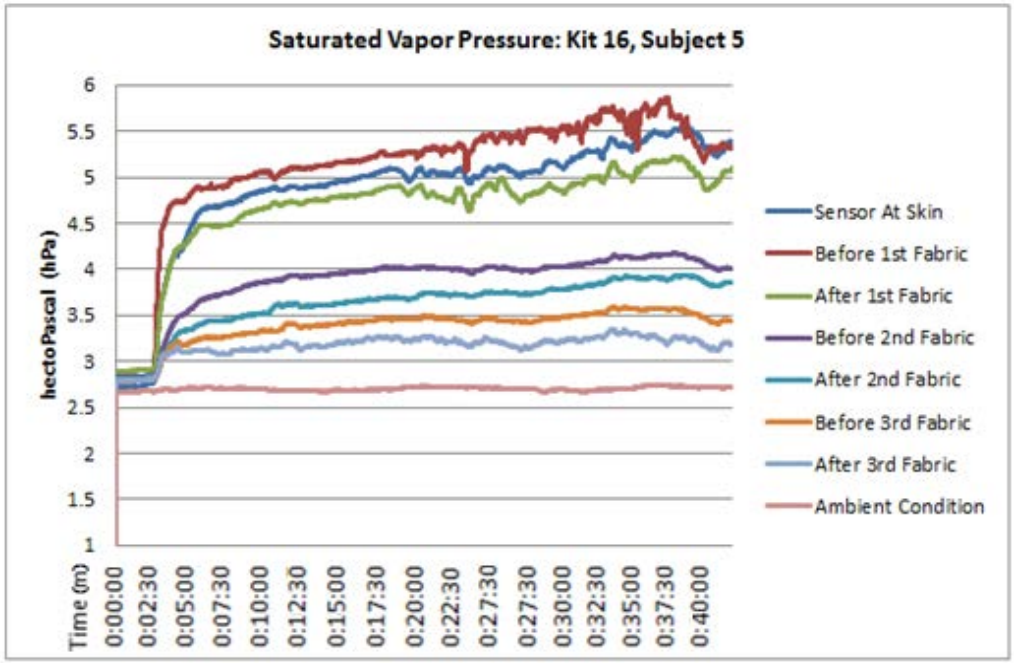

Figure 4.19: Saturated Vapor Pressure for Fabric Testing Kit 16, Subject 5

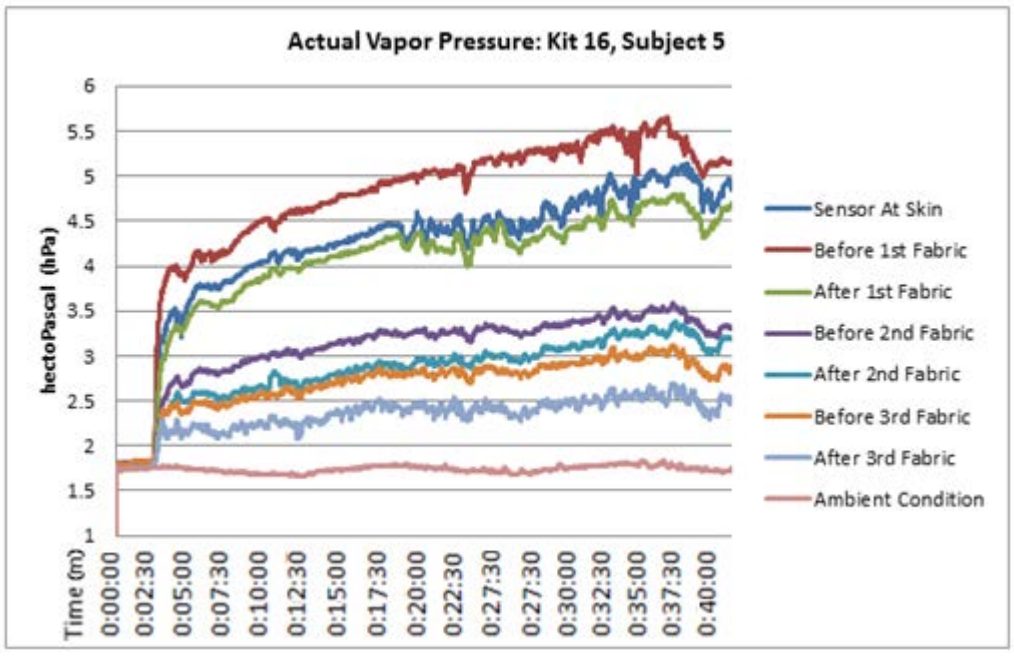

Figure 4.20: Actual Vapor Pressure for Fabric Testing Kit 16, Subject 5

The vapor movement change across each layer and each fabric was calculated from the difference between saturated vapor pressure and actual vapor ($e_s - e_a$) before and after each clothing layer as shown in Figure 4.19 and 4.20. As shown in Figure 4.21 the vapor pressure gradient or difference between saturated and actual vapor pressure during the first ten to twelve minutes of the test created the diffusion of moisture through the kit. After approximately ten minutes the difference between actual and saturated vapor pressure for the first fabric layer approaches and eventually reaches zero. At this point, the water vapor within this fabric is saturated.

Finding 8 of 17: from the sequence of temperature and humidity sensors, the research has confirmed that heat energy and vapor pressure flows from an area of higher temperature to an area of lower temperature.

Finding 9 of 17: it can be inferred from the graphical results that once actual vapor pressure reaches saturated vapor pressure the diffusion of moisture in the form of vapor is hindered. This may support theories of moisture of diffusion covered in Chapter 2 section 2.7, whereas if capillary actions are moving water vapor along the fibers, and these capillaries are blocked by saturation or liquid; diffusion would no longer occurs across these capillaries.

Finding 10 of 17: evidence in this data shows that once this saturation level has been achieved within fabric worn during exercise; without any outside disturbance i.e. air flow, temperature change, etc. diffusion of water vapor through the fabric will not recommence during an exercise routine.

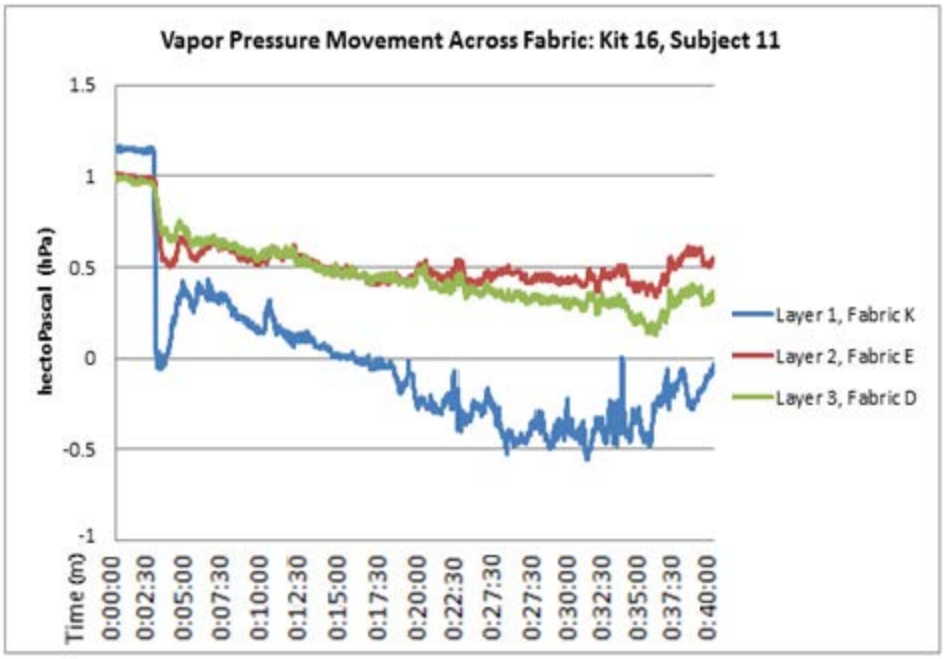

4.21: Vapor Pressure Change across Fabric Layers for Fabric Testing Kit 16, Subject 11

4.2.2. Conduction

Figure 4.22 which show these differences between the temperatures across fabrics as recorded by the sensors which can be used to calculate heat transfer by conduction. These results from the human trials also further confirm that heat energy flows from higher temperature to the lower temperature.

Finding 11 of 17: as shown in graphical form in Figure 4.22, there were distinct differences in temperature measurements at sensors on either side of a fabric layer. This supports what is known about textiles in that they prevent air movement and provide a shield against heat losses (Abdel-Rehim, Saad, El-Shakankery & Hanafy, 2006). Figure 4.22 shows these differences between the temperatures across fabrics as recorded by the sensors which can be

used to calculate heat transfer by conduction. These results from the human trials also further confirm that heat energy flows from higher temperature to the lower temperature.

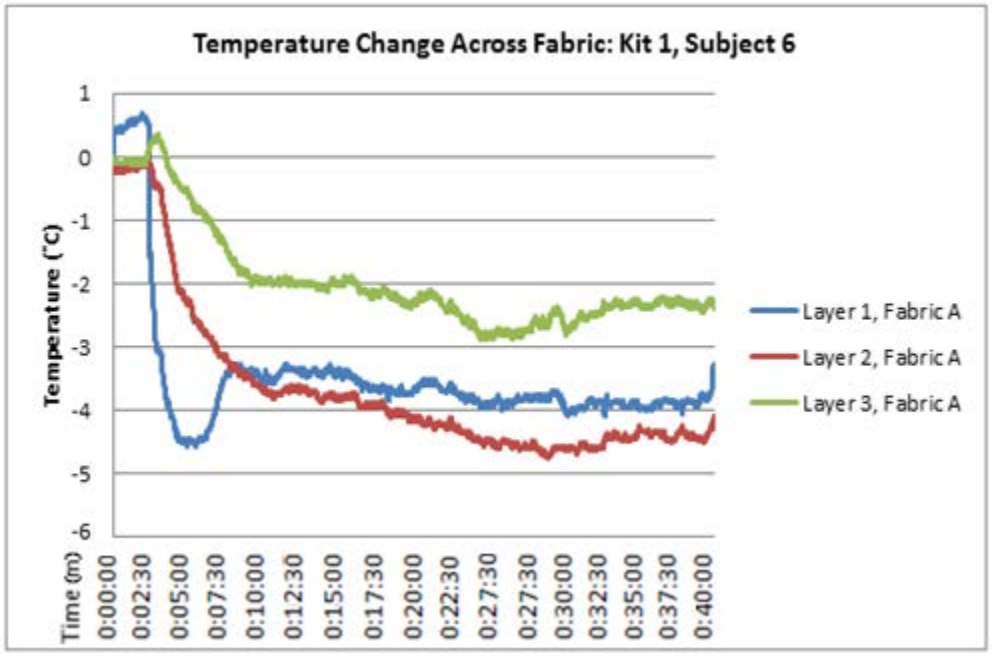

Figure 4.22: Temperature Change across Fabric Layers Kit 1

According to Fourier's law, the thermal resistance of the layer is an inverse relationship with the amount of heat energy flow, as shown in the following relationship:

$$R = \frac{\Delta T}{Q}$$

where ΔT is temperature gradient between two sides of a material, Q is heat flow, and R is thermal resistance or conductivity. This equation indicates that thermal resistance (R) is small when heat flow (Q) is large. The measurements gathered in this research's human subject trials allow for the calculation of the heat flow (Q) from the change in temperature

measurement ($T_1 - T_2$), the area (A), the material's thickness (L) and the fabric's conductivity (k) with the following equation:

$$Q = -kA(T_1 - T_2)/L.$$

For analysis, a conductivity value (k) of 0.05 $W/m\,℃$ was used for polyester fabrics or 0.04 $W/m\,℃$ was used for cotton and cotton blend fabrics (http://www.engineeringtoolbox.com/thermal-conductivity-d_429.html, http://physics.info/conduction/). It must be noted that conductivity values for fabrics vary depending not only on fiber type but other factors including but not limited to density, weave or knit structure, etc. (none of these parameters were measured in this study). The material's area and thickness were measured in this study. Figure 4.23 shows the heat transferred by conduction across each of the fabric layers within Kit 1. As shown graphically, the conduction values across the layer closet to the skin (Layer 1) increases rapidly as the fabric testing kit is placed on the body and the subject begins to warm up with exercise within the first 2-4 minutes. The second fabric layer increases less rapidly but, eventually reaches the same level as Layer 1. Fabric Layer 3 increases the least and never reaches the same level as the first two layers of fabric.

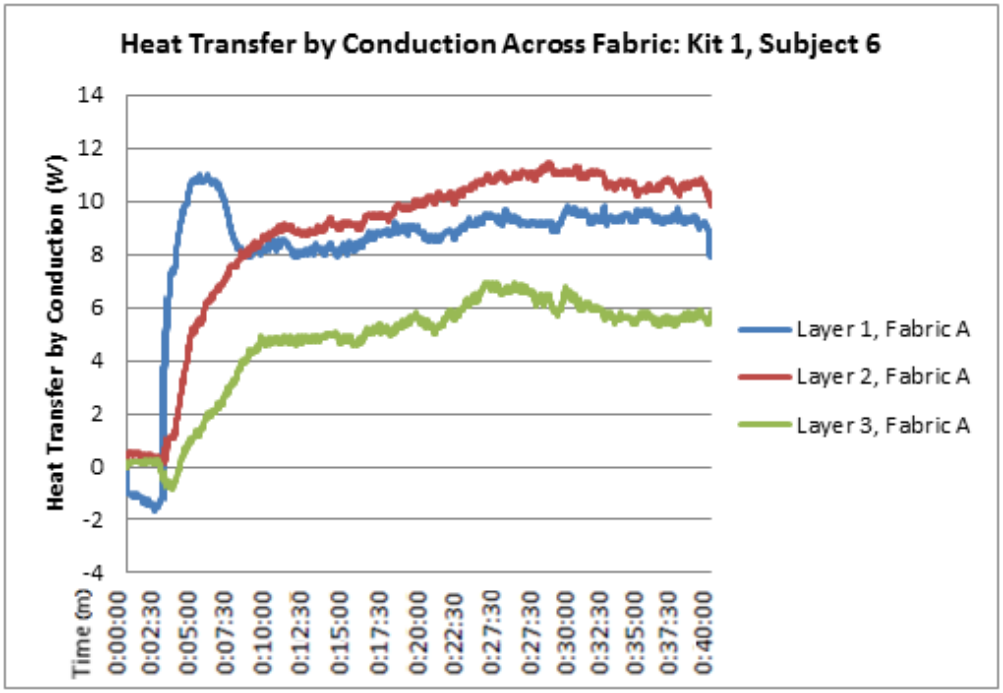

4.23: Heat Transfer by Conduction across Fabric Layers for Kit 1

4.2.3. Convection

Newton's Law of Cooling was used to in to calculate the amount of heat transferred through the fabric testing kits during the human subject trials. Newton's Law of Cooling equation:

$$Q = -hA(T_2 - T_1)$$

Where convection is (Q), the heat transfer coefficient is (h), area is (A), and the temperature difference is represented by (T_1) and (T_2). The temperature difference shown in Figure 4.22 is between the surface of the fabric on the side facing the body (T_2) and the side facing away from the body (T_1) and can also be used to calculate convection. The heat transfer coefficient value 3.122 (W/m^2) was taken from the ASHRAE handbook, while the other variables were

measured in this study. Figure 4.24 shows the heat transferred by convection across each of the fabric layers within Kit 1.

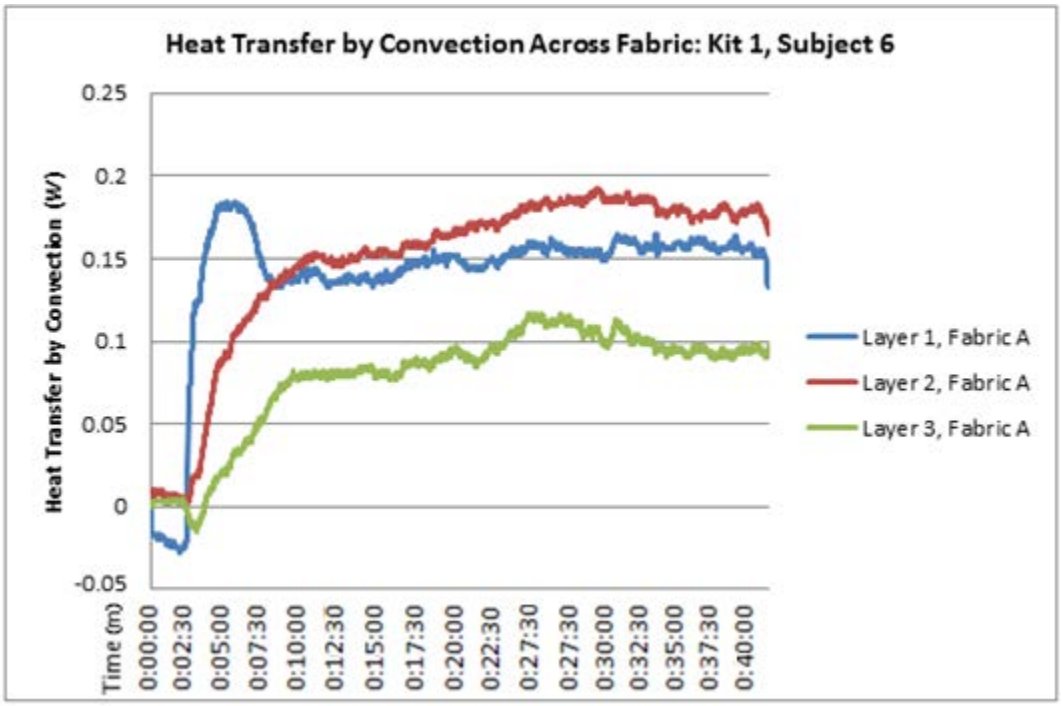

Figure 4.24: Convective Heat Transfer across Fabric Layers for Kit 1

4.2.4. Radiant Heat

To calculate radiant heat from the temperature measurements gathered during the trial using the following equation:

$$P = A\varepsilon\sigma(T_2^4 - T_1^4)$$

where σ is the Stefan-Boltzmann constant ($5.67\ X\ 10^{-8} W/m^2K^4$), ε is the thermal emissivity of 0.85 (http://www.optotherm.com/emiss-table.htm), and T_1 and T_2 are the

temperature measurements on either side of the fabric layer. Figure 4.25 shows the radiant energy flow across each of the fabric layers within Kit 1.

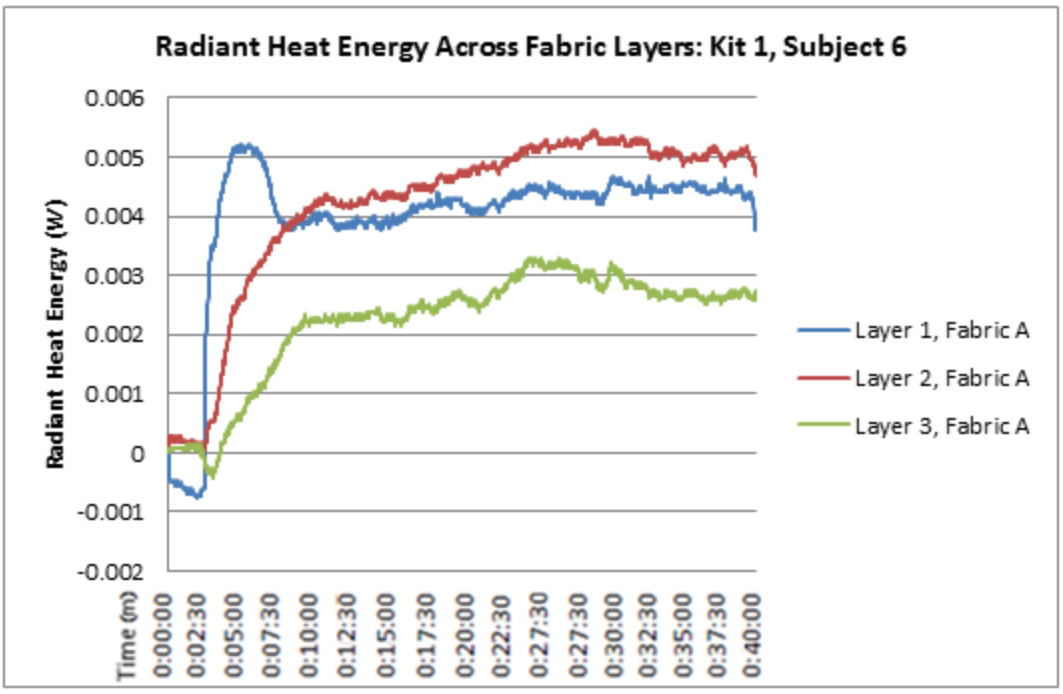

Figure 4.25: Radiant Heat across Fabric Layers for Kit 1

4.2.5. Enthalpy of Vaporization

The Clausius-Clapeyron Relation discussed in section 2.82 of this paper will be used to calculate the change in enthalpy governing the kinetic and potential energy of perspiration and heat released from the human subject's body during the duration of the trial. The enthalpy of vaporization is the energy that must be supplied to vaporize a mole of perpiration in the liquid state and is always positive, the enthalpy of condensation is the reverse and is always negative (Saha, 2008). The form of the Clausius-Clapeyron equation used to measure

the enthalpy of vaporization or condensation from the natural log of its vapor pressure versus temperature, as follows:

$$\Delta H_{vap} = \frac{R * \ln\left(\frac{P_2}{P_1}\right)}{\frac{1}{T_2} - \frac{1}{T_1}}$$

where T_1 and P_1 are temperature and vapor pressure at point 1, T_2 and P_2 are temperature and vapor pressure at point 2, ΔH_{vap} is the molar enthalpy of vaporization and R is the gas constant (8.314 $J\ mol^{-1}\ K^{-1}$). Figure 4.26 shows the enthalpy of vaporization and condensation with the point 1 measurements taken on fabric surface closest to the body and point measurements taken on the outside surface of the fabric for Kit 16 throughout the duration of the human subject trial.

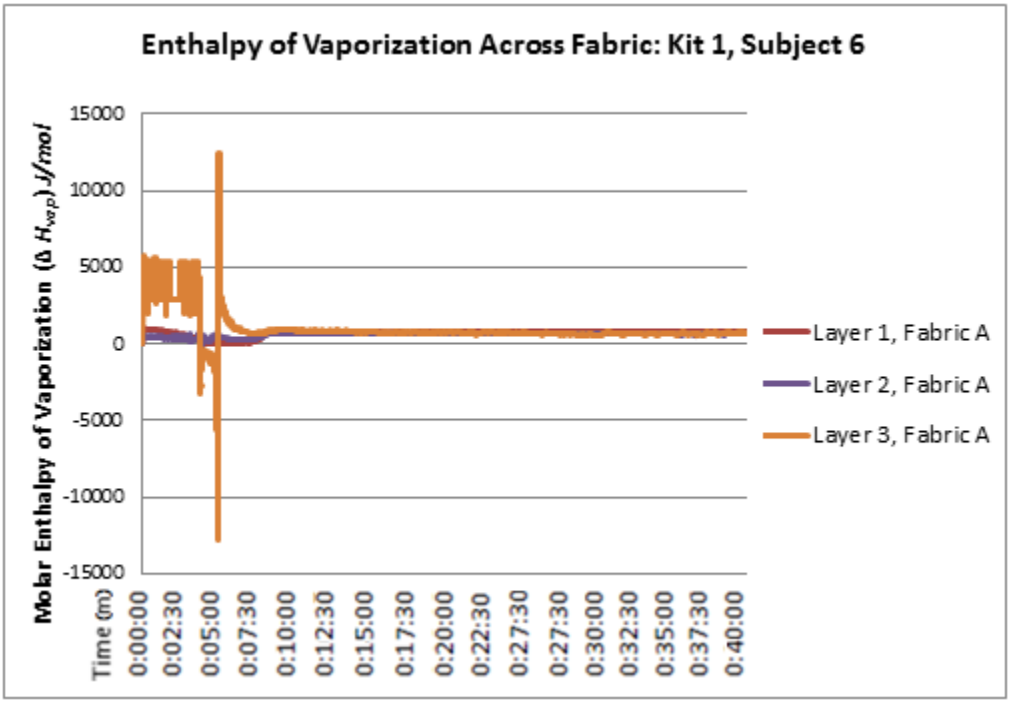

4.26: Molar Enthalpy of Vaporization and Condensation (Δ H_{vap}) *J/mol* for Kit 16

For the outer fabric layer of the kit (Fabric A), the enthalpy shows much fluctuation with high positive and high negative values as it interacts directly with the outside environment. According to the Clausius-Clapeyron relation, the negative values indicate enthalpy of condensation which is consistent with the saturated vapor pressures (e_s) calculated. Finding 12 of 17: as shown (Figure 4.26), the enthalpy fluctuation occurs across Layer 3 in Zones 1 and 2 of the trial which supports the previous analysis of vapor pressure and heat flow and the finding that the diffusion of moisture and heat occurs primarily in the first ten to twelve minutes of the trial. For the remainder of the trial, the enthalpy of vaporization remains between 600 and 900 J/mol (1000 J/mol is equal to 0.239 $kcal/mol$). The diffusion of moisture has slowed down during this period, but evaporation is a most important mechanism of heat transfer.

4.3. Fabric and Kit Consideration

4.3.1. Layer 1, Fabric A

100% PET thermal-lined double jersey fabric was used for the base layer of four different kits that were analyzed graphically calculating vapor pressure, conduction, convection, radiant heat, and enthalpy of vaporization, including: Kit 1, Kit 8, Kit 9, and Kit 18.

Vapor Pressure Layer 1, Fabric A

As shown graphically (Figure 4.27), each kit experienced a similar change with regards to vapor pressure during the first 2-4 minutes of the human subject trials with initial values in the range of 1.5 hPa +/- 0.5. After the initial warm-up period the vapor pressure change is rapid as shown by the sharp negative slope for all the kits shown in Figure 4.27. For all of

the kits shown with 100% PET thermal-lined double jersey (Fabric A), the first two layers of fabric all reach and surpass zero on the graph which has been identified as the theoretical point of vapor pressure saturation. However, the final layer, approaches but never reaches zero in all cases. This finding supports the hypothesis that vapor transfer is slowed by the saturated vapor pressure in the microclimate separating the layers of fabric. Other researchers have suggested that fabrics become saturated with liquid and they then become barriers preventing moisture movement to the fabric layer which interacts with the external environment. This research recorded very high relative humidity in the Kit but only was able to observe wetted fabric in the first layer. It can be observed from Figure 4.27 that vapor pressure differences measured either side of a fabric layer show the effect of the fabric types comprising the Kit.

Finding 13 of 17: the outer fabric layer (Layer 3) is least affected by the moisture from the human subject while Layers 1 and 2 are most critical in managing the moisture transfer, and when the vapor pressure difference becomes negative, the movement of moisture will slow or stall.

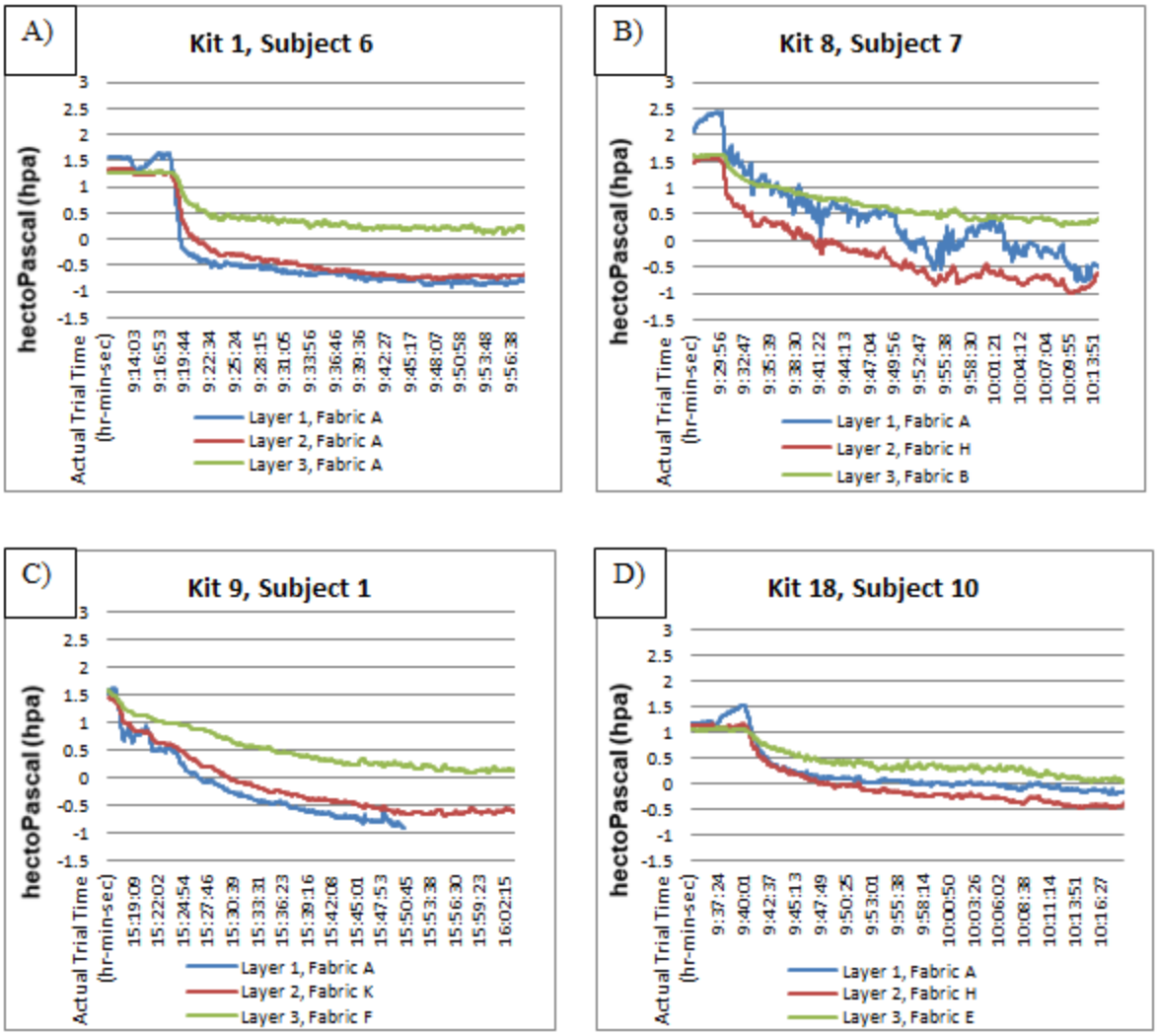

Figure 4.27: Vapor Pressure Movement across Fabric Layers (e_s-e_a) hectoPascal (hPa), Layer 1, Fabric A: A) Kit 1, Subject 6, B) Kit 8, Subject 7, C) Kit 9, Subject 1, and D) Kit 18, Subject 10

Conduction Layer 1, Fabric A

The conduction rates across the four fabric testing kits with 100% PET thermal-lined fabric are shown in Figure 4.28. As shown, once the fabric kit is attached to the body the conduction rate increases for each kit. Overall, the rate of conduction across the fabrics in the third layer (Layer 3) which interacts with the ambient environment changes the least throughout the trials especially Kits 8 and 9. As graphically shown the heat flow due to conduction for Kit 8 varies significantly for Layer 1 which indicates that the fabric used for the second and third layers of the fabric testing kit may be affecting the energy flow through the first fabric. Recall from Figure 4.27 the Layer 2 in Kit 8 became saturated most quickly and remained saturated throughout the duration of the trial while Layer 1 remained graphically similar to that of Layer 3 in terms of vapor pressure movement. As shown in Figure 4.19 were the vapor pressure movement ($e_s - e_a$) Layer 3 in Kit 8 and 9 remains at a higher level than the other fabric testing kits; in other words this less moisture is reaching Layer 3.

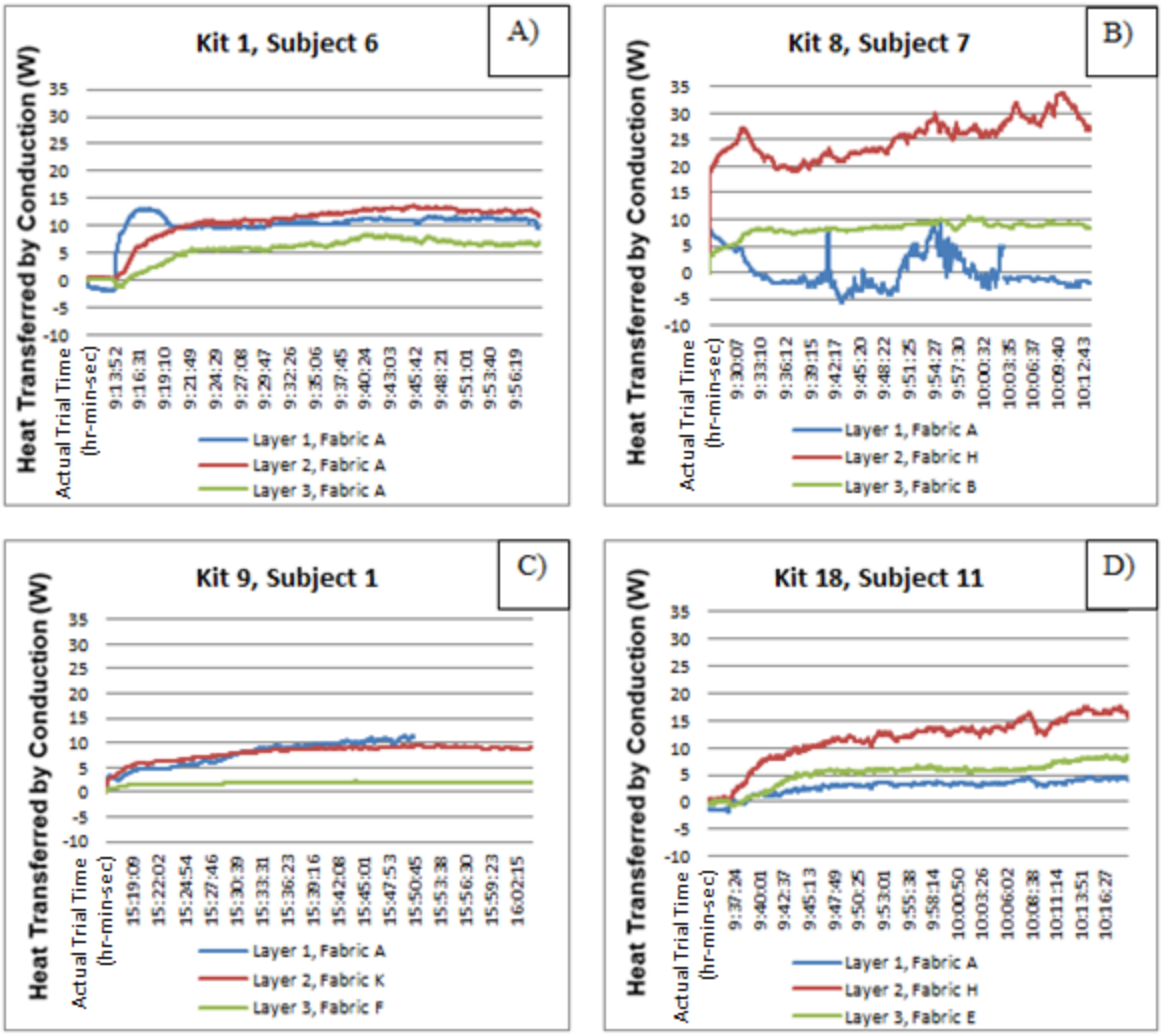

Figure 4.28: Heat Transfer across Fabric Layers by Conduction (W) Layer 1, Fabric A: A) Kit 1, Subject 6, B) Kit 8, Subject 7, C) Kit 9, Subject 1, D) Kit 18, Subject 11

Convection Layer 1, Fabric A

The convection rates across the four fabric testing kits with 100% PET thermal-lined polyester are shown in Figure 4.29. As shown, before the kit is attached to the body the rate of convection across the fabrics in the kits is approximately zero for all for kits. Once the fabric kit is attached to the body the convection rate increases for each kit and each fabric

layer with the exception of Kit 8. As shown in Figure 4.29, the first layer in Kit 8 decreases as the human subject exercises. In general, the rate of convection across the fabrics in the third layer which interacts with the ambient environment changes the least throughout the trials while Layer 2 changes the most throughout the trials with the exception of Kit 8. As graphically shown the rate convection for Kit 8 varies significantly for Layer 1 which supports Finding 14 of 17: that fabric used for the second and third layers of the fabric testing kit affects the energy flow through the first fabric. As with the conduction decrease shown in Figure 4.28, the convection decreases across Kit 8, Layer 1, Fabric A. The rate of convection does not react in the same manner at Kit 8, Layer 2, Fabric H which results in less moisture is reaching the third layer suggesting that in the case of Kit 8 the first fabric layer is creating a barrier impacting moisture and heat flow through the fabric testing kit.

Radiant Heat Layer 1, Fabric A

Figure 4.30 shows the radiant heat change across the four fabric testing kits with 100% PET thermal-lined polyester (Fabric A). For all kits shown (Figure 4.30), before the kit is attached to the body the radiant heat across the fabrics in the kits is approximately zero and remains a relatively small value throughout the human subject trial. Once the fabric kit is attached to the body the radiant heat increases with the exception of Kit 8, Layer 2, Fabric H.

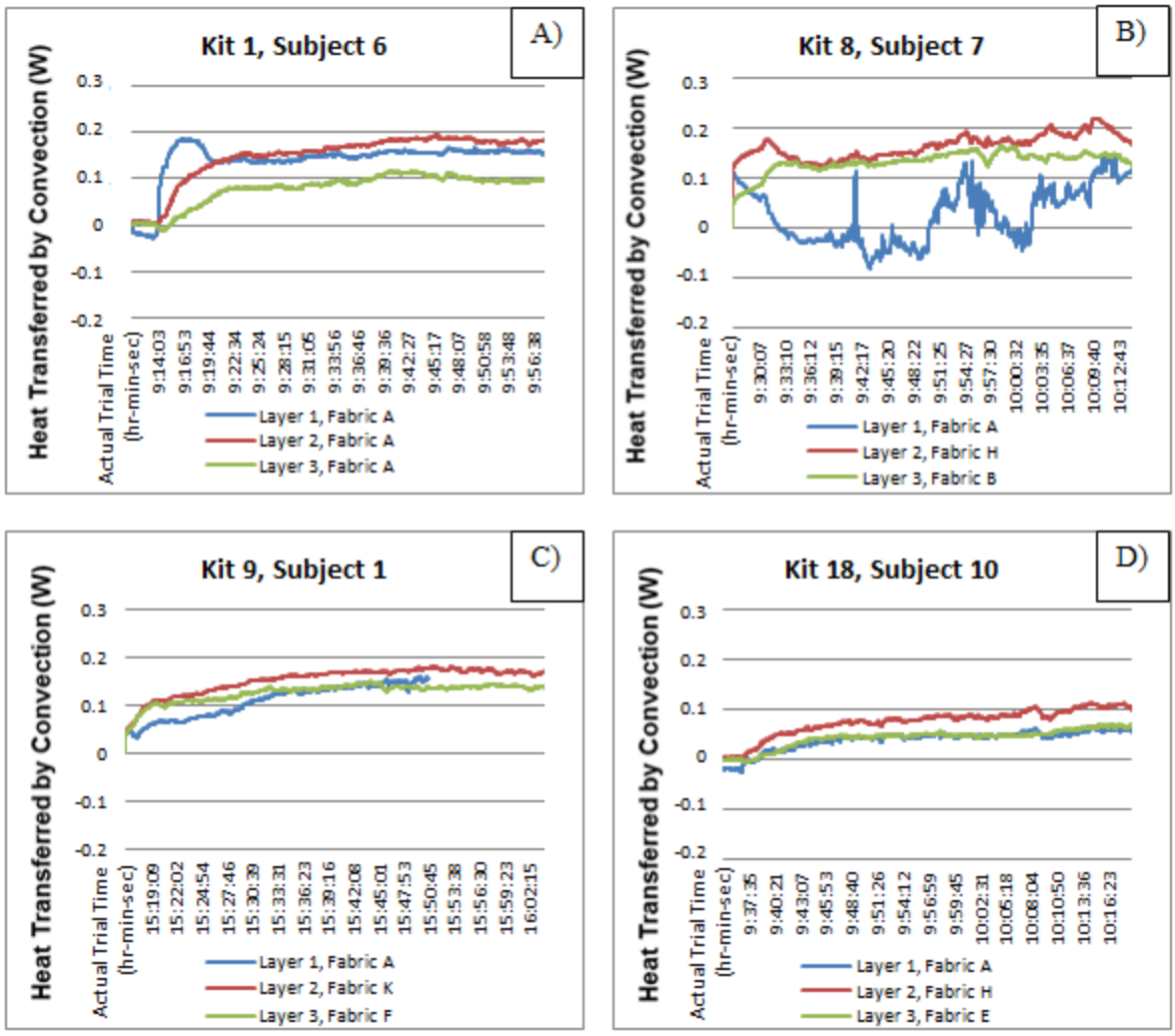

Figure 4.29: Heat Transfer across Fabric Layers by Convection (W), Layer 1, Fabric A: A) Kit 1, Subject 6, B) Kit 8, Subject 7, C) Kit 9, Subject 1, D) Kit 18, Subject 11

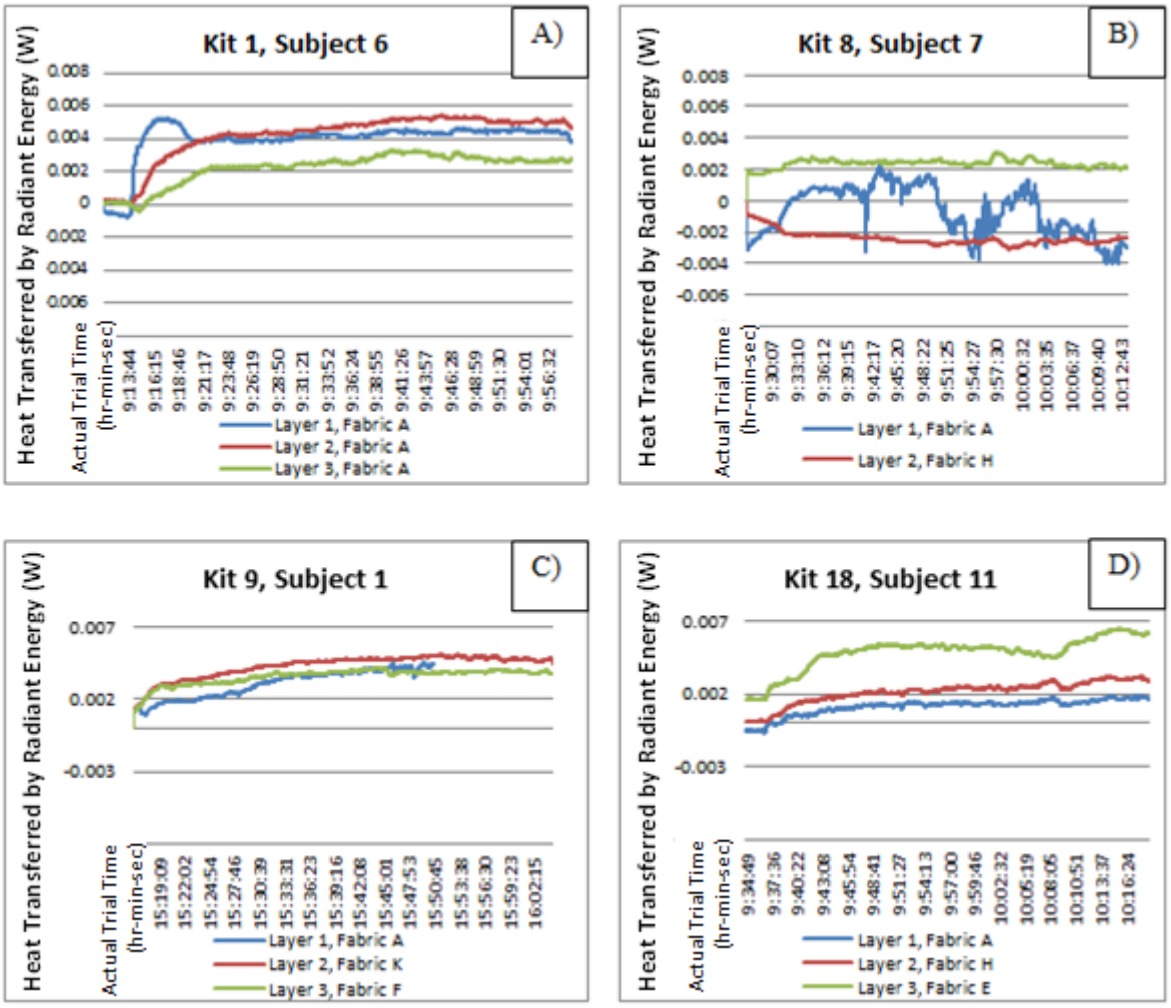

Figure 4.30: Radiant Heat Transfer (W) across Fabric, Layer 1, Fabric A: A) Kit 1, Subject 6, B) Kit 8, Subject 7, C) Kit 9, Subject 1, D) Kit 18, Subject 11

Enthalpy of Vaporization Layer 1, Fabric A

As shown in Figure 4.31, the majority of the enthalpy fluctuation occurs across in Zones 1 and 2 of the human subject trials as the diffusion of moisture and heat occurs primarily in the first ten to twelve minutes of the trial. The exception to this rule is Kit 8, Layer1, Fabric A which was the exception in each of the previous analyses in this section as thermal and

moisture management was hindered by the combination of fabrics within Kit 8 not allowing the energy flow to the outer layer (Fabric B).

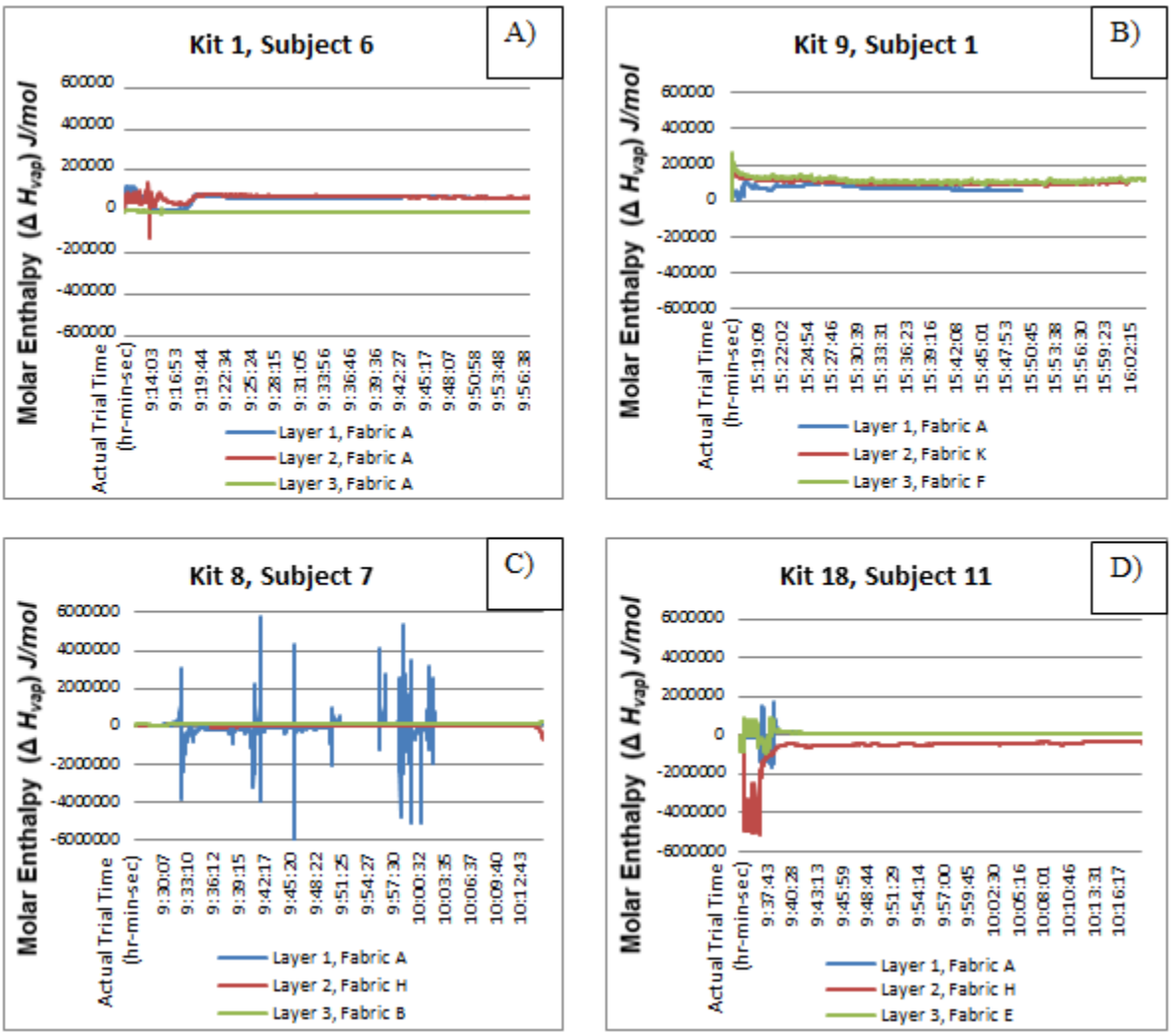

Figure 4.31: Molar Enthalpy of Vaporization and Condensation across Fabric (Δ H_{vap}) *J/mol,* Layer 1, Fabric A: A) Kit 1, Subject 6, B) Kit 8, Subject 7, C) Kit 9, Subject 1, D) Kit 18, Subject 11

4.3.2. Layer 1, Fabric K

95% Cotton, 5 % Elastane single jersey knit was used for the first layer of three different kits that were analyzed graphically calculating vapor pressure, conduction, convection, radiant heat, and enthalpy of vaporization, including: Kit 3, Kit 16, and Kit 19.

Vapor Pressure Layer 1, Fabric K

As shown graphically (Figure 4.32), each kit experienced a similar change with regards to vapor pressure during the first 2-4 minutes of the human subject trials with initial values in the range of 1.5 hPa +/- 0.5. After the initial warm-up period the vapor pressure change is rapid as shown by the sharp negative slope for all the kits shown in Figure 4.32. As with the previous fabric analyzed in section 4.3.1, the third fabric layer approaches but never reaches zero in all cases. Demonstrating that as the layer(s) closet to the body record a saturated vapor pressure and this becomes a barrier preventing moisture movement to the final layer whose role is to evaporate moisture to the outside environment. Kit 16, Layer 1, Fabric K exhibits a quick diffusion of vapor pressure early on in the trial giving a saturated vapor pressure very quickly but, the positive values shown on the graph indicates that some of that moisture was transported away from that fabric during that point of the trial. At this point in the trial, the fabric testing kit slipped on the subjects body and had to be readjusted which would introduce air flow into the system which affected the vapor pressure throughout the kit.

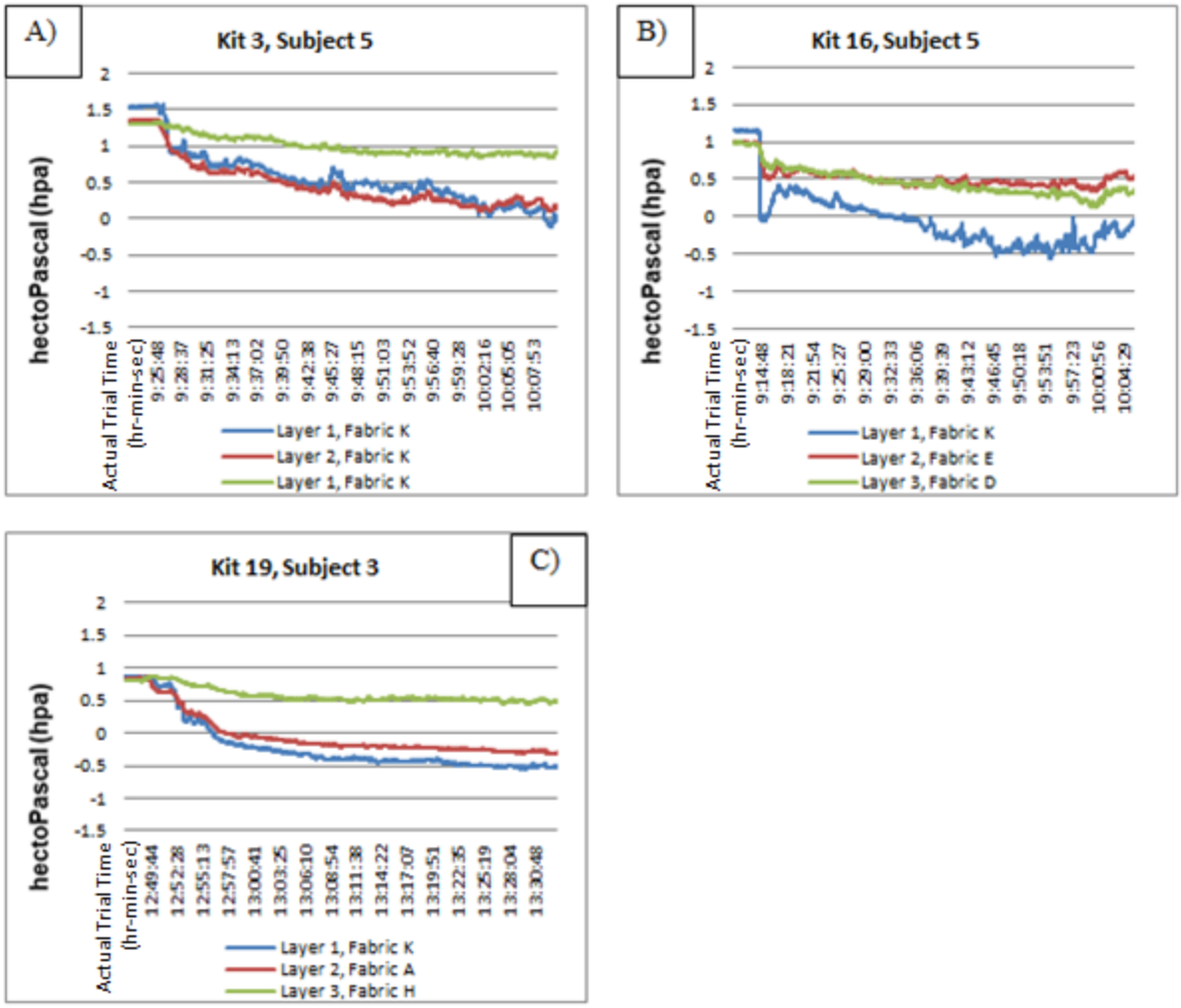

Figure 4.32: Vapor Pressure Movement across Fabric (e_s-e_a) hectoPascal (hPa), Layer 1, Fabric K: A) Kit 5, Subject 5, B) Kit 16, Subject 5, C) Kit 19, Subject 3

Conduction Layer 1, Fabric K

The conduction rates across the three fabric testing kits with 95% Cotton, 5 % Elastane single jersey knit fabric are shown in Figure 4.33. As depicted graphically, before the kit is attached to the body the rate of conduction across the fabrics in the kits is close to zero for all for kits. Once the fabric kit is attached to the body the conduction rate increases for each kit and each fabric layer with the exception of Kit 3. As shown in Figure 4.33, Kit 3, Layer 1, Fabric K decreases rapidly as the fabric testing kit is attached to the human subject and continues to increase for about a minute. This increase can be attributed to the temperature rising more rapidly at sensor 3 than sensor 2. Kit 16, which had to be re-attached due to pack slippage, is quite different from the other kits shown in Figure 4.33 in that the fabric at Layer 3 increases most rapidly and dramatically when compared layers 1 and 2. Layer 3 in Kit 16 consisted of Fabric D which is ultra-lightweight fabric (measured thickness 0.021 mm); heat flow due to conduction as defined in section 4.2.2 is dependent on fabric thickness.

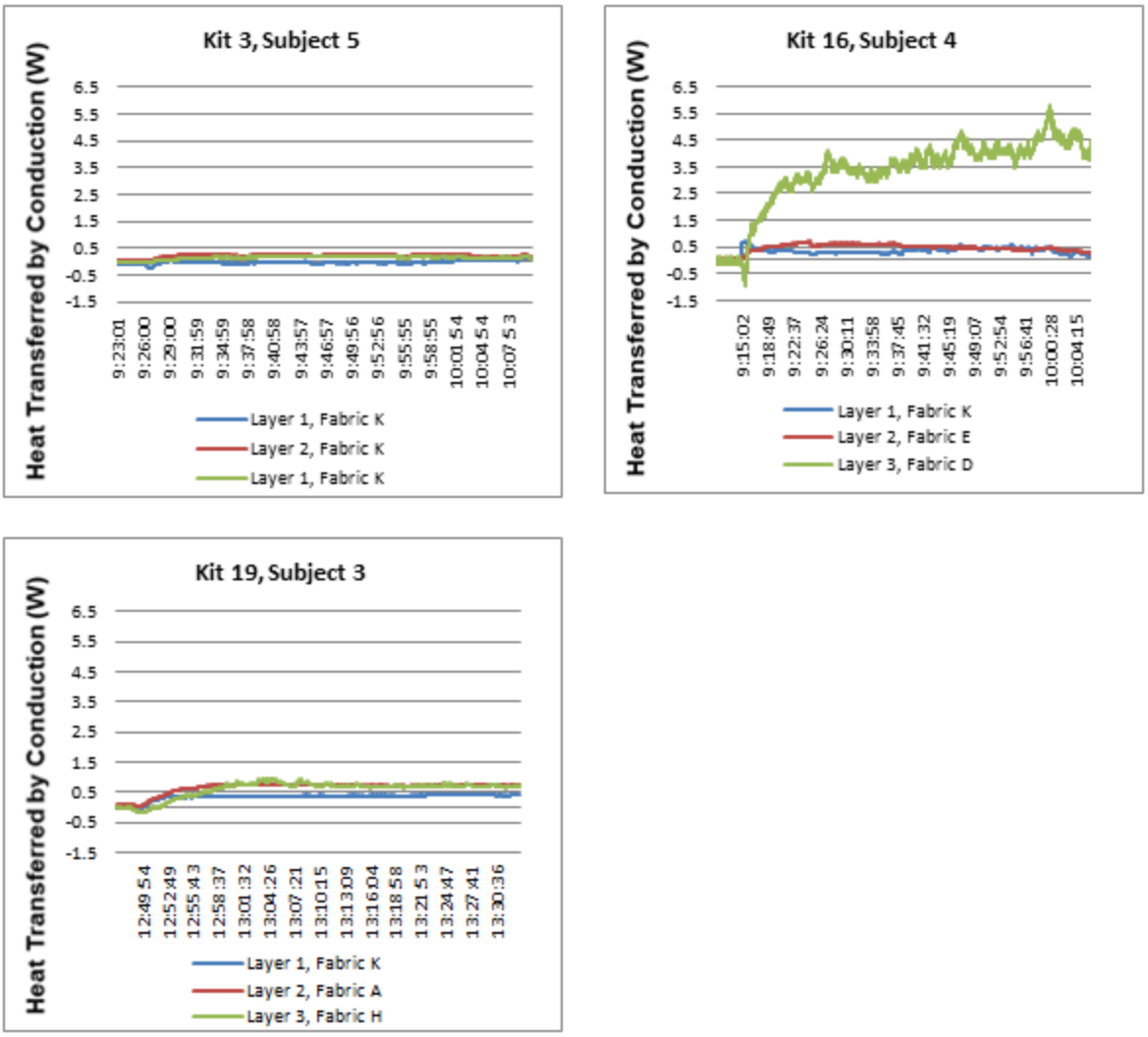

Figure 4.33: Heat Transfer across Fabric by Conduction (W), Layer 1, Fabric K: A) Kit 5, Subject 5, B) Kit 16, Subject 5, C) Kit 19, Subject 3

Convection Layer 1, Fabric K

Figure 4.34 depicts the convection rates across the three fabric testing kits consisting of 95% Cotton, 5 % Elastane single jersey knit fabric for their first layer. Before the kit is attached to the body the rate of convection across the fabrics in the kits is approximately zero for all for kits. Once the fabric kit is attached to the body the convection rate increases for each kit and each fabric layer with the exception of Layer 1, Fabric K in Kit 3. Layer 1, Fabric K in Kit 3 decreases as the fabric testing kit is attached to the human subject and continues to decrease for about a minute corresponding to the increase in conduction resulting from the temperature rising more rapidly at sensor 3 than sensor 2. For the all the kits in Figure 4.34, the rate of conduction across the third layer varies the least throughout the trials while Layer 2 changes the most throughout the trials with the exception of Kit 16. As shown in Figure 4.34, Layer 1 in Kit 16 shows an decrease in rate of convection early on in the trial and begins a positive slope afterwards as the fabric testing kit slipped on the subject's body and had to be readjusted. Similar to the case of conduction, the rate of convection for Layer 1 varies when different fabrics are used for the second and third layers of the fabric testing kit.

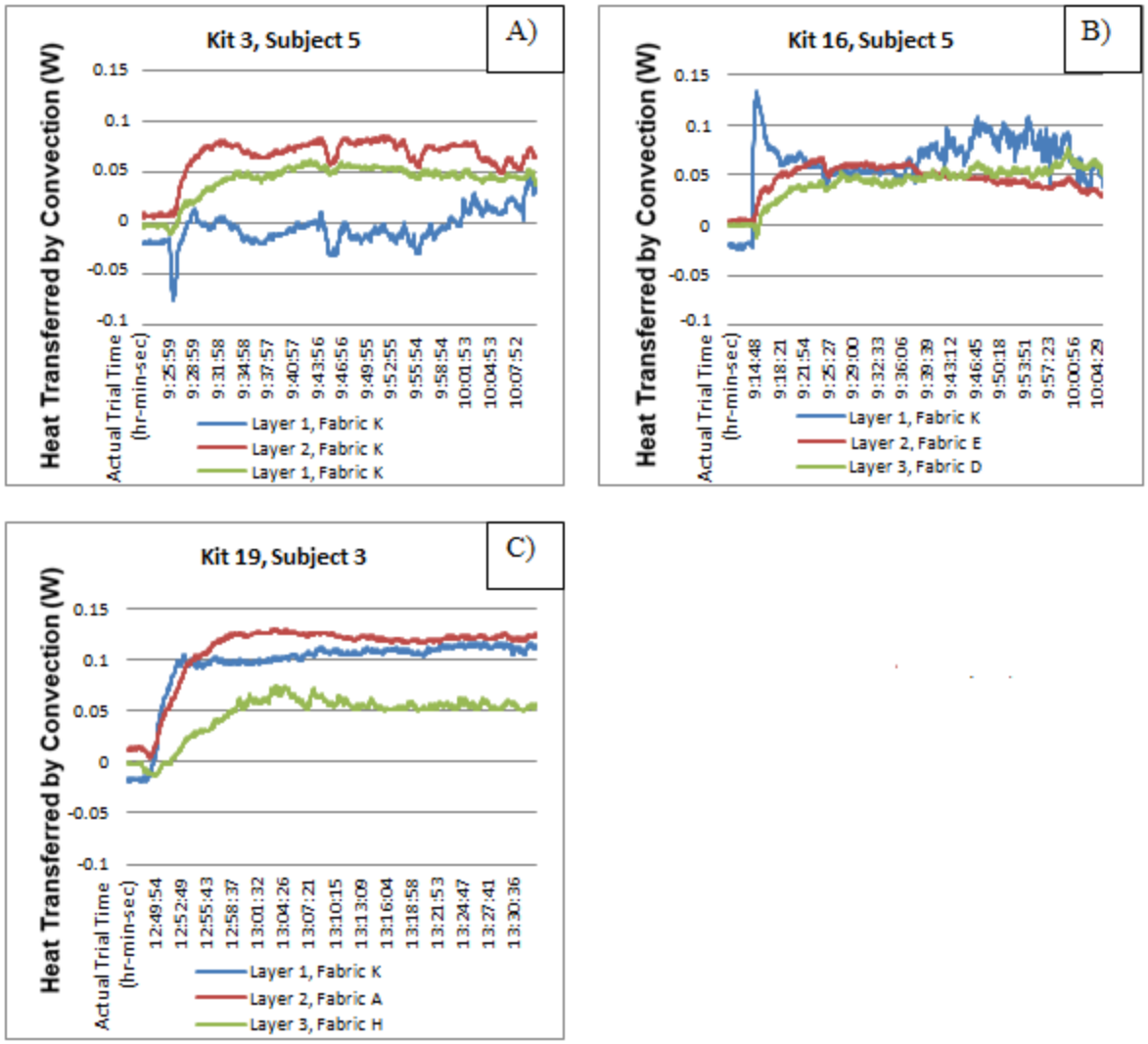

Figure 4.34: Heat Transfer across Fabric by Convection (W), Layer 1, Fabric K: A) Kit 5, Subject 5, B) Kit 16, Subject 5, C) Kit 19, Subject 3

Radiant Heat Layer 1, Fabric K

Figure 4.35 shows the rate of radiant heat change across the three fabric testing kits with 95% Cotton, 5 % Elastane single jersey knit (Fabric K) for Layer 1. For all kits shown (Figure 4.34), before the kit is attached to the body the radiant heat across the fabrics in the kits is approximately zero and once the fabric kit is attached to the body the radiant heat rate increases but remains a relatively small value throughout the human subject trial. Kit 3, Layer 1, Fabric K is the most unique of the graphs shown in Figure 4.35 whereas shown the heat flow due to radiant heat remains negative for the majority of the trial.

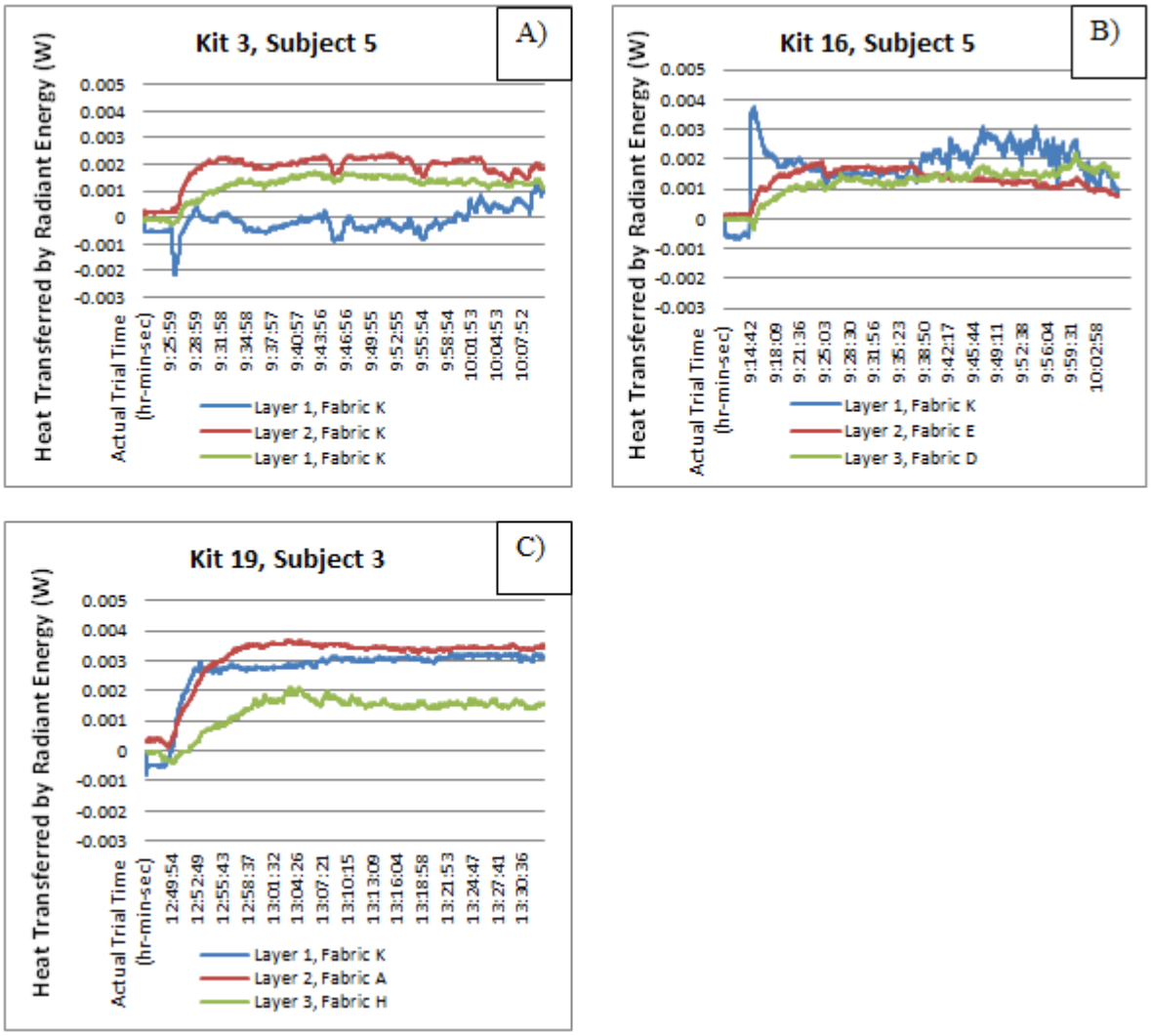

Figure 4.35: Radiant Heat Transfer across Fabric (W), Layer 1, Fabric K: A) Kit 5, Subject 5, B) Kit 16, Subject 5, C) Kit 19, Subject 3

Enthalpy of Vaporization Layer 1, Fabric K

As shown in Figure 4.36, the majority of the enthalpy fluctuation occurs across Layer 3 in Zones 1 and 2 of the human subject trials as the diffusion of moisture and heat occurs primarily in the first ten to twelve minutes of the trial. The exception where noteable fluctuations occur in Zone 3 was Kit 3, Layer1, Fabric A which was also an exception in each of the previous heat flow analyses in this section: conductivition, convection, and radiation.

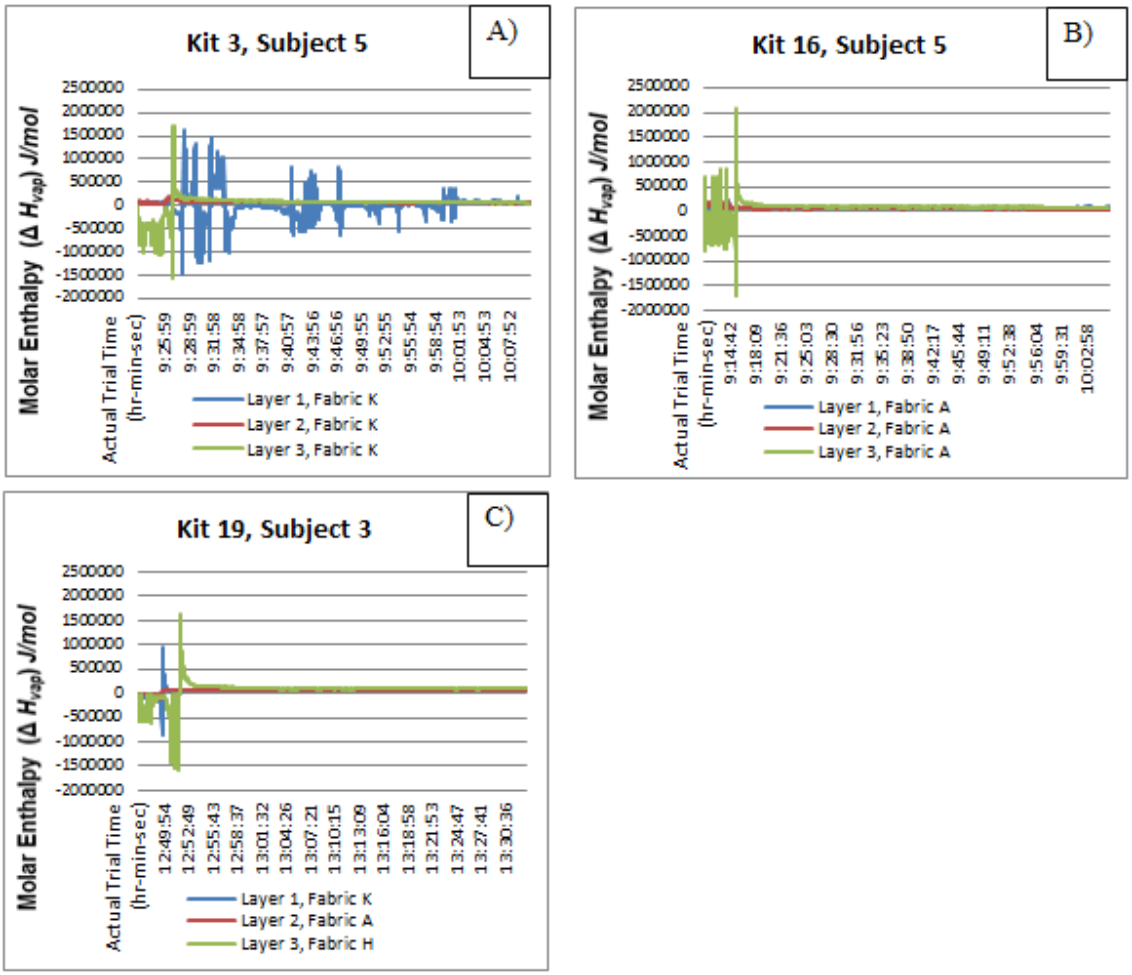

Figure 4.36: Molar Enthalpy of Vaporization and Condensation across Fabric (Δ H_{vap}) *J/mol*, Layer 1, Fabric K: A) Kit 5, Subject 5, B) Kit 16, Subject 5, C) Kit 19, Subject 3

4.3.3. Layer 1, Fabric H

100% PET double knit was used for the first layer of three different kits that were analyzed graphically calculating vapor pressure, conduction, convection, radiant heat, and enthalpy of vaporization, including: Kit 2, Kit 15, and Kit 17. These kits were also compared by dividing the trials into the three specific Zones: warm up, diffusion, and stability.

Vapor Pressure Layer 1, Fabric H

As shown graphically (Figure 4.37), each kit experienced a similar change with regards to vapor pressure during the first 2-4 minutes of the human subject trials with initial values in the range of 1.5 hPa +/- 0.5. After the initial warm-up period the vapor pressure change is rapid as shown by the sharp negative slope for all the kits shown in Figure 4.37. As with the other fabric choices for the first layer shown in this section (4.3), for the fabric testing kits shown in Figure 4.21, the vapor pressure movement varies quite noticeably with the fabric choice for the second and third layer. Finding 15 of 17: individual fabric performance is more dependent on the combination of fabrics used for a fabric testing kit rather than its own performance characteristics. Kit 2 consisted of 100% PET double knit for all three layers while Kit 17 consisted of 100% PET double knit for Layer 1, G- 86% PET, 14% Elastane single jersey knit for the Layer 2, and 100% Recycled PET ultra-lightweight plain weave for Layer 3. Fabric layers 1 and 2 have graphically similar moisture vapor movement profiles in both Kit 2 and Kit 17. Fabric layers 2 and 3 have graphically similar moisture vapor movement profiles in Kit 15 where the kit consisted of 100% PET double knit for Layer 1, 100% PET Mesh knit for Layer 2, and 100% Mesh Fleece knit for Layer 3.

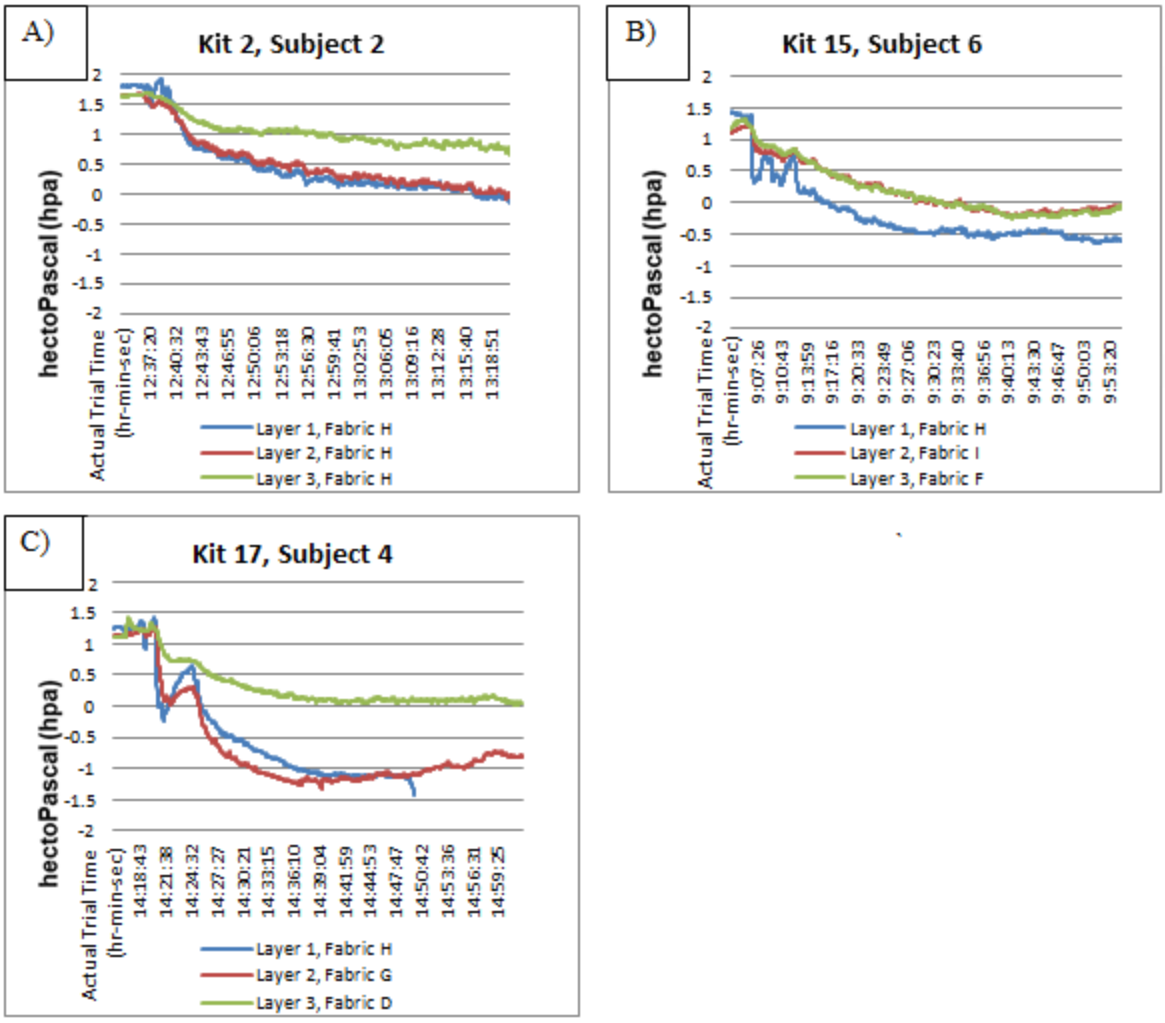

Figure 4.37: Vapor Pressure Movement across Fabric (e_s-e_a) hectoPascal (hPa), Layer 1, Fabric H: A) Kit 2, Subject 2, B) Kit 15, Subject 6, C) Kit 17, Subject 4

Conduction Layer 1, Fabric H

The conduction rates across the three fabric testing kits with 100% PET double knit used for the first layer of fabric are shown in Figure 4.38. As shown, before the kit is attached to the body the rate of conduction across the fabrics in the kits is roughly zero for all for kits. When the fabric kit is attached to the body the conduction rate increases for each kit and each fabric layer with the exception of Layer 3 in Kit 15 which stays graphically flat with a very slight downward slope throughout the human subject trial. Layer 3 consists of Fabric F a heavyweight fleece fabric (thickness measured 1.321 mm) that has a higher thickness which affects heat flow due to conduction. Kit 17, Layer 3 consists of Fabric D that is very thin as mentioned previously which accounts for the dramatic reduction in heat flow as shown graphically.

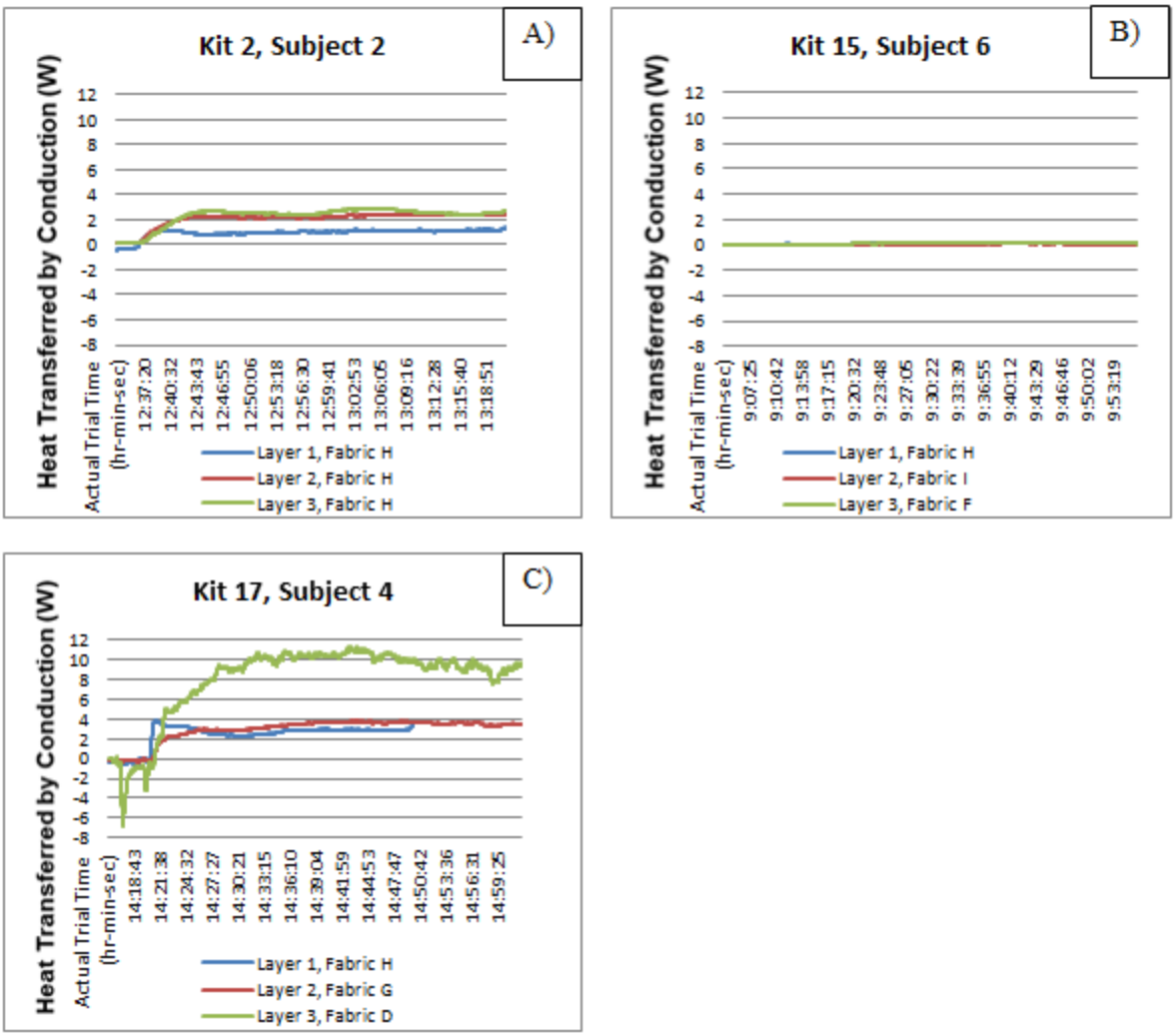

Figure 4.38: Heat Transfer by Conduction across Fabric (W), Layer 1, Fabric H: A) Kit 2, Subject 2, B) Kit 15, Subject 6, C) Kit 17, Subject 4

Convection Layer 1, Fabric H

The convection rates across the three fabric testing kits with 100% PET double knit for the first layer are shown in Figure 4.39. Before the kit is attached to the body the rate of convection across the fabrics in the kits is approximately zero for all for kits. After the fabric kit is attached to the body the convection rate increases for each kit and each fabric layer. In

general, the rate of convection across varies significantly for Layer 1 further supporting the idea that fabric used for the second and third layers of the fabric testing kit affects the energy flow through the first fabric.

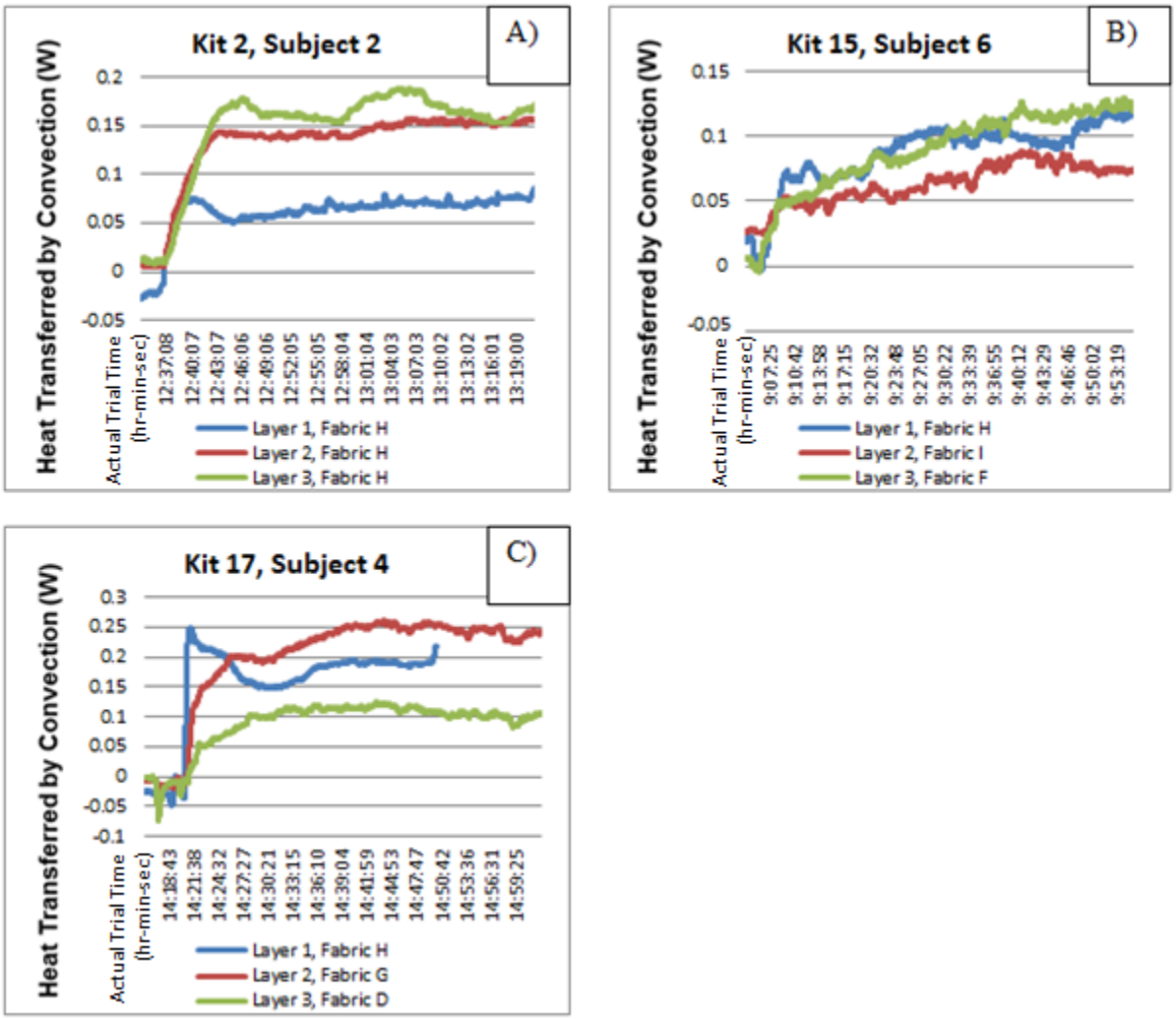

Figure 4.39: Heat Transfer by Convection across Fabric (W), Layer 1, Fabric H: A) Kit 2, Subject 2, B) Kit 15, Subject 6, C) Kit 17, Subject 4

Radiant Heat Layer 1, Fabric H

Figure 4.39 shows the radiant heat change across the three fabric testing kits with 100% PET double knit (Fabric H) for the first layer. For all kits shown (Figure 4.39), remains a relatively small value throughout the human subject trial. Once the fabric kit is attached to the body the radiant heat increases with the exception of Layer 1 and 2 in Kit 15 and Layer 1 in 17.

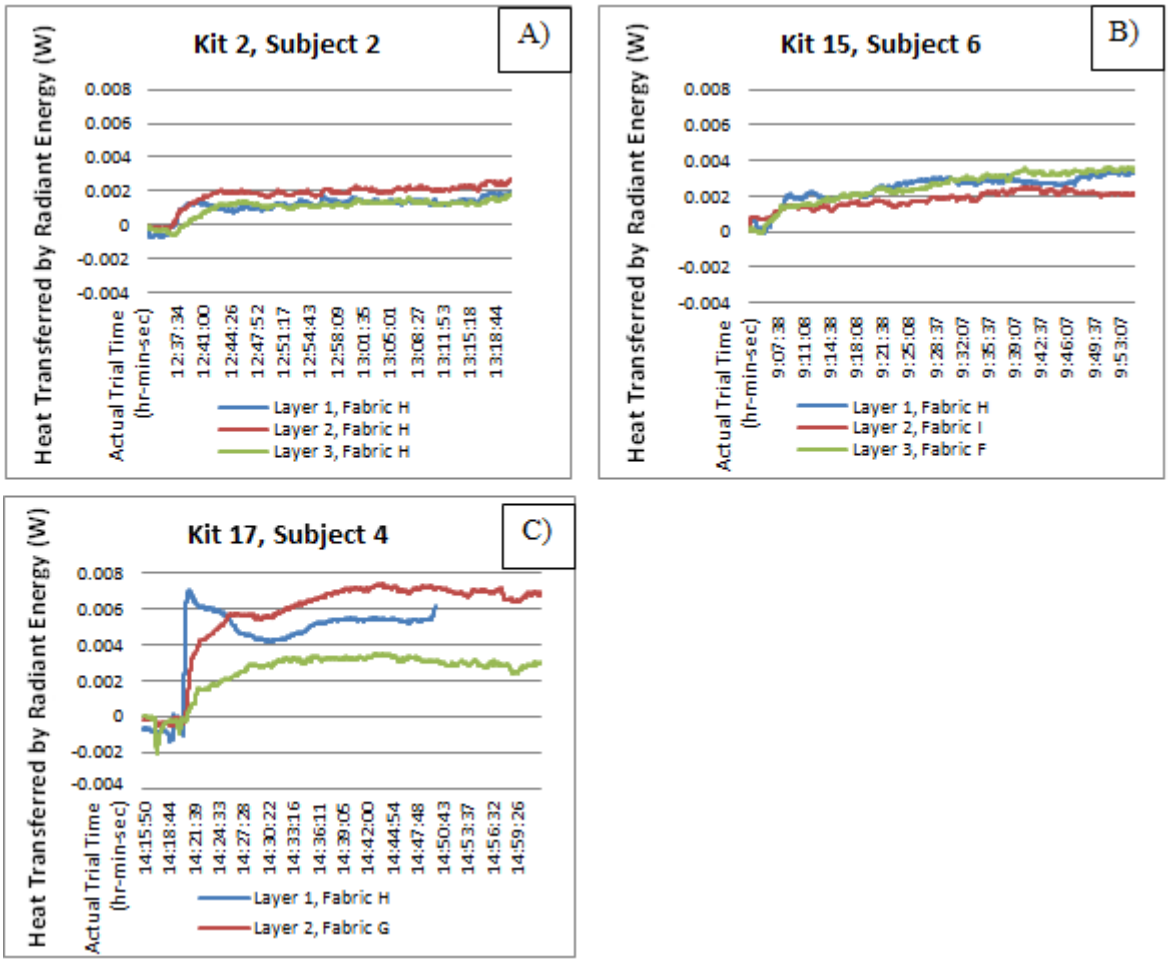

Figure 4.40: Radiant Heat Transfer across Fabric (W), Layer 1, Fabric H: A) Kit 2, Subject 2, B) Kit 15, Subject 6, C) Kit 17, Subject 4

Enthalpy of Vaporization Layer 1, Fabric H

As shown in Figure 4.41, the majority of the enthalpy fluctuation occurs across Layer 3 in Zones 1 and 2 of the human subject trials as the diffusion of moisture and heat occurs primarily in the first ten to twelve minutes of the trial. Kit 17 was an extreme example of the trends shown in the previous analyses.

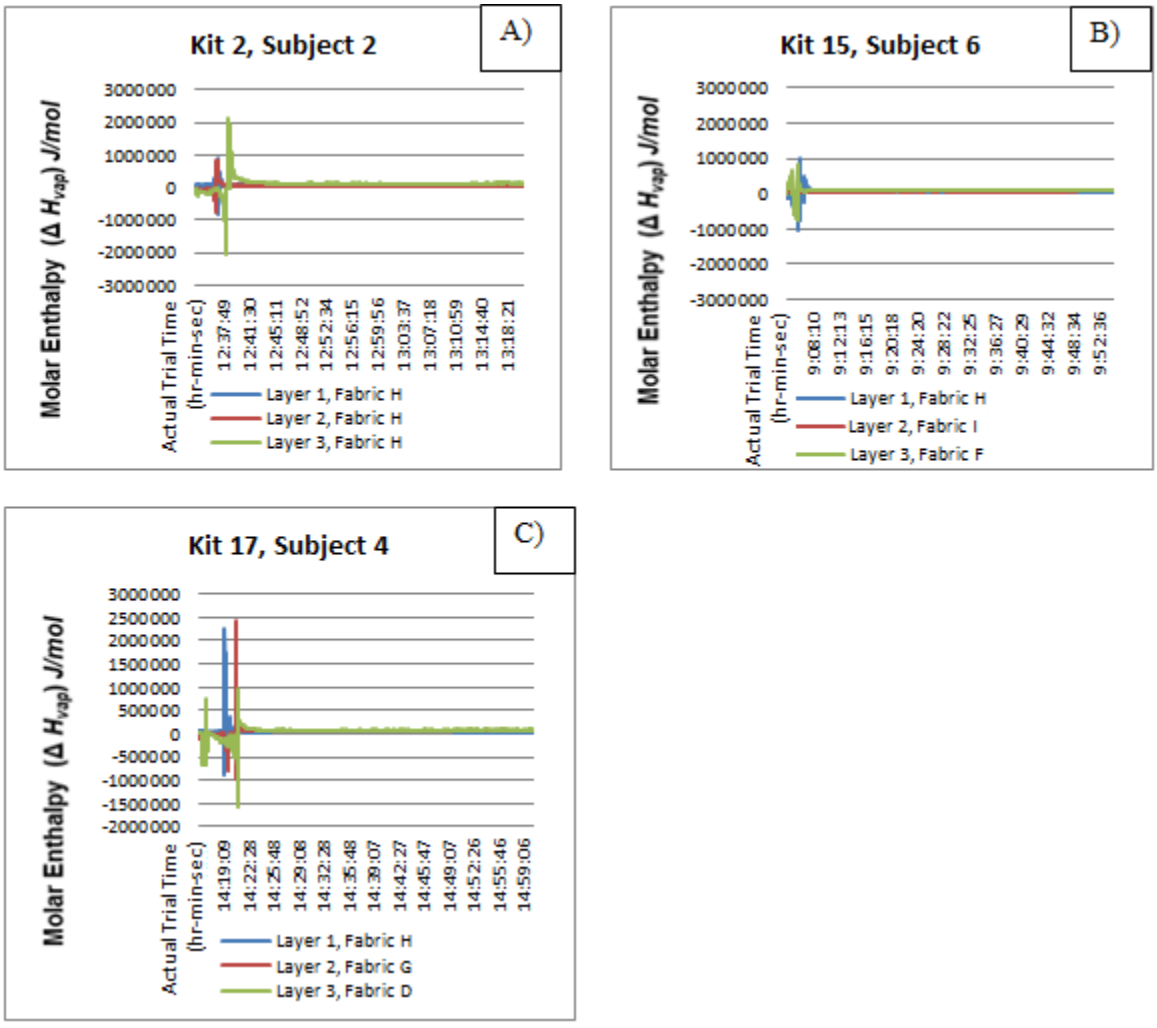

Figure 4.41: Molar Enthalpy of Vaporization and Condensation across Fabric (Δ H_{vap}) *J/mol*, Layer 1, Fabric H: A) Kit 2, Subject 2, B) Kit 15, Subject 6, C) Kit 17, Subject 4

4.3.4. Layer 1, Fabric E or G

86% PET, 14% Elastane single jersey knit and 100% Mercerized cotton poplin fabrics were used for Kit 4 and Kit 5 respectively for the first layer of two different kits that were analyzed graphically calculating vapor pressure, conduction, convection, radiant heat, and enthalpy of vaporization. These kits were also compared by dividing the trials into the three specific Zones: warm up, diffusion, and stability.

Vapor Pressure Layer 1, Fabric E or G

As shown graphically (Figure 4.42), both kits experienced a similar change with regards to vapor pressure during the first 2-4 minutes of the human subject trials with initial values in the range of 1.5 hPa +/- 1. After the initial warm-up period the vapor pressure change is rapid as shown by the sharp negative slope for all the kits shown in Figure 4.42. As shown, sensor 2 in Kit 4 stopped measuring relative humidity during the trial after Fabric 1 reached saturation. Sensor 2 measured only temperature throughout the remainder of the trial.

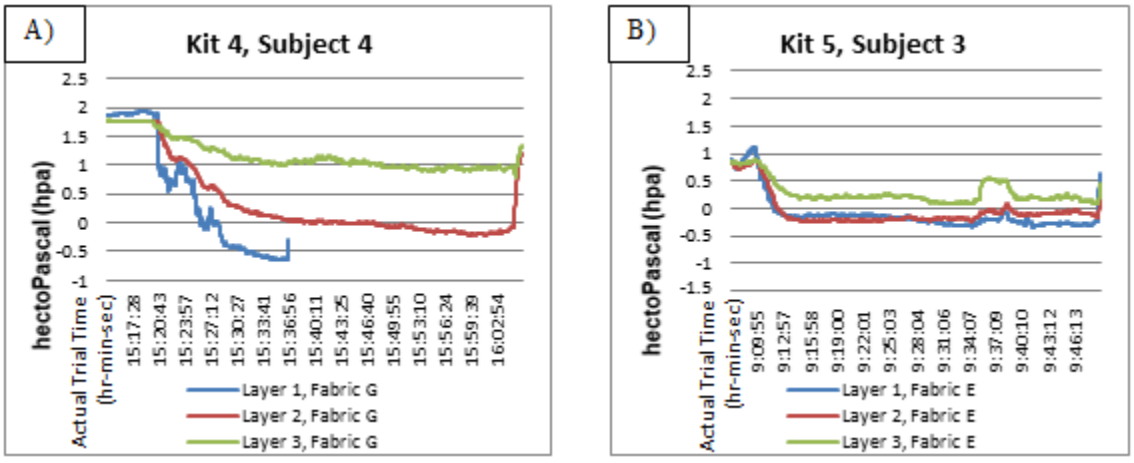

Figure 4.42: Vapor Pressure Movement across Fabric (e_s-e_a) hectoPascal (hPa), A) Layer 1, Fabric G; B) Layer 1, Fabric E

Conduction Layer 1, Fabric E or G

The heat flow if all contributed to conduction across 86% PET, 14% Elastane single jersey knit and 100% Mercerized cotton poplin fabrics used in the first layer of Kit 4 and Kit 5 respectively are shown in Figure 4.43. As depicted graphically, before the kit is attached to the body the rate of conduction across the fabrics in the kits is approximately zero for both for kits. After the fabric kit is attached to the body the conduction rate increases for both kits.

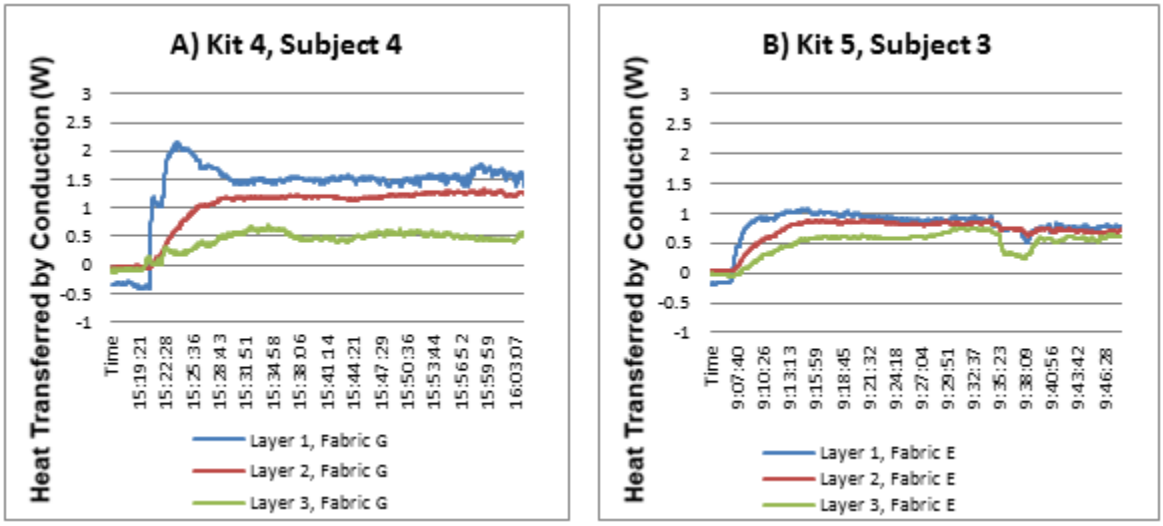

Figure 4.43: Heat Transfer by Conduction across Fabric (W), A) Layer 1, Fabric G; B) Layer 1, Fabric E

Conduction Layer 1, Fabric G

The conduction rates across 86% PET, 14% Elastane single jersey knit and 100% Mercerized cotton poplin fabrics used in the first layer of Kit 4 and Kit 5 respectively are shown in Figure 4.43. As depicted graphically, before the kit is attached to the body the rate of

conduction across the fabrics in the kits is approximately zero for both for kits. After the fabric kit is attached to the body the conduction rate increases for both kits.

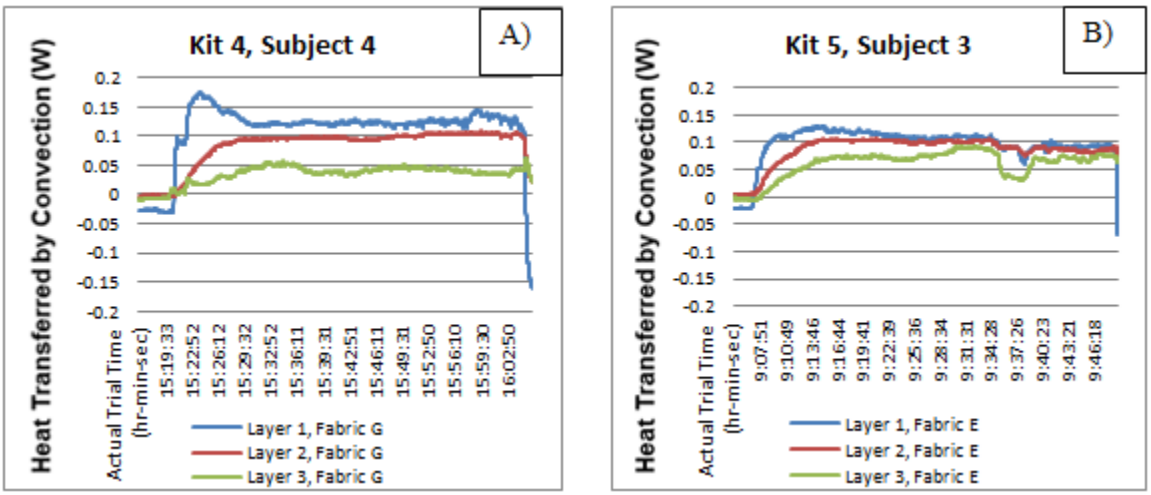

Figure 4.44: Heat Transfer by Convection across Fabric (W), A) Layer 1, Fabric G; B) Layer 1, Fabric E

Radiant Heat Layer 1, Fabric G

Figure 4.45 shows the radiant heat change across the fabric testing kits with 86% PET, 14% Elastane single jersey knit and 100% Mercerized cotton poplin fabrics used in the first layer of Kit 4 and Kit 5 respectively. For both kits shown, before the kit is attached to the body the rate of radiant heat across the fabrics in the kits is approximately zero and once the fabric kit is attached to the body the radiant heat rate increases but remains a relatively small value throughout the human subject trial.

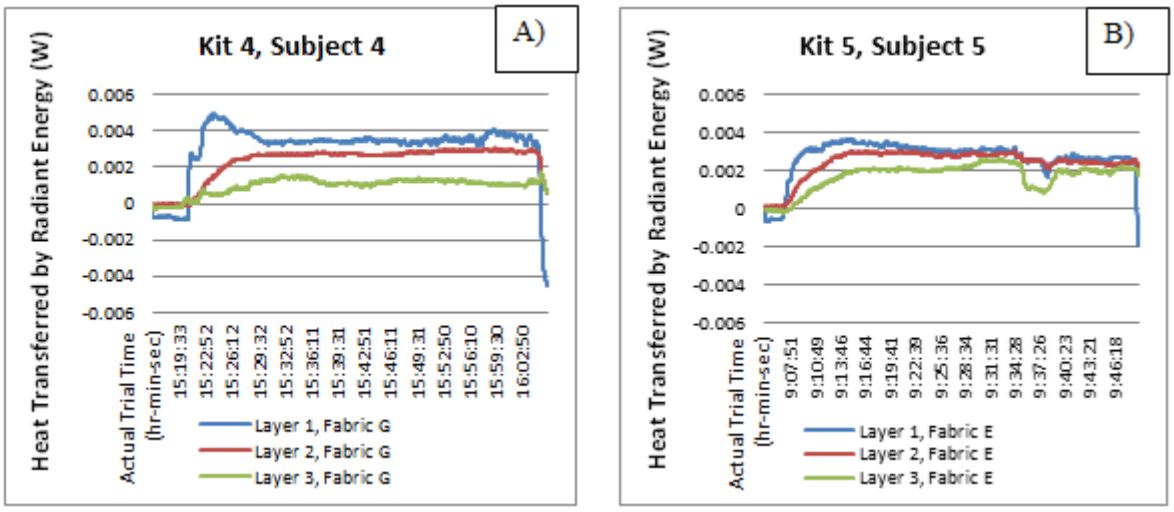

Figure 4.45: Radiant Heat Transfer across Fabric (W), A) Layer 1, Fabric G; B) Layer 1, Fabric E

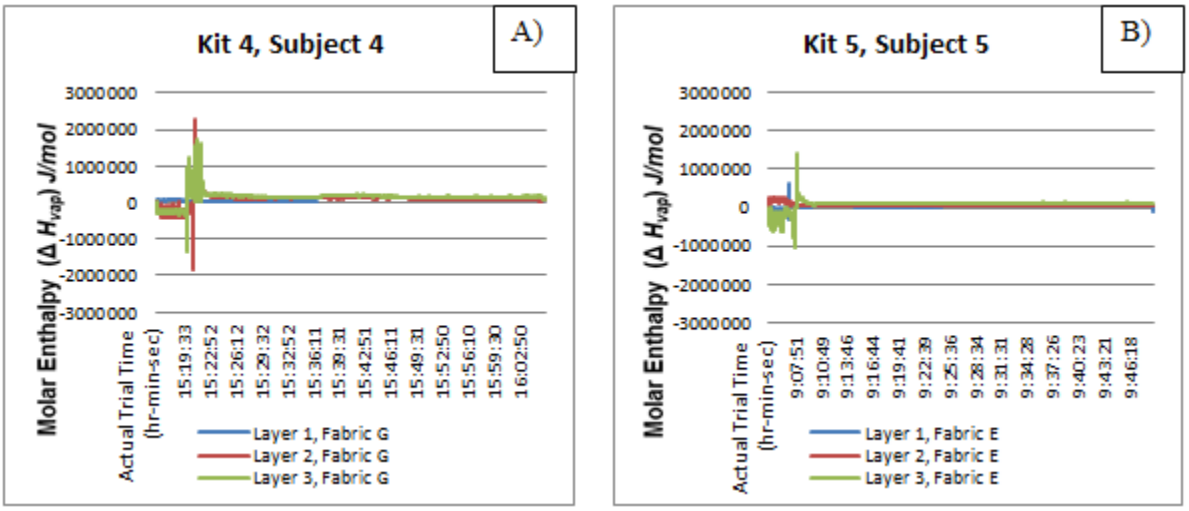

Figure 4.46: Molar Enthalpy of Vaporization and Condensation across Fabric (Δ H_{vap}) *J/mol,* A) Layer 1, Fabric G; B) Layer 1, Fabric E

Enthalpy of Vaporization Layer 1, Fabric H

As shown in Figure 4.46, the majority of the enthalpy fluctuation occurs in Zones 1 and 2 of the human subject trials as the diffusion of moisture and heat occurs primarily in the first ten to twelve minutes of the trial.

4.4. Layer to Layer Consideration

It is instructive to calculate the change in vapor pressure across each fabric layer in the range of Kits evaluated. When e_s-e_a is negative, moisture in the form of vapor can advance through the Kit. However, when e_s-e_a is positive, this means that the moisture transfer has slowly dramatically or even stalled. The following analysis compares the moisture transfer by Zone and by fabric location in the Kit.

4.4.1. Layer 1

Figure 4.47 shows fabric testing kits which exhibit a negative vapor pressure change during the first four minutes of the human subject trail or Zone 1. As shown, Kits 3, 9, 15 initially experienced changes in vapor pressure through fabric 1 at similar rates. However, only Kit 1 and 15 remained at similar levels throughout Zone 1. Kits 4, 8, 15 and 16 all experienced reductions of over 1 hPa within 30 seconds. The first fabric layer for Kits 3 consisted of 95% Cotton, 5 % Elastane single jersey knit while the first fabric in Kit 9 consisted of 100% PET thermal-lined double jersey; different fabrics tested by different human subjects but performed similar within this first portion of the human subject trial. Figure 4.48 shows the fabric testing kits that change the least during Zone 1. As shown, Kits 1, 18, and 17 are at similar initial levels at the beginning of the human subject trial (note Kit 1 and Kit 18 are the

same fabric for Fabric 1) and Kits 1, 18, and 5 follow a very similar path in terms of vapor pressure change during Zone 1. Kit 19 changes the least during Zone 3 of the trial followed by Kit 17 while Kit 2 fluctuates the most among the kits shown in Figure 4.48.

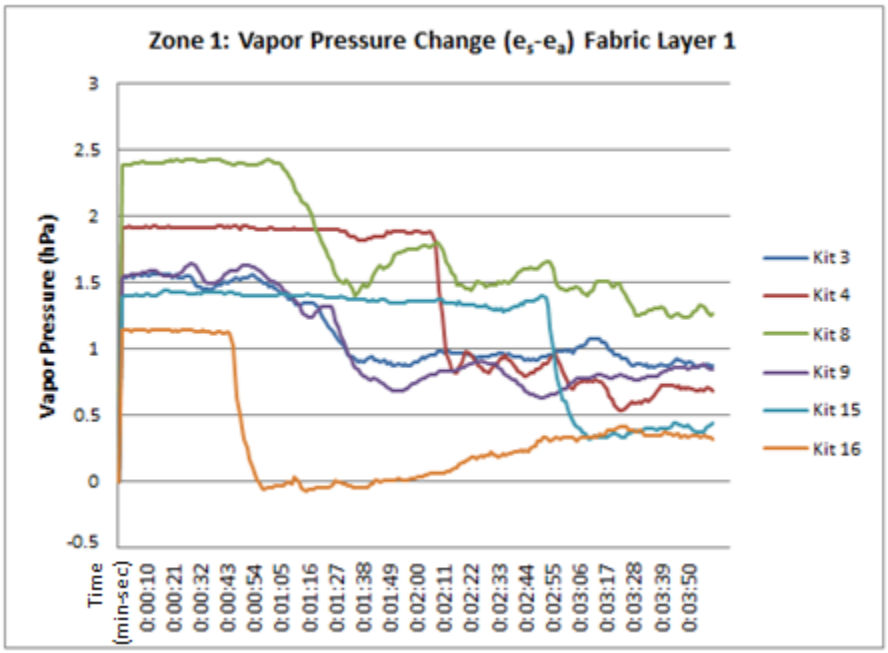

4.47: Vapor Pressure (e_s-e_a) for Fabric 1 Kits with Most Change during Zone 1

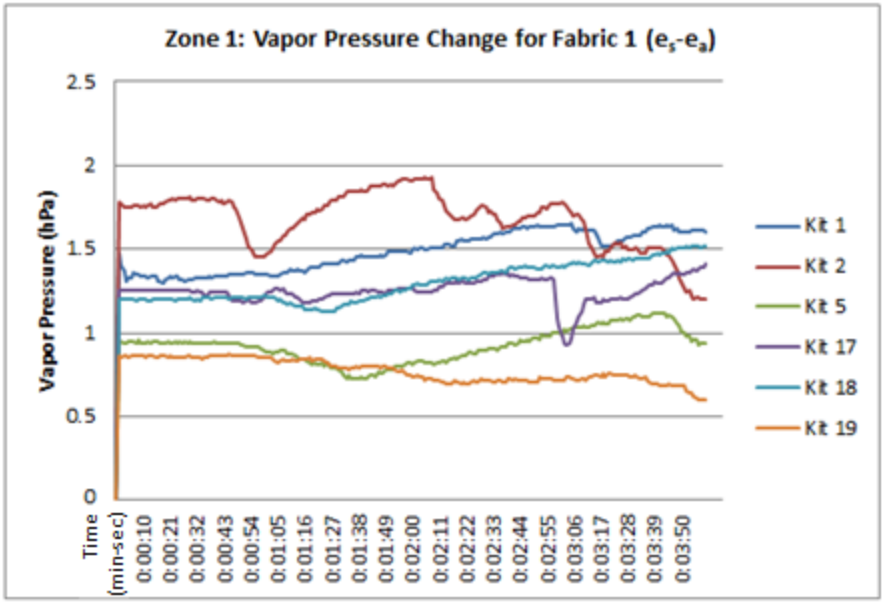

Figure 4.48: Vapor Pressure (e_s-e_a) for Fabric 1 Kits with Least Change during Zone 1

Figure 4.49 follows the kits with the most change at Fabric 1 during Zone 1 into Zone 2 which is the next ten minutes of the human subject trial. Notice that Kit 3 and Kit 16 change very little in terms of vapor pressure throughout Zone 2; these kits both consist of 95% Cotton, 5 % Elastane single jersey knit for Fabric 1. Overall, Kits 4, 8, 9 and 15 show the negative slopes through Zone 2 with Kits 4, 9 and 15 at the lowest levels all dropping under zero. Kit 8 drops below zero at one point in the trial but a positive vapor pressure change follows. Figure 4.50 shows the fabric Kits which changed the least during Zone 1, however, these Kits do not necessarily change the least during Zone 2 of the human subject trials. As shown, Kits 1,2,5,17,18 and 19 all exhibit distinct negative slopes during this portion of the trial. Kit 17 has a positive slope which corresponds to the documented pack slip which introduced air flow into the kit. As in Zone 1, Kit 19 changes the least but, is followed by Kit

(recall had fluctuated the most during Zone 1). Kit 1 and 17 show the most negative change among the kits in Figure 4.50.

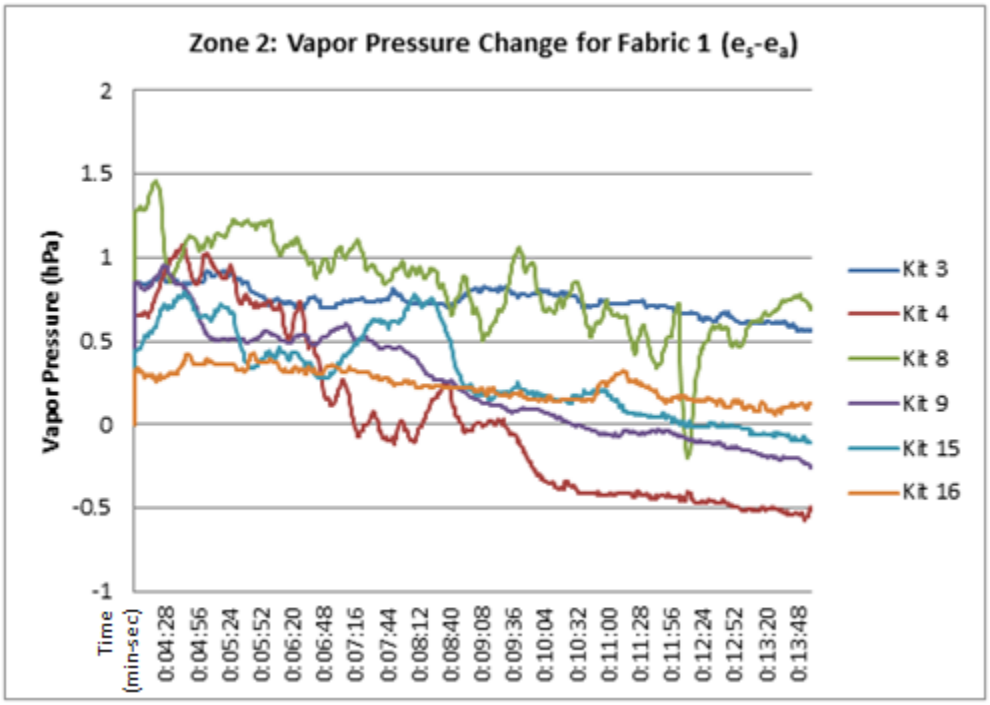

Figure 4.49: Vapor Pressure (e_s-e_a) for Fabric 1 during Zone 2: Kits 3, 4, 8, 9, 15, and 16

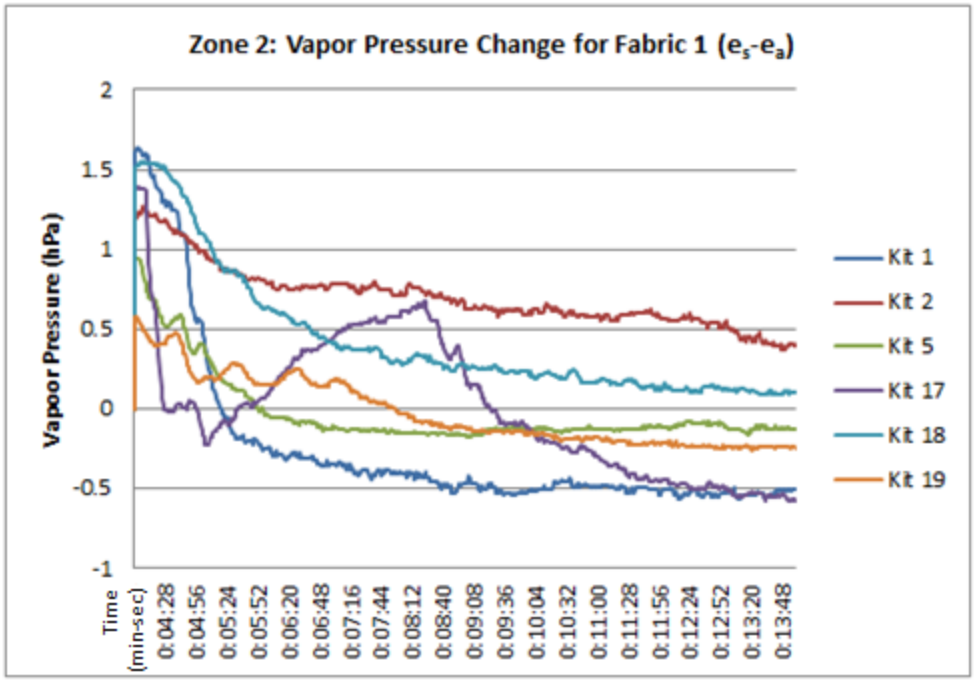

Figure 4.50: Vapor Pressure (e_s-e_a) for Fabric 1 Kits during Zone 2: Kits 1, 2, 5, 17, 18, 19

As shown in Figure 4.51, Kit 4 loses a sensor to saturation during Zone 3. Overall, Kit 8 and 9 experience the most negative slopes in Zone 3 but, Kit 9 reaches lower levels than Kit 8. Kit 8 exhibits more significant gains in vapor pressure during Zone 3 than any of the other kits. Kit 3 never reaches the negative range during the last portion of the trial. Although consisting of different fabrics, Kit 15 and 16 follow similar paths during Zone 3 of the trial and at the end of the trial the vapor pressure change is at almost the same level. Figure 4.52 shows the fabric Kits which changed the least during Zone 1 which is also true for Zone 3. Kit 2, 18, 5, 19, 1, and 17 all have similar flat paths throughout Zone 3 at varying levels and listed in descending order. Note, only Kit 2 never reaches the zero level for vapor pressure change during Zone 3 or any other portion of the human subject trial.

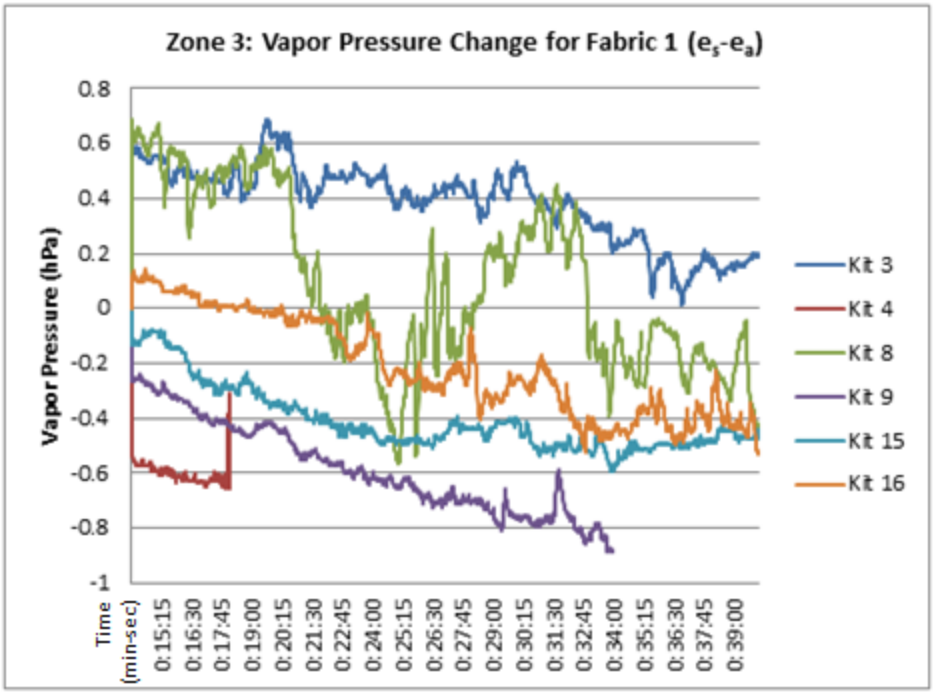

Figure 4.51: Vapor Pressure (e_s-e_a) for Fabric 1 Kits with Most Change during Zone 3

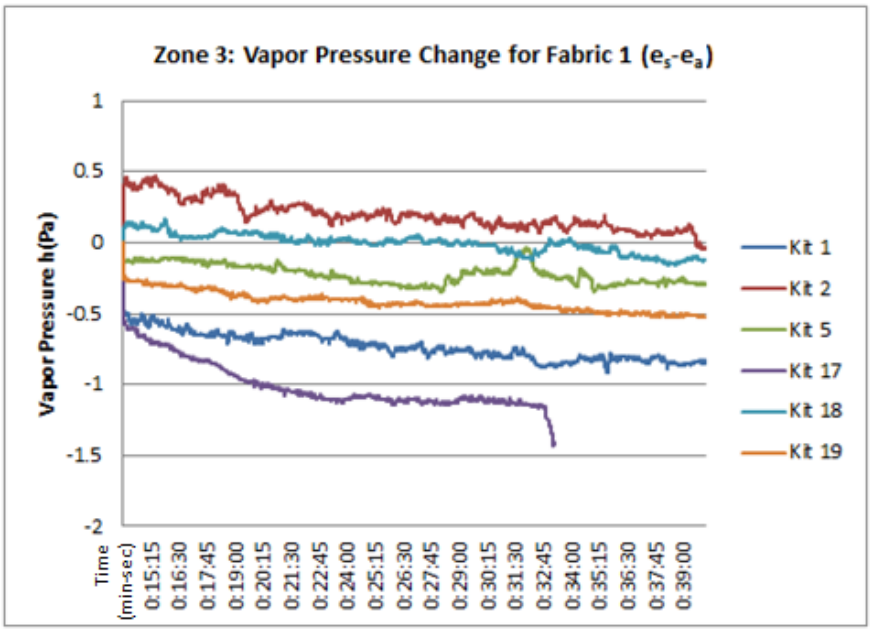

Figure 4.52: Vapor Pressure (e_s-e_a) for Fabric 1 Kits with Least Change during Zone 3

4.4.2. Layer 2

Figure 4.53 shows Fabric 2 fabric kits which changed the most during Zone 1. Recall, Fabric 1 in these kits changed the most during Zone 1 as well. Overall, these kits exhibited a negative change in vapor pressure. Kit 15 exhibits a positive vapor pressure change for the first three minutes of the trial and then begins to drop. Kits 3, 9 and 19 follow similar paths in terms of change in vapor pressure but at varying levels. Kit 8 has the most negative change in vapor pressure while Kit 3 and 15 have the least change during Zone 1. Figure 4.54 shows Fabric 2 in the kits which changed the least, again, in both Zone 1 and 2. As shown, Kits 1, 18 and 17 have the most similar slopes at varying levels during Zone 1. Kit 5 shows a negative change then a positive change and Kit 19 have the most negative change.

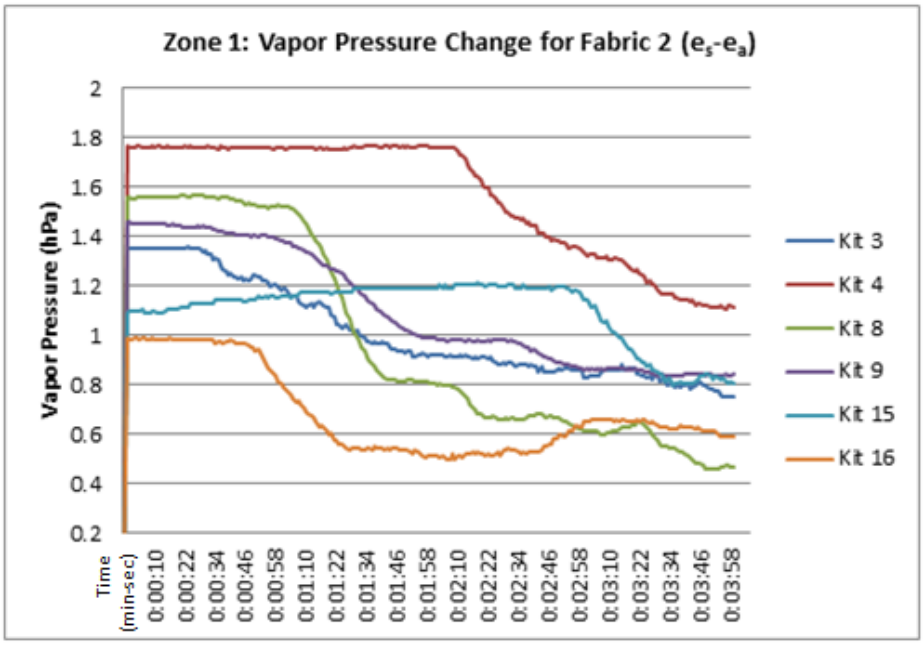

Figure 4.53: Vapor Pressure (e_s-e_a) for Fabric 2 Kits with Most Change During Zone 1

Kit 2 has the highest initial vapor pressure change and has the largest slope of change in vapor pressure over the course of Zone 1. Figure 4.55 depicts the vapor change for Fabric 2 during Zone 2 for the fabric kits that experienced the most change during Zone 1 of the human subject trials but not necessarily Zone 2. Note that Kit 16 experiences very little change during Zone 2. As shown, Kits 3, 15 and 16 change the least of the kits in the graph while Kits 9 and 4 change the most followed by Kit 8. Overall, each of the kits shown in Figure 4.56 has a negative change in vapor pressure during Zone 2. Figure 4.56 shows graphically the vapor pressure change for Fabric 2 for the kits that change the least during Zone 1 but not Zone 2. As shown, Kit 2 and 19 changes the least for Fabric 2 (recall Kits 2 and 19 also changed the least for Fabric 1). Again, as with Fabric 1, Kits 1 and 17 changes the most for Fabric 2 followed by Kit 18 the Kit 5.

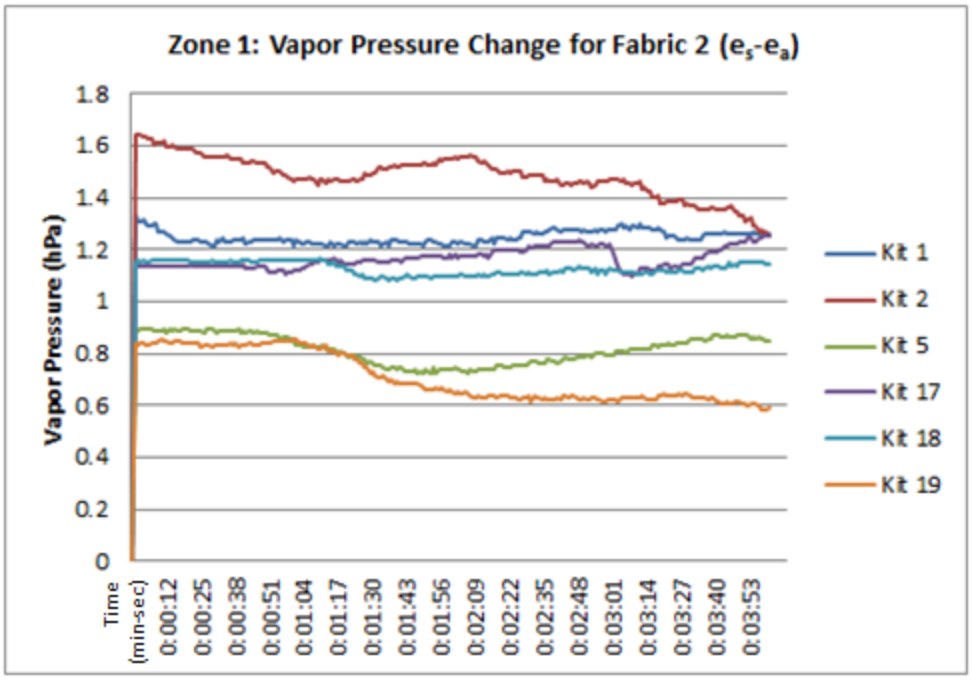

Figure 4.54: Vapor Pressure (e_s-e_a) for Fabric 2 Kits with Least Change During Zone 1

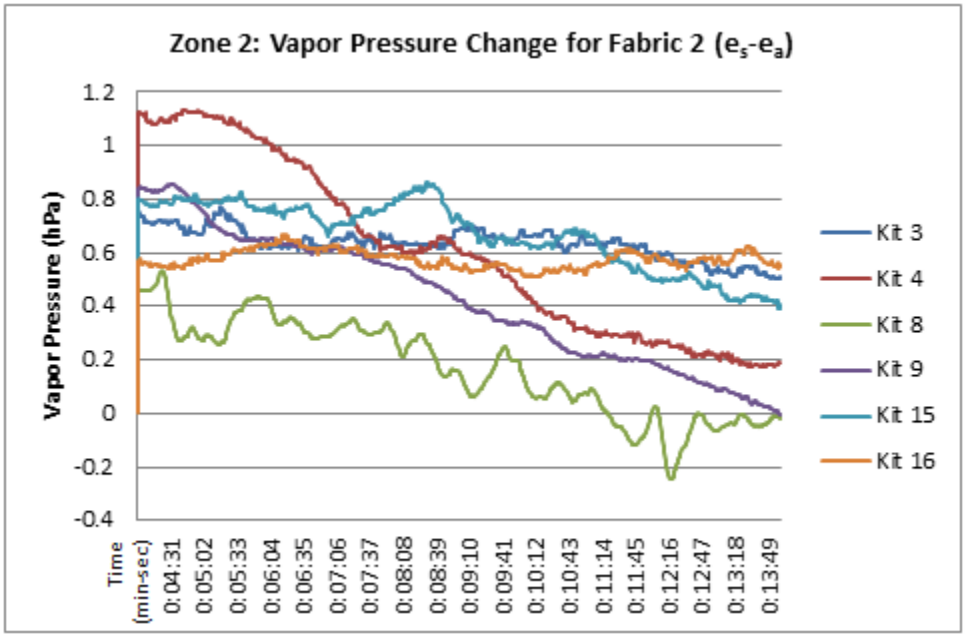

Figure 4.55: Vapor Pressure (e_s-e_a) for Fabric 2 Kits During Zone 2: Kits 3, 4, 8, 9, 15 and 16

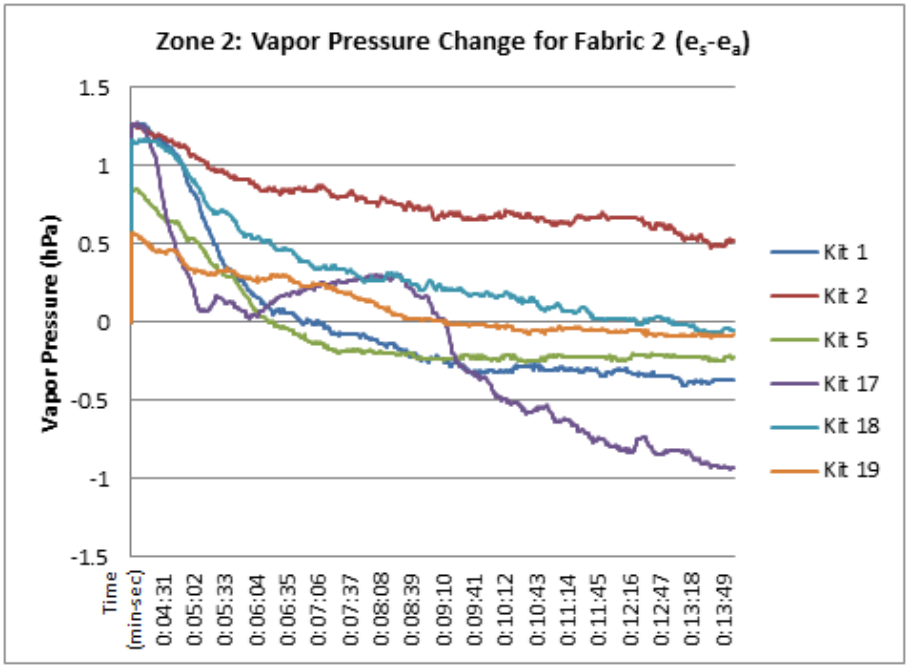

Figure 4.56: Vapor Pressure (e_s-e_a) for Fabric 2 Kits During Zone 2: Kits 1, 2, 5, 17, 18 and 19

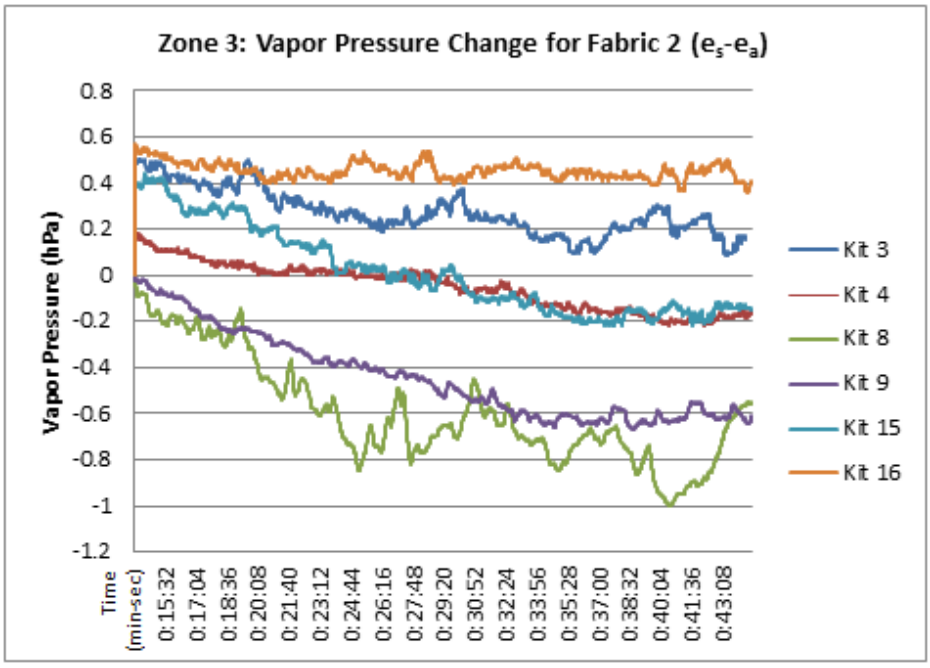

Figure 4.57: Vapor Pressure (e_s-e_a) for Fabric 2 Kits During Zone 3: Kits 3, 4, 8, 9, 15 and 16

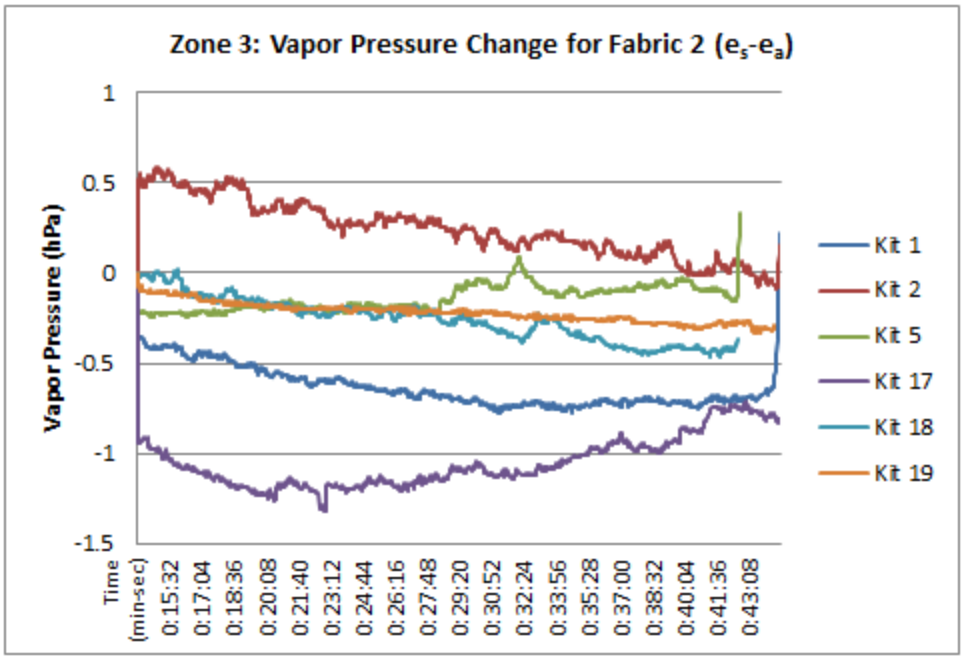

Figure 4.58: Vapor Pressure (e_s-e_a) for Fabric 2 Kits During Zone 3: Kits 1, 2, 5, 17, 18 and 19

4.4.3. Layer 3

Figure 4.59 and Figure 4.60 graphically depict the vapor pressure change for Fabric 3 for Zone 1 of the human subject trials. As shown, Fabric 3 experiences low levels of change for all the fabric testing kits especially Kits 3, 15, 1, 18, and 19. In Figure 4.55, Kits 4, 8, 9, 16 have similar paths but, Kit 9 and Kit 16 maintain very different levels as Kit 16 starts at the lowest level of vapor pressure change of the kits shown. Each of the kits shown in Figure 4.60 depicts low levels of change in terms of vapor pressure but at varying levels. Kits 5 and 19 are most similar graphically. Kit 2 has the most significant downward sloping graph during Zone 1.

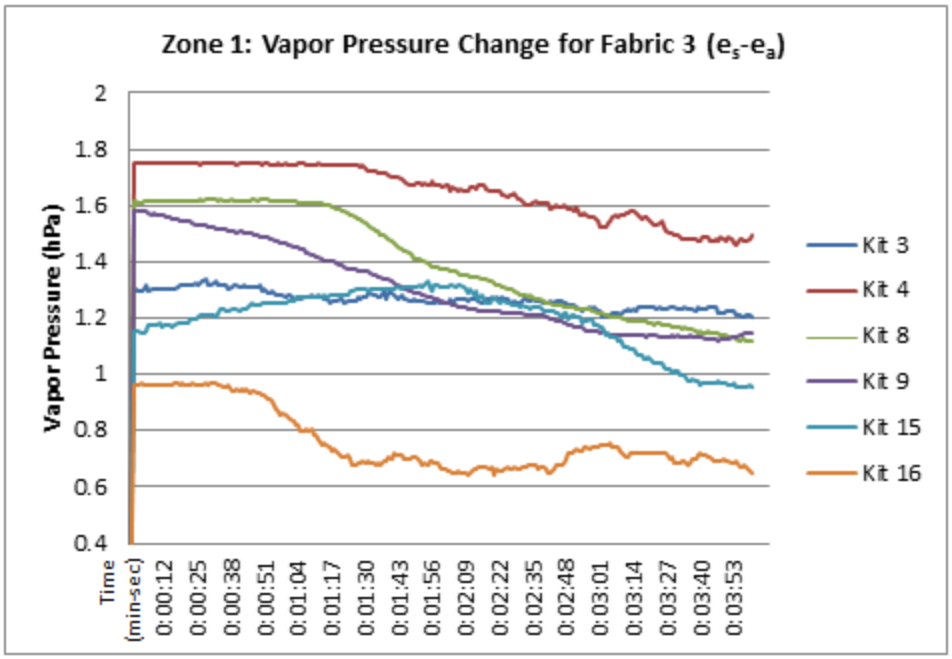

Figure 4.59: Vapor Pressure (e_s-e_a) for Fabric 3 during Zone 1: Kits 3, 4, 8, 9, 15 and 16.

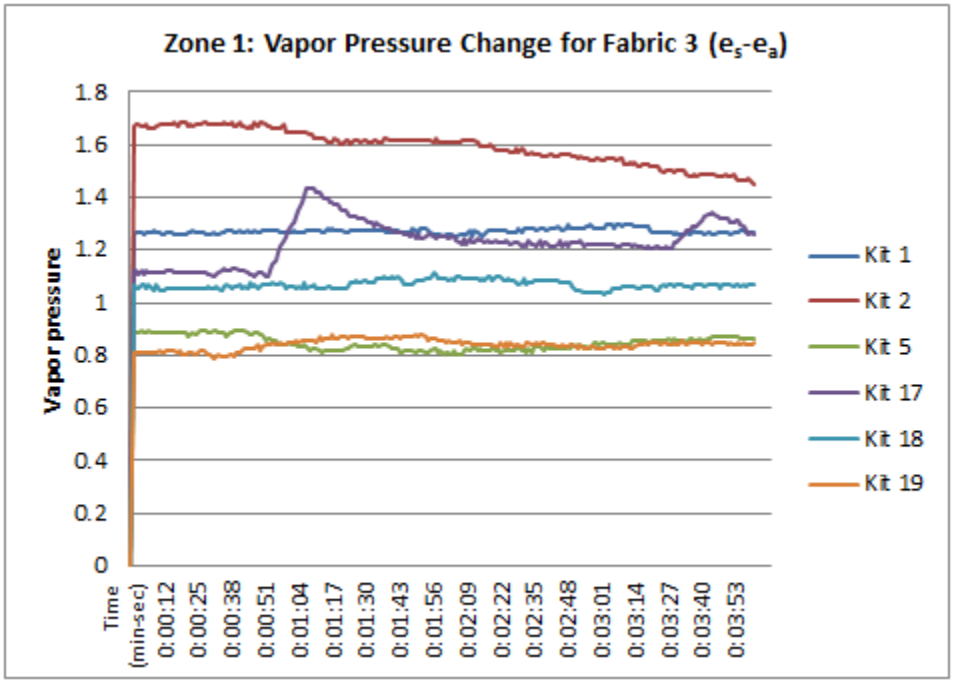

Figure 4.60: Vapor Pressure (e_s-e_a) for Fabric 3 Kits with Least Change during Zone 1

Figures 4.61 and 4.62 show the vapor pressure change for Fabric 3 during Zone 2 of the human subject trials. As shown, all of the fabric kits exhibit an overall negative slope during this portion of the trial. Kits 3, 15 and 9 in Figure 4.61 have similar initial levels of vapor pressure change, however, only Kits 3 and 15 remain the most similar graphically throughout Zone 2. Of the kits shown in Figure 4.57 Kits 3, 15, and 16 exhibit the least change while Kits 4, 8, and 9 change the most. As shown in Figure 4.62, Kits 2 and 19 change the least while Kits 17, 1, 18, and 5 change the most (listed in ascending order).

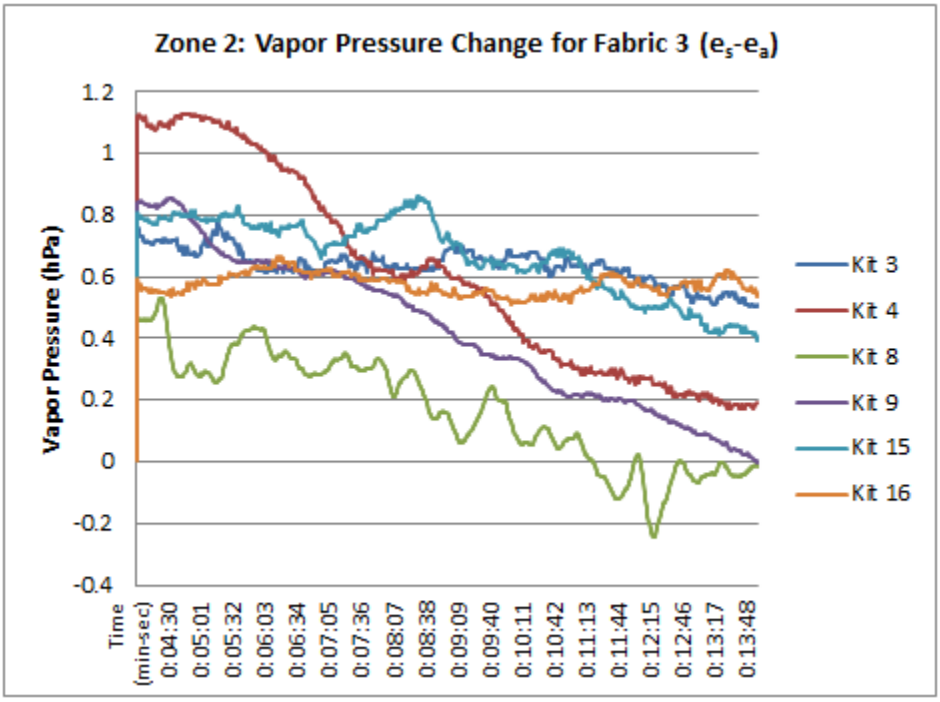

Figure 4.61: Vapor Pressure (e_s-e_a) for Fabric 3 Kits During Zone 2: Kit 3, 4, 8, 9, 15 and 16

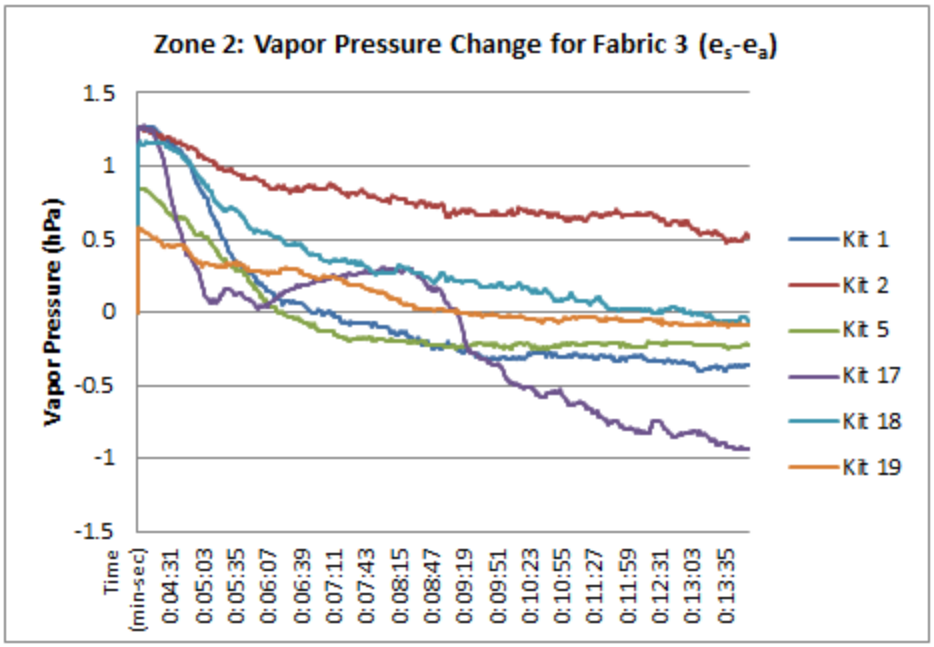

Figure 4.62: Vapor Pressure (e_s-e_a) for Fabric 3 Kits During Zone 2: Kit 1, 2, 5, 17, 18 and 19

Figure 4.63 and 4.64 graphically show the change in vapor pressure exhibited by Fabric 3 during Zone 3 of the human subject trials. As shown in Figure 4.63, Kits 8, 9, and 16 maintain very similar changes in terms of vapor pressure, this is also true for Kits 3 and 4 but these two kits change very little throughout Zone3. Kit 15 experiences the most change of the kits shown in Figure 4.63 and is also most negative. Kit 15 is the only kit that reaches the zero point on the graph. Figure 4.64 shows very little change within Fabric 3 for all the kits with the exception of Kit 2 which slopes downward during this portion of the trial.

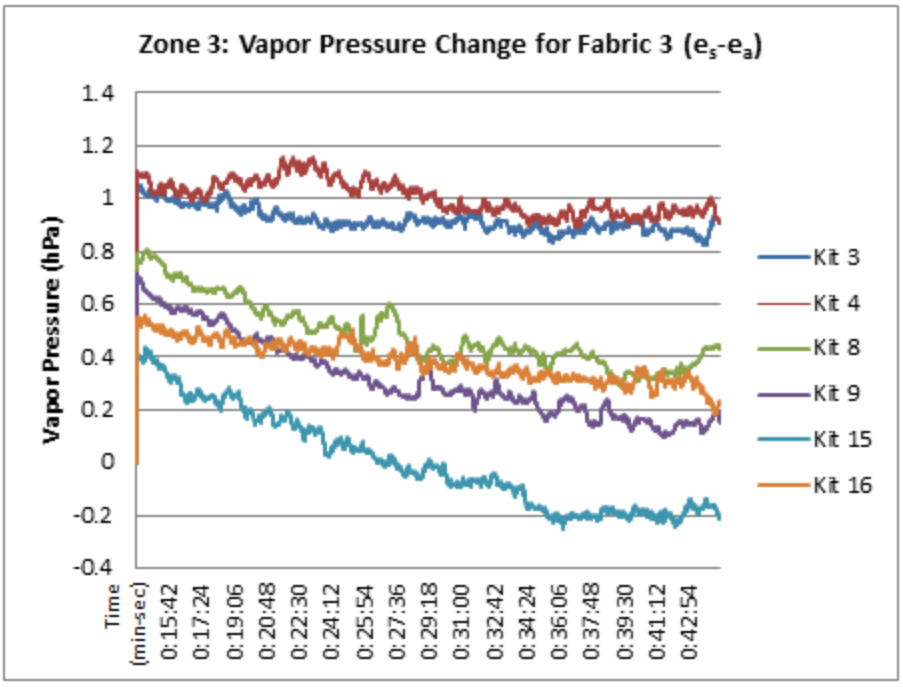

Figure 4.63: Vapor Pressure (e_s-e_a) for Fabric 3 Kits During Zone 2: Kit 3, 4, 8, 9, 15 and 16

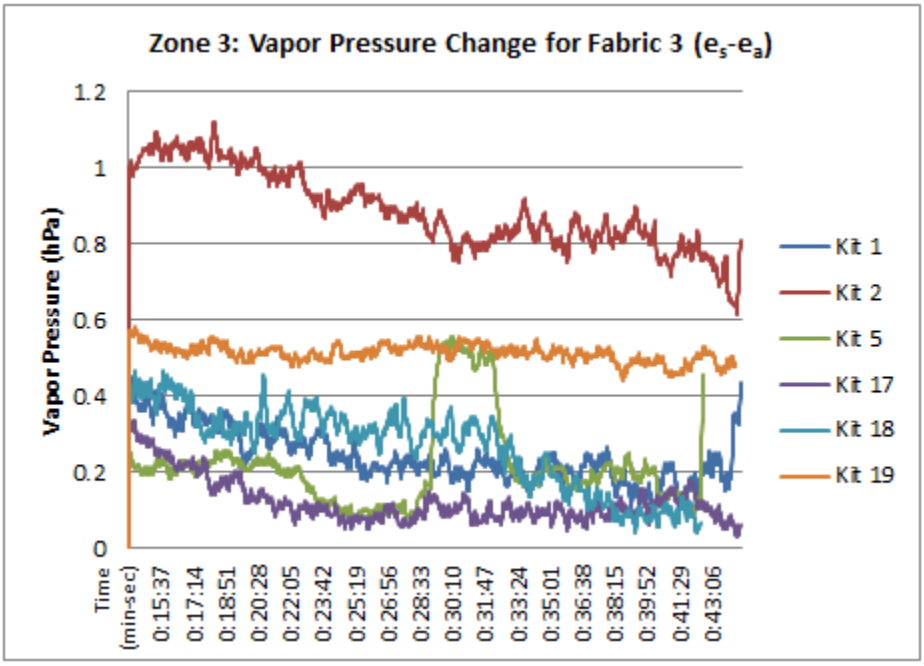

Figure 4.64: Vapor Pressure (e_s-e_a)subscript for Fabric 3 Kits during Zone 2: Kit 1, 2, 5, 17, 18 and 19

Through comparing the moisture transfer by Zone and by fabric location within the fabric testing kit evidence supporting prior findings can be found. The human subjects are not that different in terms of the amount of heat and humidity that they generate given a certain activity such as the bicycle protocol used in this study, Finding 2 of 17. The human subject trials can be divided into three distinct Zones, Finding 6 of 17. The outer fabric layer (Layer 3) is least affected by the moisture from the human subject while, Layers 1 and 2 are most critical in managing the moisture transfer, Finding 13 of 17. The fabric used for the second and third layers of the fabric testing kit affects the energy flow through the first fabric, Finding 14 of 17. Within a fabric testing kit fabric performance is more dependent on the combination and location of fabrics used for a fabric testing kit rather than its own performance characteristics, Finding 15 of 17.

4.5. Temperature, Relative Humidity, and Heat Flow

It has been shown that within each kit that if during the human subject the actual vapor pressure (e_a) becomes greater than the saturated vapor pressure (e_s) moisture transfer through the kit from the skin to the outside environment is slowed or halted. The amount of water vapor in air is dependent on temperature; higher temperatures have the capacity to increase water vapor in air. A mechanism to efficiently transfer heat, keeping the temperature levels higher could therefore optimize moisture vapor movement by increasing the saturated vapor pressure (e_s). Conduction, Convection, Radiation, and Evaporation are the mechanisms in which heat can be transferred to the environment. Conduction, Convection, and Radiation are related to material's physical properties and temperature and have been

analyzed within this study. If Conduction was considered the most significant or only mechanism for heat flow throughout this system; the conductivity value (k) of these fabrics could increase the moisture movement by more effectively keeping temperatures higher.

4.5.1. Microclimates

When the fabric testing kit was attached to the human subject's body it created three separate microclimates between layers: the subject's skin and the innermost fabric layer, the first fabric layer and the second, and the second fabric layer and the third or outermost fabric layer. Each of these microclimates size was controlled by the design of the kit which had a structured area of 20.125 in^2 and was 0.125 inches thick. With these parameters and the thermal conductivity value (k) of atmospheric air 0.024 1 $W/(m * ℃)$ the heat flow (Q) of air was calculated based on Fourier's law. Figure 4.65 shows the heat flow from conduction versus the temperature changes for all microclimate layers for all the fabric testing kits. Figure 4.66 shows a range of temperature change for the microclimate of -5.92˚C to 3.72˚C which is large considering the microclimate consists of a small distance of atmospheric air. The larger value measurements were concentrated in the humidity range from 41% to 55% relative humidity which was the period of the human subject trial characterized as Zone 1 discussed previously in this Chapter where the pack was placed on the body and an immediate rapid change in temperature and relative humidity occurred. As shown in Figure 4.66 the majority of the temperature changes in the microclimate fell between -2 and 2˚C. The temperature change was calculated by subtracting the sensor measurement of the outer sensor from the inner sensor for each microclimate layer within the fabric testing kit. Therefore a negative temperature change indicates a heat flow towards the outside

environment and a positive temperature change indicates a heat flow towards the human subject's body. As Figure 4.65 shows for the relative humidity range 20 to 40%, the heat flow due to conduction remains mostly within the positive but crosses zero. A positive heat flow value as shown in Figure 4.65, indicates heat flowing away from the body through the fabric testing kit to the outside environment. The range from 41 to 55% relative humidity shows the most positive heat flow value due to conduction reaching values up to 1.5 W. Recall from previous sections of this Chapter, throughout the human subject trials to unanimous overall trend was that relative humidity only rose overtime. After the relative humidity reaches 55% and for the remainder of the ranges shown in Figure 4.66 the range is concentrated around zero from -1 to 1 W. These findings are consistent with what is known about conduction and heat flow through air, which was found to act as an insulator within the fabric testing kits.

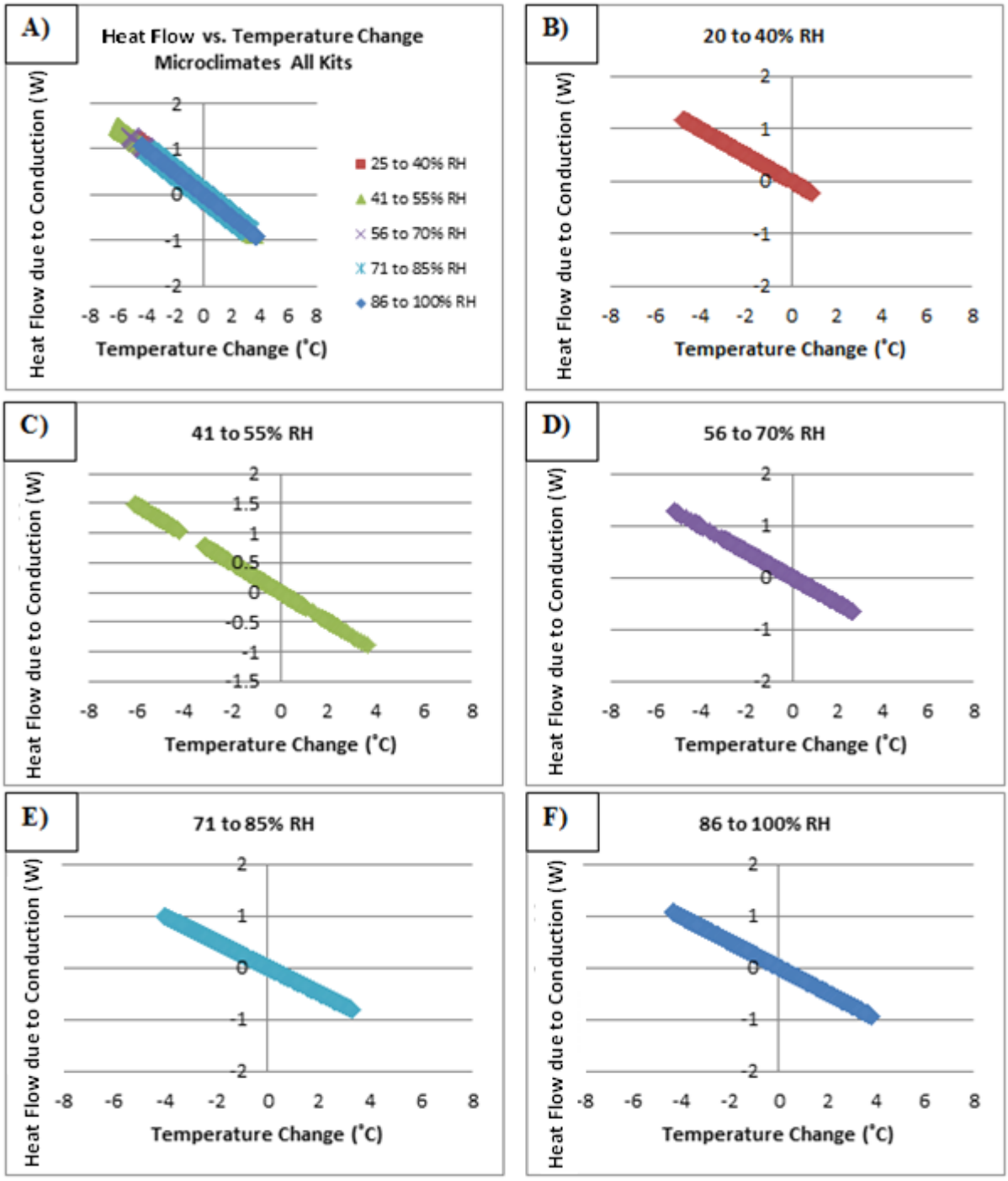

Figure 4.65: Heat Flow due to Conduction in Watts (W) by versus Temperature Change for the Microclimate All Layers All Kits: A) All Relative Humidity Ranges, B) 20 to 40% R.H., C) 41 to 55% R.H., D) 56 to 70% R.H., E)71 to 85% R.H., and F) 86 to 100% R.H

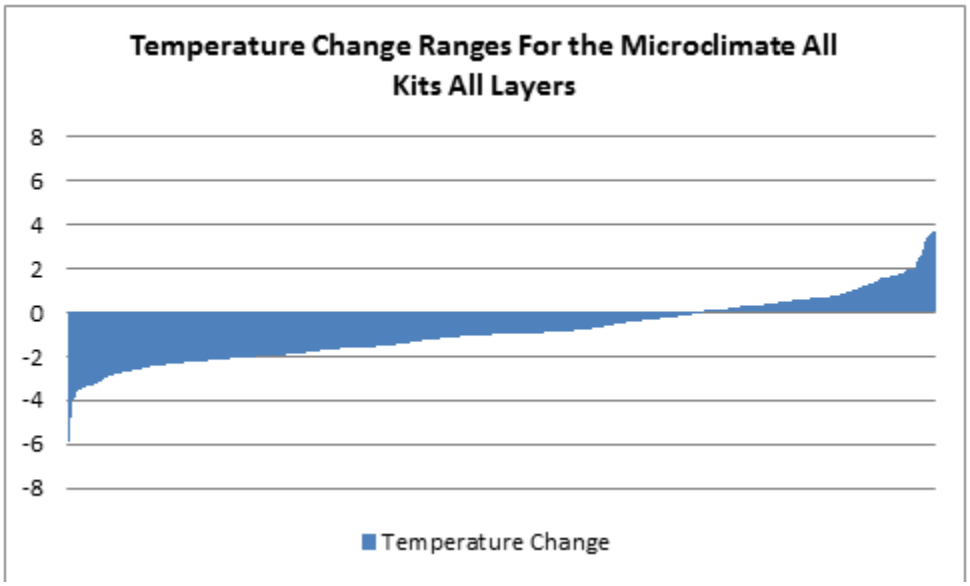

Figure 4.66: Temperature Change Ranges for the Microclimate All Layers All Kits

4.5.2. Fabric A

As shown in Figure 4.67, the heat flow due to conductiion range for Fabric A is much greater than what was seen in the previous section for the microclimate. The heat flow due to conduction range for Fabric A 13.43 to -10.31 W, while the range for temperature change remained between -4.64 and 3.56 ˚C. During the relative humidity range from 41 to 55%, which corresponds to Zone 1 for the human subject trials, the heat flow due to conduction remains mostly positive indicating that once the pack was placed on the subject's body the heat was flowing to the outside environment. During relative humidity range from 56 to 70% the heat flow due to conduction continues to remain mostly positive as the human subject trial would within the time period of Zone 1 and Zone 2. The relative humidity range from 71 to 85% shows the largest range in terms of the heat flow due to conduction, reaching

negative values as low as -10.31 W and as high as 13.43 W. In terms of human subject trial Zones, these relative humidity measurements were concentrated in Zone 2 and 3 were the kit was reaching its highest temperature and relative humidity measurements and heat flowed both away and back towards the subject's skin. However, as shown in Figure 4.68, Fabric A only reached the extreme negative values for heat flow due to conduction when used in Kit 1 where it was placed in all three fabric layers of the kit. This exchange with the outside environment occurred for this fabric when it was used as the outermost layer of the kit. Also, as Figure 4.68 shows Kit 1 had the largest range for values of heat flow due to conduction. For the relative humidity range from 86% to 95%, the human subject trial would be into Zone 3 which means that at this point the fabric vapor pressure would be saturated from the definition discussed in the previously in this Chapter. During this relative humidity range this Fabric A only exhibits a positive heat flow due to conduction indicating that this particular fabric is a better thermal conductor when saturated or wet. As shown in Figure 4.68 the range for heat flow due to conduction for each of the Kits where Fabric A was used only as the first layer is quite similar. When Fabric A is used as the second layer, it reached the same positive value of heat flow due to conduction as it did in the kits were it was for only the first layer but, did not reach the same level of negative values as the other kits allowing as much heat flow towards the body.

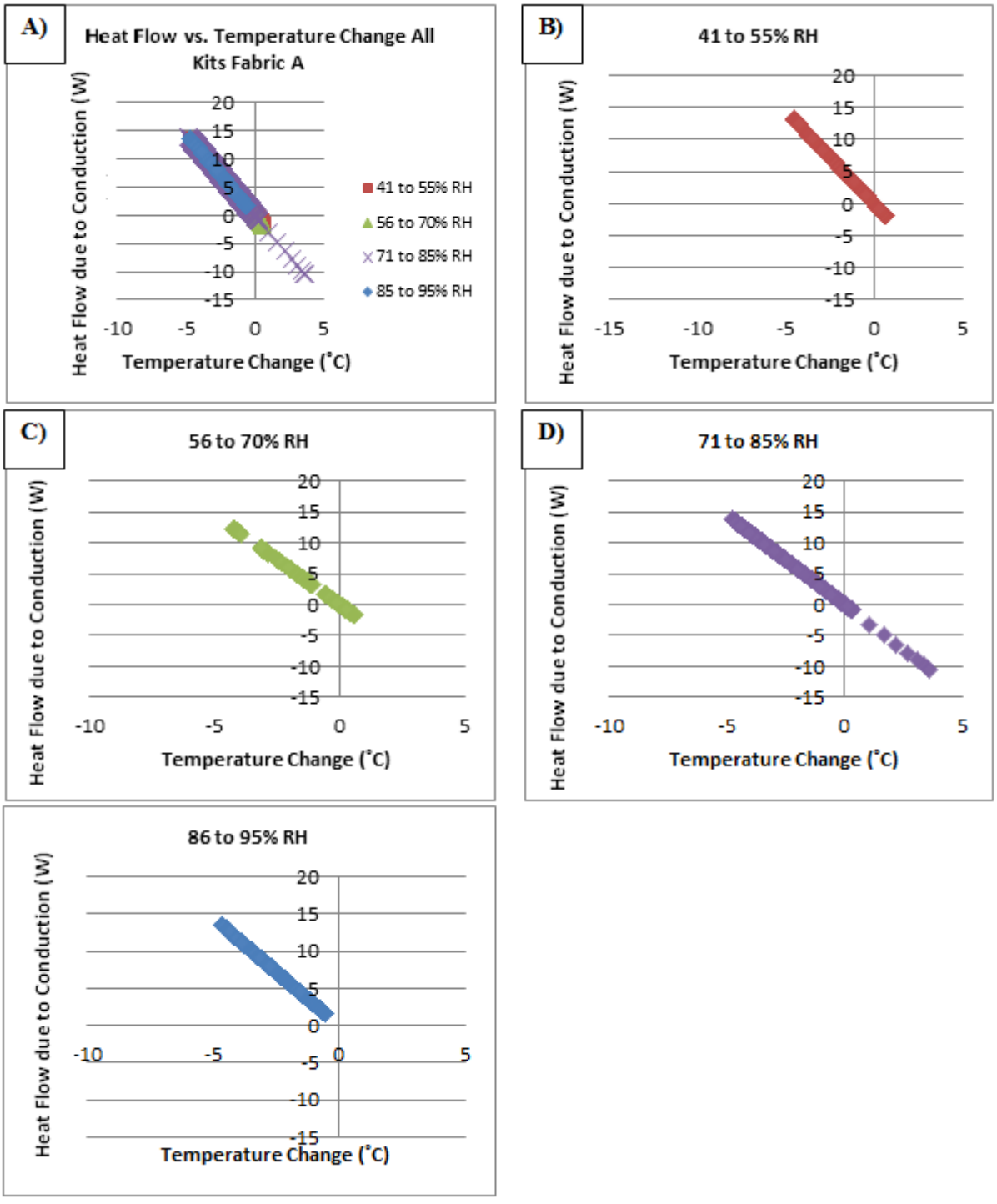

Figure 4.67: Heat Flow due to Conduction in Watts (W) versus Temperature Change All Kits Fabric A: A) All Relative Humidity Ranges, B) 41 to 55% R.H., C) 56 to 70% R.H., D)71 to 85% R.H., and E) 86 to 95% R.H.

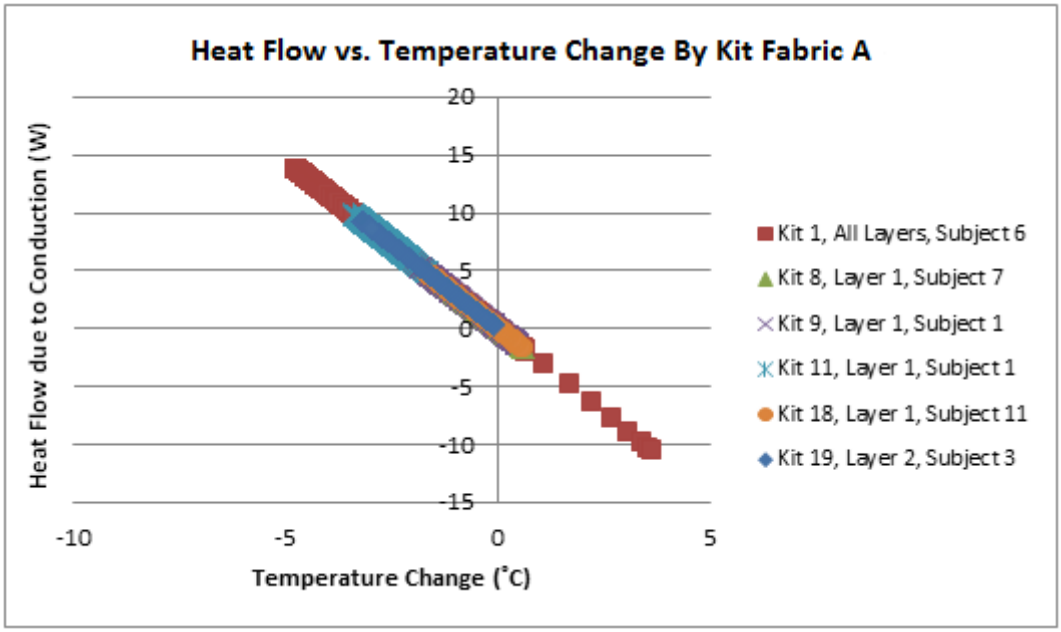

Figure 4.68: Heat flow (Q) due to Conduction in Watts (W) versus Temperature Change by Kit for Fabric A

4.5.3. Fabric B

As shown in Figure 4.69, the heat flow due to conduction range for Fabric B is greater than what was seen in the previous section for the microclimate, but not as large as Fabric A. The heat flow due to conduction range for Fabric B -0.98 to 10.25 W, and the range for temperature change is only between -1.17 and 3.22˚C. During the relative humidity range from 41 to 55%, which corresponds to Zone 1 for the human subject trials, the heat flow due to conduction is only positive when the pack was placed on the subject's body and the heat was flowing to the outside environment. During relative humidity range from 56 to 70% the heat flow due to conduction continues to remain mostly positive but, reaches zero. The relative humidity range from 71 to 85% shows the largest range in terms of the heat flow due

to conduction. These relative humidity measurements would be concentrated in Zones 2 and 3 were the kit was reaching its highest temperature and relative humidity measurements and heat flowed both away and back towards the subject's skin. For the relative humidity range from 86 to 95%, the human subject trial would be into Zone 3 and for this particular fabric the range does drop slightly into the negative values but only slightly. As shown in Figure 4.70, Fabric B was only used for the second and third fabric layers as it is a dense French terry knit suitable for a jacket end use. As shown in Figure 4.70 the range for heat flow due to conduction for each of the Kits where Fabric B was used as the second layer (Kit 7) is larger than that when used as the third and final layer (Kit 8). When Fabric B is used as the second layer, the range of values for the heat flow from conduction reaches the most negative and most positive values for the fabric which shows the effect of that the outside fabric choice can have on the clothing system. The third fabric layer of Kit 7 consisted of moisture blocking membrane sandwiched between two layers of thick fleece; this acted as a barrier for moisture and heat flow to the outside environment and may account for the heat flow back towards the body.

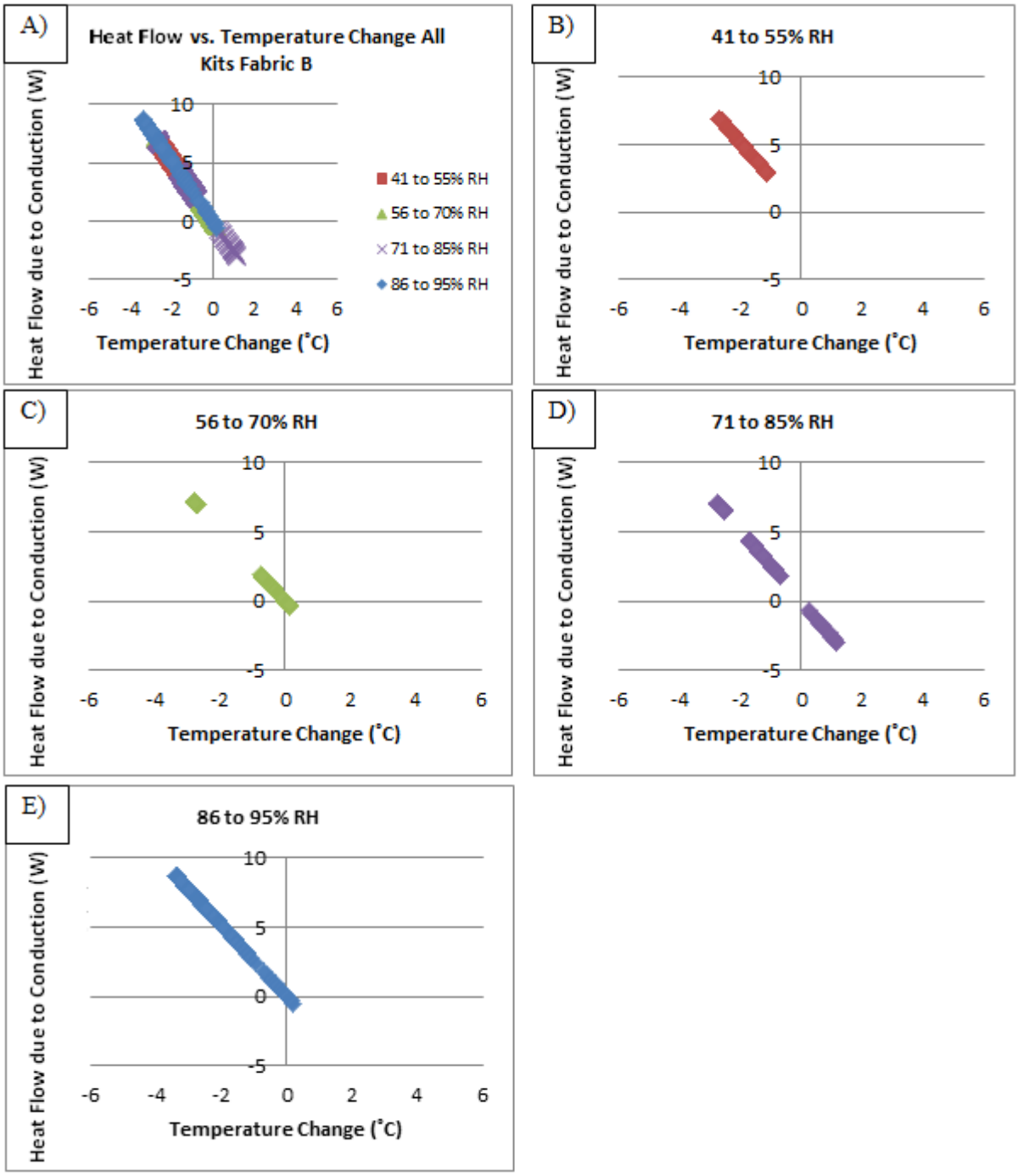

Figure 4.69: Heat Flow (Q) due to Conduction in Watts (W) versus Temperature Change for All Kits Fabric B: A) All Relative Humidity Ranges, B) 41 to 55% R.H., C) 56 to 70% R.H., D)71 to 85% R.H., and E) 86 to 95% R.H.

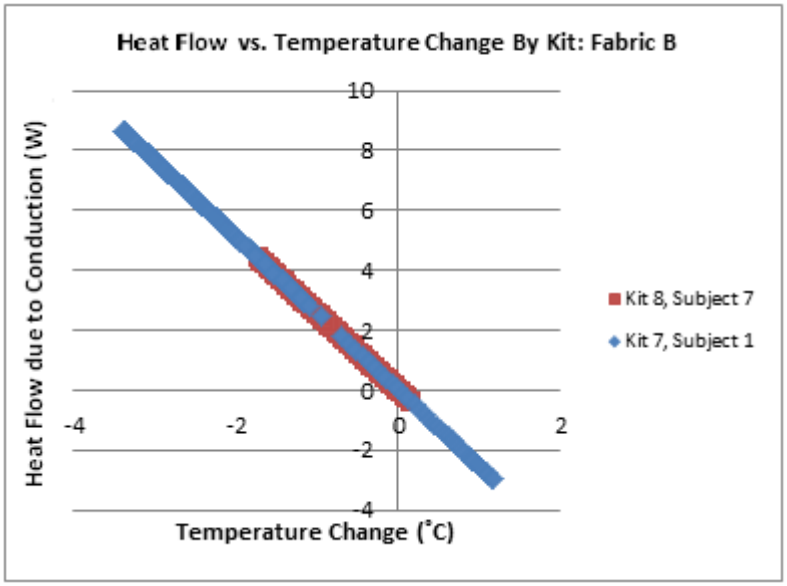

Figure 4.70: Heat Flow (Q) due to Conduction in Watts (W) versus Temperature Change by Kits Fabric B

4.5.4. Fabric D

As shown in Figure 4.71, the heat flow due to conduction range for Fabric D is largest of all the fabrics tested. The heat flow due to conduction range for Fabric D was between -65.29 and 111.29 W, while the range for temperature change was between -2.92 and 1.72 ˚C. This particular fabric was only used as a third fabric layer due to suitability of end use. The relative humidity range from 56 to 70% shows the largest range in terms of the heat flow due to conduction and shows that the heat flow movement away from and back towards the subject's skin. For the relative humidity range from 86 to 95%, the range is mostly contained within the positive values but, drops slightly into the negative values measuring 0.24 W at the lowest point. As shown in Figure 4.72 the range for heat flow due to conduction for Kit 17 was much wider than that of Kit 16.

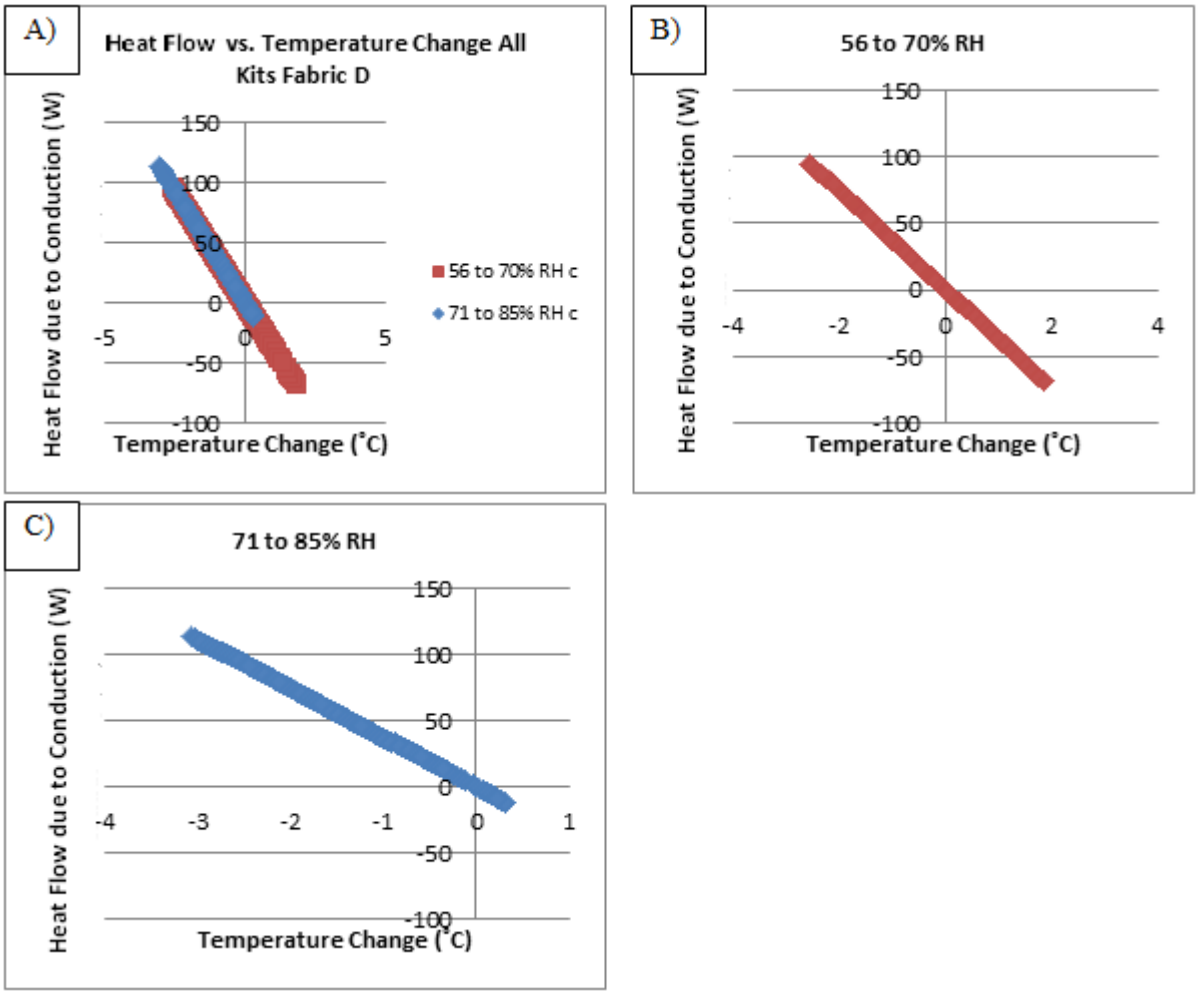

Figure 4.71: Heat Flow (Q) due to Conduction in Watts (W) versus Temperature Change All Kits Fabric D: A) All Relative Humidity Ranges, B) 56 to 70% R.H., and C) 71 to 85% R.H.

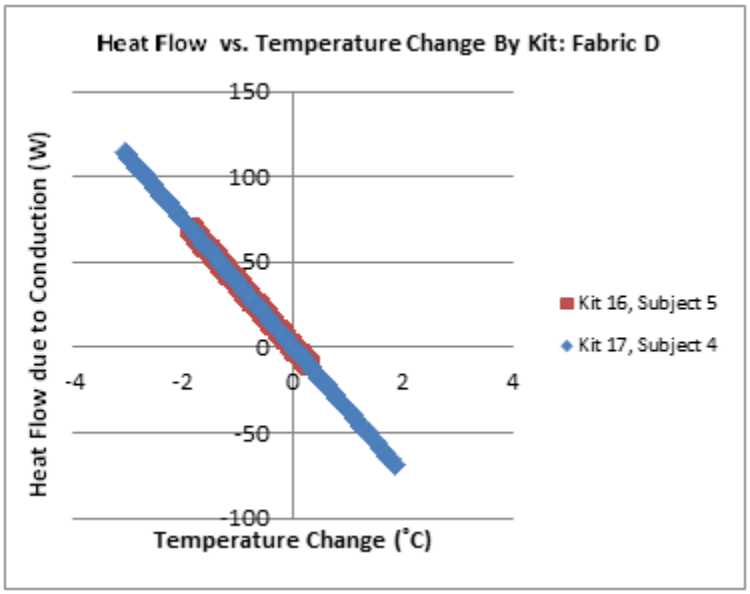

Figure 4.72: Heat Flow (Q) due to Conduction in Watts (W) versus Temperature Change by Kit Fabric D

This difference could be attributed to the other fabric layers used within the kit or the difference between subjects. However, the heat flow within the kit varies. The initial temperature and relative humidity measurements from the sensor closest to the skin for both kits were 22.71, 23.51˚C and 63.14, 63.96%. The highest temperature and relative humidity measurement reached within the trial at the sensor closet to the skin for both kits were 34.67, 35.15 ˚C and 92.74, 97.64%. Figure 4.73 shows what happened with the temperature measurements within these two kits where the largest build-up of heat for Kit 16 occurred after the first fabric layer and before the second fabric layer in the microclimate between these two fabrics. Build-ups of heat occurred in Kit 17 within fabric layers.

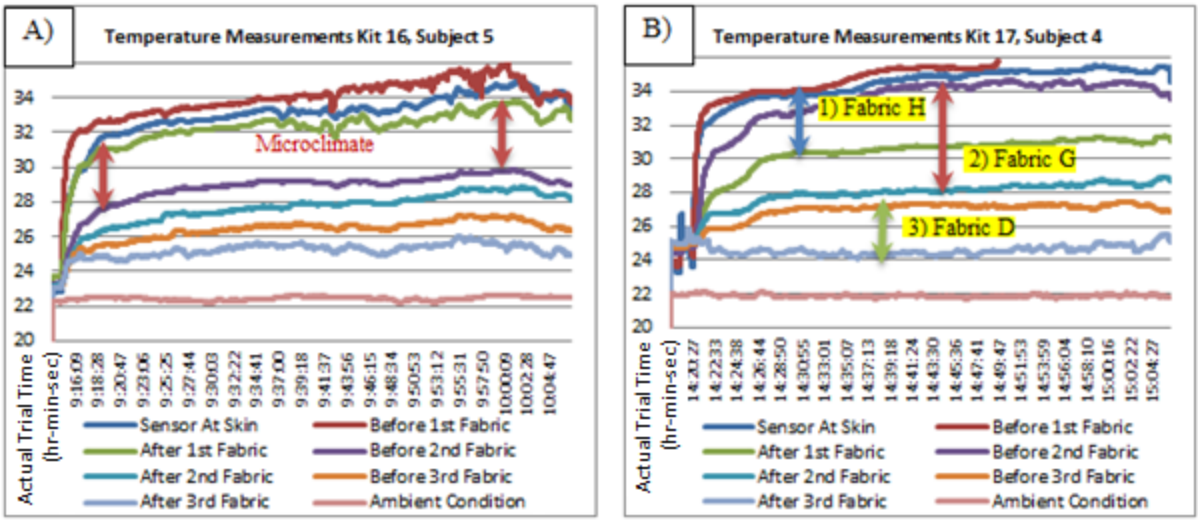

Figure 4.73: Temperature Change Across Microclimate and Fabric: A) Kit 16 and B) Kit 17

4.5.5. Fabric E

As shown in Figure 4.74, the heat flow due to conduction range for Fabric E is much greater than what was seen in the previous section for the microclimate. The heat flow due to conduction range for Fabric A -7.99 to 15.78 W, and the range for temperature change remained between -3.16 to -1.6 ˚C. During the relative humidity ranges from 20 to 55%, the heat flow due to conduction remains mostly positive. During relative humidity range from 56 to 70% the heat flow due to conduction continues to remain mostly positive, but moves into the negative ranges. The relative humidity range from 71 to 85% is only in the positive ranges for heat flow due to conduction meaning that the direction of flow was away from the skin. However, for the relative humidity range from 86 to 95%, the heat flow due to conduction continues to remain mostly positive, but becomes negative and reaches a low point of -7.99 W.

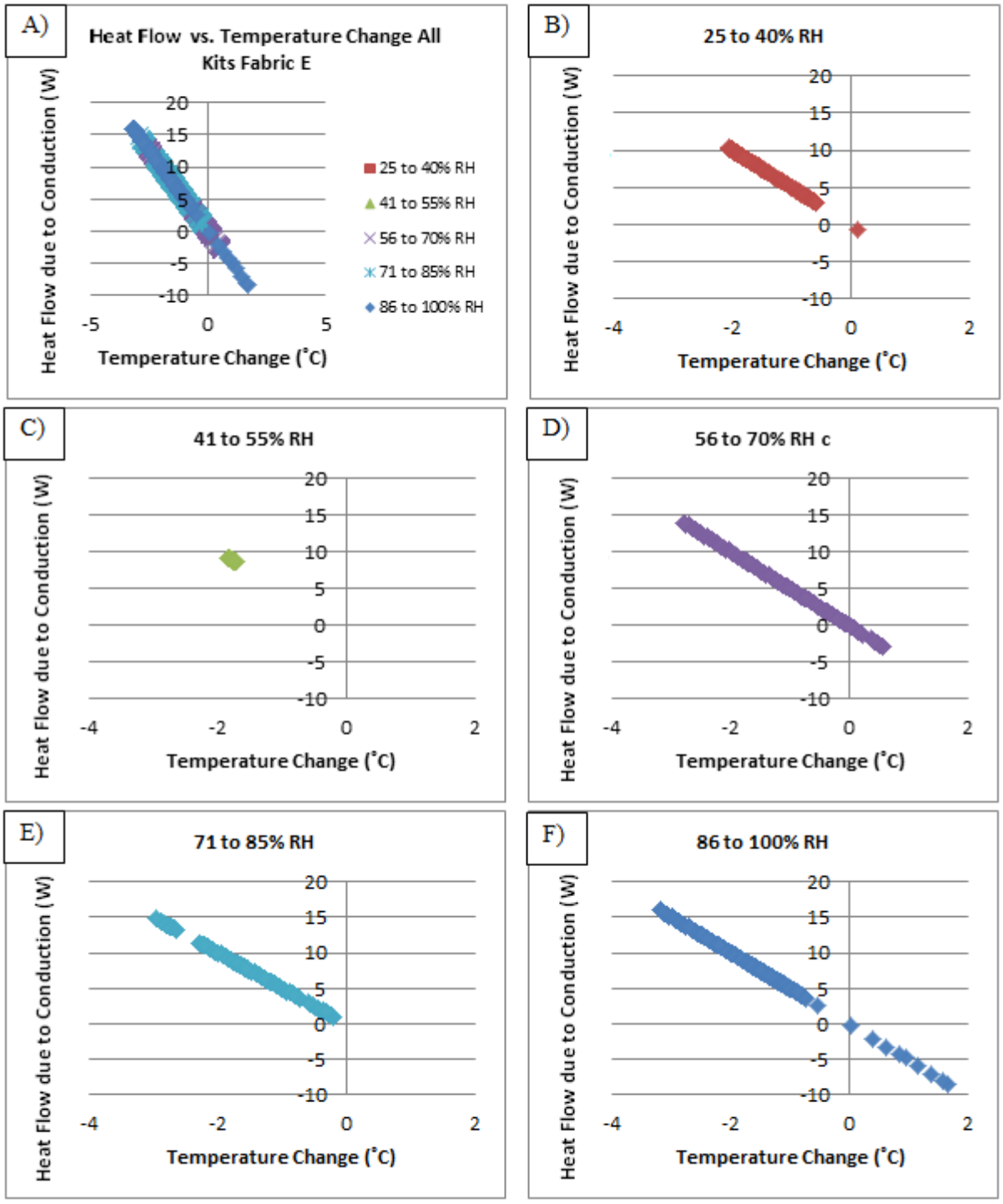

Figure 4.74: Heat Flow (Q) due to Conduction in Watts (W) versus Temperature Change All Kits Fabric E: A) All Relative Humidity Ranges, B) 25 to 40% R.H., C) 41 to 55% R.H., D) 56 to 70% R.H., E)71 to 85% R.H., and F) 86 to 100% R.H.

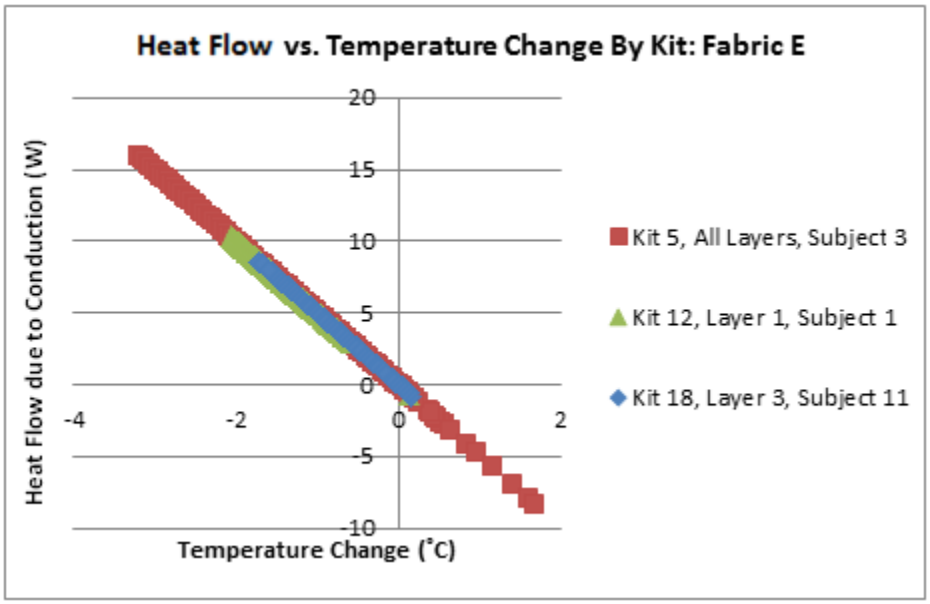

Figure 4.75: Heat flow (Q) due to Conduction in Watts (W) versus Temperature Change by Kit Fabric E

Similar to Fabric A, as shown in Figure 4.75, Fabric E has the greatest range of heat flow due to conduction with used in all three layers (Kit 5). It should be noted that when used in the first layer in Kit 12 that the heat flow only moved away from the body for Fabric E.

4.5.6. Fabric F

As shown in Figure 4.76, the heat flow due to conduction range for Fabric E was between -0.14 and 1.5 W, while the range for temperature change was between -2.56 and 0.24 ˚C. This particular fabric was only used as a third fabric layer due to suitability of end use. The relative humidity range from 20 to 70% shows the largest range in terms of the heat flow due to conduction and shows that the heat flow movement away from and back towards the subject's skin. For the relative humidity range from 71to 75%, the range is contained within the positive values. The range for heat flow due to conduction for varies by kit.

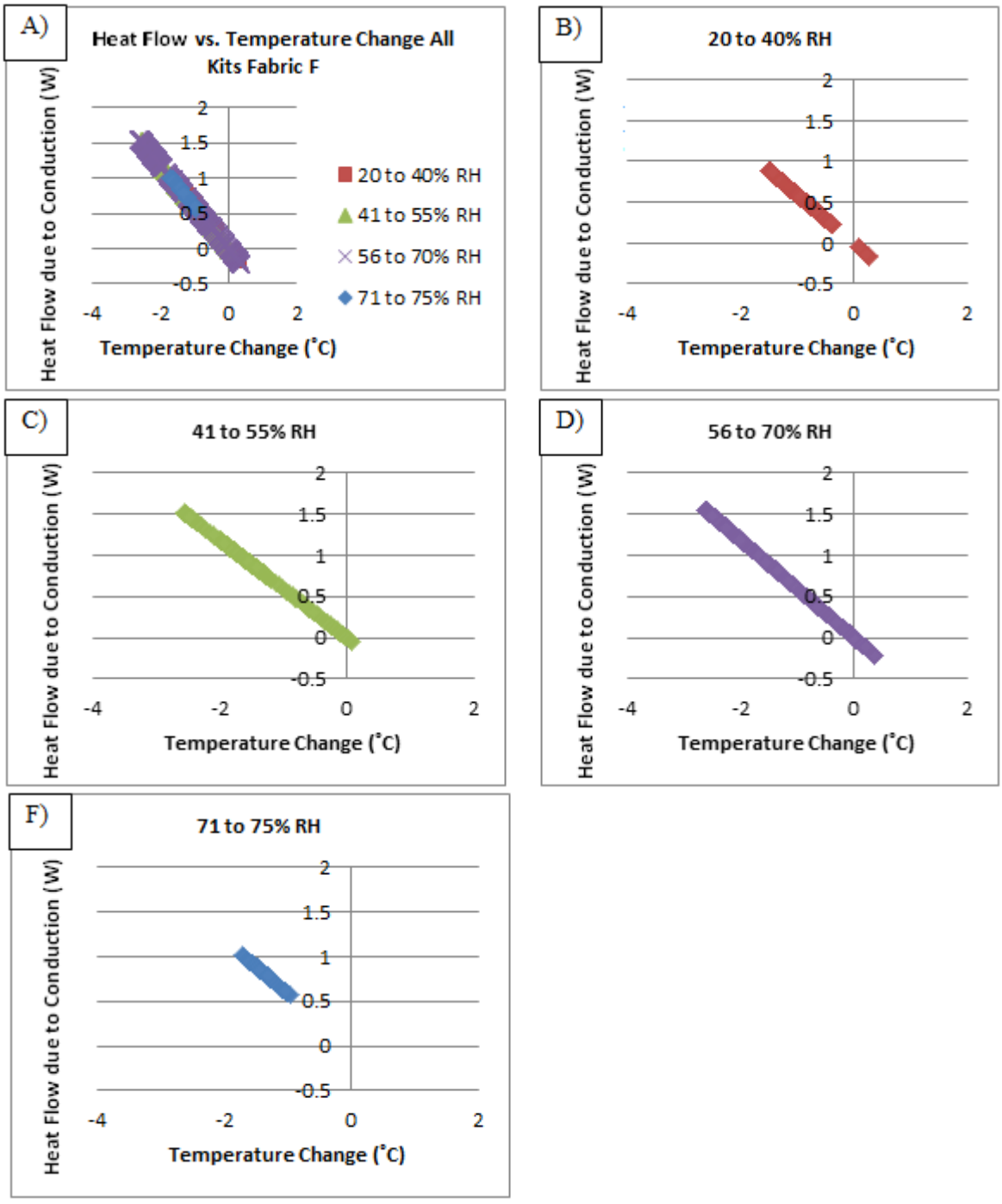

Figure 4.76: Heat Transferred (W) versus Temperature Change All Kits Fabric F: A) All Relative Humidity Ranges, B) 20 to 40% R.H., C) 41 to 55% R.H., D) 56 to 70% R.H., and E)71 to 75% R.H.

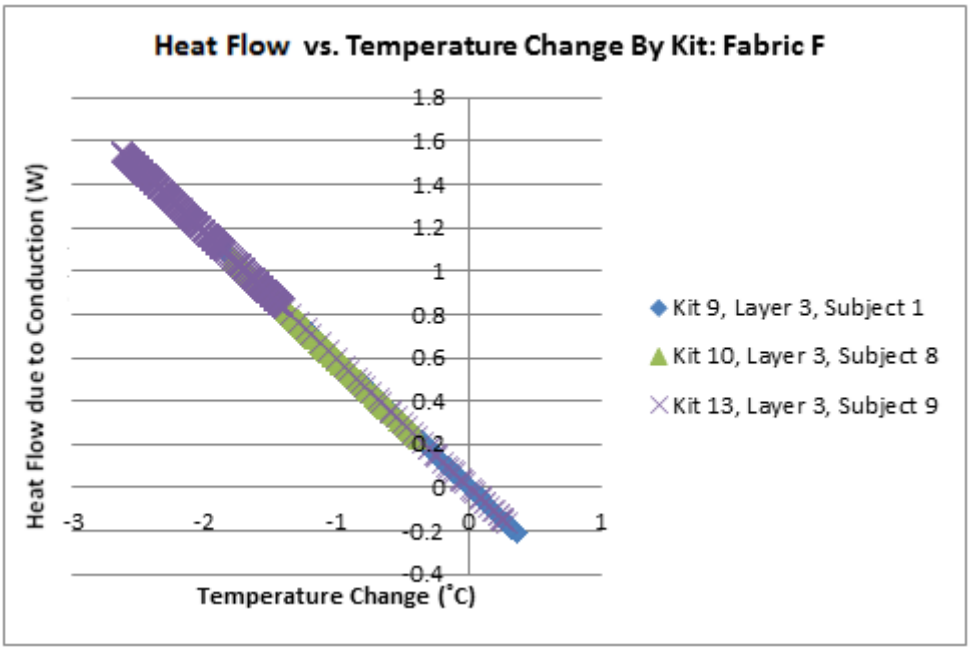

Figure 4.77: Heat Transferred (W) versus Temperature Change By Kit Fabric F

4.5.7. Fabric G

As shown in Figure 4.78, the heat flow due to conduction ranges for Fabric G -14.98 to 36.87 W, while the range for temperature change remained between -6.2 and 2.52 ˚C. During the relative humidity range from 20 to 40%, the heat flow due to conduction remains mostly negative. During relative humidity ranges from 40 to 85% the heat flow due to conduction shows a large range in terms of the heat flow due to conduction, indicating heat flowed both away and back towards the subject's skin. However, as shown in Figure 4.79, Fabric G reaches the largest positive values for heat flow due to conduction when used in Kit 17. It should also be noted that in Kit 13 the heat does not flow back towards the body through Fabric G during the human subject trial.

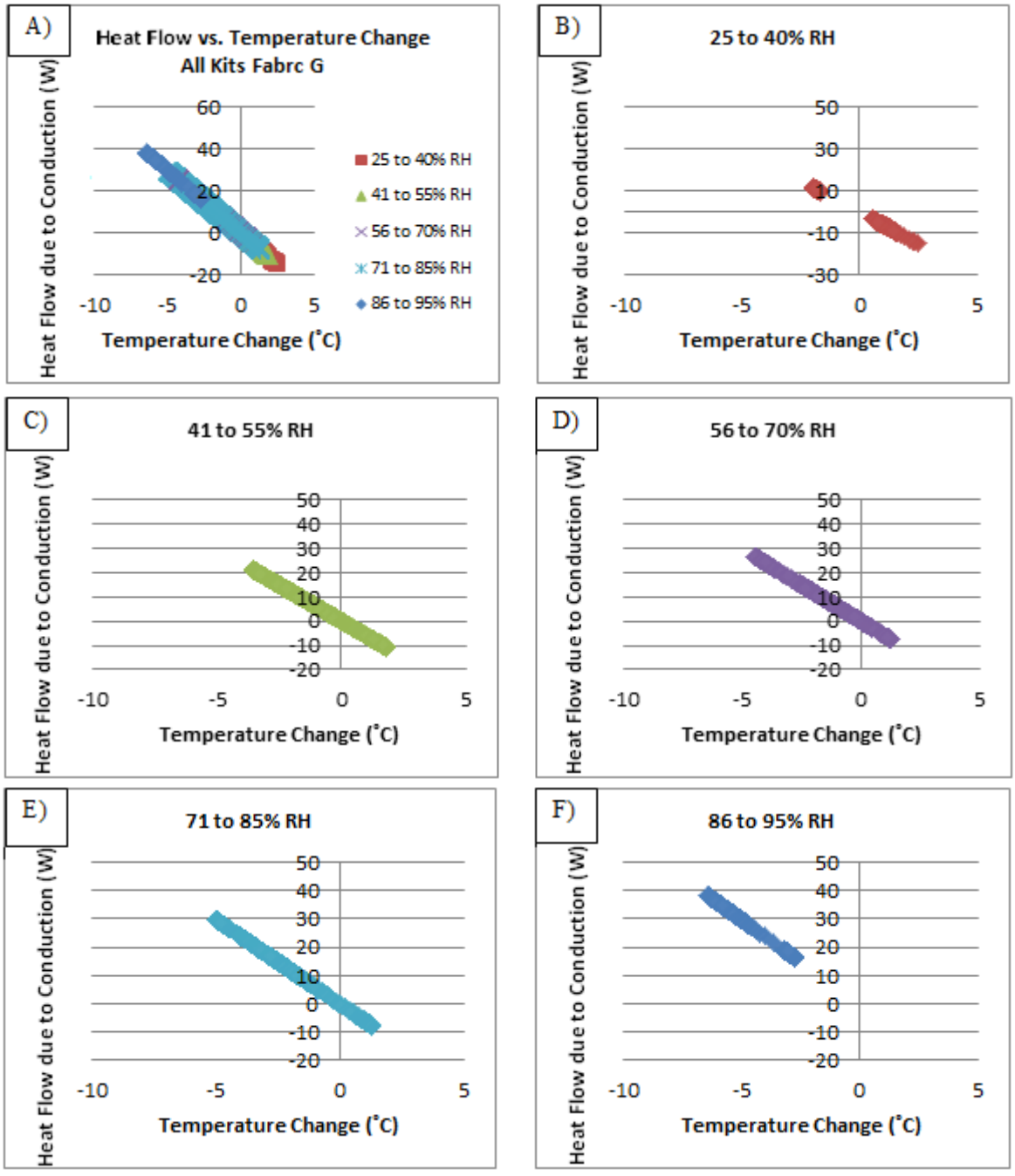

Figure 4.78: Heat Flow (Q) due to Conduction in Watts (W) versus Temperature Change All Kits Fabric G: A) All Relative Humidity Ranges, B) 25 to 40% R.H., C) 41 to 55% R.H., D) 56 to 70% R.H., E) 71 to 75% R.H., and F) 86 to 95% R.H.

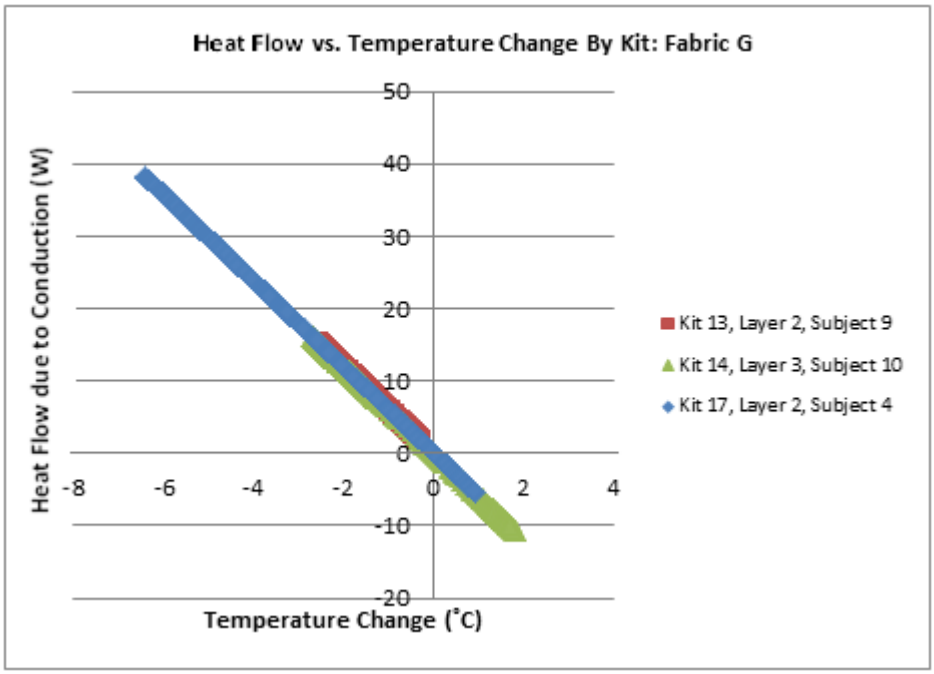

Figure 4.79: Heat Flow (Q) due to Conduction in Watts (W) versus Temperature Change by Kit Fabric G

4.5.8. Fabric H

As shown in Figure 4.80, the heat flow due to conduction ranges for Fabric H from -13.01 to 43.22 W, while the range for temperature change remained between -6.88 and 2.07 ˚C. During the relative humidity range from 25 to 40%, which only accounts for a small fraction of the data points, the heat flow due to conduction is positive. For the remainder of the human subject trials using Fabric H, the relative humidity range from 40 to 95% the heat flow due to heat flowed both away and back towards the subject's skin. As shown in Figure 4.81 all of the kits using Fabric H except Kit 8 and 18 where the fabric was used in the second layer, the heat flow due to conduction exhibited negative values.

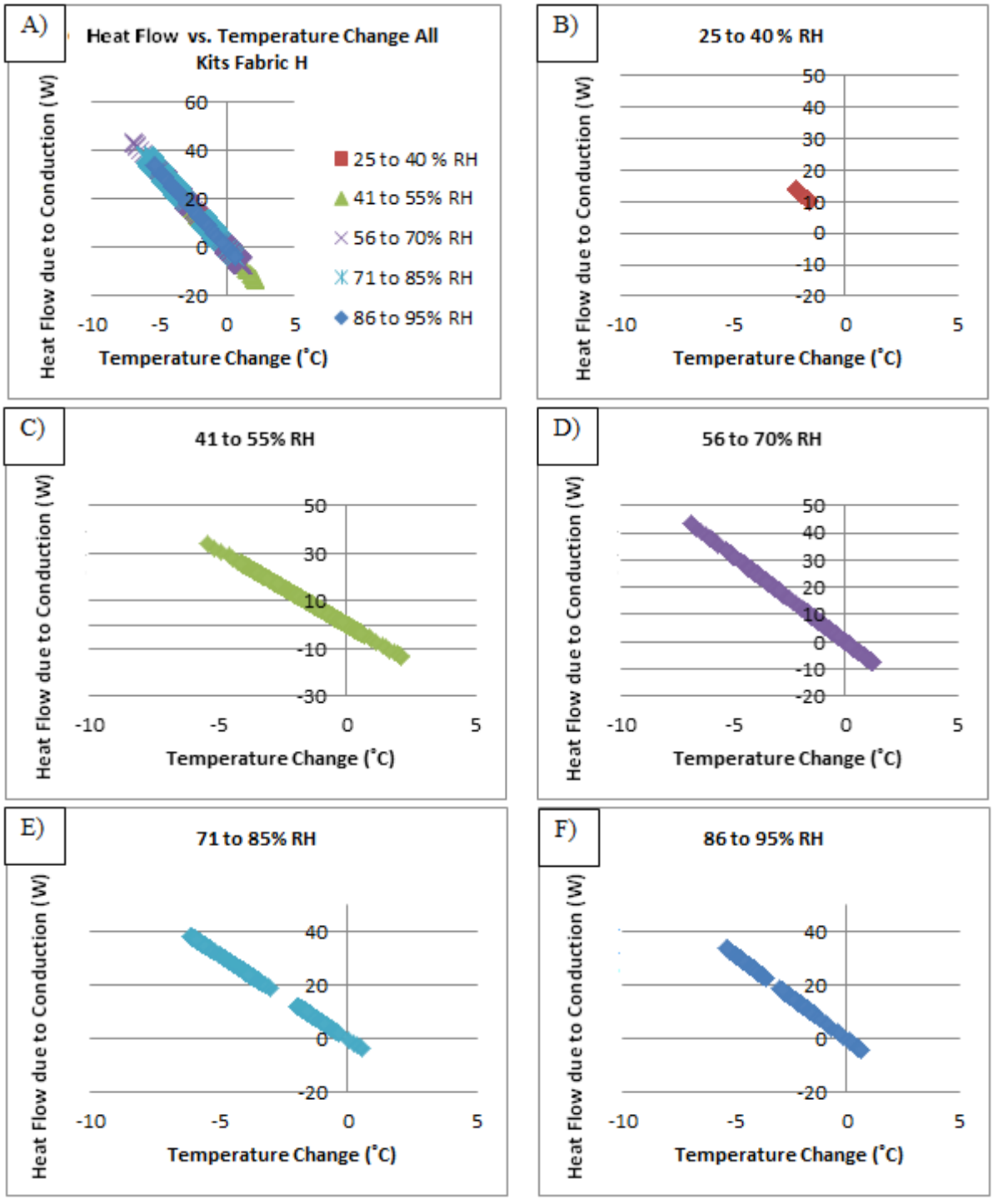

Figure 4.80: Heat Flow (Q) due to Conduction in Watts (W) versus Temperature Change All Kits Fabric H: A) All Relative Humidity Ranges, B) 25 to 40% R.H., C) 41 to 55% R.H., D) 56 to 70% R.H., E) 71 to 75% R.H., and F) 86 to 95% R.H.

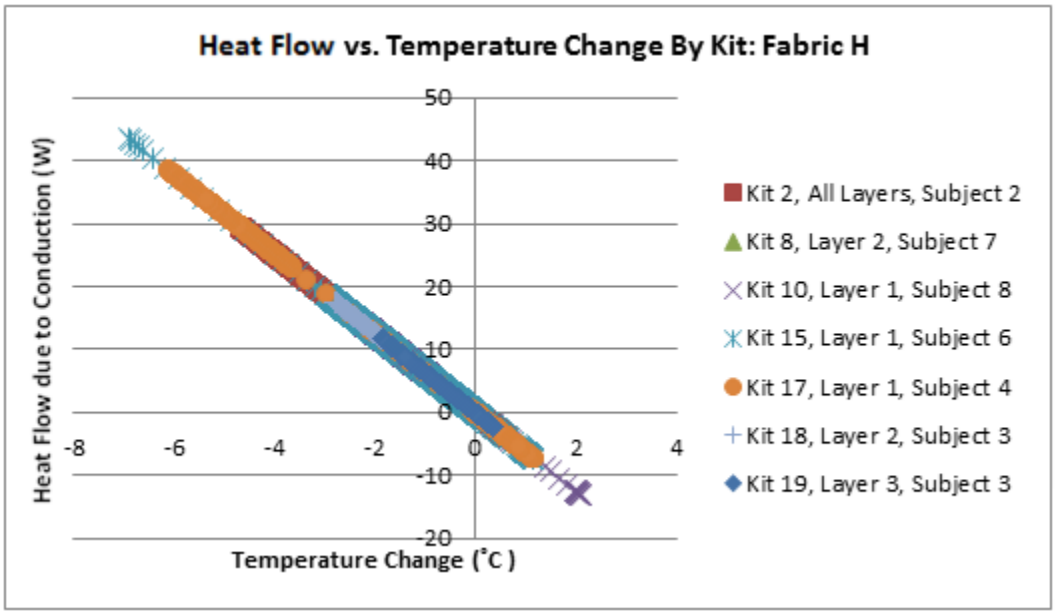

Figure 4.81: Heat Flow (Q) due to Conduction in Watts (W) versus Temperature Change by Kit Fabric H

4.5.9. Fabric I

As shown in Figure 4.82, the heat flow due to conduction range for Fabric I was -10.71 to 19.04 W, while the range for temperature change remained between -3.52 and 1.98 ˚C. During the relative humidity ranges from 41 to 85%, the heat flow due to conduction remains mostly positive indicating that once the pack was placed on the subject's body the heat was flowing to the outside environment. During relative humidity range from 56 to 70% the heat flow due to conduction continues to remain mostly positive but, also reaches into the negative values so, heat flowed both away and back towards the subject's skin (with the exception of Kit 6). For the relative humidity range from 86 to 95%, where Fabric I would be saturated, the heat flow due to conduction is positive indicating that this particular fabric is a better thermal conductor wet.

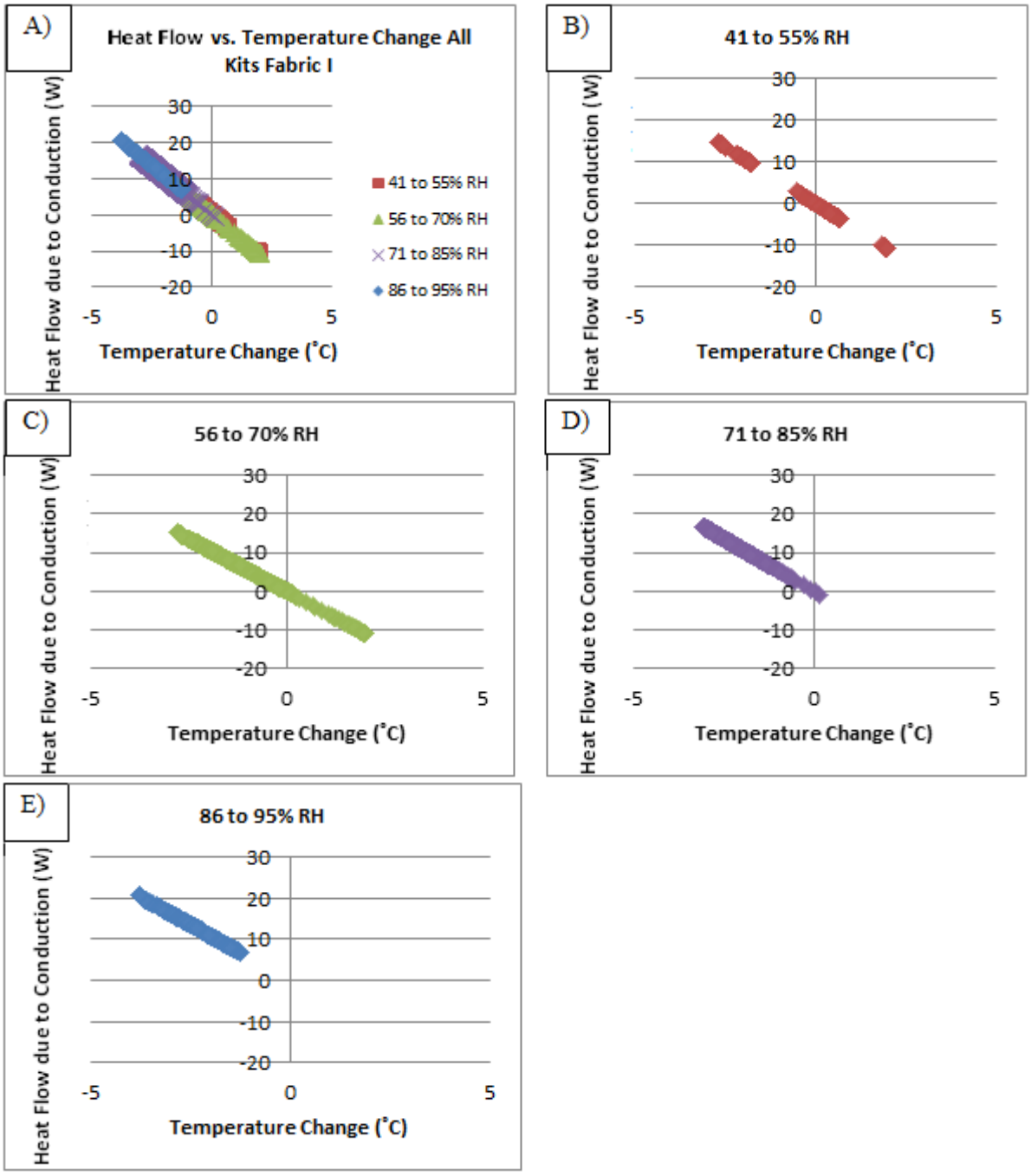

Figure 4.82: Heat Flow (Q) due to Conduction in Watts (W) versus Temperature Change All Kits Fabric I: A) All Relative Humidity Ranges, B) 41 to 55% R.H., C) 56 to 70% R.H., D) 71 to 75% R.H., and E) 86 to 95% R.H.

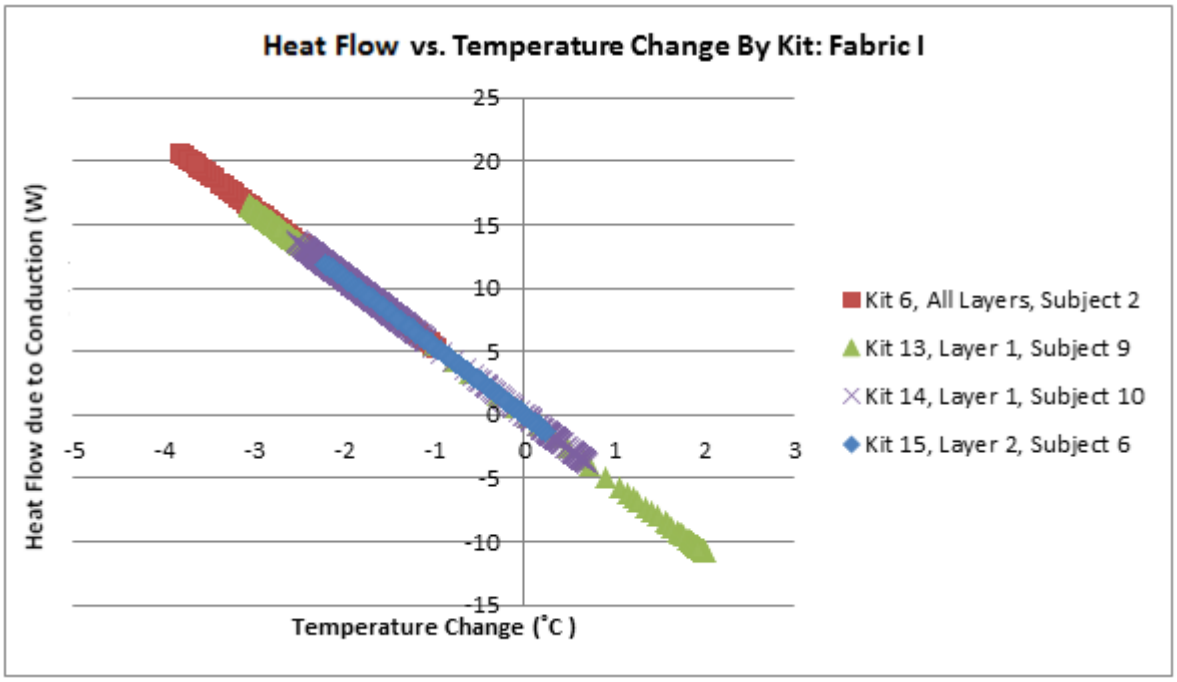

Figure 4.83: Heat Flow due to Conduction in Watts (W) versus Temperature Change By Kit Fabric I

4.5.10. Fabric K

As shown in Figure 4.84, the heat flow due to conduction ranges for Fabric K from -8.56 to 8.56 W, while the range for temperature change remained between -4 and 4 ˚C. During all the relative humidity ranges, from 20 to 95%, the heat flow due to heat flowed both away and back towards the subject's skin. As shown in Figure 4.85, Kit 11 and 14 have the smallest range of values for heat flow due to conduction while Kit 3 has the largest range. However, all of the Kits with Fabric K have instances within the trial where the heat flow due to conduction was negative and flowing back towards the human subject's skin.

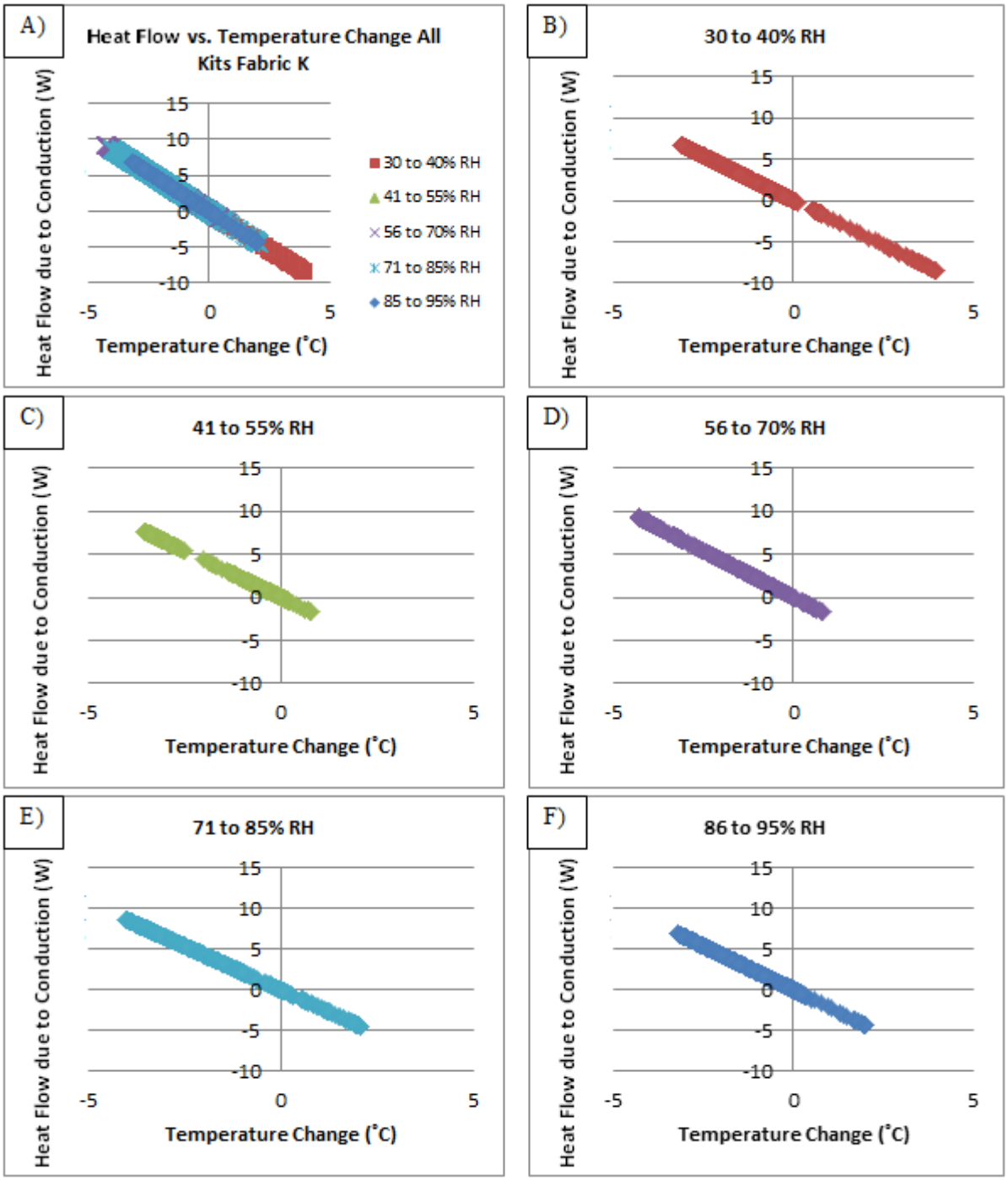

Figure 4.84: Heat Flow (Q) due to Conduction in Watts (W) versus Temperature Change All Kits Fabric K: A) All Relative Humidity Ranges, B) 30 to 40 R.H., C) 41 to 55% R.H., D) 56 to 70% R.H., E) 71 to 75% R.H., and F) 86 to 95% R.H.

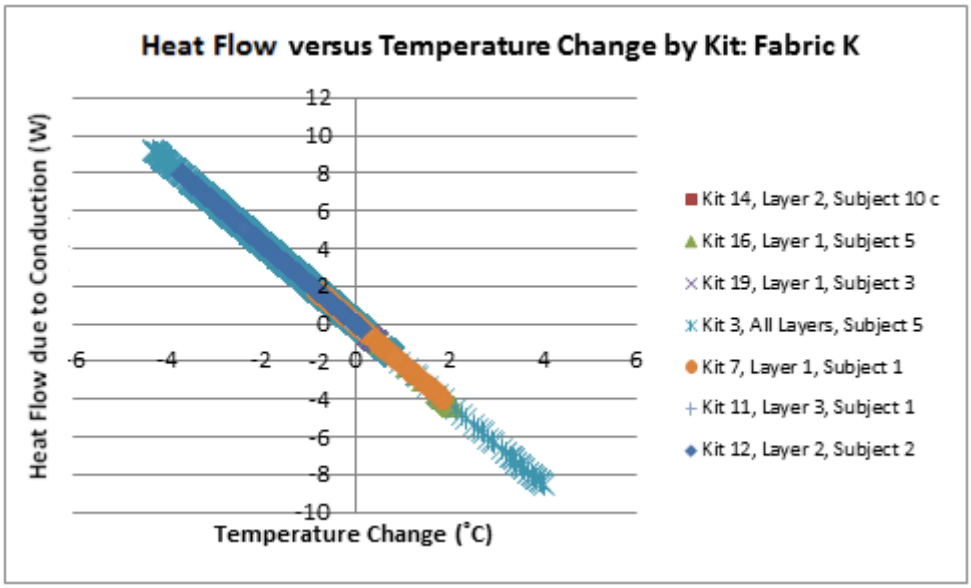

Figure 4.85: Heat Flow (Q) due to Conduction in Watts (W) versus Temperature Change by Kit Fabric K

Figure 4.86 depicts heat flow due to conduction versus temperature change for all the fabrics used in this study as well as for the microclimate within each of the fabric testing kits for different ranges of humidity. Finding 16 of 17: fabric thickness alters heat flow due to conduction with no apparent effect from changes in relative humidity (as measured in this study between 25 and 95% R.H.). As shown in Figure 4.86, Fabric D allowed by far the most heat flow due to conduction of the fabrics tested in this study. Fabric D is an ultra-lightweight woven material that is very thin so, it has very little insulation due to air within the fabric. However, when layered in a clothing system, this type of fabric is not traditionally worn next to the skin as a t-shirt or undergarment so, it was only tested as an outer garment on the third layer of the fabric testing kit. Figure 4.87 shows the buildup of relative humidity in the kits using Fabric D represented by the red arrows in the graph, where the fabric

combination of Kit 16 allowed more relative humidity escape to the outside environment through Fabric D. The next fabric which allowed more heat flow due to conduction than the others was Fabric H followed by Fabric G, I, and E. The rest of the fabrics were lumped together at a lower level allowing less heat flow due to conduction, were Fabric K, B, and A. Fabric F was by far the thickest fabric and allowed the least heat flow due to conduction at almost the same level as Microclimate which consisted of atmospheric air. Finding 17 of 17: the microclimate within these fabric testing kits serves as an insulation layer that humidity changes have no effect which could be found with this study.

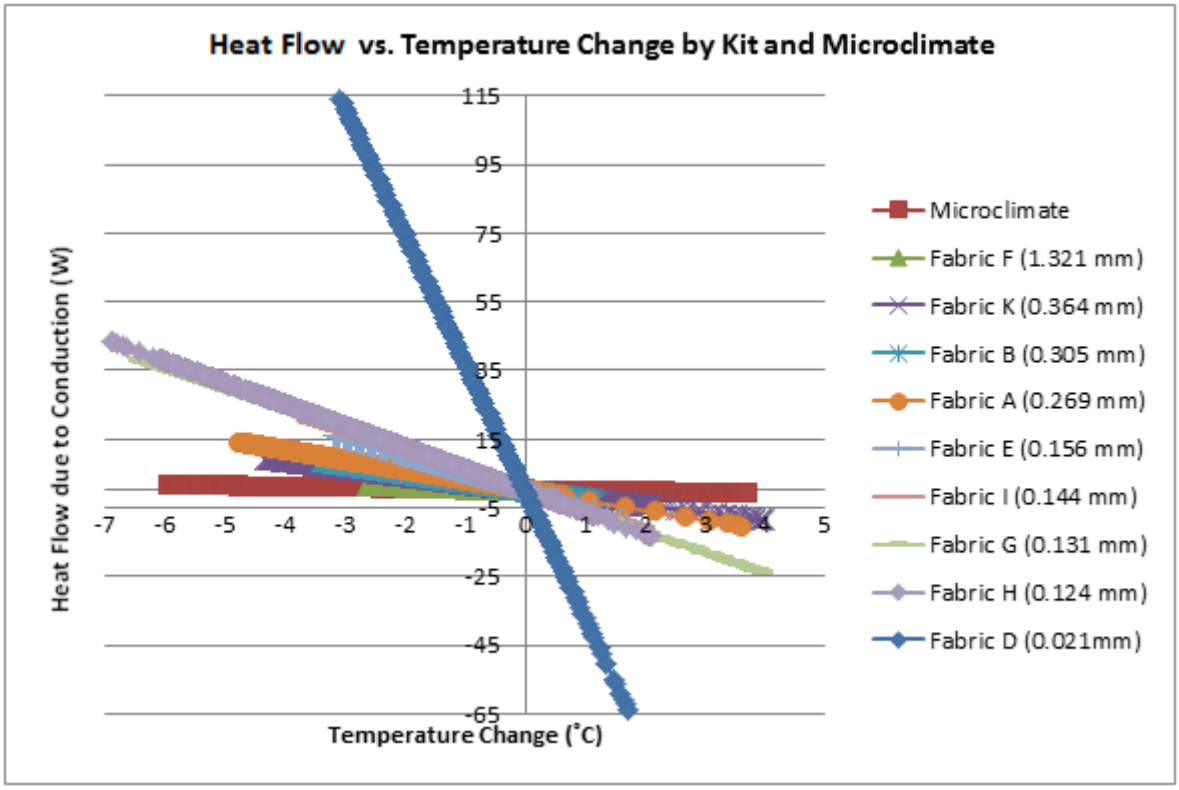

Figure 4.86: Heat Flow (Q) due to Conduction in Watts (W) versus Temperature Change by Kit and Microclimate

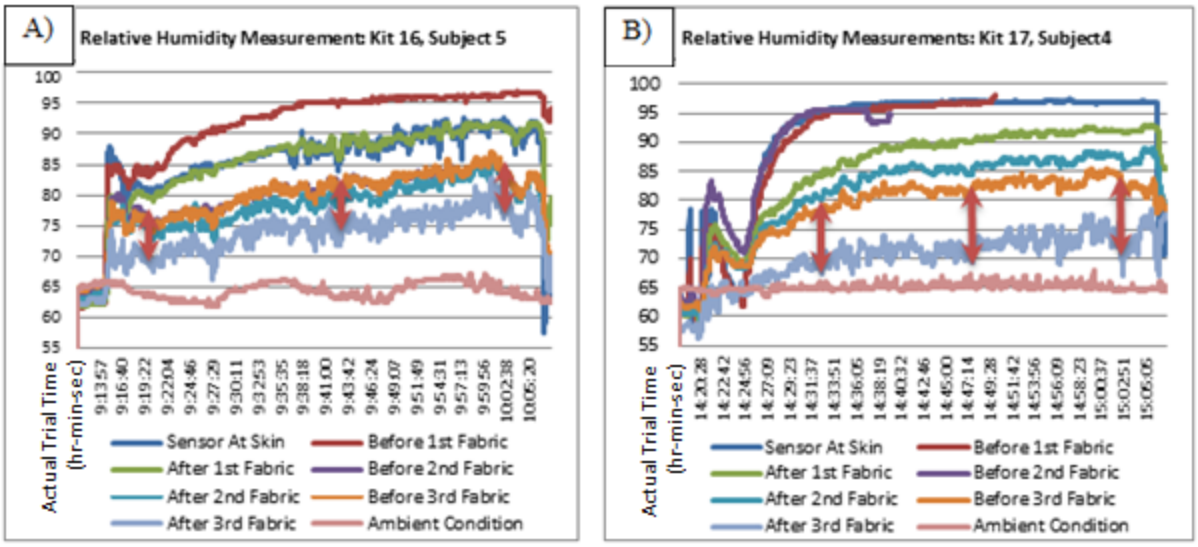

Figure 4.87: Relative Humidity Measurement A) Kit 16 and B) Kit 17

As previously concluded, individual fabric performance is more dependent on the combination of fabrics used for a fabric testing kit rather than its own performance characteristics. Overall, every fabric testing kit experienced buildups of temperature and relative humidity which hindered energy flow from the body to the ambient environment. As far as fabric performance within a kit is concerned, the heat and moisture buildup occurred within the microclimate or the fabric layer itself. Logically, the most successful kits would be those that allowed moisture and heat to move the farthest away from the body. In other words the kits in which the buildup of temperature and relative humidity occurred within the microclimate before the final layer of fabric or within the final layer of fabric as shown in Figure 4.87. On the other hand, the worst scenario would be large heat and humidity buildup within one of the inner layers of the kit as seen in Figure 4.88. Kit 9 had the greatest difference between the temperature and humidity measurements at the skin and that of the outside of the third layer.

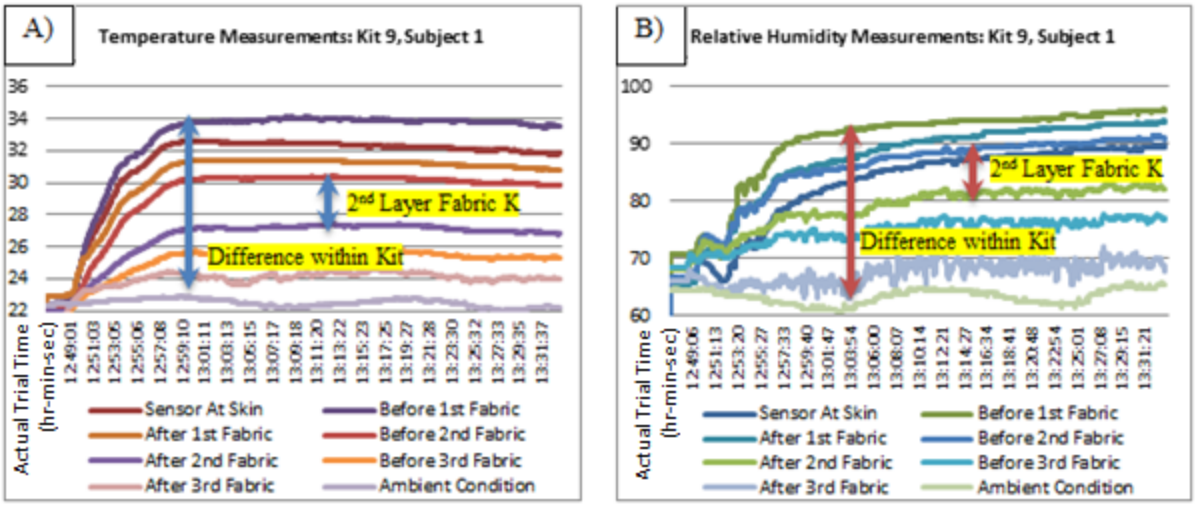

Figure 4.88: A) Temperature Measurements Kit 9 and B) Relative Humidity Measurements Kit 9

It should be noted that each of the kits shown in Figure are standard kits meaning the same fabric is used for each of the three layers. This supports the idea that the individual moisture management properties of fabrics used in a clothing system are less important than the combination of moisture management for the clothing system as a whole. Another scenario is to have the humidity buildup fairly evenly spaced within the kit and the best example of this was found in Kit 18 which is shown in Figure. As shown, the overall difference between the relative humidity coming off the skin is smaller compared to any of the other even those kits that moved the moisture majority buildup to the outside microclimate and third fabric layer. Based on Findings 1 through 17, in terms of building clothing systems, there are two outcomes: for summer or hot environments, thin fabrics with no microclimate are ideal; for winter or cold environments, fabrics which create microclimates on the outer layer away from the skin are important but, it is ideal to avoid microclimates or insulative layers involving atmosphereic air close to the skin.

Figure 4.89: Relative Humidity Measurements: A) Kit 2, B) Kit 3, C) Kit 5, and D) Kit 6

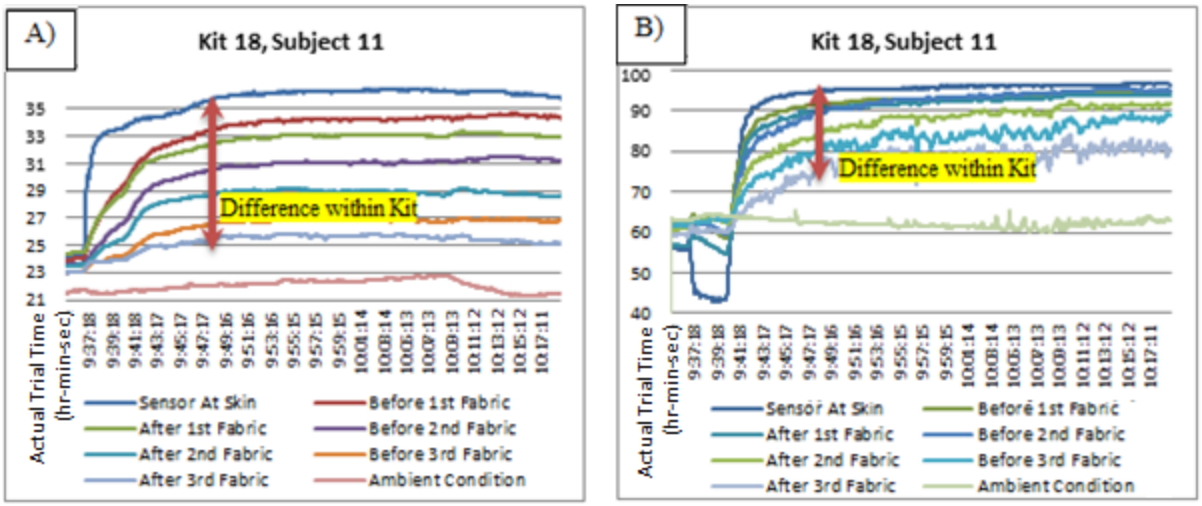

Figure 4.90: A) Temperature Measurements Kit 18 and B) Relative Humidity Measurements Kit 18

4.6. Summary of Findings

The findings of this research study were compiled in a list of nineteen findings (described in detail in Chapter 4) which cover several aspects of the research such as the use of fabric testing kits for the human subject trials, the onset of perspiration which occurred among the human subjects, the choice of fabric for the fabric testing kits, and the moisture transfer by Zone and by fabric location within the fabric testing kit. Also, these findings include an analysis of the heat flow due to conduction and the temperature changes across the fabrics and the microclimate for relative humidity ranges measured in this study.

- Finding 1 of 17: each trial was successful in inducing perspiration in the human subject early in the trial protocol,
- Finding 2 of 17: there are only small variations in temperature at the skin from subject to subject,

- Finding 3 of 17: there was little variation from subject to subject in terms of the relative humidity measured at the skin,
- Finding 4 of 17: definite patterns emerge which apply all the human subject trials,
- Finding 5 of 17: the eight sensors are capable of measuring differences in both temperature and relative humidity within the kit,
- Finding 6 of 17: the temperature and relative measurements can be divided into three distinct zones for analysis,
- Finding 7 of 17: for each human subject the onset of perspiration was sudden and the humidity increased inside the fabric testing kit at a rapid rate,
- Finding 8 of 17: heat energy and vapor pressure flows from an area of higher temperature to an area of lower temperature,
- Finding 9 of 17: when actual vapor pressure reaches saturated vapor pressure the diffusion of moisture vapor is hindered or stalled,
- Finding 10 of 17: once a saturation level has been achieved within a fabric worn during exercise; without any outside disturbance i.e. air flow, temperature change, etc. diffusion of water vapor through the fabric will not recommence during an exercise routine,
- Finding 11 of 17: there were distinct differences in temperature measurements at sensors on either side of a fabric layer,
- Finding 12 of 17: the enthalpy fluctuations calculated coincide with vapor pressure movement and heat flow,

- Finding 13 of 17: the outer fabric layer was least affected by the moisture from the human subject while, the first two layers are most critical in managing the moisture transfer,
- Finding 14 of 17: that fabric used for the second and third layers of the fabric testing kit affects the energy flow through the first fabric,
- Finding 15 of 17: individual fabric performance is more dependent on the combination and location of fabrics used for a fabric testing kit rather than its own performance characteristics,
- Finding 16 of 17: fabric thickness alters heat flow due to conduction with no apparent effect from changes in relative humidity (as measured in this study between 25 and 95% R.H),
- Finding 17 of 17: the microclimate within these fabric testing kits serves as an insulation layer that humidity changes had no effect upon,
- Based on Findings 1 through 17: for summer or hot environments thin fabrics with no microclimate are ideal, and for winter or cold environments fabrics which create microclimates on the outer layer away from the skin are important but, microclimates or insulative layers close to the skin should be avoided.

These findings were drawn from a detailed analysis of multilayer clothing performance during an exercise routine and can be used to better understand how an athlete's body responds to exercise and help in the design of clothing systems that are better suited for athletes or regular exercisers will be perspiring for prolonged periods of time such as long distance runners and cyclists. These findings were also drawn from an in depth analysis of an

athletes' warm up prior to training or competing, which can aid in the development of clothing systems that effectively warm muscles to a competing temperature and prevent formation of lactic acid build up before or after the competition.

CHAPTER FIVE

5. Conclusions, Summary, and Recommendations

This research investigated how to build a layered clothing system that would optimize moisture management and performance during athletic end use through some very decisive conclusions. Athletic apparel manufacturers must consider the market moisture and heat management as a clothing system where the layers work together. The fabric testing kits show it is the combination of the fabric layers that determines the performance of the clothing system. This means that the undergarment must be designed to work with the t-shirt, tank, top, jacket, pullover, etc. in order to optimize the athlete's experience. As the results of this research show, within the fabric testing kits the temperature movement across multiple layers of fabric is not sufficient to prevent saturated vapor pressure build-up. When the saturated vapor pressure produced a build-up a stall in vapor pressure movement occurred within each fabric testing kit. This highlights opportunities to redesign athletic wear to conduct better. Fabrics which can increase the heat transferred would increase the vapor pressure movement from the body to the outside environment thus optimizing moisture management and athletic wear performance.

5.1. Summary

It is well known that clothing can modify the body's heat loss from the skin as well as the moisture loss from the skin. During physical activity muscles burn nutrients which releases energy, some of which is released outside the body as external work, but the majority of it is released as heat. The human should maintain a constant core temperature of about 37

degrees Celsius, only a small change (+/-) ~4°C can lead to serious injury or death. Also, there are only four mechanisms that allow the body to lose heat to the environment in order to maintain its thermal balance: conduction, convection, radiation, and evaporation. This research utilizes a test method where multiple fabric layers are tested simultaneously as a person would wear multiple garment layers together. Typically, existing testing procedures for the measure of heat and moisture transport in textile materials are successful in measuring one layer of fabric at a time with the exceptions of the guarded sweating hotplate and the sweating manikin which measure multiple fabric layers by combining the fabric layers and the air layers. However, people typically wear more than one layer of clothing especially on their upper torso which could include a foundation garment such as a sports bra, undershirt or t-shirt, and an additional layer consisting of a shirt or jacket. As part of this research, fabric testing kit was designed in order to test three different fabric layers at the same time while mounted on a human subject during exercise. This fabric testing kit measured coupled heat and moisture transfer in relation to temperature and humidity across the microclimates, the interaction between clothing to skin, and the layer to layer interactions of a clothing system.

5.1.1. Human Subjects

Human subjects were recruited from active bicyclist and athletes who use the bicycle frequently in their training routines. All of the human subjects were accustomed to riding a bicycle for an extended period of time. These individuals were all athletic and capable of performing the human trial where they would be asked to ride a bicycle to produce perspiration. Both males and females participated in this study. A total of eleven different subjects were used in this research including seven males and four females. The test protocol

was approved by the Institutional Review Board – Human Subjects and was adhered to for every human subject and for every trial. Each trial was performed on a stationary bicycle located in an athletic training facility. All subjects were asked survey questions (see Appendix) to further verify and document their capability of performing the test protocol.

The test protocol was successful in inducing perspiration in each human subject. After all the data from the human subject trials was collected and analyzed, it was found that during the bicycle protocol used in this study the temperatures measured at the subject's skin varied no more than 4 ˚C and relative humidity varied no more than 10% throughout the trial. The sensors within the fabric testing kit measured changes in temperature and relative measurements as the energy created by the human subject passed through each fabric and out to the outside environment. The measurements gathered by each fabric testing kit were divided into three distinct time zones for analysis. The first zone was the warm up zone when the kit was first placed on the body and the sensors responded to the body's temperature (approximately two to four minutes). The second zone was when the diffusion of moisture and heat took place within the kit and this zone extended approximately ten to twelve minutes after the first zone. The third and final zone was marked by stability in the measurements and usually occurred for the last twenty minutes or more of the trial.

5.1.2. Fabric Testing Kit and Data Collection

The fabric testing kits used in this study were constructed of foam sheets with known thickness. The foam sheets were flexible, easily cut, and gave the fabric testing kit the ability to flex somewhat to the shape of the human subject. Also, the foam sheets served as the

structure to house the three fabric layers and the sensors which measured the temperature and relative humidity within the kit. The data was generated by sensors (SHT-71) and data loggers (EK-H4).

To collect data from each of the fabric testing kits in terms of their ability to manage heat and humidity generated by a human body, a bicycle protocol was created. This bicycle protocol was designed to induce perspiration from the human subject. Several devices for monitoring the subject's vital signs were attached to their body including: heart rate, blood pressure, and blood oxygen monitors were attached to the subject before the trial. Once this vital sign monitoring was set-up, the fabric testing kit was attached to the subject using approved medical adhesive tape. The sensors begin recording at the time right before the kit is attached to the subject's body in order to capture the initial response of the sensors as both the temperature and relative humidity changes immediately as it is placed near the skin even before the subject begins pedaling on the stationery bicycle.

Clothing when worn on the human body introduces a number of complex variables such as construction or garment design, fit on the body, physical movement as well as the individual wears sensational perception. The cost and difficulty implementing human testing has driven the research towards finding an alternative method that can best represent the "real world." The testing instruments discussed in Chapter 2 of this research include: the cup testing method, DMPC, GATS, Alambeta (Permetest) instrument, Guarded Sweating Hotplate, Sweating Manikin, MMT, Dynamic Surface Moisture method, HCE simulator as well as methods for testing wicking and wettability. All of these fabric testing methods are focused on the evaluation of single layer textile systems as far as moisture management is

concerned with the exception of the Human-Clothing-Environment Stimulator. People typically wear more than one layer of clothing and there is a need to test fabrics in combination with other fabrics as accomplished by the fabric testing kit used in this research.

Ten different fabrics were chosen to be evaluated by the fabric testing kit. Recall, the fabric kit consisted of three layers designed to represent how a human body would dress: underwear as a base layer (Fabric Layer 1), t-shirt or top (Fabric Layer 2), and jacket (Fabric Layer 3) as an outer shell. The choice of fabric to be used for each layer within the kit was based upon a survey of current active wear products available at several retail outlets. The ten fabrics used in this study varied in terms of suitability of end use which was a consideration when building each kit. Many of the fabrics were suitable for use in more than one layer but, other fabrics were only suitable for the outside layer. For example, a heavy fleece fabric would only be placed in the third layer position on the outside of the fabric testing kit.

5.1.3. Synopsis of Findings

The findings of this research study were compiled in a list of nineteen findings which can be found at the end of each section of Chapter 4. These findings covered various aspects of the research analysis including: using the fabric testing kits for the human subject trials, the onset of perspiration which occurred among the human subjects, the fabric choices for the fabric testing kits, the moisture transfer by Zone and by fabric location within the fabric testing kit, the heat flow due to conduction, and the temperature changes and relative humidity ranges across the fabrics and the microclimate.

This research offers a new way of characterizing heat and moisture transfer through a multilayered fabric assembly using human subjects. It is demonstrated that as the vapor

pressures in the middle layers of the multilayered fabric kit become saturated and prevent moisture vapor flow. In turn, the rate of heat transfer is not adequate to raise the saturated vapor pressure in a timely manner since the fabric and microclimates behave as insulators. The findings of this research aid in designing clothing systems that provide better heat and moisture management for athletes, particularly those spend extended periods of time training or competing. Also, this research provides a characterization of an athletes' warm up prior to competing, which is important for the functional design of a clothing system that can warm muscles to a competing temperature and prevent formation of lactic acid build up before or after the competition.

5.2. Recommendations and Limitations

This fabric testing kit was able to measure heat and moisture transfer across fabric and microclimates, the interaction between clothing to skin, and the layer to layer interactions of a clothing system. However, there were limitations in this study based on the use of simple models such as Fourier's Law, Newton's Law of Cooling, Stefan-Boltzmann Law, and the Clausius–Clapeyron relation. This study also assumed that certain values for conductivity (k), the heat transfer coefficient (h), and thermal emissivity (ε) used to calculate the heat transfer would be the same or similar for all fabrics used in this study. The source of energy in this study which was different human beings vary especially in terms of their metabolic rate which is determined by many complex factors including but not limited to diet, physical fitness, hormone levels, mental state, etc. In addition, there are some recommendations for further work to consider. The major area for improvement would be kit design where the kit

could be made to be portable, easily reloadable with fabric, and more true to life. Other recommendations arise when considering the testing environment.

5.2.1. Kit Design- Portability

As constructed, the fabric testing kit wired sensors limited the range of motion and movement of the human subject. Because of the wires connecting the sensors to the data logger and the computer, the bicycle protocol used in this study was ideal. If the sensors were made portable this type of research could more easily be conducted during many physical activities a human subject could perform such as a treadmill or even a particular sport. Also, if the kit were more portable the fabric testing kit could be used in practically any environment.

5.2.2. Kit Design- Reloadable

A new fabric testing kit was built for each human subject trial using new materials. However, if the fabric testing kit was made to be reloadable, different fabrics could quickly and easily be tested without building a new kit for each trial. Another advantage that a reloadable fabric testing kit could offer is that it would allow a layer to be removed during a trial. Much like an athlete might remove a layer of clothing once their muscles have warmed up, a layer could be removed during a trial and the effect of removing that layer could be measured.

5.2.3. Kit Design- True to Life

The fabric testing kit as designed for this research held each fabric in its relaxed state meaning that special care was taken when building each kit not to stretch or distort the fabric in anyway. However, many of these fabrics as worn in their intended end use would be stretched considerably while worn over the body. Also, when fabrics are worn against the

body in layers the space between layers can vary depending on the garment. A fabric testing kit could also be designed to be intelligent or adaptable to the fit or end use of a particular garment design.

5.2.4. Testing Environment

The athletic facility used to conduct the human trials for this research was not a controlled environment. However, the facility was generally kept within a temperature and relative humidity range. Some valuable insight may be gained from conducting similar human subject trials using the fabric testing kit in a controlled environment. These external environments could also be adjusted to cold or hot conditions.

5.2.5. Body Mapping

The fabric testing kit could be used to measure temperature and relative humidity in locations of the body other than the lower back. This kit could be used to study how the body perspires in various sweat zones aiding in body mapping of heat and perspiration during exercise activities.

REFERENCES

Abdel-Rehim, Z.S., Saad, M.M., El-Shakankery, M., and Hanafy, I. (2006). Textile Fabrics as Thermal Insulators. *AUTEX Research Journal, 6*(3), 148-161.

Ainsworth, B. E., Haskell, W. L., Herrmann, S. D., Meckes, N., Bassett, D. R., Tudor-Locke, C., Leon, A. S. (2011). 2011 compendium of physical activities: A second update of codes and MET values. *Medicine & Science in Sports & Exercise, 43*(8), 1575-1581.

Albert, R. E., & Palmes, E. D. (1951). Evaporation rate patterns from small skin areas as measured by an infrared gas analyzer. *Journal of Applied Physiology, 4*(3), 208-214.

Albert-Wallerstrom, B., & Holmer, I. (1985). Efficiency of sweat evaporation in unacclimatized man working in a hot humid environment. *European Journal of Applied Physiology, 54*(5), 480-487.

Alduchov, O. A., & Eskridge, R. (1996). Improved magnus form approximation of saturation vapour pressure. *Journal of Applied Meteorology, 35*, 601-609.

American Heart Association. (2012). Exercise Standards for Testing and Training. Retrieved on 11/7/2012 From: http://circ.ahajournals.org/content/104/14/1694.full

Anonymous. (2007). Moisture Management Fabrics for Performance Apparel. Defense Update. Retrieved on 6/21/2013 from: http://defense-update.com/products/m/moisture_management_fabric.htm

Anonymous. (2011). Outlast Debuts Polyester Heat-Management Fiber. *Textile World, 161*(1), 40.

Anderson, D.B. (1936). Relative humidity or vapour pressure deficit. *Ecology, 17*(2), 277–282.

Arabuli, S., Vlasenko, V., Havelka, A., & Kus, Z. (2010). Analysis of modern methods for measuring vapor permeability properties of textiles. *7th International Conference - TEXSCI 2010,* Liberec, Czech Republic.

ASHRAE Handbook, (2009). Two-Phase Flow, American Society of Heating, Refrigerating and Air-Conditioning Engineers, Inc. Atlanta, GA.

Backer, S. (1951). The relationship between the structural geometry of a textile fabric and its physical properties. Part IV: Interstice geometry and air permeability. *Textile Research Journal, 21*(10), 703–713.

Barker, R. L. (2002). From fabric hand to thermal comfort: The evolving role of objective measurements in explaining human comfort response to textiles. *International Journal of Clothing Science and Technology, 14*(3/4), 181-200.

Bass, D. E., & Henschel, A. (1956). Responses of body fluid compartments in heat and cold. *Physiological Reviews, 36*(1), 128-144.

Baxter, S. & Cassie, A.B.D. (1943). Thermal Insulating Properties of Clothing. *Journal of the Textile Institute Journal of the Textile Institute Transactions, 34,* T41-T59.

Benyus, J. M. (1997). *Biomimicry: Innovation inspired by nature*. New York: William Morrow. Retrieved from http://www2.lib.ncsu.edu/catalog/record/NCSU963711

Bhattacharjee, D. & Kothari, V.K. (2008). Measurement of Thermal Resistance of Woven Fabrics in Natural and Forced Convections. *Research Journal of Textile and Apparel, 12*(2), 39-49.

Bligh, J. (1978). Thermoregulation: what is regulated and how? In Y. Houdas & J.D. Guieu (Eds.), New trends in thermal physiology. (pp. 124-126). Masson: New York.

Bogaty, H., Hollies, N. R. S., & Harris, M. (1956). The judgment of harshness of fabrics. *Textile Research Journal, 26*(5), 355-360.

Boron, W. F., & Boulpaep, E. L. (2012). *Medical physiology* (2nd ed.). Philadelphia, P.A.: Saunders Elsevier.

Branson, D. H., & Sweeney, M. (1991). Conceptualization and measurement of clothing comfort: Toward a metatheory. *Critical linkages in textiles and clothing: Theory, method and practice* (S. Kaiser & M. L. Damhorst ed., pp. 94-105). Monument, CO: International Textile and Apparel Association.

Burdett, R. G., & Skrinar, G. S. (1983). Comparison of mechanical work and metabolic energy consumption during normal gait. *Journal of Orthopedic Research, 1*(1), 63-72.

Bullard, R.W., Banerjee, M.R., MacIntyre, B.A. (1967). The role of the skin in negative feedback regulation of eccrine sweating. *Int. J. Biometeorol, 1* (11), 93-104.

Candas, V., Libert, J. P., & Vogt, J. J. (1979). Human skin wettedness and evaporative efficiency of sweating. *Journal of Applied Physiology, 46*(3), 522-528.

Carter, J.G., Brooks, K.A. & Sparks, J.R. (2012). Comparison of the YMCA Cycle Sub-Maximal VO2 Max Test to a Treadmill VO2 Max Test. Retrieved on 11/7/2012 From: http://digitalcommons.wku.edu/cgi/viewcontent.cgi?article=1305&context=ijesab

Celcar, D., Meinander, H., & Geršak, J. (2008). Heat and moisture transmission properties of clothing systems evaluated by using a sweating thermal manikin under different environmental conditions. *International Journal of Clothing Science and Technology, 20*(4), 240-252.

Chen, Q., Fan, J.T., Sarkar, M.K. (2012). Biomimetics of branching structure in warp knitted fabrics to improve water transport properties for comfort. *Textile Research Journal, 82*(11), 1131–1142.

Chinta, S. K., Landage, S. M. and Kumar, S.M. (2012). Plasma Technology in Wet Processing. International Journal of Engineering Research & Technology (IJERT). Retrieved 6/19/2013 from: http://www.ijert.org/browse/july-2012-edition?start=10

Clayton, F.H. (1935). The measurement of the air permeability of fabrics. *Journal of the Textile Institute, 26,* 171–186.

Colin, J., & Houdas, Y. (1965). Initiation of sweating in man after abrupt rise in environmental temperature. *Journal of Applied Physiology, 20*(5), 984-990.

Das, B., Kothari, V. K., Fangueiro, R., & Araujo, M. (2007a). Moisture transmission through textiles - part II: Evaluation methods and mathematical modeling. *AUTEX Research Journal, 7*(3), 194-216.

Das, B., Kothari, V. K., Fangueiro, R., & Araujo, M. (2007b). Moisture transmission through textiles -part I: Processes involved in moisture transmission and the factors at play. *AUTEX Research Journal, 7*(2), 100-110.

David, H., & Nordon, P., (1969). Case Studies of Coupled Heat and Moisture Diffusion in Wool Beds, *Textile Research Journal, 39*, 166-172.

Dionne, J. P., Semeniuk, K. & Makris, A. (2003). Thermal manikin evaluation of liquid cooling garments intended for use in hazardous waste management. Retrieved August 21, 2012, from http://www.wmsym.org/archives/2003/pdfs/58.pdf

DuBois, D., & DuBois, E. F. (1916). A formula to estimate the approximate surface area if height and weight be known. *Archives of Internal Medicine, 17*, 863-871.

Easter, E.P. & Ankenman, B.E. (2006). Evaluation of the care and performance of comfort-stretch knit fabrics. *AATCC Review, 6*(11), 1-6.

Egan, M. D. (1975). Concepts in Thermal Comfort, Prentice-Hall, Inc.: Englewood Cliffs, New Jersey.

Elnashar, E.A. (2005). Volume porosity and permeability in double-layer woven fabrics. *Autex Research Journal, 5*(4), 207–218.

Epps, H.H. (1988). Insulation characteristics of fabric assemblies. *Journal of Coated Fabrics, 17*, 212–218.

Fan, J., & Chen, Y. S. (2002). Measurement of clothing thermal insulation and moisture vapour resistance using a novel perspiring fabric thermal manikin. *Measurement Science and Technology, 13*(7), 1115. Retrieved from http://stacks.iop.org/0957-0233/13/i=7/a=320

Fan, J., & Qian, X. (2004). New functions and applications of water, the sweating fabric manikin. *European Journal of Applied Physiology, 92*(6), 641-644.

Farnworth, B. (1983). Mechanisms of heat flow through clothing insulation. *Textile Research Journal, 53*(12), 717-725.

Ferrero, F. (2003). Wettability measurements on plasma treated synthetic fabrics by capillary rise method. *Polymer Testing, 22*(5), 571-578.

Fohr, J. P., Couton, D., & Treguier, G. (2002). Dynamic heat and water transfer through layered fabrics. *Textile Research Journal, 72*(1), 1-12.

Fourt, L., & Hollies, N. R. S. (1970). *Clothing: Comfort and function*. New York, NY, USA: Marcel Dekker, Inc.

Fowler, M. (2005). Heat transport. Retrieved 7/19, 2012, from http://galileo.phys.virginia.edu/classes/152.mf1i.spring02/HeatTransport.htm

Franklin, K., Muir, P., & Scott, T. (2010). *Introduction to biological physics for the health and life sciences*. Hoboken, N.J.: Wiley.

Frydrych, I., Dziworska, G., & Bilska, J. (2002). Comparative analysis of the thermal insulation properties of fabrics made of natural and man-made cellulose fibres. *Fibres & Textiles in Eastern Europe, 10*(4), 40-44.

Fukazawa, T., Havenith, G. (2009). Differences in comfort perception in relation to local and whole body skin wettedness. *European Journal of Applied Physiology, 106*(1), 15-24.

Gagge, A.P. (1937). A new physiological variable associated with sensible and insensible perspiration. *American Journal of Physiology, 120*, 277-287.

Gibson, P., and Charmchi, M., (1997). The Use of Volume-averaging Techniques to Predict Temperature Transients Due to Water Vapor Sorption in Hygroscopic Porous Polymer Materials, *Journal of Applied Polymer Science, 64*(3), 493-505.

Gibson, P., Kendrick, C., Rivin, D., Charmchii, M., & Sicuranza, L. (1995). *Army Natick research development and engineering center MA.*

Givoni, B. (1976). *Man, climate and architecture* (2nd ed.). London: Applied Science Publishers.

Givoni, B., Berner-Nir, E. (1967) Expected sweat rate as function of metabolism, environmental factors and clothing. Israel Institute of Technology UNESCO: Haifa, Israel.

Gooijer, H., Warmoesjerjen, M.M.C.G., & Groot Wassink, J. (2003a). Flow resistance of textile materials, Part I: Monofilament fabrics. *Textile Research Journal, 73*(5), 437–443.

Gooijer, H., Warmoesjerjen, M.M.C.G., & Groot Wassink, J. (2003b). Flow resistance of textile materials. *Textiles Research Journal, 73*(6), 480–484.

Gorjanc, D. Š, Dimitrovski, K., & Bizjak, M. (2012). Thermal and water vapor resistance of the elastic and conventional cotton fabrics. *Textile Research Journal, 82*(14), 1498-1506.

Guyton, A. C. (2000). *Textbook of Medical Physiology.* Philadelphia, PA: Sanders.

Grottenmuller, R. (1998). Fluorocarbons- an Innovative Auxiliary for the Finish of Textile Surfaces. Melliand Textilberichte, 79(10), 743-746. E 195.

Harnett, P., & Mehta, P. (1984). A survey and comparison of laboratory test methods for measuring wicking. *Textile Research Journal, 54*(7), 471-478.

Hatch, K. L. (1993). *Textile science*. Minneapolis/Saint Paul: West Pub. Retrieved from http://www2.lib.ncsu.edu/catalog/record/NCSU845804

Havenith, G. (1999). Heat balance when wearing protective clothing. *The Annals of Occupational Hygiene, 43*(5), 289-296.

Havenith, G. (2005). Temperature regulation, heat balance and climatic stress. *Extreme weather events and public health responses.* Retrieved on 10/21/12 From: *http://link.springer.com/chapter/10.1007%2F3-540-28862-7_7*

Havenith, G., Fogarty, A., Bartlett, R., Smith, C.J. & Ventenat, V. (2008a). Male and female upper body sweat distribution during running measured with technical absorbents. *European Journal of Applied Physiology 104*(2), 245–255.

Havenith, G., Richards, M.G., Wang, X., Brode, P., Candas, V., den Hartog, E., Holmer, I., Kuklane, K., Meinander, H. & Nocker, W. (2008b). Apparent latent heat of evaporation from clothing: attenuation and ‘‘heat pipe’’ effects. *Journal of Applied Physiology 104*(1) 142–149.

Havrdová, M. (2007). Air permeability of multi layer system of fabrics. Retrieved September 15, 2009, from http://centrum.tul.cz/centrum/centrum/2Pristroje/2.2_publikace/%5B2.2.07%5D.pdf

Henry, P. S. (1939). Diffusion in Absorbing Media, *Proceedings of the Royal Society A: Mathematical, Physical and Engineering Sciences, 171*(A), 215-241.

Hes, L., Bernardo, C. A., & Queirós, M. A. (1996). A new method for the determination of water-vapour permeability of polymer films based on the evaluation of the heat of evaporation. *Polymer Testing, 15*(2), 189-201.

Hes, L. (2009). Permetest manual. Retrieved September 16, 2012, from http://www.sensora.eu/PermetestManual09.pdf

Hock, C. W., Sookne, A. M., & Harris, M. (1944). Thermal properties of moist fabrics. *Journal of the Franklin Institute, 237*(6), 469-470.

Hocker, H. (2002). Plasma treatment of textile fibers. *Pure and Applied Chemistry, 74*(3), 423-427.

Hoffman, R. M., & Beste, J. F. (1951). Some relations of fiber properties to fabric hand. *Textile Research Journal, 21*(2), 66-77.

Hollies, N. R., Custer, A. G., Morin, C. J., & Howard, M. E. (1979). A human perception analysis approach to clothing comfort. *Textile Research Journal, 49*(10), 557-564.

Holme, I. (2003). In Water Repellency and Waterproofing. D. Heywood (Ed.) Textile Finishing, Society of Dyers and Colourists. (pp. 137-213). West Yorkshire: UK.

Houdas, Y., Lecroart, J.L., Ledru, C., Carette, G., Guieu, J.D. (1978). The thermo-regulatory mechanisms considered as a follow-up system. In Houdas Y. and Guieu J.D. (Eds.) New trends in thermal physiology. (pp. 11-19). Masson: New York.

Hope, P. R. (1993). Heat balancing model. *Experientia, 49*, 741-746.

Howell, J. R., & Buckius, R. O. (1992). *Fundamentals of engineering thermodynamics* (2nd ed.). New York, NY: McGraw-Hill.

Howorth, W. S., & Oliver, P. H. (1958). The application of multiple factor analysis to the assessment of fabric handle. *Journal of the Textile Institute, 49*(11), T540-T553.

Huang, J., & Qian, X. (2008). Comparison of test methods for measuring water vapor permeability of fabrics. *Textile Research Journal, 78*(4), 342-352.

Huang, J. (2006). Sweating guarded hot plate test method. *Polymer Testing*, *25*(5), 709-716

Huang, J., & Qian, X. (2007). A new test method for measuring the water vapour permeability of fabrics. *Measurement Science and Technology*, *18*(9), 3043-3047.

Huang, J., Zhanga, C., Qian, X. (2013). A simple test method for measuring water vapor resistance of porous polymeric materials. Polymer Testing, 32(6), 1037–104.

Isamil, M. I., Ammar, A. S. A., and El-Okeily, M. (1985). On Thermal Conductivity of Some Fabric, *Journal of Applied Polymer Science*. 30(6), 2343-2350.

Janna, W. S. (2000). Engineering Heat Transfer. Washington, D.C.: CRC Press.

Jost, W. (1960). . New York, NY: Academic Press.

Kato Tech Company Ltd. (2007). History of product development. Retrieved September 19, 2012, from http://english.keskato.co.jp/company/outline.php

Kerslake, D. M. (1972). The Stress of Hot Environments. Cambridge: Cambridge University Press.

Kim, E., Yoo, S. J., & Shim, H. (2006). Performance of Selected Clothing Systems under Subzero Conditions: Determination of Performance by a Human-Clothing-Environment Simulator. *Textile Research Journal, 76*(4), 301-308.

Kim, E., & Yoo, S. (2010). In Shah K. S. (Ed.), *Human-clothing-environment simulator* (7680638th ed.). United States:

Kim, S. H., Lee, J. H., Lim, D. Y., & Jeon, H. Y. (2003). Simultaneous Heat and Moisture Transfer with Moisture Sorption, Condensation, and Capillary Liquid Diffusion in Porous Textiles. *Textile Research Journal, 73*(5), 455-460.

Kissa, E. (1996). Wetting and Wicking. *Textile Research Journal, 66*, 660-668.

Kondepudi, D. K. (2008). *Introduction to modern thermodynamics* (1st ed.). Hoboken, NJ: John Wiley & Sons, Inc.

Koutsoyiannis, D. (2012). Reply to ‘Comment on “Clausius–Clapeyron equation and saturation vapour pressure: Simple theory reconciled with practice”’. *European Journal of Physics, 33*(3), L13. Retrieved from http://stacks.iop.org/0143-0807/33/i=3/a=L13

Kulichenko, A.V. (2005). Theoretical analysis, calculation and prediction of the air permeability of textiles. *Fibre Chemistry, 37*(5), 371–380.

Kulichenko, A.V., & Van Langenhove, L. (1992). The resistance to flow transmission of porous materials. *Journal of the Textile Institute, 83*(1), 127–132.

European Journal of Applied Physiology, *111*Kyunghoon, M., Yangsoo S., & Chongyoup, K. (2007). Heat and moisture transfer from skin to environment through fabrics: A mathematical model. *International Journal of Heat and Mass Transfer, 50*(25-26) 5292–5304.

Lee, J.Y., Nakao, K., Tochihara, Y. (2011). Validity of perceived skin wettedness mapping to evaluate heat strain. *European Journal of Applied Physiology, 111*(10), 2581-2591.

Lee, S., Obendorf, S.K. (2012). Statistical modeling of water vapor transport through woven fabrics. *Textile Research Journal, 82*(3), 211–219.

Li, Y. (2001). The science of clothing comfort. *Textile Progress, 31*(1-2), 1-135.

Li, Y. (2002). Influence of Thickness and Porosity on Coupled Heat and Liquid Moisture Transfer in Porous Textile. *Textile Research Journal, 72*(5), 435-446.

Li, Y. (2005). Perceptions of temperature, moisture and comfort in clothing during environmental transients. *Ergonomics, 48*(3),234–248.

Li, Y. & Luo, Z.X. (1999). An Improved Mathematical Simulation of the Coupled Diffusion of Moisture and Heat in Wool Fabric, *Textile Research Journal (610),* 7960-768.

Li, Y., Zhu, Q. Y. & Luo, Z. X. (2001). Numerical Simulation of Heat Transfer Coupled with Moisture Sorption and Liquid Transport in Porous Textiles, *6th Asian Textile Conference, Hong Kong, August 22-24.*

Li, Y., Zhu, Q. & Yeung, K.W. (2002). Influence of thickness and porosity on coupled heat and liquid moisture transfer in porous textiles. *Textile Research Journal, 72*(5), 435-446.

Liu, R., Little, T.J., & Williams, M.E. (2012). Evaluation of elite athletes psycho-physiological responses to compression form-fitted athletic wear in intensive exercise based on 5Ps model. *Fibers and Polymers,13*(3), 380-389.

Logan, E. (1999). *Thermodynamics: Processes and applications* (1st ed.). New York, NY: Marcel Dekker, Inc.

Lord, J. (1959). The determination of the air permeability of fabrics. *Journal of the Textile Institute, 50,* 569–582.

Lundgren, H. P. (1969). New concepts in evaluating fabric hand. *Textile Chemists and Colorists, 1*(1), 35-45.

Luo, Z. X., Fan, J. T. & Li, Y. (2000). Heat and Moisture Transfer with Sorption and Condensation in Porous Clothing Assemblies and Numerical Simulation, *International Journal of Heat and Mass Transfer (4163),* 2989-3000.

Lustinec, K. (1973). Sweat rate, its prediction and interpretation. Arch Sci Physiol (Paris). *27*(2):127-36.

Mao, N. and Russell, S. J. (2007). The Thermal Insulation Properties of Spacer Fabrics with a Mechanically Integrated Wool Fiber Surface, *Textile Research Journal*. *77*(12), 914-922.

McCallrey, T.V., Wurster, R.D., Jacobs, H.K., Euler, D.E., and Geis, G.S. (1979). Role of skin temperature in the control of sweating. Journal of Applied Physiology, 47(3), 591-597.

McCullough, E. A., Kwon, M., & Shim, H. (2003). A comparison of standard methods for measuring water vapour permeability of fabrics. *Measurement Science and Technology, 14*(8), 1402-1408.

Macpherson, R.K. (1960). Physiological responses to hot environments. Medical Research Council Special Report Series No. 298. (pp. 219, 294-299). London, England: Her Majesty's Stationery Office.

MacRae, B., Cotter, J. & Laing, R. (2011). Compression Garments and Exercise Garment Considerations, Physiology and Performance. *Sports Medicine, 41*(10), 815-843.

MacRae, B., Laing, R., Niven, B.E. & Cotter, J. (2012). Pressure and coverage effects of sporting compression garments on cardiovascular function, thermoregulatory function, and exercise performance. *European Journal of Applied Physiology, 112*(5), 1783–1795.

Melesse, A., Abtew, W. (2013). Vapor Pressure Calculation Methods. In A. Wossenu & A. Melesse (Eds.) *Evaporation and Evapotranspiration: Measurements and Estimations* (pp. 53-62). Dordrecht: Springer Netherlands.

Mehrtens, D. G., & McAlister, K. C. (1962). Fiber properties responsible for garment comfort. *Textile Research Journal, 32*(8), 658-665.

Milenkovic, L., & Skundric, P. (1999). Comfort properties of defense protective clothings. *The Scientific Journal FACTA UNIVERSITATIS, 4*, 101-106.

Militky, J., & Havrdová, M. (2001). Porosity and air permeability of composite clean room textiles. *International Journal of Clothing Science and Technology, 12*(3/4), 280–288.

Miller, A. T. (1968). *Energy metabolism*. Philadelphia, PA: Davis Co.

Moran, M. J., & Shaprio, H. N. (2008). *Fundamentals of engineering thermodynamics* (6th ed.). Hoboken, NJ: John Wiley & Sons, Inc.

Morris, C. J. (1953). Thermal properties of textile materials. *Journal of the Textile Institute, 44*(10), T449-T476.

Mukhopadhyay, A., Midha, V.K. (2008). A review on designing the waterproof breathable fabrics. *Journal of Industrial Textiles, 37*(3), 225–262.

Nadel, E.R., Bullard, R.W., Stolwijk, J.A. (1971). Importance of skin temperature in the regulation of sweating. Journal of Applied Physiology, 31(1),80–87.

Nadel, E.R., Stolwijk, J.A. (1973). Effect of skin wettedness on sweat gland response. *Journal of Applied Physiology, 35*(5):689–694.

Ostwald, W. (1891). Solutions. New York: Longmans, Green, And Co.

Parsons, K. C. (2002). The estimation of metabolic heat for use in the assessment of thermal comfort. Retrieved 8/23/12 From: http://nceub.commoncense.info/uploads//Paper27_Parsons.pdf

Pause, B. (1996). Measuring the water vapor permeability of coated fabrics and laminates. *Journal of Industrial Textiles, 25*(4), 311-320.

Pierce, F. T. (1930). The handle of cloth as a measurable quantity. *Shirley Institute Memoirs, 9*(8), 83-122.

Pontrelli, G. J. (1977). Partial analysis of comfort's gestalt. *Clothing comfort: Interaction of thermal, ventilation, construction, and assessment factors* (N. R. S. Hollies & R. F. Goldman ed., pp. 71-80). Ann Arbor, MI: Ann Arbor Science Publishers.

Pontrelli, G. J. (1990). Comfort by design. *Textile Asia, 21*(1), 52-61.

Prahsarn, C., Barker, R. L., & Gupta, B. S. (2005). Moisture vapor transport behavior of polyester knit fabrics. *Textile Research Journal, 75*(4), 346-351.

Rainard, L.W. (1946). Air permeability of fabrics. *Textile Research Journal, 16,* 473–480.

Rainard, L.W. (1947). Air permeability of fabrics II. *Textile Research Journal, 17,* 167–170.

Rees, W. H. (1941). The transmission of heat through textile fabrics. *Journal of the Textile Institute, 32,* 149-165.

Reilly, T. and Waterhouse, J. (2009). Circadian aspects of body temperature regulation in exercise. Journal of Thermal Biology. 34(4), 161–170.

Ren, Y. J., & Ruckman, J. E. (2003). Water vapour transfer in wet waterproof breathable fabrics. *Journal of Industrial Textiles, 32*(3), 165-175.

Rodrigues, K. A. (2000). *Hydrophilic finish for textiles* (US Patent 6046120 ed.)

Rushton, A., & Griffiths, P. (1971). Fluid flow in monofilament filter media. *Transactions of the Institution of Chemical Engineers, 49,* 49–59.

Saha, K. (2008). Water Vapour in the Atmosphere: Thermodynamics of Moist Air. In The Earth's Atmosphere Its Physics and Dynamics, (pp. 43-58). Springer: New York.

Sarkar, M., Jintu, F., Szeto, Y., & Xiaoming, T. (2009). Biomimetics of plant structure in textile fabrics for the improvement of water transport properties. *Textile Research Journal, 79*(7), 657-668.

Sato, M., Nakagawa, M., Tokura, H., Zhang, P., & Gong, R. H. (2007). Physiological effects of outerwear moisture transfer rate during intermittent bicycle exercise. *Journal of the Textile Institute, 98*(1), 73-79.

Saville, B. P. (1999). In Knovel (Firm), Textile Institute (Manchester E. (Eds.), *Physical testing of textiles [electronic resource]*. Cambridge, England; Boca Raton, Fla.: Woodhead Pub., in association with the Textile Institute; In North and South America by CRC Press. Retrieved from http://www2.lib.ncsu.edu/catalog/record/NCSU2201602

Scheurell, D. M., Spivak, S. M., & Hollies, N. R. (1985). Dynamic surface wetness of fabrics in relation to clothing comfort. *Textile Research Journal, 55*(7), 394-399.

Shapiro, Y., Pandolf, K. B., and Goldman, R. F. (1982). Predicting Sweat Loss Response to Exercise, Environment and Clothing. *European Journal Applied Physiology. 48*(1), 83-96.

Shuttleworth, W.J. (2012). Water Vapor in the Atmosphere. In W. Shuttleworth (Eds.), Terrestrial Hydrometeorology. (pp. 14-24). John Wiley & Sons, Ltd: West Sussex.

Slater, K. (1985). The meaning of comfort. *Human comfort* (pp. 3-11). Springfield, IL: Charles C. Thomas Publisher.

Smith, C.J. & Havenith, G. (2011). Body mapping of sweating patterns in male athletes in mild exercise-induced hyperthermia. *European Journal Applied Physiology 111*(7), 1391–1404.

Smith, C.J., and Havenith, G., 2011. Sweat mapping in humans and applications for clothing design. *The Fourth International Conference on Human-Environment System* (ICHES 2011), Sapporo, Japan, 3-6 October, 782-787.

Sontag, S. M. (1985). Comfort dimensions of actual and ideal insulative clothing for older women. *Clothing and Textiles Research Journal, 4*(9), 9-17.

Stoecker, W. F., & Jones, J. W. (1982). *Refrigeration and air conditioning* (2nd ed.). New York, NY: McGraw-Hill.

Su, C.I., Fang, J.X., Chen, X.H., and Wu, W.Y. (2007). Moisture Absorption and Release of Profiled Polyester and Cotton Composite Knitted Fabrics. Textile Research Journal, 77(10), 764-769.

Sampath, M.B., Mani, S., and Nalankilli, G. (2011). Effect of filament fineness on comfort characteristics of moisture management finished polyester knitted fabrics. Journal of Industrial Textiles, 41(2), 160-173.

Sundaramoorthy, S., Nallampalayam, P.K., & Jayaraman, S. (2011). Air permeability of multilayer woven fabric systems. *The Journal of the Textile Institute, 102*(3), 189–202.

Tazelaar, D. J. (1999). Long Cotton Wool Rolls as Compression Enhancers in Macrosclerotherapy for Varicose Veins. *Dermatol Surg, 25*, 38-40.

Tugrul, O.R. (2006). Air permeability of woven fabrics. *Journal of Textile and Apparel Technology and Management, 5*(2), 1–10.

Tzanov, T., Betcheva, R., & Hardalov, I. (1999). Thermophysiological comfort of silicone softeners-treated woven textile materials. *International Journal of Clothing Science and Technology, 11*(4), 189-197.

U.S. Environmental Protection Agency (2013). Perfluorooctanoic Acid (PFOA) and Fluorinated Telomers. Retrieved 6/13/2013 from: http://www.epa.gov/opptintr/pfoa/index.htm

Vigneswaran, C. and Chandrasekrara, K. (2009). Effect of Thermal Conductivity Behavior of Jute/Cotton Blended Knitted Fabrics, *Journal of Industrial Textiles. 38*(4), 289-306.

Wang, J., Kaynak, A., Wang, L. & Liu, X. (2206). Thermal conductivity studies on wool fabrics with conductive coatings. *Journal of the Textile Institute, 97*(3), 265-270.

Wang, Q., Maze, B., Vahedi, T.H., & Pourdeyhimi, B. (2006). A note on permeability simulation of multifilament woven fabrics. *Chemical Engineering Science, 61*, 8085–8088.

Wang, J., & Yasuda, H. (1991). Dynamic water vapor and heat transport through layered fabrics, part 1:Effect of surface modification. *Textile Research Journal, 61*(1), 10-20.

Wilhelm, A., Hilmar, F., & Walter, K. (2006). Nonwoven Fabrics: Raw Materials, Manufacture, Applications, Characteristics, Testing Processes. Weinheim, Germany: Wiley-VCH.

Wehner, J. A. (1988). Dynamics of water vapor transmission through fabric barriers. *Textile Research Journal, 58*(10), 581-592.

Wilusz, E. (2012). Creating the future of textiles: Protective clothing Advancements in protective clothing applications including super-repellent coatings, nanotechnology and intelligent textiles. Specialty Fabrics Review. Retrieved 6/19/2013 from http://specialtyfabricsreview.com/articles/1112_fot_protective_clothing.html

Wu, X. R., Cao, J. D., & Chen, Y. (2011). Testing of fabric dynamic moisture transfer based on munsell color HV/C value. *Applied Mechanics and Materials, 58*(60), 1854-1859.

Xu, G., & Wang, F. (2005). Prediction of the permeability of woven fabrics. *Journal of Industrial Textiles, 34*(4), 243–254.

Ye, C., Li, B. & Sun, W. (2010). Quasi-steady-state and steady-state models for heat and moisture transport in textile assemblies. *Proceedings of the Royal Society A: Mathematical, Physical and Engineering Sciences, (466)*2122, 2875-2896.

Yi, L., Aihua, M., Ruomei, W., Xiaonan, L., Zhong, W., Wenbang, H., Yubei, L. (2006). P-smart—a virtual system for clothing thermal functional design. *Computer-Aided Design, 38*(7), 726-739.

Yoo, S., & Barker, R. L. (2005). Comfort properties of heat resistant protective workwear in varying conditions of physical activity and environment. part II: Percieved comfort response to garments and its relationship to fabric properties. *Textile Research Journal, 75*, 531-541.

Yoo, S., & Barker, R. L. (2004). Moisture management properties of heat-resistant workwear fabrics— effects of hydrophilic finishes and hygroscopic fiber blends. *Textile Research Journal, 74*(11), 995-1000.

Yoo, S., & Kim, E. (2008). Effects of multilayer clothing system array on water vapor transfer and condensation in cold weather clothing ensemble JF textile research journal. *Textile Research Journal, 78*(3), 189-197.

Zhu, F. & Li, K. (2010). Determining Effective Thermal Conductivity of Fabrics by Using Fractal Method. *International Journal of Thermophysics*, 31(3), 612-619.

APPENDICES

Appendix A- *Institutional Review Board Documents*

North Carolina State University
Institutional Review Board for the Use of Human Subjects in Research
SUBMISSION FOR NEW STUDIES

GENERAL INFORMATION

1. **Date Submitted:** _____ 1a. **Revised Date:** _____
2. **Title of Project:** *Temperature and Relative Humidity Control in Multilayered Garments*
3. **Principal Investigator:** *Kelly Ross*
4. **Department:** *Textiles*
5. **Campus Box Number:** *8301*
6. **Email:** *kelly_ross@ncsu.edu*
7. **Phone Number:** *919-858-6383*
8. **Fax Number:** *9195153733*
9. **Faculty Sponsor Name and Email Address if Student Submission:** *Trevor Little; trevor_little@ncsu.edu*
10. **Source of Funding? (required information): Departmental Funds**
11. **Is this research receiving federal funding?:** *no*
12. **If Externally funded, include sponsor name and university account number:**_____
13. RANK: ☐ Faculty ☐ Student: ☐Undergraduate; ☐ Masters; or ☒PhD ☐ Other (specify): _____

As the principal investigator, my signature testifies that I have read and understood the University Policy and Procedures for the Use of Human Subjects in Research. I assure the Committee that all procedures performed under this project will be conducted exactly as outlined in the Proposal Narrative and that any modification to this protocol will be submitted to the Committee in the form of an amendment for its approval prior to implementation.

Principal Investigator:

Kelly Ross	Kelly Ross *	*11-7-12*
(typed/printed name)	(signature)	(date)

*As the faculty sponsor, my signature testifies that I have reviewed this application thoroughly and will oversee the research in its entirety. I hereby acknowledge my role as the **principal investigator of record**.*

Faculty Sponsor:

Trevor Little	Trevor Little *	_____
(typed/printed name)	(signature)	(date)

***Electronic submissions to the IRB are considered signed via an electronic signature. For student submissions this means that the faculty sponsor has reviewed the proposal prior to it being submitted and is copied on the submission.**

Please complete this application and email as an attachment to: debra_paxton@ncsu.edu or send by mail to: Institutional Review Board, Box 7514, NCSU Campus (Administrative Services III). **Please include consent forms and other study documents with your application and submit as one document.**

****

For SPARCS office use only

Reviewer Decision (Expedited or Exempt Review)

☐ Exempt ☐ Approved ☐ Approved pending modifications ☐ Table

Expedited Review Category: ☐ 1 ☐ 2 ☐ 3 ☐ 4 ☐ 5 ☐ 6 ☐ 7 ☐ 8a ☐ 8b ☐ 8c ☐ 9

_____

Reviewer Name Signature Date

North Carolina State University
Institutional Review Board for the Use of Human Subjects in Research
GUIDELINES FOR A PROPOSAL NARRATIVE

In your narrative, address each of the topics outlined below. Every application for IRB review must contain a proposal narrative, and failure to follow these directions will result in delays in reviewing/processing the protocol.

A. INTRODUCTION

1. Briefly describe in lay language the purpose of the proposed research and why it is important.

The purpose of this research is to determine how to build a multiple layer clothing system that would optimize performance during athletic end use. The tests are intended to measure coupled heat and moisture transfer in relation to temperature and humidity across the microclimates, interaction between clothing to skin and layer to layer interactions of a clothing system. The human trials are necessary to research how multiple layer clothing systems manage moisture and heat transfer.

2. If student research, indicate whether for a course, thesis, dissertation, or independent research.

Dissertation

B. SUBJECT POPULATION

1. How many subjects will be involved in the research?
Estimates or ranges are acceptable. Please be aware that if you recruit over 10% more participants than originally requested, you will need to submit a request to modify your recruitment numbers.

There will be a minimum of 10 subjects involved in this study, a mixture of both male and female, and ages ranging between 18 to 45 years.

2. Describe how subjects will be recruited. Please provide the IRB with any recruitment materials that will be used.

The subjects will be recruited from a group of bicycle enthusiasts known to the researcher. These enthusiasts ride leisurely and competitively in teams and are very familiar with riding a bicycle for an extended period of time. The researcher will also recruit athletes who incorporate the stationery bicycle into their training routines.

3. List specific eligibility requirements for subjects (or describe screening procedures), including those criteria that would exclude otherwise acceptable subjects.

The subjects of this study must be in good health and physical condition that would enable them to ride a stationary bicycle for an extended period of time. The researcher will recruit subjects that are athletes or experienced bicyclists.

4. Explain any sampling procedure that might exclude specific populations.

As stated previously, the researcher will recruit from a population of athletes and bicycle enthusiasts because, this population has been training with stationery bicycles or are experienced bicycle riders. This method of sampling will exclude those that are not athletes or that do not ride bicycles. Bicycle riders that are outside the 18-45 years old age range are also excluded.

5. Disclose any relationship between researcher and subjects - such as, teacher/student; employer/employee.

The subjects may be current or former NC State students; others may not have any affiliation with the University.

6. Check any vulnerable populations included in study:

- ☐ minors (under age 18) - if so, have you included a line on the consent form for the parent/guardian signature
- ☐ fetuses
- ☐ pregnant women
- ☐ persons with mental, psychiatric or emotional disabilities
- ☐ persons with physical disabilities
- ☐ economically or educationally disadvantaged
- ☐ prisoners
- ☐ elderly
- ☐ students from a class taught by principal investigator
- ☐ other vulnerable population.

7. If any of the above are used, state the necessity for doing so. Please indicate the approximate age range of the minors to be involved.

na

C. PROCEDURES TO BE FOLLOWED

1. In lay language, describe completely all procedures to be followed during the course of the experimentation. Provide sufficient detail so that the Committee is able to assess potential risks to human subjects. In order for the IRB to completely understand the experience of the subjects in your project, please provide a detailed outline of everything subjects will experience as a result of participating in your project. Please be specific and include information on all aspects of the research, through subject recruitment and ending when the subject's role in the project is complete. All descriptions should include the informed consent process, interactions between the subjects and the researcher, and any tasks, tests, etc. that involve subjects. If the project involves more than one group of subjects (e.g. teachers and students, employees and supervisors), please make sure to provide descriptions for each subject group.

Prior to the experiment the subject will be introduced to the equipment and the procedure for the trial. The equipment includes an exercise cycle and various sensors. The placement of sensors for monitoring heart rate, blood pressure, skin temperature, and blood oxygen content will be explained and demonstrated. The researcher will also go over the informed consent form and address any of the subject’s questions or concerns. Before the subjects use the stationery bicycle, they will fill out a research survey form that includes height, weight, and gender (see attached survey form). Approximately 30 minutes will be allowed for the equipment explanation and survey

form completion.

The subject will change into an exercise outfit, provided by the researcher, in a dressing room. The following sensors will be attached to the body: blood pressure cuff on the bicep, heart rate monitor on the chest, and blood oxygen level monitor on the fingertip. The oxygen saturation of the arterial blood will be measured via an Adult Articulated Finger Clip Senor which is placed on the finger tip. The oxygen is recorded automatically every minute through the data recording system See Figure1a) for placement of the heart rate and blood pressure sensors. The flexible fabric test kit will be attached to the subject's lower back using medical/sports tape. The fabric test kit used in this study will house seven sensors (SHT-71). The sensors will be positioned on either side of each fabric within the kit making the 1st and the 2nd sensors' positions close to the body. The sensors are powered by a 3V supply from a data logger. These sensors are connected with Data loggers (EK-H4) by using seven specific cables. There is no electrical shock risk for the subject from these sensors. An additional sensor will measure the external environment around the human subjects including the ambient temperature and relative humidity. Initial skin temperature, blood pressure, heart rate and blood oxygen level will be taken before the bicycle trial begins. Before beginning the trial, the sensors measuring the temperature and relative humidity in the fabric test kit will be activated. If the subject feels discomfort with from the exercise garment, the attachment of the fabric test kit, or from any of the sensors; adjustments will be made until the subject indicates that they are comfortable. Skin temperature will be measured on the forehead at the beginning of the trial and at 2 minute intervals throughout the trial. Blood pressure and Heart rate will be taken (automatically) at 2 minute intervals throughout the trial and blood oxygen level is continuously monitored and recorded. The Life Fitness 97C Lifecycle Upright Bike (shown in Figure 1b)) in the Weisiger-Brown Athletics Building at NC State University will be utilized in this study. The bicycle has 25 programmable resistance settings that progressively increase the amount of resistance applied while pedaling. For this study the bicycle will be set at level 6, as suggested by the strength & conditioning coach at Weisiger-Brown. The strength and conditioning coach as well as the 97C Lifecycle manual suggests maintaining a specific heart rate while exercising as the optimal way to monitor the intensity of a workout.

Figure 1a): Sensor Placement 1

Figure 91b): Lifecycle 97C

Bicycle protocol: 1) 5 minutes to warm up on bicycle during this time the subject can slowly work up to the target heart rate zone; 2) 30 minutes at target heart (135-155 beats per minute); 3) 10 minutes slower pace; 4) 10-15 minutes cool down after trial and not on bicycle
Heart rate, skin temperature, humidity, blood oxygen level, and blood pressure will be monitored throughout the bicycle test.
If the subject feels discomfort or ill at any time; the trial will be stopped and medical attention sought if needed.

After the trial the remaining questions on the research survey form will be asked.

2. How much time will be required of each subject?

Approximately 1 hour and 30 minutes

D. POTENTIAL RISKS

1. State the potential risks (psychological, social, physical, financial, legal or other) connected with the proposed procedures and explain the steps taken to minimize these risks.

The potential risk for any type of injury or distress to the subject in this research is very minor. It is possible that the sensor cables could become tangled or wrapped around pedals, cable ties will be used to prevent this issue. The subject can stop pedaling the bicycle at any time. Also, subjects will be monitored continuously by two trial observers. Physiological measurements will be monitored at all times during the trials. If a subject's heart rate exceeds 155 beats per minute then, the subject will be asked to pedal more slowly. If a subject's blood pressure exceeds 175/90, the trial will be stopped immediately and the subject will be excluded from the study.

2. Will there be a request for information that subjects might consider to be personal or sensitive (e.g. private behavior, economic status, sexual issues, religious beliefs, or other matters that if made public might impair their self-esteem or reputation or could reasonably place the subjects at risk of criminal or civil liability)?

No

a. If yes, please describe and explain the steps taken to minimize these risks.

na

3. Could any of the study procedures produce stress or anxiety, or be considered offensive, threatening, or degrading? If yes, please describe why they are important and what arrangements have been made for handling an emotional reaction from the subject.

No

4. How will data be recorded and stored?

Data will be generated by Sensors (SHT-71) and data loggers (EK-H4). The data will be recorded by Microsoft's excel program on a password protected laptop. After completing the research and analyzing the data, the data will be coded in such a way that any identifiers that could link the data to a particular subject will be removed.

a. How will identifiers be used in study notes and other materials?

No names – The researcher will use a unique code for each subject . The list of codes connecting code and subject will be maintained in a separate password protected file in my University computer account.

b. How will reports will be written, in aggregate terms, or will individual responses be described?

Individual data will be recorded without name of the human subjects. The subject will be given a unique code at the beginning of the trial when the subject is given the survey form. The researcher will use the unique code to be able to analyze the results. Codes will be used at the data collection stage.

5. If audio or video recordings are collected, will you retain or destroy the recordings? How will recordings be stored during the project and after, as per your destruction/retention plans?

The researcher will take pictures of the human subjects to show the experimental setup. However, the researcher will not include faces in these photos. Any identifying features such as tattoos, jewelry scars, and/or birthmarks will be covered up or not included in photographs to illustrate the experimental set up. After coding the records for the research, the original images will be deleted from the camera. Images may be used to illustrate the experimental set-up of the research in publications after all personal identifiers have been removed.

6. Is there any deception of the human subjects involved in this study? If yes, please describe why it is necessary and describe the debriefing procedures that have been arranged.

No

E. POTENTIAL BENEFITS

This does not include any form of compensation for participation.

1. What, if any, direct benefit is to be gained by the subject? If no direct benefit is expected, but indirect benefit may be expected (knowledge may be gained that could help others), please explain.

Although there are no direct benefits to the subjects, the information produced from their participation in this study regarding heat and moisture transfer through fabric layers will ultimately lead to develop better athletic performance apparel.

F. COMPENSATION

Please keep in mind that the logistics of providing compensation to your subjects (e.g., if your business office requires names of subjects who received compensation) may compromise anonymity or complicate confidentiality protections. If, while arranging for subject compensation, you must make changes to the anonymity or confidentiality provisions for your research, you must contact the IRB office prior to implementing those changes.

1. Describe compensation

None

2. Explain compensation provisions if the subject withdraws prior to completion of the study.

None

3. If class credit will be given, list the amount and alternative ways to earn the same amount of credit.

None

G COLLABORATORS

1. If you anticipate that additional investigators (other than those named on **Cover Page**) may be involved in this research, list them here indicating their institution, department and phone number.

No

2. Will anyone besides the PI or the research team have access to the data (including completed surveys) from the moment they are collected until they are destroyed.

No

H. CONFLICT OF INTEREST

1. Do you have a significant financial interest or other conflict of interest in the sponsor of this project? *No*

2. Does your current conflicts of interest management plan include this relationship and is it being properly followed? *No*

I. ADDITIONAL INFORMATION

1. If a questionnaire, survey or interview instrument is to be used, attach a copy to this proposal.

2. Attach a copy of the informed consent form to this proposal.

3. Please provide any additional materials that may aid the IRB in making its decision.

J. HUMAN SUBJECT ETHICS TRAINING

*****Please consider taking the Collaborative Institutional Training Initiative (CITI), a free, comprehensive ethics training program for researchers conducting research with human subjects. Just click on the underlined link.

Research Survey Form

College of Textiles

Date:

Subject Information

Subject Code:

For your safety, you must answer yes to the following three questions in order to be a subject in this study.

	Yes	No
1. Are you comfortable using a stationary bicycle?	_____	
2. Are you able to use a bicycle for an extended period of time (at least 30 minutes)?	_____	
3. Are you between the ages of 18 and 45?	_____	

Statistics

Height: _____ Weight: _____ Gender: _____

Size: S____M____L____XL____

Check List	Before	After
1. Skin Temperature (T):	_____	_____
2. Blood Pressure (BP):	_____	_____
3. Heart Rate (HR):	_____	_____
4. Blood O_2 Pressure (O_2)	_____	_____

Questions?

Before		After	
Yes	No	Yes	No

1. Do you feel tired?
2. Do you feel thirsty?
3. Do you feel too hot?
4. Does your body feel cold?
5. Does your skin feel cold?
6. Do you feel discomfort in any area?

Appendix B- *Sensor Performance Datasheets*

SENSIRION
THE SENSOR COMPANY

Datasheet SHT7x (SHT71, SHT75)

Humidity and Temperature Sensor IC

- Fully calibrated
- Digital output
- Low power consumption
- Excellent long term stability
- Pin type package – easy integration

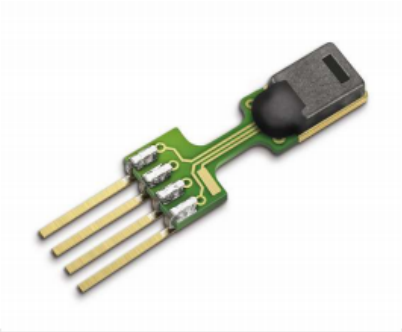

Product Summary

SHT7x (including SHT71 and SHT75) is Sensirion's family of relative humidity and temperature sensors with pins. The sensors integrate sensor elements plus signal processing in compact format and provide a fully calibrated digital output. A unique capacitive sensor element is used for measuring relative humidity while temperature is measured by a band-gap sensor. The applied CMOSens® technology guarantees excellent reliability and long term stability. Both sensors are seamlessly coupled to a 14bit analog to digital converter and a serial interface circuit. This results in superior signal quality, a fast response time and insensitivity to external disturbances (EMC).

Each SHT7x is individually calibrated in a precision humidity chamber. The calibration coefficients are programmed into an OTP memory on the chip. These coefficients are used to internally calibrate the signals from the sensors. The 2-wire serial interface and internal voltage regulation allows for easy and fast system integration. The small size and low power consumption makes SHT7x the ultimate choice for even the most demanding applications.

SHT7x is supplied on FR4 with pins which allows for easy integration or replacement. The same sensor is also available as surface mountable packaging (SHT1x) or on flex print (SHTA1).

Dimensions

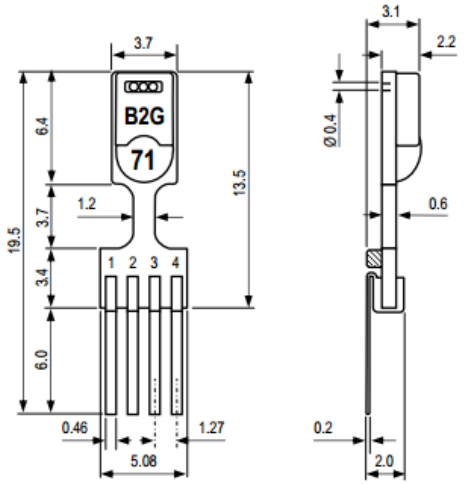

Figure 1: Drawing of SHT7x (applies to SHT71 and SHT75) sensor packaging, dimensions in mm (1mm = 0.039inch). Contact assignment: 1: SCK, 2: VDD, 3: GND, 4: DATA. Hatched item on backside of PCB is a 100nF capacitor – see Section 2.1 for more information.

Sensor Chip

SHT7x V4 – for which this datasheet applies – features a version 4 Silicon sensor chip. Besides a humidity and a temperature sensor the chip contains an amplifier, A/D converter, OTP memory and a digital interface. V4 sensors can be identified by the alpha-numeric traceability code on the sensor cap – see example "B2G" code on Figure 1.

Material Contents

While the sensor is made of a CMOS chip the sensor housing consists of an LCP cap with epoxy glob top on an FR4 substrate. Pins are made of a Cu/Be alloy coated with Ni and Au. The device is fully RoHS and WEEE compliant, thus it is free of Pb, Cd, Hg, Cr(6+), PBB and PBDE.

Evaluation Kits

For sensor trial measurements, for qualification of the sensor or even experimental application (data logging) of the sensor there is an evaluation kit *EK-H4* available including SHT71 (same sensor chip as SHT1x) and 4 sensor channels, hard and software to interface with a computer. For other evaluation kits please check www.sensirion.com/humidity.

Sensor Performance

Relative Humidity

Parameter	Condition	min	typ	max	Units
Resolution[1]		0.4	0.05	0.05	%RH
		8	12	12	bit
Accuracy[2] SHT71	typ		±3.0		%RH
	max	see Figure 2			
Accuracy[2] SHT75	typ		±1.8		%RH
	max	see Figure 2			
Repeatability			±0.1		%RH
Hysteresis			±1		%RH
Nonlinearity	raw data		±3		%RH
	linearized		<<1		%RH
Response time[3]	tau 63%		8		s
Operating Range		0		100	%RH
Long term drift[4]	normal		< 0.5		%RH/yr

Temperature

Parameter	Condition	min	typ	max	Units
Resolution[1]		0.04	0.01	0.01	°C
		12	14	14	bit
Accuracy[2] SHT71	typ		±0.4		°C
	max	see Figure 3			
Accuracy[2] SHT75	typ		±0.3		°C
	max	see Figure 3			
Repeatability			±0.1		°C
Operating Range		-40		123.8	°C
		-40		254.9	°F
Response Time [6]	tau 63%	5		30	s
Long term drift			< 0.04		°C/yr

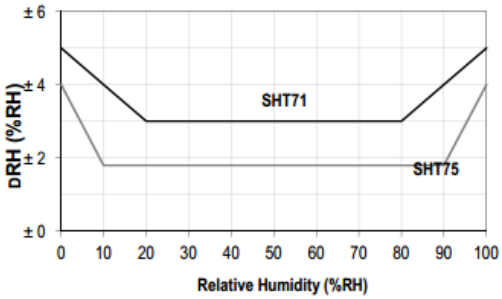

Figure 2: Maximal RH-tolerance at 25°C per sensor type.

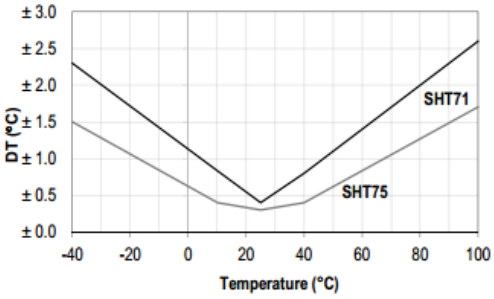

Figure 3: Maximal T-tolerance per sensor type.

Electrical and General Items

Parameter	Condition	min	typ	max	Units
Source Voltage		2.4	3.3	5.5	V
Power Consumption[5]	sleep		2	5	µW
	measuring		3		mW
	average		90		µW
Communication	digital 2-wire interface, see Communication				
Storage	10 – 50°C (0 – 80°C peak), 20 – 60%RH				

Packaging Information

Sensor Type	Packaging	Quantity	Order Number
SHT71	Tape Stripes	50	1-100092-04
SHT75	Tape Stripes	50	1-100071-04

This datasheet is subject to change and may be amended without prior notice.

[1] The default measurement resolution of is 14bit for temperature and 12bit for humidity. It can be reduced to 12/8bit by command to status register.

[2] Accuracies are tested at Outgoing Quality Control at 25°C (77°F) and 3.3V. Values exclude hysteresis and are only applicable to non-condensing environments.

[3] Time for reaching 63% of a step function, valid at 25°C and 1 m/s airflow.

[4] Value may be higher in environments with high contents of volatile organic compounds. See Section 1.3 of Users Guide.

[5] Values for VDD=3.3V at 25°C, average value at one 12bit measurement per second.

[6] Response time depends on heat capacity of and thermal resistance to sensor substrate.